Award Number:
W81XWH-10-1-0146

TITLE:
Oxidative Lung Injury in Virus-Induced Wheezing

PRINCIPAL INVESTIGATOR: Roberto P. Garofalo, M.D.

CONTRACTING ORGANIZATION: The University of Texas Medical Branch at Galveston
Galveston, TX 77555-5302

REPORT DATE: July 2015

TYPE OF REPORT: Final

PREPARED FOR:
U.S. Army Medical Research and Materiel Command
Fort Detrick, Maryland 21702-5012

REPORT DOCUMENTATION PAGE

Form Approved
OMB No. 0704-0188

1. REPORT DATE	2. REPORT TYPE	3. DATES COVERED
July 2015	Final	05/01/2010 - 04/30/2015

4. TITLE AND SUBTITLE

Oxidative Lung Injury in Virus-Induced Wheezing

5a. CONTRACT NUMBER
W81XWH-10-1-0146

5b. GRANT NUMBER

5c. PROGRAM ELEMENT NUMBER

6. AUTHOR(S)

Roberto P. Garofalo, M.D.

E-Mail: rpgarofa@utmb.edu

5d. PROJECT NUMBER

5e. TASK NUMBER

5f. WORK UNIT NUMBER

7. PERFORMING ORGANIZATION NAME(S) AND ADDRESS(ES)
University of Texas Medical Branch at Galveston

301 University Boulevard
Galveston, TX 77555-0372

8. PERFORMING ORGANIZATION REPORT NUMBER

9. SPONSORING / MONITORING AGENCY NAME(S) AND ADDRESS(ES)

U.S. Army Medical Research and Materiel Command

Fort Detrick, Maryland 21702-5012

10. SPONSOR/MONITOR'S ACRONYM(S)

11. SPONSOR/MONITOR'S REPORT NUMBER(S)

12. DISTRIBUTION / AVAILABILITY STATEMENT
Approved for Public Release; Distribution Unlimited

13. SUPPLEMENTARY NOTES

14. ABSTRACT

We have focused on the role of the transcription factor Nrf2 in controlling expression of antioxidant enzymes (AOE) genes in the lung following infection by respiratory viruses, in particular respiratory syncytial virus (RSV). We have shown that an NRF2-inducing agent, BHA, can restore in part expression of the antioxidant genes SOD1 and catalase following RSV infection in mice. We have also shown that EUKs antioxidant mimetics modulate oxidative stress and inflammatory response in human epithelial cells infected by RSV. Our data show that RSV infection induces NRF2 deacetylation, ubiquitination, and degradation via the proteasome pathway both in vitro and in vivo. Histone deacetylase (HDAC) and proteasome inhibitors block NRF2 degradation and increase NRF2 binding to endogenous promoter ARE sites, resulting in increased AOE expression. Known inducers of NRF2 are able to increase NRF2 activation and subsequent AOE expression during RSV infection in AECs, as well as in an animal model of infection, with significant amelioration of oxidative stress, which is an important pathogenic component of virus-induced lung disease, adding additional support to the concept that therapeutic strategies aimed to increase airway antioxidant capacity by increasing NRF2 activity could be beneficial in RSV infection. Recently, using an *in vitro* model of RSV infection of airway epithelial cells, we discovered that RSV infection inhibits the expression of the CSE enzyme and reduces the ability to generate cellular hydrogen sulfide (H_2S), an endogenous gasotransmitter that we have identified as a novel antiviral pathway. We have presented these data at several national and international meetings and published our findings in high impact factor scientific journals.

15. SUBJECT TERMS
Nothing listed

16. SECURITY CLASSIFICATION OF:			17. LIMITATION OF ABSTRACT	18. NUMBER OF PAGES	19a. NAME OF RESPONSIBLE PERSON
a. REPORT	b. ABSTRACT	c. THIS PAGE			USAMRMC
U	U	U	UU	112	19b. TELEPHONE NUMBER *(include area code)*

Table of Contents

Page

Journal Publications

1. Hosakote YM, Jantzi P, Esham D, Kurosky A, Casola A, Garofalo RP. Viral-mediated inhibition of antioxidant enzymes contributes to the pathogenesis of severe RSV bronchiolitis. Amer J Resp Critic Care Med. 2011; 183(11):1550-60.
2. Hosakote, Y.M., Komaravelli, N., Mautemps, N., Liu, T., Garofalo, R.P., & Casola, A. Antioxidant mimetics modulate oxidative stress and cellular signaling in airway epithelial cells infected with respiratory syncytial virus. Am J Physiol-Lung C 2012; 303:L991-1000.
3. Komaravelli, N, Tian, B., Ivanciuc, T., Mautemps, N., Brasier, A.R., Garofalo, R.P., Casola, A. Respiratory syncytial virus infection downregulates antioxidant enzyme expression by triggering deacetylation-proteasomal degradation of Nrf2. Free Radical Biology and Medicine, Special Issue, Volume 88, Part B, 2015; 391-403.
4. Li, H., Ma, Y., Ivanciuc, T., Komaravelli, N., Kelley, J.P., Ciro, C., Szabo, C., Garofalo, R.P., Casola, A. Role of hydrogen sulfide in paramyxovirus infections. Journal of Virology, 2015. 89(10):5557-68.
5. Ivanciuc, T., Sbrana, E., Ansar, M., Bazhanov, N., Szabo, C., Casola, A., Garofalo, R.P. Hydrogen Sulfide: Antiviral and anti-inflammatory endogenous gastotransmitter in the airways role in respiratory syncytial virus infection. Am J Resp Cell and Mol Biol. 2016; accepted.

FINAL REPORT FOR THE PERIOD ENDING APRIL 30, 2015

I. INTRODUCTION

This project is in response to the Department of Defense Congressionally Directed Medical Research Programs, Investigator-Initiated Research Award and is addressing the topic area "Childhood asthma". The project focuses on respiratory syncytial virus (RSV), the single most important pathogen causing acute respiratory-tract infections in children. RSV infections are a major precipitating factor of wheezing in asthmatic children and have been linked to both the development and the severity of asthma. Our group has established a multidisciplinary and highly integrated pre-clinical and translational research program that focuses on the role of oxidative injury in the pathogenesis of severe RSV infections. We have discovered that in the course of RSV infections reactive oxygen species (ROS) are rapidly generated along with viral-mediated inhibition of protective antioxidant enzyme (AOE) genes in the lung. We have focused on the role of the transcription factor Nrf2 in controlling expression of antioxidant enzymes (AOE) genes in the lung following infection by respiratory viruses, in particular(RSV. Recently, using an *in vitro* model of RSV infection of airway epithelial cells, we discovered that RSV infection inhibits the expression of the CSE enzyme and reduces the ability to generate cellular hydrogen sulfide (H_2S), an endogenous gasotransmitter that we have identified as a novel antiviral pathway. Thus, we propose a new molecular pathway by which respiratory viruses induce lung inflammation, with implication for novel therapeutic strategies of lower respiratory infections and virus-triggered precipitation of asthma attacks.

II. BODY (STATEMENT OF WORK)

This project is in response to the Department of Defense Congressionally Directed Medical Research Programs, Investigator-Initiated Research Award and is addressing the topic area "Childhood asthma". The project focuses on respiratory syncytial virus (RSV), the single most important pathogen causing acute respiratory-tract infections in children. RSV infections are a major precipitating factor of wheezing in asthmatic children and have been linked to both the development and the severity of asthma. Our group has established a multidisciplinary and highly integrated pre-clinical and translational research program that focuses on the role of oxidative injury in the pathogenesis of severe RSV infections. We have discovered that in the course of RSV infections reactive oxygen species (ROS) are rapidly generated along with viral-mediated inhibition of protective antioxidant enzyme (AOE) genes in the lung. Thus, we propose a new molecular pathway by which respiratory viruses induce lung inflammation, with implication for novel therapeutic strategies of lower respiratory infections and virus-triggered precipitation of asthma attacks. The scope of our work is summarized below.

Specific Aim 1 - To determine the mechanism(s) of inhibition of AOE expression in the lung during the course of RSV infection by dissecting the role of Nrf2-mediated transcription pathways.

Aim 1a – Establish expression profile, kinetics and cellular source of AOE in mouse lung.

Task # 1. Perform WB analysis of AOE in lung tissue and BAL* (Year 1, Q1-2*).

Task # 1a. Submit amendment to IACUC protocol # 9001002A to cover experiments in Aim 1 and 2. **(Year 1, Q1-2)**

Milestone # 1. Approval of amendment(s) to IACUC protocol. (Year 1, Q1)

Task # 1b. Experiment 1: RSV or sham infection of BALB/c mice (total 80 animals) and extraction of lung and BAL proteins at different time points (day 1, 3, 5, 7, 9, 15, 21). **(Year 1, Q1-2)**

Task # 1c. Perform WB of normalized lung and BAL proteins with specific antibodies for AOE. **(Year 1, Q1-2)**

Task # 1d. Analysis and quantification of WB results. **(Year 1, Q1-2)**

Task # 1e. Experiment 2: repeat experiment in 1a-d (80 animals). Statistical analysis of AOE expression in RSV-infected vs sham-infected (control) lungs. **(Year 1, Q1-2)**

Results

Respiratory syncytial virus (RSV) is one of the most important causes of upper and lower respiratory tract infections in infants and young children. A recent meta-analysis has estimated that in 2005, 33.8 million new episodes of RSV-associated lower respiratory tract infections occurred worldwide in children younger than 5 years of age, with at least 3.4 million episodes representing severe RSV-associated infections necessitating hospital admission and up to 199,000 fatal cases. In the United States the number of children hospitalized each year with viral lower respiratory tract infections has recently been estimated at more than 200,000, with 500 deaths occurring per year in children under 5 years of age. The mechanisms of RSV-induced airway disease and associated long-term consequences remain incompletely defined, although lung inflammatory response is believed to play a central pathogenetic role. Reactive oxygen species (ROS) are important regulators of cellular signaling, and oxidative stress has been implicated in the pathogenesis of acute and chronic lung inflammatory diseases, such as asthma, cystic fibrosis, and chronic obstructive pulmonary disease (COPD). We have previously shown that RSV infection of airway epithelial cells induces ROS production, which is involved in transcription factor activation and chemokine gene expression. We have also shown that RSV induces oxidative stress in the lung in a mouse model of experimental RSV infection, and that antioxidant treatment significantly ameliorates RSV-induced clinical disease and pulmonary inflammation. In addition, we found that RSV infection of airway epithelial cells results in a significant decrease of antioxidant enzyme (AOE) expression, as well as in increased levels of markers of oxidative stress, indicating an imbalance between ROS production and antioxidant cellular defenses.

As proposed in Specific Aim 1, Milestone # 1, to determine whether RSV infection results in decreased expression of antioxidant proteins *in vivo*, similar to our observation in cultured cells, groups of BALB/c mice were infected intranasally with RSV or sham-inoculated. BAL was collected at Days 1, 3, 5, and 9 after infection to assess levels of

catalase, GST-mu, and SOD 1, 2, and 3 by Western blot. Mouse lung tissue was homogenized in 5 ml ice-cold Buffer A (10 mM 2-hydroxyethyl-piperazine N′-2-ethanesulfonic acid [HEPES]–KOH, pH 7.9, 1.5 mM $MgCl_2$, 10 mM KCl, 0.5 mM dithiothreitol [DTT], 0.2 mM phemylmethyl sulfonyl fluoride [PMSF], 0.6% nonident P40 [NP-40]) and centrifuged at 350 × *g*, 4 °C for 30 secs. The supernatant was kept on ice for 5 min and centrifuged for 5 min at 6,000 × *g* at 4 °C, and the pellet was resuspended in 200 μl Buffer B (10 mM HEPES–KOH, pH 7.9, 1.5 mM $MgCl_2$, 10 mM KCl, 1.2 M sucrose, 0.5 mM DTT, 0.2 mM PMSF). After centrifugation (13,000 × *g*, 4 °C, 30 min), the pellet was resuspended in 100 μl Buffer C (20 mM HEPES–KOH, pH 7.9, 1.5 mM $MgCl_2$, 420 mM NaCl, 0.2 mM ethylenediamine-tetraacetic acid, 0.5 mM DTT, 0.2 mM PMSF, 2 mM benzamidine, 5 μg/ml leupeptin, 25% glycerol), incubated on ice for 20 min, and centrifuged (6,000 × *g*, 4 °C, 2 min). Equal amount of proteins (10-20 μg, depending on the antibody used) were loaded and separated by SDS-PAGE, and transferred onto Hybond-polyvinylidene difluoride membrane (Amersham Pharmacia Biotech, Piscataway, NJ). Nonspecific binding was blocked by immersing the membrane in Tris-buffered saline-Tween (TBST) blocking solution (10 mM Tris-HCl, pH 7.6, 150 mM NaCl, 0.05% Tween-20 [v/v]) containing 5% skim milk powder for 30 min. After a short wash in TBST, the membranes were incubated with the primary antibody overnight at 4 °C, followed by the appropriate secondary antibody (Santa Cruz Biotechnology, Santa Cruz, CA), diluted 1:5–10,000 in TBST for 1h at room temperature. After washing, the proteins were detected using enhanced-chemiluminescence assay (Amersham Biosciences, Piscataway, NJ) according to the manufacturer's recommendations. The primary antibodies used for Western blots were anti-SOD 1, 2, and 3 rabbit polyclonal antibodies (Stressgen Bioreagents, Ann Arbor, MI), anti-catalase rabbit polyclonal antibody, and anti-lamin B mouse monoclonal antibody (Calbiochem), anti-Nrf2 (C20) rabbit polyclonal (Santa Cruz Biotechnology), and anti–β-actin mouse monoclonal antibody from Sigma-Aldrich (Saint Louis, MO). The anti-GST rabbit polyclonal antibody was a generous gift from Dr. Yogesh Awasthi, University of North Texas Health Science Center.

As shown in **Fig. 1**, RSV-infected mice showed a significant reduction in the expression levels of most of the tested enzymes in BAL samples at days 1 and/or 3 after infection compared with control animals. SOD 3 was decreased at days 3 and 5 after infection in most but not all of the RSV-infected animals and therefore did not reach statistical significance. Overall, levels of AOE in RSV-infected mice returned to control levels by day 9 after infection, with the exception of SOD 2, whose expression normalized earlier (day 5 after infection).

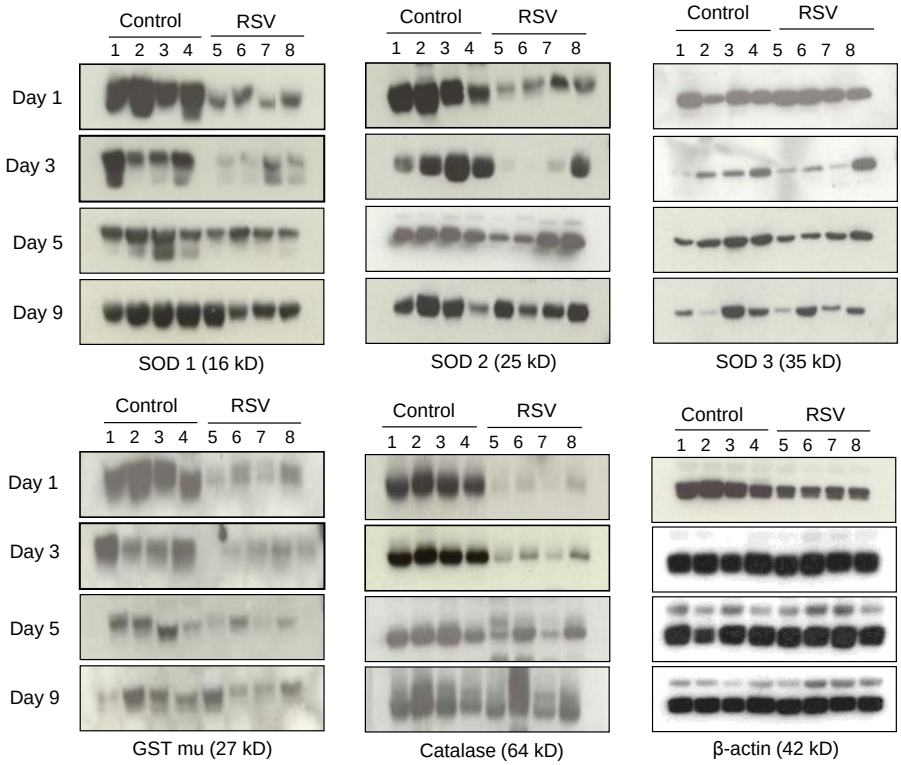

Fig 1. Antioxidant enzymes (AOE) are reduced in BAL of RSV-infected mice. Groups of mice were infected with RSV or sham inoculated with saline (Control) and BAL was collected at days 1, 3, 5, and 9. BAL proteins were resolved on 10% SDS-PAGE and Western blots were performed using antibodies against SOD 1, 2, 3, catalase and GST-mu. Membranes were stripped and reprobed for β-actin as an internal control for protein integrity and loading. Lanes 1-4 are BAL from four control and 5-8 from four RSV-infected mice at each time point.

Milestone # 2. Complete quantitative kinetics of AOE protein expression in the lung/BAL after infection – 5 animal/each time point/each condition X 2 independent experiments. (Year 1, Q2)

Task #2. Perform real time PCR analysis of AOE in lung tissue and BAL cells. **(Year 1, Q2-3)**

Task # 2a. Experiment 1: RSV or sham infection of BALB/c mice (total 80 animals) and extraction of lung and BAL cell RNA (day 1, 3, 5, 7, 9, 15, 21). **(Year 1, Q2-3)**

Task # 2b. Perform real time PCR of lung and BAL RNA with specific muse primers for AOE. **(Year 1, Q2-3)**

Task # 2c. Analysis and quantification of real time PCR results. **(Year 1, Q2-3)**

Task # 2d. Experiment 2: repeat experiment in 2a-c (80 animals) – Statistical analysis. **(Year 1, Q2-3)**

Results

Based on the results of AOE WB analysis, we have performed focused real-time PCR of AOE in the lung at 48h post-infection. These studies were performed in relation to the

modulatory effect of BHA treatment and are described under Specific Aim 2 (see below). In addition, to determine whether changes in AOE protein expression resulted in changes in their activities in response to RSV infection, BAL was collected from groups of RSV-infected or sham-inoculated mice at Days 1, 3, 5, and 9 after infection, and total SOD, catalase, GST, and GPx enzymatic activity were assessed by biochemical assays. There was a significant reduction of all AOE activities in RSV-infected mice compared with control animals (**Fig. 2**). In particular, in RSV-infected mice, total SOD and GPx activities decreased significantly at Days 1 (86 and 59%, respectively) and 3 (52 and 46%, respectively), compared with sham-inoculated mice, with levels returning to those in control mice by Day 9. In addition, catalase and GST activities were significantly lower in RSV-infected mice compared with control mice at all tested time points, but different from our findings with SOD and GPx, they did not return to control levels by Day 9 (76, 63, 37, and 50% reduction for catalase and 75, 59, 50, and 48% reduction for GST at Days 1, 3, 5, and 9 after infection). Overall, these results indicate that RSV significantly reduces antioxidant defenses of the airways.

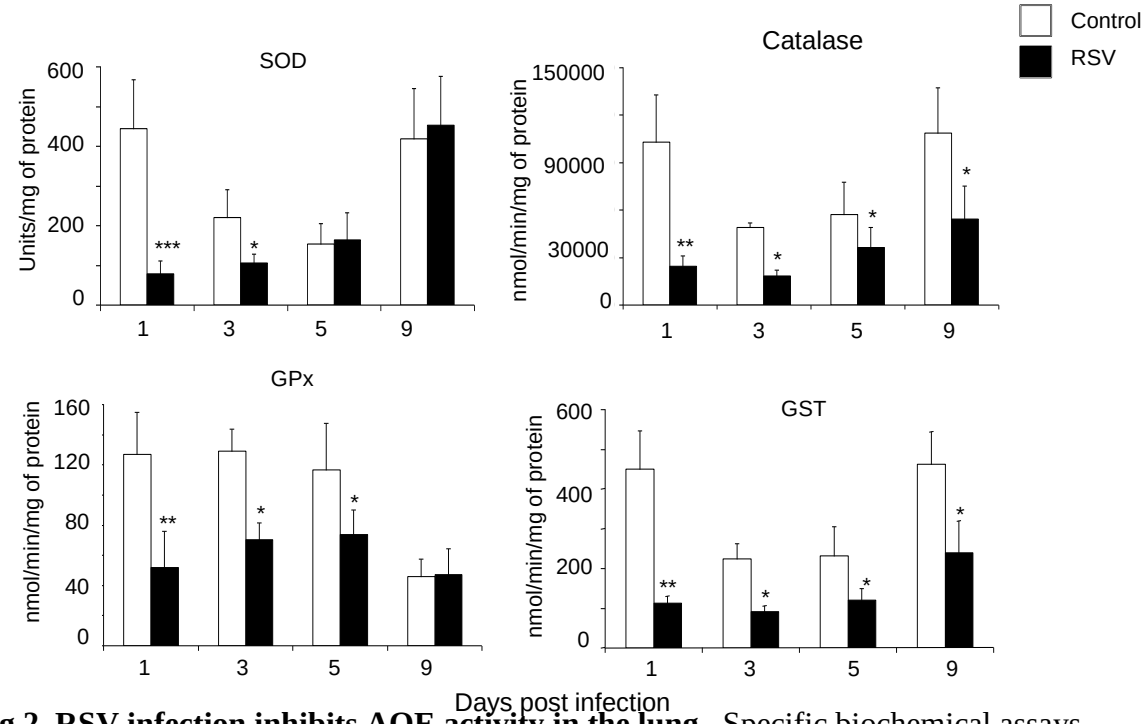

Fig 2. RSV infection inhibits AOE activity in the lung. Specific biochemical assays were used to determine total SOD, catalase, GPx, and GST activity in BAL of group of mice that were RSV infected or sham inoculated. The figure is representative of three independent experiments, each experiment with 4-5 mice/group/time point. Data are presented as mean ± SEM of 4 mice/group/each time point. *$p < 0.05$; ** $p < 0.01$ and ***$p < 0.001$ relative to control mice.

Milestone # 3. Complete quantitative kinetics of AOE mRNA in the lung/BAL cells after infection – 5 animal/each time point/each condition X 2 independent experiments. (Year 1, Q3)

***Task # 3. Identification of lung cells involved in RSV-mediated AOE modulation.* (Year 1, Q3-4)**

Task # 3a. Refine methodology to isolate total proteins from epithelial cells of the distant airways and alveolar macrophages. **(Year 1, Q3-4)**

Results

As proposed in Milestone # 3, to determine whether levels of AOE detected in the BAL reflected changes in the AOE in airway epithelium, a major target of RSV infection, we performed Western blot analysis of SOD 1, 2, and 3 in proteins isolated from airway epithelial cells of infected mice. A lysis-lavage method described by Wheelock and colleagues was used to isolate epithelial cell proteins of conductive airways. Briefly, mice were killed and trachea was exposed and cannulated, lungs were then removed from the thorax and inflated with 0.5 ml agarose solution (0.75% low-melting agarose, 5% dextrose) immediately followed by 0.5 ml dextrose solution (1% dextrose, 2% protease inhibitor cocktail) through a three-way valve. Both solutions were preheated at 37°C. The inflated lungs were incubated in 5% dextrose for 15 min at room temperature. Dextrose solution was then removed by repeated steps of inversion of the lungs and gentle suction with a syringe. The airways were then lavaged with 0.5 ml of lysis buffer (2 M thiourea, 7 M urea, 4% 3-((3-cholamidopropyl)dimethylammonio)-1-propanesulfonic acid, 0.5% Triton X 100, 1% DTT, and protease inhibitors). The lysis buffer containing the proteins was immediately recovered, flash frozen on dry ice and stored at −80 °C until further use. As shown in **Fig. 3**, we found a significant decrease of SOD 1 and 3 in epithelial proteins of RSV-infected mice compared with epithelial proteins from control mic. On the other hand, SOD 2 levels were similar in epithelial proteins of RSV-infected and control mice, suggesting that the reduction of such enzymes observed in Western blots of infected BAL samples may reflect a non-epithelial source/cell target of such enzymes after RSV infection.

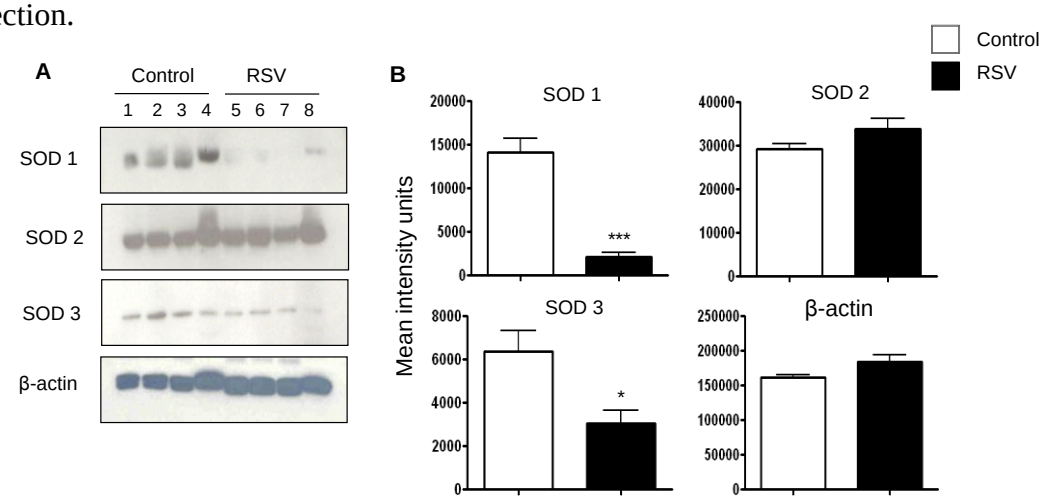

Fig 3. SOD 1, SOD 2, and SOD 3 in conductive airway epithelial cells. (**A**) Proteins of conductive airway epithelial cells were obtained by lysis-lavage from RSV-infected or control mice (day 1 p.i.). Proteins were analyzed by Western blot for content of SOD 1, SOD 2, and SOD 3 as in Fig. 1 (**B**) Densitometric analysis of Western blot band intensities was performed using Alpha Ease software, version 2200 (2.2d) (Alpha

Innotech Co., San Leandro, CA). Bands in RSV-infected samples were normalized to uninfected control sample background and are presented as mean ± SEM of n = 4. *p < 0.05; ***p < 0.001 relative to control mice.

Milestone # 4. Obtain > 90% cell-specific proteins from either distal airway epithelial cells or alveolar macrophages. (Year 1, Q4)

Task 3b. Experiment 1: based on results in Task # 1, infect mice and obtain epithelial and macrophage proteins at three to four representative time points (30-40 animals). **(Year 1, Q4)**

Task # 3c. Perform WB analysis of cell proteins with specific antibodies for AOE enzymes. **(Year 1, Q4)**

Task # 3d. Experiment 2: repeat experiment in 3b-c (30-40 animals). Statistical analysis. **(Year 1, Q-4)**

Results

Please see above in Milestone # 3 the detailed description of isolation of specific proteins from distal airway epithelial cells. The isolation of proteins form alveolar macrophages (AM) after RSV infection of mice has proven to be difficult given the fact that we discovered that these cells undergo rapid necrosis (within 3-6h) after inoculation of the virus (1). We are currently pursuing alternative approaches, including studies in which we will deplete AM from the airways and will assess the contribution of these cells to the overall AOE expression in the lung.

Milestone # 5. Complete analysis of specific cell source of AOE during RSV infection and its expression pattern. (Year 1, Q4)

Aim 1b – Activation of Nrf2 and Nrf3 in the lung of RSV-infected mice.

Task # 4 – Perform WB and EMSA analysis of lung and BAL nuclear proteins. **(Year 1, Q3-4)**

Task # 4a. Experiment 1: RSV or sham infection of BALB/c mice (total 80 animals) and extraction of lung and BAL nuclear proteins (day 1, 3, 5, 7, 9, 15, 21). **(Year 1, Q3-4)**

Task # 4b. WB of normalized nuclear lung and BAL proteins with specific antibodies for Nrf2 and Nrf3. Analysis and quantification. **(Year 1, Q3-4)**

Task # 4c. EMSA of normalized nuclear lung and BAL proteins with specific Nrf2 and Nrf3 DNA-binding sequences. Analysis and quantification. **(Year 1, Q3-4)**

Task # 4d. Experiment 2: repeat experiment in 4a-c (80 animals). Statistical analysis. **(Year 1, Q3-4)**

Milestone # 6. Complete analysis of RSV-mediated inhibition and/or activation of Nrf2 and Nrf3 as critical regulatory elements of AOE transcriptional activity. (Year 1, Q4)

Results

Recent findings have demonstrated that Nrf2 is a crucial transcription factor that binds to antioxidant responsive element (ARE) sequences and regulates the expression of antioxidant and phase 2 metabolizing enzymes in response to oxidative stress. To examine the effect of RSV infection on Nrf2 activation, we performed Western blot analysis of mouse lung nuclear extracts. Groups of BALB/c mice were infected with RSV or sham inoculated, and nuclear extracts were obtained from lungs at 12, 24, 48, and 72 hours after infection. There was a significant decrease of Nrf2 nuclear abundance in RSV-infected mice compared with control mice at 12 hours and 24 hours after infection (average percentage change of Nrf2 in RSV over control is 61 and 97% at 12 and 24 hours, respectively)(**Fig. 4**), with nuclear levels in RSV-infected mice still below control at 48 and 72 hours after infection (data not shown). These results suggest that decreased AOE expression after RSV infection could be due to reduced basal activation of Nrf2 in the airways of mice. Based on these results, the Nrf3 hypothesis was not further pursued. Further results of the Nrf2 pathways are presented in relation to Specific Aim 2 (see below).

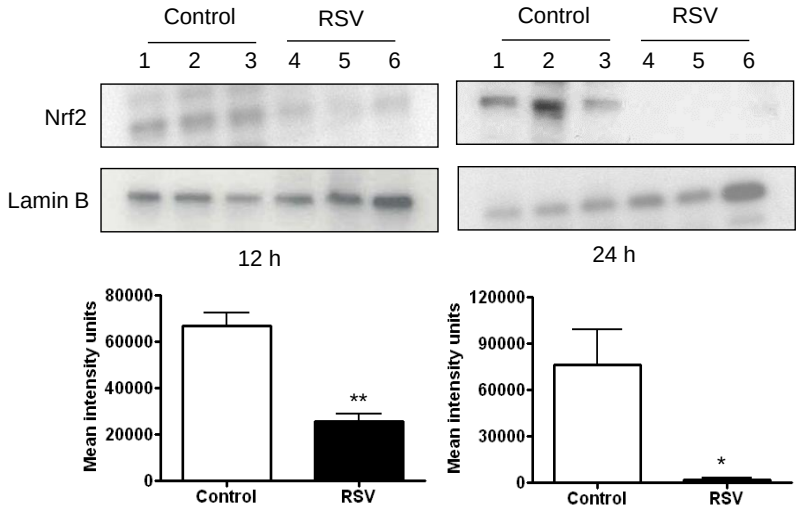

Fig. 4. RSV infection is associated with decreased levels of nuclear Nrf2 in the lung. Mice were infected with RSV or sham inoculated and lungs were harvested at 12 and 24 h to isolate nuclear proteins. Equal amounts of nuclear proteins were analyzed by Western blot using anti-Nrf2 antibody. Membranes were stripped and reprobed for Lamin B, as control for equal loading of the samples. Lanes 1-3 are lung nuclear proteins from control and 4-6 from RSV-infected mice at each time point. The figure is representative of three independent experiments, each experiment with 4-5 mice/group/time point. Densitometric analysis of Western blot band intensities was performed using Alpha Ease software presented as mean ± SEM of n = 3. *$p < 0.05$; ** $p < 0.01$ relative to control mice.

Specific Aim 2 - To establish whether pharmacologic intervention aimed to increase Nrf2 activation in the airways or to supplement the antioxidant response via synthetic antioxidant mimetics results in protection from viral-induced lung injury and clinical disease.

Aim 2a – Effect of activation of Nrf2-dependent AOE expression by synthetic triterpenoids on RSV-induced lung oxidative injury and clinical disease.

Task # 5. Establish appropriate treatment of mice with triterpenoids (CDDO) that results in increased Nrf2 activation in the lung and AOE expression. **(Year 2, Q1-2)**

Task # 5a. Treatment of groups of BALB/c mice with the synthetic triterpenoid CDDO to establish proper pharmacologic dose (two i.p. doses, three groups of mice, including one group treated with control vehicle, total 150 mice) – Lung nuclear protein extraction five days after initial dose. Potential drug toxicity monitored by daily body weight assessment. **(Year 2, Q1-2)**

Task # 5b. WB and EMSA of nuclear lung proteins with specific antibodies for Nrf2 as in Task # 4b-c. Analysis and quantification comparing CDDO-treated vs vehicle-treated mice. **(Year 2, Q1-2)**

Task # 5c. Treatment of BALB/c mice with dose and schedule of CDDO established in task # 5a-b. Extraction of total lung proteins for assessment of AOE expression by WB and/or real time PCR
(total 100 mice). Repeat experiment twice. **(Year 2, Q2)**

Milestone # 7. Establish dose and schedule of CDDO that result in Nrf2 activation and AOE expression in lung of BALB/c mice. (Year 2, Q2)

Task # 6. Effect of CDDO treatment on RSV-induced clinical disease, AHR and oxidative damage in the lung. **(Year 2, Q2-3)**

Task # 6a. RSV infection of CDDO-treated or vehicle-treated (control) BALB/c mice and determination of clinical disease by body weight loss, clinical disease score, and AHR by Buxco, over 21 days (50 animals total). Peak viral replication will be determined at day 5. Experiment will be repeated twice. Statistical analysis. **(Year 2, Q2-3)**

Task # 6b. RSV infection of CDDO-treated or vehicle-treated (control) BALB/c mice and analysis of lung and BAL for lipid peroxidation markers (MDA and 4-HNE) and for measurement of 8-isoprostane (total 50 mice). Experiment will be repeated twice. Statistical analysis. **(Year 2, Q2-3)**

Milestone # 8. Complete determination of protective effect of triterpenoids on RSV-induced clinical disease and oxidative damage in a mouse model. (Year 2, Q3)

Aim 2b – Effect of catalytic scavengers on RSV-induced lung oxidative injury and clinical disease.

Task # 7. ***Effect of synthetic SOD and catalase mimetics on RSV-induced clinical disease and AHR.*** **(Year 2, Q3-4)**

Task # 7a. Mice treated with the mimetics EUK-8 or EUK-134 or with vehicle control by gavage. Dose and schedule treatment will be established based on published data by scientists who developed these compounds and experience

by the PI with the anti-oxidant BHA. Anticipated need for 200 mice to set up conditions. Potential toxicity will be monitored by body weight loss. **(Year 2, Q3-4)**

Task # 7b. RSV infection of EUK-treated or vehicle-treated (control) BALB/c mice and determination of clinical disease by body weight loss, clinical disease score, and AHR by Buxco, over 21 days (100 animals total). Peak viral replication will be determined at day 5. Experiment will be repeated twice. Statistical analysis. **(Year 2, Q3-4)**

Results

Initial experiments revealed that the Nrf2-inducer triterpenoid CDDO was indeed toxic to mice and therefore this approach was not further pursued. Among the compounds known to stimulate ARE-driven transcription, butylated hydroxynanisole (BHA) and its metabolite *tert*-butylhydroquinone (tBHQ) have been shown to increase HO-1, NQO1, and Nrf2 protein expression in both primary and cultured cells. We investigated whether tBHQ treatment could rescue Nrf2 activity following viral infection. Initial studies were performed in vitro. A549 cells were transiently transfected with the ARE-driven reporter plasmid and infected with RSV in the presence or absence of tBHQ. RSV infection was associated with a significant decrease in reporter gene activity, compared with uninfected cells, which was restored close to levels of uninfected cells by tBHQ treatment [Fig. 8 in (2)]. AOE gene and protein expression, as well as Nrf2 nuclear levels, were also significantly increased in RSV-infected cells by tBHQ treatment [Fig. 8B and 8C and supplementary material, Figs 6A and 6B in (2)], indicating that Nrf2 inducers can restore ARE-dependent gene expression following RSV infection. Restoration of AOE cellular capacity was paralleled by significant reduction of RSV-induced oxidative stress, as shown by a significant decrease of the oxidative marker 8-isoprostane in virus-infected tBHQ-treated cells [Fig. 8D in (2)].

As tBHQ treatment of cells was able to restore Nrf2 activation, we tested whether BHA (precursor of tBHQ) had a similar effect in the airways of infected mice. Lungs of mice either sham-inoculated or infected with RSV for 48 h in the presence or absence of BHA (250 mg/kg) were harvested to prepare bronchoalveolar lavages (BALs), nuclear extracts, or total RNA. Mice infected with RSV showed significantly reduced Nrf2 nuclear levels, compared with sham-inoculated mice, and in most of the infected mice, BHA treatment was able to restore Nrf2 activation to levels close to that in uninfected mice [Fig. 9A in (2)], as well as the expression of the Nrf2 target genes catalase and SOD1 [Fig. 9B in (2)]. In addition, there was a very significant reduction in RSV-induced lung oxidative stress in BHA-treated mice, as indicated by a significant reduction of 8-isoprostane levels in BALs, compared with untreated, infected mice [Fig. 9C in (2)], supporting our previous finding that BHA treatment has a positive impact on RSV-induced lung disease (3).

Milestone # 9. Complete determination of protective effect of synthetic SOD and catalase mimetics on RSV-induced clinical disease and AHR in a murine model. (Year 2, Q4)

Results

In these studies, we first tested whether treatment with the antioxidant mimetics EUK-8 and -189, which possess significant catalase and peroxidase activity in addition to SOD, could restore AOE capacity in RSV-infected airway epithelial cells (AECs) and thereby exert a protective effect against RSV-induced oxidative stress. A549 cells were treated 1 h before infection and throughout the length of infection with increasing concentration of EUK and infected with RSV. Cells were harvested at a different time postinfection to measure AOE activity in the presence or absence of EUK treatment. RSV infection induced a progressive increase in SOD activity with a concomitant decrease in catalase and peroxidase activity [Fig. 1 in (4)]. EUK-8 treatment further increased SOD activity but, more importantly, reversed the loss of catalase and peroxidase activity observed in response to RSV infection, with the highest dose of EUK-8 increasing the latter two AOE activities above values of uninfected cells. Similar results were obtained in cells treated with EUK-189. To determine whether EUK treatment could reduce RSV-induced ROS production and cellular oxidative stress, A549 cells were treated with different concentrations of the two antioxidant mimetics either 1 h before and throughout the length of infection, or at a different time postinfection. Cells were harvested at 24 h post-infection to measure ROS generation and concentration of the lipid peroxidation markers MDA and F_2-8-isoprostane. RSV infection of AECs induced a time-dependent increase in ROS generation, starting between 1 and 3 h postinfection [Fig. 3A in (4)], which was significantly reduced by pretreatment with both EUK-8 and EUK-189, in a dose-dependent manner [Fig. 3B in (4)]. In agreement with the observed reduction in ROS production, EUK pretreatment of AECs significantly decreased the elevated cellular levels of the lipid peroxidation markers MDA and 8-isoprostane generated in response to RSV infection [Fig. 4 in (4)], indicating that antioxidant mimetic pretreatment can effectively counteract viral-induced cellular oxidative stress. EUK treatment was still effective, leading to a significant reduction in 8-isoprostane generation, even after RSV infection was established. When we tested the EUKs in mice, we found that they were modestly effective in reducing RSV-mediated oxidative response and secretion of inflammatory cytokines. Therefore, we turned to a new approach to overexpress AOE in the lung. In collaboration with Dr. Sergei Atamas at University of Maryland, Baltimore, we have recently generated a recombinant replication-deficient adenovirus (AdV) expressing human SOD1, using the RAPAd system described elsewhere in details [Vira-Quest, North Liberty, IA) (5)]. The resultant purified adenovirus vector has a concentration of $0.9X10^{12}$ particles/ml and an infectious titer of $4X10^{10}$ plaque-forming units (PFU)/ml and was termed AdV-hSOD1. Control adenovirus vector AdV-Null with no insert in the E1 region was produced in the same manner. Both vectors have green fluorescent protein (GFP)-encoding gene inserts in the E3 region, to permit detection in the lung by green fluorescence. In preliminary experiments performed in BALB/c mice we have shown peak expression of GFP in the lung at 5 days after either intratracheal or intranasal instillation of the AdV constructs at a range from 1 to $5X10^8$ PFU/mouse. Importantly, we have shown that the replication-deficient AdV *per se* does not affect the subsequent infection with RSV in terms of viral replication or disease. We are currently examining expression of human SOD1 by WB analysis in lung protein extracts. Conditions shown to be optimal for SOD1 expression will be used to investigate RSV

lung titers at different days post-inoculation (day 1, 3, 5, 7) and other parameters of RSV-induced oxidative injury and lung disease. Similarly we have generated a murine AdV-Nrf2 construct which is currently undergoing testing in mice.

Aim 3 - Analyze whether distinct AOE expression patterns at the airway mucosal site can discriminate between infants with different severity of illness and/or degree of oxidative-associated injury following naturally-acquired RSV infection.

Aim 3a – Expression of AOE and oxidative stress markers in NPS of RSV-infected infants.

Task # 8. Perform WB for AOE in NPS of RSV-infected infants that were previously collected. **(Year 2, Q1-2)**

Task # 8a. Submit amendment to IRB protocol # 03-117: addition of new investigators and scope of the work covered in this grant. **(Year 1, Q1)**

Milestone # 10. Approval of amendment(s) to IRB protocol. (Year 1, Q1)

Task # 8b. Set up conditions for WB of AOE in NPS, including clean-up of mucus from samples, amount of protein, concentration of primary antibodies, secondary antibody. Set up conditions for measurement of lipid peroxidation markers (MDA and 4-HNE) and for measurement of 8-isoprostane. **(Year 2, Q1-2)**

Task # 8c. Perform WB for AOE and oxidative marker assays in 150 previously collected and stored (- 70^0 C) samples of NPS from RSV-infected infants. **(Year 2, Q1-2)**

Task # 8d. Analysis and quantification of WB results. **(Year 2, Q1-2)**

Results

Samples of NPS were collected at UTMB from infants and children who were enrolled in an ongoing study on the pathogenesis of viral bronchiolitis. The study protocol and consent forms have been approved by the UTMB Institutional Review Board. The study population comprised groups of infants and children younger than 12 months old recruited from the UTMB Emergency Department, the pediatrics outpatient clinics, or inpatient areas of Children's Hospital. These subjects were assigned a diagnosis of upper respiratory tract infection (URTI) alone (absence of crackles or wheezing on auscultation of the chest, oxygen saturation ≥ 97% on room air, and normal chest radiograph when obtained), "nonhypoxic bronchiolitis" (defined for the purposes of this study as wheezing on auscultation with oxygen saturation > 95% on room air), or "hypoxic bronchiolitis" (wheezing on auscultation and oxygen saturation ≤ 95% on room air or, in the absence of wheezing, hyperinflation on chest radiograph and oxygen saturation ≤ 95% on room air). Hypoxia was assessed at the time that secretion samples were obtained, with subjects breathing ambient air without oxygen supplementation. Subjects with recurrent wheezing were not included, nor were those with history of chronic lung disease or congenital heart disease. Infants who were intubated (VS, ventilatory support) because of acute

respiratory failure caused by RSV infection were also included in the study. RSV infection was confirmed in all subjects by detection of viral antigen in NPS samples by antigen detection. All samples were obtained within the first 5 days of respiratory illness and within 24 hours after the onset of wheezing.

Milestone # 11. Complete analysis of AOE in stored samples of human NPS collected from RSV infections. (Year 2, Q2)

Task # 9. Analysis of AOE, protein patterns, and oxidative markers in prospectively enrolled infants with different clinical severity of RSV infection.

Task # 9a. Enroll infants and young children with RSV infections, URTI or LRTI (bronchiolitis, with or without hypoxemia). Enrollment on the ward, outpatient clinic, or emergency room. Collect NPS samples for virus identification, protein analysis. Collect clinical data. **(Year 1, Q2-4;Year 2, Q1-4;Year 3,1-2)**

Task # 9b. Perform WB for AOE and assays for MDA, 4-HNE, and 8-isoprostane in samples of NPS (total samples over 3 year study ~ 200). **(Year 2, Q1-4; Year 3, Q1-2)**

Task # 9c. Analysis and quantification of WB and other assays, statistical analysis and correlation with clinical severity, other parameters of infection. **(Year 3, Q2)**

Results

Samples of NPS were obtained by passing size 5F feeding tubes into the nasopharynx and applying gentle suction. Secretions then were rinsed into collecting traps with 3 ml of PBS. After centrifugation to precipitate cells, samples were digested with sputolysin (Calbiochem, San Diego, CA), a mucolytic agent in 6.5 mM dithiothreitol in 100 mM phosphate buffer, pH 7.01, and stored at −80 °C for subsequent protein and biomarker analysis. For WB analysis, please see description under Milestone # 1. As shown in an example in **Fig. 5**, we measured levels of SOD 1, 2, and 3, catalase, and GST-mu in NPS of infected children by WB. For this analysis, infants on VS (i.e., those with most severe illness) were included in a separate group. SOD 1 levels were lower in infants with bronchiolitis, hypoxic bronchiolitis, and VS compared with those with URTI alone. The VS group showed also significantly lower levels of SOD 3, catalase, and GST-mu compared with the other illness groups. SOD 2 levels were similar in all illness groups.

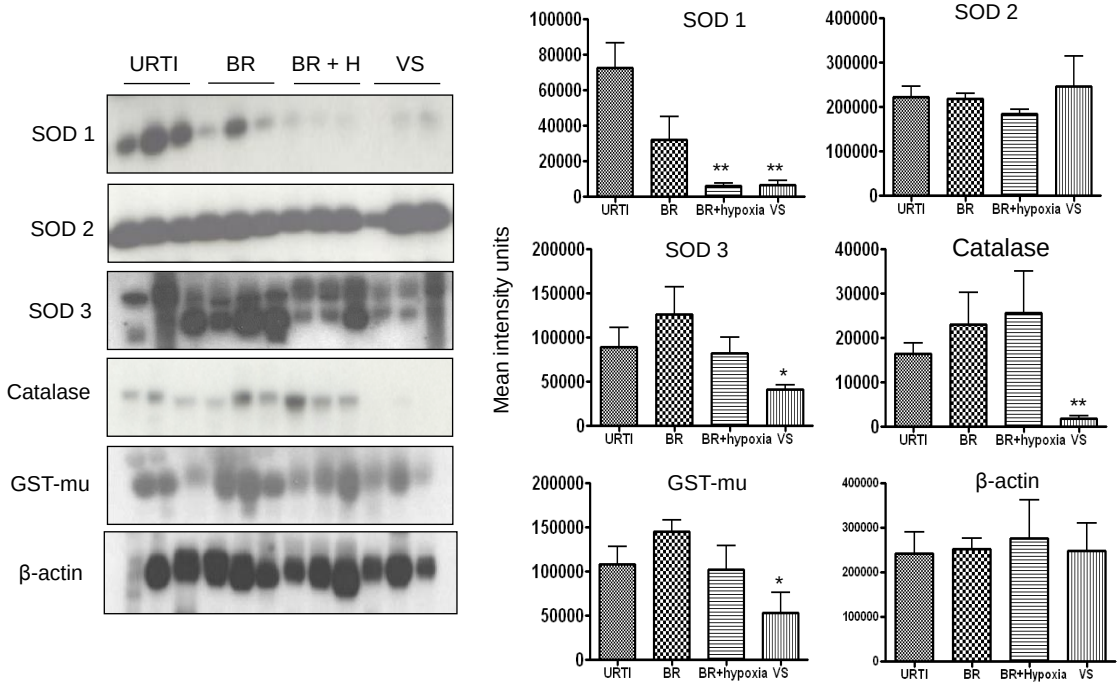

Fig. 5. AOE expression in NPS of infants with naturally-acquired RSV infections. Western blot analysis of SOD 1, 2 and 3, catalase and GST-mu in NPS of children with upper respiratory tract infections (URTI), bronchiolitis (BR), bronchiolitis with hypoxia (BR + H) and patients on ventilatory support (VS). β-actin was used as a control for protein integrity and equal loading of the samples. Densitometric analysis of Western blot band intensities was performed using Alpha Ease software. *$p < 0.05$; ** $p < 0.01$, compared to URTI.

Milestone # 12. Assessment of AOE and oxidative markers in NPS and their relationship to disease severity in RSV-infected infants. (Year 3, Q3)

Aim 3b – Differential protein expression in fractionated NPS samples by 2DE and MALDI/TOF/TOF.

Task # 10. Set up conditions for NPS fractionation and subsequently analysis by 2DE gels or Electrospray MS/MS. **(Year 2, Q1)**

Task # 10a. NPS fractionation by size exclusion chromatography (SEC) and 2DE gels of proteins with MW > 26kDA: set up conditions using previously collected and stored (- 70^0 C) samples of NPS from RSV-infected infants. Run samples in duplicate. **(Year 1, Q4; Year 2, Q1-4, Year 3, Q1)**

Task # 10b. Trypsin digestion and Electrospray MS/MS of protein fractions < 26 kDA - Run sample in duplicate. **(Year 2, Q2-4; Year 3, Q1)**

Results

We have previously shown that RSV is a potent inducer of ROS in airway epithelial cells *in vitro* and causes significant oxidative stress damage *in vivo*, as demonstrated by the increase of lipid peroxidation markers F_2 8-isoprostane, MDA, and 4-hydroxynonenal in the lung of experimentally infected mice. Thus, we measured the levels of F_2 8-isoprostane and MDA in NPS of children with RSV-proven infections of increasing clinical severity, from milder URTI to bronchiolitis without or with hypoxia. As shown in **Fig. 6.**, concentration of F_2 8-isoprostane in NPS was slightly increased in subjects with mild bronchiolitis compared with those with URTI, but the difference was not statistically significant. However, subjects with hypoxic bronchiolitis had significantly more F_2 8-isoprostane in NPS than did subjects with URTI alone ($P < 0.01$) or with nonhypoxic bronchiolitis ($P < 0.001$). A similar trend was observed for MDA concentrations in a smaller number of NPS samples that were tested. Analysis of additional markers is ongoing.

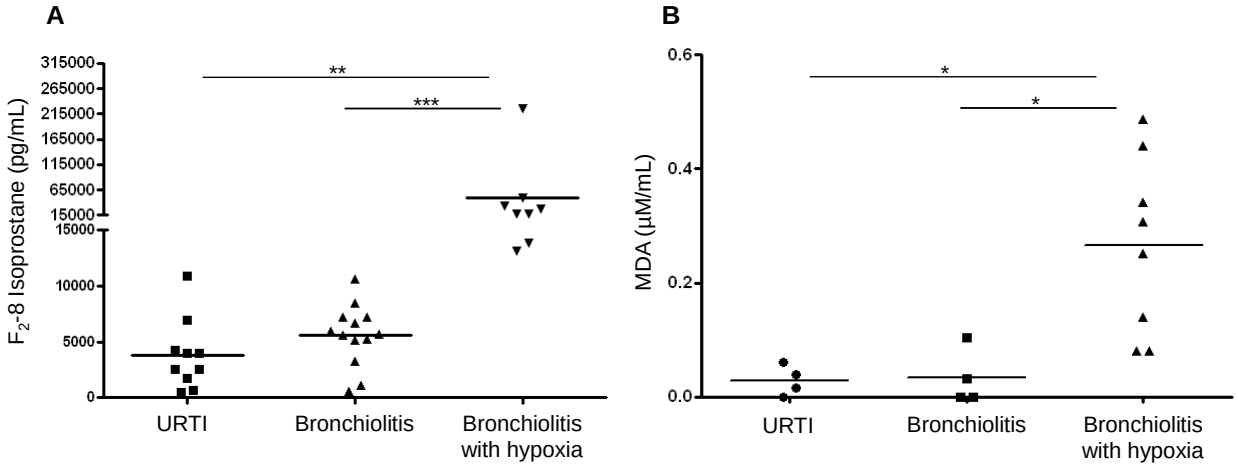

Fig 6. Concentrations of the oxidative stress markers in NPS of infants with naturally-acquired RSV infections. NPS collected from infants and young children with RSV-proven upper respiratory tract infections (URTI) and bronchiolitis were tested for F2-isoprostane (**A**) or MDA (**B**) concentrations. Horizontal lines indicate the mean concentration. ** $p < 0.01$ and ***$p < 0.001$ compared to URTI.

Milestone # 13. Establish a reproducible methodology to fractionate proteins in NPS by SEC.

Task # 11. Identify differential expressed proteins in fractionated NPS from infants with URTI or bronchiolitis. **(Year 3, Q1)**

Task # 11a. Perform mass fingerprinting of prospectively collected NPS by MALDI-TOF and MS of proteins and a Bayesian statistical algorithm. **(Year 3, Q3)**

Task # 11b. Sequencing of selected proteins by LC/MS/MS **(Year 3, Q4)**

Milestone # 14. Build a map of NPS proteins that are quantitatively or functionally associated with more severe manifestations of RSV infections. (Year 3, Q4)

Results

We have established conditions to obtain proteins from human NPS for proteomics studies (2DE gels). Briefly, sputolysin-digested human NPS samples were lyophilized and reconstituted in 100 µl of reagent 1 procured from Bio-Rad (Hercules, CA; 50 mM Tris buffer), desalted using protein desalting columns from Pierce (Rockford, IL) (7,000 MW cutoff), followed by albumin depletion by a Montage albumin depletion kit. Then 200 µl of 1 mg/ml protein aliquots were isoelectrofocused (IEF) on 11 cm–long nonlinear precast immobilized pH gradient (IPG) strips (pH 3–10; Bio-Rad) using the IPGPhor isoelectrofocusing system. Protein samples were loaded onto an IPG strip and rehydrated overnight. IEF was performed at 20°C with the following parameters: 50 V for 11 hours, 250 V for 1 hour, 500 V for 1 hour, 1,000 V for 1 hour, 8,000 V for 2 hours, and 8,000 V for 6 hours, with a total of 48,000 V. After IEF, the IPG strips were stored at −80°C until two-dimensional sodium dodecyl sulfate polyacrylamide gel electrophoresis (SDS-PAGE) was performed. For the two-dimensional SDS-PAGE, the IPG strips were incubated in 4 ml of equilibration buffer (6 M urea, 2% SDS, 50 mM Tris-HCl [pH 8.8], 20% glycerol) containing 10 µl of 0.5 M TCEP [Tris(2-carboxyethyl) phosphine] for 15 minutes at 22 °C with shaking. The strips were then incubated in another 4 ml of equilibration buffer with 25 mg of iodoacetamide/ml for 15 min at 22 °C with shaking. Electrophoresis was performed at 150 V for 2.25 hours at 4 °C with 8 to 16% precast polyacrylamide gels in Tris-glycine buffer (25 mM Tris-HCl, 192 mM glycine, 0.1% SDS [pH 8.3]). After two-dimensional gel electrophoresis (2DE), the gels were fixed (10% methanol [MeOH], 7% acetic acid in double-distilled water), stained with SYPRO Ruby (Bio-Rad), and destained (10% ethanol in double-distilled water).

The destained gels were scanned at a 100-µm resolution using the Perkin-Elmer (Boston, MA) ProXPRESS ProFinder Proteomic Imaging System with 480-nm excitation and 620-nm emission filters. The exposure time was adjusted to achieve a value of approximately 55,000- to 63,000-pixel intensity on the most intense protein spots on the gel. The 2DE gel images were subsequently analyzed using Progenesis Discovery software version 2006.03 (Nonlinear Dynamics, Ltd., Newcastle Upon Tyne, UK). An average gel was created from gels run on NPS proteins from infants with URTI, nonhypoxic bronchiolitis, bronchiolitis with hypoxia, and patients on VS. The software automatically selected one of the six gels for mice experiment and one of the four gels for human NPS as the base image of the reference gel. The gel with the highest number of spots was set as the reference gel. Unmatched spots present in five of the six other gels were subsequently added to the reference gel image by the software to give a comprehensive reference gel. Subsequent to automatic spot detection, spot filtering was also manually performed. The matching of spots between the gels was manually reviewed and adjusted as necessary. Moreover, the log-transformed spot volumes were normally distributed, indicating that nonparametric statistical comparisons, such as *t* tests, could be applied to identify those proteins whose expression was significantly changed by infection. The spot volumes were normalized based on the total spot volume for each gel, and the control and RSV-infected samples were compared.

Protein gel spots were excised and prepared for matrix-assisted laser desorption ionization-time of flight mass spectrometry (MALDI-TOF-MS) analysis using Genomic Solutions' ProPic and ProPrep robotic instruments following the manufacturer's protocols. Briefly, gel pieces were incubated with trypsin (20 µg/ml in 25 mM ammonium bicarbonate, pH 8.0; Promega Corp., Madison, WI) at 37 °C for 4 hours. The peptide mixture was purified with an in-tip reversed-phase column (C18 Zip-Tip; Millipore) to remove salts and impurities. MALDI-TOF-MS was performed using an Applied Biosystems Voyager model DE STR (Applied Biosystems, Framingham, MA) for peptide mass fingerprinting. The peptide masses were matched with the theoretical peptide masses of all the proteins from mouse and human species of the Swiss-Prot and National Center for Biotechnology database. Protein identification was performed using a Bayesian algorithm, in which high-probability matches are indicated by an expectation score, an estimate of the number of matches that would be expected in that database if the matches were completely random. As part of our analysis of 2DE gel proteins we discovered that two critical enzymes that regulate the endogenous production of hydrogen sulfide (H_2S), cystathionine β-synthase (CBS) and cystathionine γ-lyase (CSE) are indeed significantly reduced in NPS of infants with more sever RSV infections. This pathway regulates the generation and catabolism of H_2S. For several hundred years, H_2S has been known to exist in animal tissues as a noxious gas. As H_2S is typically formed by commensal bacteria, it was not regarded as physiologically significant. However, recent studies have established that H_2S is indeed a biologically relevant signaling molecule in mammals [reviewed in (6)]. H_2S acts as a messenger molecule, and together with the volatile substances nitric oxide (NO) and carbon monoxide (CO) it is defined as a gasotransmitter, playing physiological roles in a variety of functions such as synaptic transmission, vascular tone, angiogenesis, inflammation and cellular signaling (7). The generation of H_2S is catalysed by cystathionine β-synthase (CBS), cystathionine γ-lyase (CSE) and 3-mercaptopyruvate sulfurtransferase (MST)(**Fig.7**). There are no studies investigating the role of H_2S generation in pathophysiology of viral infections or the use of H_2S donors as pharmacological intervention for viral-induced airway diseases. As part of our

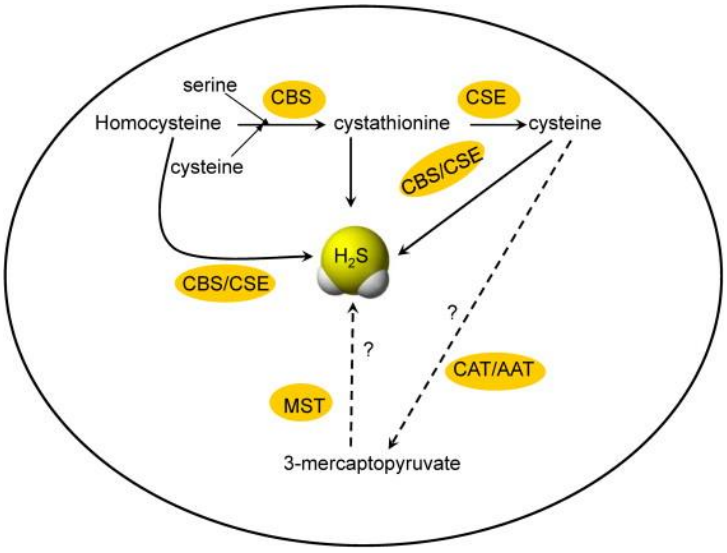

Fig. 7 Metabolic pathways for endogenous produced H_2S. (*adapted from Chen Y, Respir Physiol & Neurobiol, 184;130-134, 2012*). H_2S is produced endogenously in mammals including humans. Two cytoplasmic enzymes, cystathionine-γ-lyase (CSE) and cystathionine-β-synthase (CBS) are responsible for H_2S biogenesis. MST catalyzes the formation of H_2S from 3-mercaptopuruvate, a cysteine metabolite. CAT/AAT is an aminotransferase, which can catalyse the conversion of cysteine to 3-mercaptopuruvate. Whether CAT/AAT and MST actually produce H_2S in the respiratory have been uncertain.

comprehensive studies of protein expression in cells, mice and children supported by this DoD grant we discovered that: 1) RSV infection inhibited expression of the CSE and CBS enzymes, reduced ability to generate cellular H_2S, and increased H_2S degradation; 2) Inhibition of H_2S generation, using propargylglycine (PAG), an inhibitor of CSE, was associated with increased production of virus infectious particles, as well as increased secretion of proinflammatory cytokines; 3) Treatment of both A549 (a lung carcinoma cell line retaining features of type II alveolar epithelial cells) and primary small alveolar epithelial (SAE) cells with GYY4137 (morpholin-4-ium 4 methoxyphenyl(morpholino)phosphinodithioate), a slow-releasing H_2S compound, significantly inhibited viral replication at a step subsequent to viral adsorption. In addition, we found that genetic deficiency of CSE (using CSE -/- mice) resulted in increased airway hyperresponsiveness (AHR) in CSE -/- mice compared to WT controls, following either exposure to cigarette smoke or RSV infection (**Fig. 8**). Moreover, we found that intranasal treatment of BALB/c mice with GYY4137 significantly attenuated disease following RSV infection and similarly to our findings in cells inhibited viral replication in the lung (**Fig. 9, next page).** GYY4137 treatment was also characterized by a blunted viral-induced neutrophilia in BAL and reduced AHR (**Fig. 10, next page**). Overall, our studies have identified a previously unknown function of endogenous H_2S that may play a critical role in the pathogenesis of viral respiratory infections and development of wheezing/asthma.

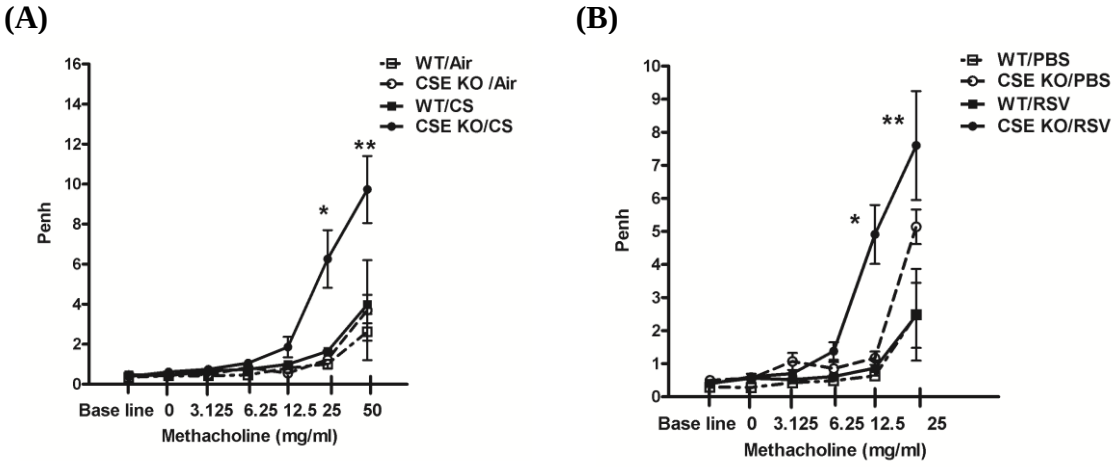

Fig. 8. CSE gene deficiency increases AHR in mice. (A) CSE gene deficiency increases AHR in mice exposed to cigarette smoke. WT and CSE -/- mice were exposed in a chamber to cigarette smoke (CS) of five cigarettes/ day (3R4F research cigarette from University of Kentucky) or air for 4 consecutive days. Unrestrained, whole-body plethysmography (Buxco Electronics, Inc. Sharon, CT) was used to measure the Enhanced Pause (Penh) to evaluate AHR. Baseline and post-methacholine challenge Penh values were determined after cigarette smoke or air exposure. Penh values are presented as mean ± SEM (n = 4 mice/group). * p<0.05 compared with WT/CS; ** p<0.01 compared with WT/CS. **(B)** CSE gene deficiency increases AHR following RSV infection. WT and CSE -/- mice were inoculated with either RSV dose 107 PFU or mock-infected. Baseline and post-methacholine challenge Penh values were determined at day 5 post-infection. Data are means ± SEM (n = 3-4 mice/group). * p<0.005 compared with WT/RSV; ** p<0.05 compared with WT/RSV.

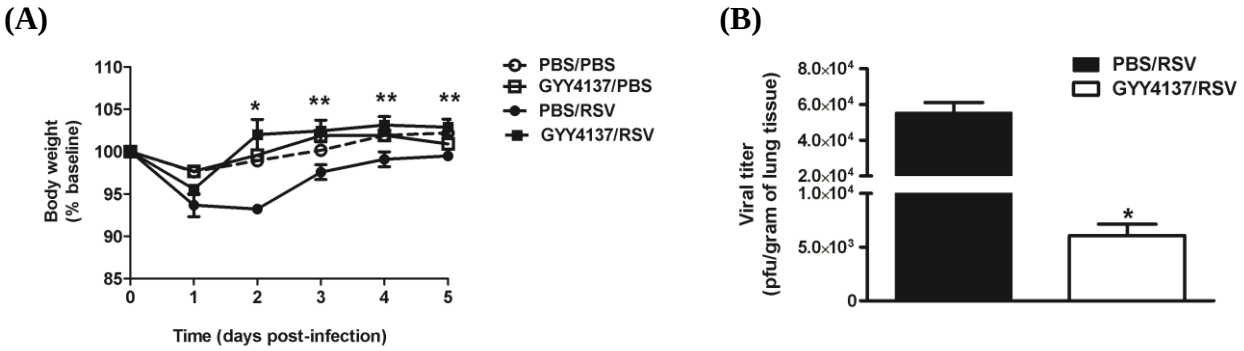

Fig. 9. H_2S donor treatment attenuates RSV-induced clinical disease and viral replication *in vivo*. (A) Disease parameters. Mice were treated i.n. with GYY4137 (50 mg/kg body weight) or an appropriate volume of vehicle (PBS) 1h before, 6h and 20h after infection. Mice were inoculated with RSV dose 10^6 PFU or mock-infected. Data are expressed as mean ± SEM (n = 4 mice/group) and is representative of two independent experiments. *p<0.01 compared with PBS/RSV at day 2 p.i., **p<0.05 compared with PBS/RSV at days 3, 4, and 5 p.i. **(B)** Viral replication in the lungs. At day 5 p.i., lungs were excised and viral replication was determined by plaque assay. The bar graph represents mean ± SEM (n = 4 mice/group).*p<0.01 compared with PBS/RSV group.

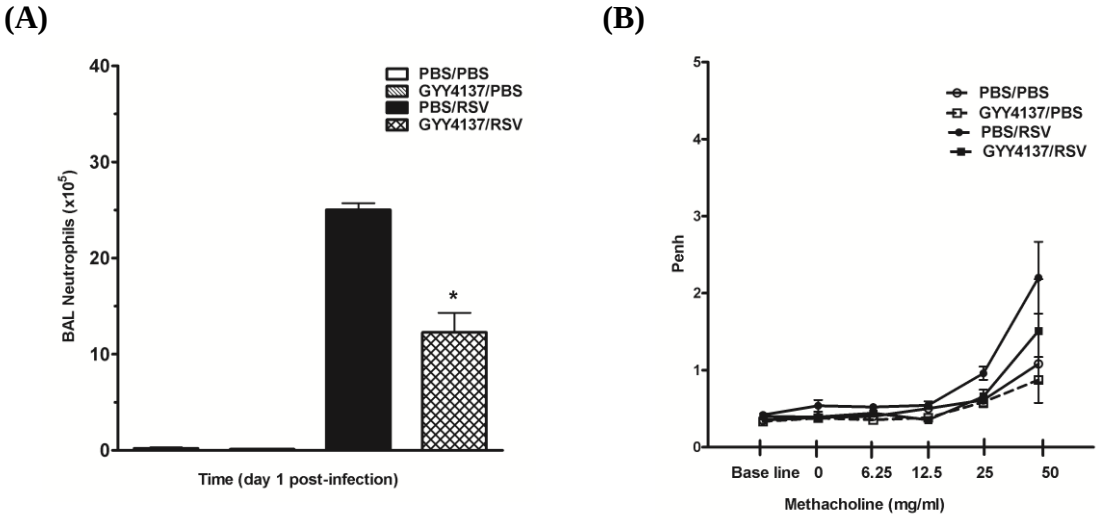

Fig. 10. Effect of H_2S donor on neutrophils populations in BAL and AHR in response to RSV infection. Mice were treated i.n. with GYY4137 (50 mg/kg body weight) or an appropriate volume of vehicle (PBS) 1h before, 6h and 20h after infection. Mice were inoculated with either RSV dose 10^6 PFU or mock-infected. **(A)** Neutrophils cell counts were determined in BAL samples at day 1 post-infection. Cell preparations were stained (Wright-Giemsa) and counted under the microscope (200 cells/slide). The bar graph represents mean ± SEM (n = 4 mice/group).*p<0.001 compared with PBS/RSV group. **(B)** Unrestrained, whole-body plethysmography (Buxco Electronics, Inc. Sharon, CT) was used to measure the Enhanced Pause (Penh) to evaluate AHR. Baseline and post-methacholine challenge Penh values were determined at day 5 post-infection. Penh values are presented as mean ± SEM (n = 4 mice/group).

III. KEY RESEARCH ACCOMPLISHMENTS

- RSV, a major respiratory pathogen which infections predispose to the development of asthma is a potent inducer of oxidative damage in the airways.

- Severe RSV infections are characterized by an overall impairment of the antioxidant defense system, as we have discovered in epithelial cells, and in the lung of experimentally infected mice and naturally infected patients.

- Specifically, we have shown by both protein and mRNA analysis that AOE levels, including SOD1, catalase, GST, GPx, are decreased in BAL fluids of RSV inoculated mice.

- RSV infection induces a progressive reduction in nuclear and total cellular levels of the transcription factor NF-E2-related factor 2 (Nrf2), resulting in decreased binding to endogenous AOE gene promoters and decreased AOE expression.

- RSV induces Nrf2 deacetylation and degradation via the proteasome pathway *in vitro* and *in vivo*. Histone deacetylase and proteasome inhibitors block Nrf2 degradation and increase Nrf2 binding to AOE endogenous promoters, resulting in increased AOE expression.

- Known inducers of Nrf2 are able to increase Nrf2 activation and subsequent AOE expression during RSV infection in vitro and in vivo, with significant amelioration of oxidative stress. This is the first demonstration of the mechanism(s) of virus-induced inhibition of AOE expression.

- In our proteomics studies of NPS obtained from children with RSV infection, we found a significant increase in markers of oxidative injury and a significant decrease in AOE expression, which correlated with the severity of lung disease.

- Our study included a balanced representation of the spectrum of disease that is caused by this pathogen in infancy.

- Thanks to our proteomics studies of BAL in mice and NPS in children, we have discovered a previously unknown antiviral function of the endogenous H_2S pathway. This pathway has a broader anti-viral activity and its upregulation may represent a novel mechanism to control a variety of infections caused by important human pathogens, including RSV, hMPV, influenza, and Ebola virus.

IV. REPORTABLE OUTCOMES (PRODUCTS)

a. Manuscripts, abstracts, presentations:

1. Hosakote YM, Jantzi P, Esham D, Kurosky A, Casola A, Garofalo RP. Viral-mediated inhibition of antioxidant enzymes contributes to the pathogenesis of severe RSV bronchiolitis. Amer J Resp Critic Care Med. 2011; 183(11):1550-60.
2. Hosakote, Y.M., Komaravelli, N., Mautemps, N., Liu, T., Garofalo, R.P., & Casola, A. Antioxidant mimetics modulate oxidative stress and cellular signaling in airway epithelial cells infected with respiratory syncytial virus. Am J Physiol-Lung C 2012; 303:L991-1000.
3. Komaravelli, N, Tian, B., Ivanciuc, T., Mautemps, N., Brasier, A.R., Garofalo, R.P., Casola, A. Respiratory syncytial virus infection downregulates antioxidant enzyme expression by triggering deacetylation-proteasomal degradation of Nrf2. Free Radical Biology and Medicine, Special Issue, 2015. Jun 11. pii: S0891-5849(15)00266-X. doi: 10.1016/j.freeradbiomed.2015.05.043. [Epub ahead of print]
4. Li, H., Ma, Y., Ivanciuc, T., Komaravelli, N., Kelley, J.P., Ciro, C., Szabo, C., Garofalo, R.P., Casola, A. Role of hydrogen sulfide in paramyxovirus infections. Journal of Virology, 2015. 89(10):5557-68.
5. Narayana Komaravelli, Roberto. P. Garofalo, Antonella Casola. NF-κB and NRF2 pathways cross talk during Respiratory Syncitial Virus pathogenesis. At RSV 2012 Symposium, SantaFe, New Mexico, USA on Sep27-30, 2012
6. Narayana Komaravelli, Tianshuang Liu,Tian Bing, Roberto. P. Garofalo, Antonella Casola. RSV Induces Oxidative Stress by Reducing Antioxidant Enzymes via Nrf2 Deprivation. At ASCB 2013 annual meeting – New Orleans, LA, USA on Dec 16, 2013.
7. 9th International respiratory Syncytial Virus Symposium - November 9-13, Cape Town, South Africa. Antiviral pathway of endogenous H2S protects against RSV-induced airway disease MilanoPediatria 2014 - November 20-23, Milano, Italy. Antiviral role of the oxidative system in the lung
8. Narayana Komaravelli1, Bing Tiang, Teodora Ivanciuc, Allan R. Brasier, Roberto P. Garofalo, and Antonella Casola Respiratory Syncytial Virus Infection Downregulates Antioxidant enzyme expression by triggering Nrf2 degradation. At American Society for Biochemistry and Molecular Biology (ASBMB) Annual meeting 2015 – Boston, MA, USA – Mar 30, 2015

b. Informatics such as databases and animal models, etc.:

1. We have generated a Nrf2-KO murine model of RSV infection. C57BL6J $Nrf2$ $+/-$ (strain name B6.129X1-Nfe2l2tm1Ywk/J) mice were purchased from Jackson laboratory. Nrf2-KO mice were generated by mating heterozygous female with homozygous male, and the offspring were genotyped. We are currently backcrossing this mouse to BALB/c.

V. CONCLUSION

In summary, as described in the previous section we have made major progress towards our goal of understanding the key role of the transcription factor Nrf2 in regulating antiviral response in the lung as well as the oxidative injury occurring in viral respiratory infections. RSV infection in cells, mice, and children leads to rapid generation of reactive oxygen species, which are associated with oxidative stress and lung damage, due to a significant decrease in the expression of airway antioxidant enzymes. Oxidative stress plays an important role in the pathogenesis of RSV-induced lung disease, as antioxidants ameliorate clinical disease and inflammation in vivo. We have shown that RSV infection induces a progressive reduction in nuclear and total cellular levels of the transcription factor NF-E2-related factor 2 (Nrf2), resulting in decreased binding to endogenous AOE gene promoters and decreased AOE expression. RSV induces Nrf2 deacetylation and degradation via the proteasome pathway *in vitro* and *in vivo* (2). Histone deacetylase and proteasome inhibitors block Nrf2 degradation and increase Nrf2 binding to AOE endogenous promoters, resulting in increased AOE expression. Known inducers of Nrf2 are able to increase Nrf2 activation and subsequent AOE expression during RSV infection *in vitro* and *in vivo*, with significant amelioration of oxidative stress. This is the first description of the mechanism(s) controlling virus-induced inhibition of AOE expression. RSV-induced inhibition of Nrf2 activation, due to deacetylation and proteasomal degradation, could be targeted for therapeutic intervention aimed to increase airway antioxidant capacity during infection.

In addition our discovery of the role of endogenous H_2S as a potent anti-inflammatory and antiviral gasotransmitter opens further possibilities for the use of H_2S modulating agents in respiratory diseases associated with viral infections. For several hundred years, hydrogen sulfide (H_2S) has been known to exist in animal tissues as a noxious gas. As H_2S is typically formed by commensal bacteria, it was not regarded as physiologically significant. However, recent studies have established that H_2S is indeed a biologically relevant signaling molecule in mammals [reviewed in (26)]. We have shown for the first time that levels of intracellular H_2S modulates cellular responses and viral replication in an *in vitro* model of paramyxovirus infection (7), including RSV. Herein, we provide evidence that H_2S has a protective role in RSV infection *in vivo* as well, by modulating both inflammatory responses and viral replication. Indeed, our study shows that treatment of mice with an H_2S donor reduced RSV peak titer in the lung and ameliorated clinical disease, including AHR. These effects were associated with a reduction in BAL and lung neutrophilia and overall lung pathology in RSV-infected H_2S-treated mice compared to RSV-infected untreated mice. These findings were further supported by the evidence that: 1) RSV infection, similarly to our observations in epithelial cells, causes a time-dependent reduction in the expression of H_2S-generating enzymes CSE and CBS; 2) CSE-deficient mice had increased RSV replication, greater disease and inflammatory mediator production compared to CSE-competent mice; and 3) anti-viral activity and lung function (AHR) could be rescued in CSE-deficient mice by treatment with GYY4137. In humans, CSE expression and activity are developmentally regulated as demonstrated by studies in premature infants, newborns and infants in the first year of life, in which this enzyme has been measured and found to be delayed in maturation (29) (30). These findings are of particular relevance in relation to natural RSV infections, which cause the most severe disease during the first year of life, when the endogenous H_2S tone would likely be reduced or in premature infants with smaller airways.

VI. REFERENCES

1. Kolli D, Gupta MR, Sbrana E, Velayutham TS, Hong C, Casola A, Garofalo RP. Alveolar Macrophages Contribute to the Pathogenesis of HMPV Infection While Protecting Against RSV Infection. *Am J Respir Cell Mol Biol* 2014.
2. Komaravelli N, Tian B, Ivanciuc T, Mautemps N, Brasier AR, Garofalo RP, Casola A. Respiratory Syncytial Virus Infection Down-Regulates Antioxidant Enzyme Expression by Triggering Deacetylation-Proteasomal Degradation of NRF2. *Free Radic Biol Med* 2015.
3. Castro SM, Guerrero-Plata A, Suarez-Real G, Adegboyega PA, Colasurdo GN, Khan AM, Garofalo RP, Casola A. Antioxidant Treatment Ameliorates Respiratory Syncytial Virus-Induced Disease and Lung Inflammation. *Am J Respir Crit Care Med* 2006;174:1361-1369.
4. Hosakote YM, Komaravelli N, Mautemps N, Liu T, Garofalo RP, Casola A. Antioxidant Mimetics Modulate Oxidative Stress and Cellular Signaling in Airway Epithelial Cells Infected With Respiratory Syncytial Virus. *Am J Physiol Lung Cell Mol Physiol* 2012;303:L991-1000.
5. Anderson RD, Haskell RE, Xia H, Roessler BJ, Davidson BL. A Simple Method for the Rapid Generation of Recombinant Adenovirus Vectors. *Gene Ther* 2000;7:1034-1038.
6. Paul BD, Snyder SH. H(2)S Signalling Through Protein Sulfhydration and Beyond. *Nat Rev Mol Cell Biol* 2012;13:499-507.
7. Chen Y, Wang R. The Message in the Air: Hydrogen Sulfide Metabolism in Chronic Respiratory Diseases. *Respiratory Physiology & Neurobiology* 2012;184:130-138.

VII.APPENDIX

1. Hosakote YM, Jantzi P, Esham D, Kurosky A, Casola A, Garofalo RP. Viral-mediated inhibition of antioxidant enzymes contributes to the pathogenesis of severe RSV bronchiolitis. Amer J Resp Critic Care Med. 2011; 183(11):1550-60.
2. Hosakote, Y.M., Komaravelli, N., Mautemps, N., Liu, T., Garofalo, R.P., & Casola, A. Antioxidant mimetics modulate oxidative stress and cellular signaling in airway epithelial cells infected with respiratory syncytial virus. Am J Physiol-Lung C 2012; 303:L991-1000.
3. Komaravelli, N, Tian, B., Ivanciuc, T., Mautemps, N., Brasier, A.R., Garofalo, R.P., Casola, A. Respiratory syncytial virus infection downregulates antioxidant enzyme expression by triggering deacetylation-proteasomal degradation of Nrf2. Free Radical Biology and Medicine, Special Issue, Volume 88, Part B, 2015; 391-403.
4. Li, H., Ma, Y., Ivanciuc, T., Komaravelli, N., Kelley, J.P., Ciro, C., Szabo, C., Garofalo, R.P., Casola, A. Role of hydrogen sulfide in paramyxovirus infections. Journal of Virology, 2015. 89(10):5557-68.
5. Ivanciuc, T., Sbrana, E., Ansar, M., Bazhanov, N., Szabo, C., Casola, A., Garofalo, R.P. Hydrogen Sulfide: Antiviral and anti-inflammatory endogenous gastotransmitter in the airways role in respiratory syncytial virus infection. Am J Resp Cell and Mol Biol. 2016; accepted.

Viral-mediated Inhibition of Antioxidant Enzymes Contributes to the Pathogenesis of Severe Respiratory Syncytial Virus Bronchiolitis

Yashoda M. Hosakote[1], Paul D. Jantzi[1], Dana L. Esham[1], Heidi Spratt[2,3], Alexander Kurosky[3,4], Antonella Casola[1,3,5], and Roberto P. Garofalo[1,3,5]

[1]Department of Pediatrics, [2]Department of Preventive Medicine and Community Health, [3]Sealy Center for Molecular Medicine, [4]Department of Biochemistry and Molecular Biology, and [5]Department of Microbiology and Immunology, The University of Texas Medical Branch at Galveston, Galveston, Texas

Rationale: **Respiratory syncytial virus (RSV) is a major cause of lower respiratory tract infections in children, for which no specific treatment or vaccine is currently available. We have previously shown that RSV induces reactive oxygen species in cultured cells and oxidative injury in the lungs of experimentally infected mice. The mechanism(s) of RSV-induced oxidative stress *in vivo* is not known.**

Objectives: **To measure changes of lung antioxidant enzymes expression/activity and activation of NF-E2-related factor 2 (Nrf2), a transcription factor that regulates detoxifying and antioxidant enzyme gene expression, in mice and in infants with naturally acquired RSV infection.**

Methods: **Superoxide dismutase 1 (SOD 1), SOD 2, SOD 3, catalase, glutathione peroxidase, and glutathione S-transferase, as well as Nrf2 expression, were measured in murine bronchoalveolar lavage, cell extracts of conductive airways, and/or in human nasopharyngeal secretions by Western blot and two-dimensional gel electrophoresis. Antioxidant enzyme activity and markers of oxidative cell injury were measured in either murine bronchoalveolar lavage or nasopharyngeal secretions by colorimetric/immunoassays.**

Measurements and Main Results: **RSV infection induced a significant decrease in the expression and/or activity of SOD, catalase, glutathione S-transferase, and glutathione peroxidase in murine lungs and in the airways of children with severe bronchiolitis. Markers of oxidative damage correlated with severity of clinical illness in RSV-infected infants. Nrf2 expression was also significantly reduced in the lungs of viral-infected mice.**

Conclusions: **RSV infection induces significant down-regulation of the airway antioxidant system *in vivo*, likely resulting in lung oxidative damage. Modulation of oxidative stress may pave the way toward important advances in the therapeutic approach of RSV-induced acute lung disease.**

Keywords: respiratory syncytial virus; airways; antioxidant enzymes; oxidative stress

AT A GLANCE COMMENTARY

Scientific Knowledge on the Subject

Although respiratory viruses, such as respiratory syncytial virus (RSV), induce reactive oxygen species production and oxidative stress responses in cultured cells and experimental infections, the mechanisms of such oxidative injury and their role in the pathogenesis of natural infections in humans are not known.

What This Study Adds to the Field

This study suggests that RSV infections cause inhibition of lung antioxidant enzymes involved in maintaining the oxidant–antioxidant cellular balance. In children with naturally acquired RSV infections, such an event is associated with the presence of biomarkers of oxidative injury and with greater severity of clinical illness.

Respiratory syncytial virus (RSV) is one of the most important causes of upper and lower respiratory tract infections in infants and young children. A recent metaanalysis has estimated that in 2005, 33.8 million new episodes of RSV-associated lower respiratory tract infections occurred worldwide in children younger than 5 years of age, with at least 3.4 million episodes representing severe RSV-associated infections necessitating hospital admission and up to 199,000 fatal cases (1). In the United States the number of children hospitalized each year with viral lower respiratory tract infections has recently been estimated at more than 200,000, with 500 deaths occurring per year in children under 5 years of age (2). The mechanisms of RSV-induced airway disease and associated long-term consequences remain incompletely defined, although lung inflammatory response is believed to play a central pathogenetic role. Reactive oxygen species (ROS) are important regulators of cellular signaling (3, 4), and oxidative stress has been implicated in the pathogenesis of acute and chronic lung inflammatory diseases, such as asthma, cystic fibrosis, and chronic obstructive pulmonary disease (COPD) (5–7). We have previously shown that RSV infection of airway epithelial cells induces ROS production, which is involved in transcription factor activation and chemokine gene expression (8, 9). We have also shown that RSV induces oxidative stress in the lung in a mouse model of experimental RSV infection, and that antioxidant treatment significantly ameliorates RSV-induced clinical disease and pulmonary inflammation (10). In addition, we found that RSV infection of airway epithelial cells results in a significant decrease of antioxidant enzyme (AOE) expression, as well as in increased levels of markers of oxidative stress, indicating an imbalance between ROS production and antioxidant cellular defenses (11). The molecular mechanism(s) responsible for RSV-induced oxidative damage in the airways *in vivo* is not known.

In this study, we found that expression of superoxide dismutase (SOD) 1 and 2, catalase, glutathione peroxidase (GPx), and glutathione S-transferase (GST) was significantly reduced

(*Received in original form October 29, 2010; accepted in final form March 4, 2011*)

Supported by National Institutes of Health grants AI062885, AI30039, HV28184, UL1RR029876, by Department of Defense W81XWH1010146, and by Flight Attendant Medical Research Institute (FAMRI) Clinical Innovator Awards 072147 (A.C.) and 42253 (R.P.G.). P.D.J. and D.L.E. were supported by Postdoctoral Fellowships from the National Institute of Environmental Health Sciences (T32–07254).

Correspondence and requests for reprints should be addressed to Antonella Casola, M.D., Department of Pediatrics, 301 University Boulevard, Galveston, TX 77555-0366. E-mail: ancasola@utmb.edu

This article has an online supplement, which is accessible from this issue's table of contents at www.atsjournals.org

Am J Respir Crit Care Med Vol 183. pp 1550–1560, 2011
Originally Published in Press as DOI: 10.1164/rccm.201010-1755OC on March 4, 2011
Internet address: www.atsjournals.org

in the bronchoalveolar lavage (BAL) of mice infected with RSV. Similarly, enzymatic assays showed that total SOD, catalase, GPx, and GST activities were decreased in the lungs of infected animals. Indeed, proteomic analysis of murine BALs found that the decrease in AOE expression involved a large number of the enzymes involved in maintaining cellular oxidant–antioxidant balance. Lungs of mice infected with RSV showed a significant decrease in nuclear expression of Nrf2, a protein belonging to the cap-n-collar (CNC) family of transcription factors, which coordinates gene transcription of antioxidant and phase 2 metabolizing enzymes in response to oxidative stress (12). In nasopharyngeal secretions (NPS) of children with naturally acquired RSV infection, there was a significant increase in markers of oxidative injury and a significant decrease in AOE expression, which correlated with the severity of clinical illness. Our findings suggest that RSV-induced oxidative damage *in vivo* is the result of an imbalance between ROS production and airway antioxidant defenses. Modulation of oxidative stress represents a potential novel pharmacological approach to ameliorate RSV-induced acute lung inflammation and its long-term consequences. Some of the results of these studies have been previously reported in the form of an abstract (13).

METHODS

RSV Preparation

RSV A2 strain was grown in HEp-2 cells and purified by centrifugation on discontinuous sucrose gradients as described elsewhere (14). Titer of the purified RSV pools was 8 to 9 $\log_{10}$ plaque-forming units (PFU)/ml using a methylcellulose plaque assay. No contaminating cytokines were found in these sucrose-purified viral preparations (15). The human metapneumovirus (hMPV) strain CAN97-83 was propagated and titrated in LLC-MK2 cells and sucrose-gradient purified as previously described (16). Virus pools were aliquoted, quick-frozen on dry ice/alcohol, and stored at −80°C until used. Virus pools were endotoxin free by routine tests using the limulus hemocyanin agglutination assay.

Experimental Infection Protocol and Sample Collection

Female, 6- to 8-week-old BALB/c mice were purchased from Harlan (Houston, TX) and maintained in pathogen-free conditions at the animal research facility of the University of Texas Medical Branch (UTMB), Galveston, Texas. Mice were used under an experimental protocol approved by the UTMB Institutional Animal Care and Use Committee. Before inoculation with RSV, mice were lightly anesthetized by intraperitoneal administration of ketamine and xylazine. Mice were infected intranasally with 50 μl of RSV diluted in phosphate-buffered saline (PBS; 10^7 PFU) or sham inoculated using the same volume of control buffer. For hMPV infection, mice were infected intranasally with 50 μl of hMPV (10^7 PFU). Groups of mice were killed at various intervals after infection and BAL was collected by flushing the lungs twice with ice-cold sterile PBS (1 ml) as described (10). BAL fluid was centrifuged at 10,000 × *g* for 2 minutes at 4°C and stored at −80°C until further analysis. Lungs were removed, quickly frozen in liquid nitrogen, and stored at −80°C until further processing.

RSV-Infected Children and Collection of Nasopharyngeal Secretion Samples

Sample of NPS were collected at UTMB from infants and children who were enrolled in an ongoing study on the pathogenesis of viral bronchiolitis. The study protocol and consent forms have been approved by the UTMB Institutional Review Board. The study population comprised groups of infants and children younger than 12 months old recruited from the UTMB Emergency Department, the pediatrics outpatient clinics, or inpatient areas of Children's Hospital. These subjects were assigned a diagnosis of upper respiratory tract infection (URTI) alone (absence of crackles or wheezing on auscultation of the chest, oxygen saturation ⩾ 97% on room air, and normal chest radiograph when obtained), "nonhypoxic bronchiolitis" (defined for the purposes of this study as wheezing on auscultation with oxygen saturation > 95% on room air), or "hypoxic bronchiolitis" (wheezing on auscultation and oxygen saturation ⩽ 95% on room air or, in the absence of wheezing, hyperinflation on chest radiograph and oxygen saturation ⩽ 95% on room air). Hypoxia was assessed at the time that secretion samples were obtained, with subjects breathing ambient air without oxygen supplementation. Subjects with recurrent wheezing were not included, nor were those with history of chronic lung disease or congenital heart disease. Three infants who were intubated (VS, ventilatory support) because of acute respiratory failure caused by RSV infection were also included in the study. RSV infection was confirmed in all subjects by detection of viral antigen in NPS samples by antigen detection. All samples were obtained within the first 5 days of respiratory illness and within 24 hours after the onset of wheezing. Samples of NPS were obtained by passing size 5F feeding tubes into the nasopharynx and applying gentle suction. Secretions then were rinsed into collecting traps with 3 ml of PBS. After centrifugation to precipitate cells, samples were digested with sputolysin (Calbiochem, San Diego, CA), a mucolytic agent in 6.5 mM dithiothreitol in 100 mM phosphate buffer, pH 7.01, and stored at −80°C for subsequent protein and biomarker analysis.

Extraction of Mouse Lung Nuclear and Epithelial Proteins

Lung nuclear proteins were prepared as previously described (17, 18). Briefly, mouse lung tissue was homogenized in 5 ml ice-cold Buffer A (10 mM 2-hydroxyethyl-piperazine N′-2-ethanesulfonic acid [HEPES]–KOH, pH 7.9, 1.5 mM $MgCl_2$, 10 mM KCl, 0.5 mM dithiothreitol [DTT], 0.2 mM phemylmethyl sulfonyl fluoride [PMSF], 0.6% nonident P40 [NP-40]) and centrifuged at 350 × *g*, 4°C for 30 seconds. The supernatant was kept on ice for 5 minutes and centrifuged for 5 minutes at 6,000 × *g* at 4°C, and the pellet was resuspended in 200 μl Buffer B (10 mM HEPES–KOH, pH 7.9, 1.5 mM $MgCl_2$, 10 mM KCl, 1.2 M sucrose, 0.5 mM DTT, 0.2 mM PMSF). After centrifugation (13,000 × *g*, 4°C, 30 min), the pellet was resuspended in 100 μl Buffer C (20 mM HEPES–KOH, pH 7.9, 1.5 mM $MgCl_2$, 420 mM NaCl, 0.2 mM ethylenediamine-tetraacetic acid, 0.5 mM DTT, 0.2 mM PMSF, 2 mM benzamidine, 5 μg/ml leupeptin, 25% glycerol), incubated on ice for 20 minutes, and centrifuged (6,000 × *g*, 4°C, 2 min).

A lysis-lavage method described by Wheelock and colleagues was used to isolate epithelial cell proteins of conductive airways (19). Briefly, mice were killed and trachea was exposed and cannulated, lungs were then removed from the thorax and inflated with 0.5 ml agarose solution (0.75% low-melting agarose, 5% dextrose) immediately followed by 0.5 ml dextrose solution (1% dextrose, 2% protease inhibitor cocktail) through a three-way valve. Both solutions were preheated at 37°C. The inflated lungs were incubated in 5% dextrose for 15 minutes at room temperature. Dextrose solution was then removed by repeated steps of inversion of the lungs and gentle suction with a syringe. The airways were then lavaged with 0.5 ml of lysis buffer (2 M thiourea, 7 M urea, 4% 3-((3-cholamidopropyl)dimethylammonio)-1-propanesulfonic acid, 0.5% Triton X 100, 1% DTT, and protease inhibitors). The lysis buffer containing the proteins was immediately recovered, flash frozen on dry ice and stored at −80°C until further use.

Two-Dimensional Gel Electrophoresis and Gel Imaging

Mouse BAL fluids and sputolysin-digested human NPS samples were lyophilized and reconstituted in 100 μl of reagent 1 procured from Bio-Rad (Hercules, CA; 50 mM Tris buffer), desalted using protein desalting columns from Pierce (Rockford, IL) (7,000 MW cutoff), followed by albumin depletion by a Montage albumin depletion kit. Then 200 μl of 1 mg/ml protein aliquots were isoelectrofocused (IEF) on 11 cm–long nonlinear precast immobilized pH gradient (IPG) strips (pH 3–10; Bio-Rad) using the IPGPhor isoelectrofocusing system. Protein samples were loaded onto an IPG strip and rehydrated overnight. IEF was performed at 20°C with the following parameters: 50 V for 11 hours, 250 V for 1 hour, 500 V for 1 hour, 1,000 V for 1 hour, 8,000 V for 2 hours, and 8,000 V for 6 hours, with a total of 48,000 V. After IEF, the IPG strips were stored at −80°C until two-dimensional sodium dodecyl sulfate polyacrylamide gel electrophoresis (SDS-PAGE) was performed. For the two-dimensional SDS-PAGE, the IPG strips were incubated in 4 ml of equilibration buffer (6 M urea, 2% SDS, 50 mM Tris-HCl [pH 8.8], 20% glycerol) containing 10 μl of 0.5 M TCEP [Tris(2-carboxyethyl) phosphine] for 15 minutes at 22°C with shaking.

The strips were then incubated in another 4 ml of equilibration buffer with 25 mg of iodoacetamide/ml for 15 minutes at 22°C with shaking. Electrophoresis was performed at 150 V for 2.25 hours at 4°C with 8 to 16% precast polyacrylamide gels in Tris-glycine buffer (25 mM Tris-HCl, 192 mM glycine, 0.1% SDS [pH 8.3]). After two-dimensional gel electrophoresis (2DE), the gels were fixed (10% methanol [MeOH], 7% acetic acid in double-distilled water), stained with SYPRO Ruby (Bio-Rad), and destained (10% ethanol in double-distilled water).

The destained gels were scanned at a 100-μm resolution using the Perkin-Elmer (Boston, MA) ProXPRESS ProFinder Proteomic Imaging System with 480-nm excitation and 620-nm emission filters. The exposure time was adjusted to achieve a value of approximately 55,000- to 63,000-pixel intensity on the most intense protein spots on the gel. The 2DE gel images were subsequently analyzed using Progenesis Discovery software version 2006.03 (Nonlinear Dynamics, Ltd., Newcastle Upon Tyne, UK). An average gel was created from gels run on BAL proteins from three separate samples from mock-infected mice (control) and three separate samples from RSV-infected mice (24 hours). For human samples, an average gel was created from gels run on NPS proteins from infants with URTI, nonhypoxic bronchiolitis, bronchiolitis with hypoxia, and patients on VS. The software automatically selected one of the six gels for mice experiment and one of the four gels for human NPS as the base image of the reference gel. The gel with the highest number of spots was set as the reference gel. Unmatched spots present in five of the six other gels were subsequently added to the reference gel image by the software to give a comprehensive reference gel. Subsequent to automatic spot detection, spot filtering was also manually performed. The matching of spots between the gels was manually reviewed and adjusted as necessary. Moreover, the log-transformed spot volumes were normally distributed, indicating that nonparametric statistical comparisons, such as *t* tests, could be applied to identify those proteins whose expression was significantly changed by infection. The spot volumes were normalized based on the total spot volume for each gel, and the control and RSV-infected samples were compared.

Protein Gel Spot Identification

Protein gel spots were excised and prepared for matrix-assisted laser desorption ionization-time of flight mass spectrometry (MALDI-TOF-MS) analysis using Genomic Solutions' ProPic and ProPrep robotic instruments following the manufacturer's protocols. Briefly, gel pieces were incubated with trypsin (20 μg/ml in 25 mM ammonium bicarbonate, pH 8.0; Promega Corp., Madison, WI) at 37°C for 4 hours. The peptide mixture was purified with an in-tip reversed-phase column (C18 Zip-Tip; Millipore) to remove salts and impurities (20). MALDI-TOF-MS was performed using an Applied Biosystems Voyager model DE STR (Applied Biosystems, Framingham, MA) for peptide mass fingerprinting. The peptide masses were matched with the theoretical peptide masses of all the proteins from mouse and human species of the Swiss-Prot and National Center for Biotechnology database. Protein identification was performed using a Bayesian algorithm, in which high-probability matches are indicated by an expectation score, an estimate of the number of matches that would be expected in that database if the matches were completely random (21).

Western Blot Analysis

Equal amount of proteins (10–20 μg, depending on the antibody used) from mouse BAL, conductive airway epithelial cells or human NPS were loaded and separated by SDS-PAGE, and transferred onto Hybond-polyvinylidene difluoride membrane (Amersham Pharmacia Biotech, Piscataway, NJ). Nonspecific binding was blocked by immersing the membrane in Tris-buffered saline-Tween (TBST) blocking solution (10 mM Tris-HCl, pH 7.6, 150 mM NaCl, 0.05% Tween-20 [v/v]) containing 5% skim milk powder for 30 minutes. After a short wash in TBST, the membranes were incubated with the primary antibody overnight at 4°C, followed by the appropriate secondary antibody (Santa Cruz Biotechnology, Santa Cruz, CA), diluted 1:5–10,000 in TBST for 1 hour at room temperature. After washing, the proteins were detected using enhanced-chemiluminescence assay (Amersham Biosciences, Piscataway, NJ) according to the manufacturer's recommendations. The primary antibodies used for Western blots were anti-SOD 1, 2, and 3 rabbit polyclonal antibodies (Stressgen Bioreagents, Ann Arbor, MI), anti-catalase rabbit polyclonal antibody, and anti-lamin B mouse monoclonal antibody (Calbiochem), anti-Nrf2 (C20) rabbit polyclonal (Santa Cruz Biotechnology), and anti–β-actin mouse monoclonal antibody from Sigma-Aldrich (Saint Louis, MO). The anti-GST rabbit polyclonal antibody was a generous gift from Dr. Yogesh Awasthi, University of North Texas Health Science Center.

Biochemical Assays for Antioxidant Activities

Catalase, GST, GPx, and SOD activities were determined in BAL fluids using specific biochemical assays (Cayman Chemical, Ann Arbor, MI; Catalog No. 707002, 703302, 703102, and 706002, respectively, for catalase, GST, GPx, and SOD), according to the manufacturer's instructions. The quantification of catalase activity in BAL was based on the reaction of the enzyme with methanol in the presence of an optimal concentration of H_2O_2. The formaldehyde produced is measured spectrophotometrically with 4-amino-3-hydrazino-5-mercapto-124-triazole as the chromogen. The catalase activity was expressed as nmol/min/mg of protein in the sample. The total GST activity was quantified by measuring the conjugation of 1-chloro-2,4-dinitrobenzene with reduced glutathione. The conjugation is accompanied by an increase in absorbance at 340 nm. The rate of increase is directly proportional to the GST activity in the sample. The GST activity was expressed as nmol/min/mg of protein in the sample. The GPx activity was determined spectrophotometrically in BAL through an indirect coupled reaction with glutathione reductase. Oxidized glutathione, produced on reduction of hydroperoxide by GPx, is recycled to its reduced state by glutathione reductase and NADP reduced. The oxidation of NADP reduced to $NADP^+$ is accompanied by a decrease in absorbance at 340 nm. Under conditions in which the GPx activity is rate limiting, the rate of decrease in the A_{340} is directly proportional to the GPx activity in the sample. SOD activity was determined by using tetrazolium salt for the detection of superoxide radicals generated by xanthine oxidase and hypoxanthine. One unit of SOD is defined as the amount of enzyme needed to exhibit 50% dismutation of the superoxide radical.

Measurement of Lipid Peroxidation Products

Measurement of F_2 8-isoprostane in human NPS was performed using a competitive enzyme immunoassay from Cayman Chemical Co. according to manufacturer's instructions. Measurement of malondialdehyde (MDA) was performed using a spectrophotometric assay (Oxis Research, Burlingame, CA).

Statistical Analysis

All results are expressed as mean ± SEM. Data were analyzed using the GraphPad Instat Biostatistics 3.0 software. Student *t* test using a 95% confidence level was used to determine the level of differences in RSV-infected versus sham-inoculated mice. Differences between RSV illness groups were assessed by use of ANOVA.

RESULTS

Expression of AOE in the Lung Is Decreased by RSV Infection

ROS generation due to the respiratory burst of activated phagocytic cells recruited to the airways during viral infections is an important antiviral defense. However, a robust production of ROS can lead to depletion of antioxidants and cause oxidative stress. In previous studies, we have shown that RSV infection causes significant oxidative stress damage as demonstrated by the increase of the lipid peroxidation markers F_2 8-isoprostane, MDA, and 4-hydroxynonenal in cultured airway epithelial cells and in the lung of experimentally infected mice (8, 10). More recently, we have demonstrated a significant reduction in the expression of several antioxidant enzymes, such as SOD 1, SOD 3, catalase, and GST, in airway epithelial cells as a result of RSV infection, suggesting that oxidative stress could be the result of imbalance between ROS production and antioxidant cellular defenses (11). To determine whether RSV infection results in decreased expression of antioxidant proteins *in vivo*, similar to our observation in cultured cells, groups of BALB/c mice were infected intranasally with RSV or sham-inoculated. BAL was

collected at Days 1, 3, 5, and 9 after infection to assess levels of catalase, GST-mu, and SOD 1, 2, and 3 by Western blot. As shown in Figure 1 and by densitometric analysis in Figure E1 in the online supplement, RSV-infected mice showed a significant reduction in the expression levels of most of the tested enzymes at Days 1 and/or 3 after infection compared with control animals. SOD 3 was decreased at Days 3 and 5 after infection in most but not all of the RSV-infected animals and therefore did not reach statistical significance. Overall, levels of AOE in RSV-infected mice returned to control levels by Day 9 after infection, with the exception of SOD 2, whose expression normalized earlier (Day 5 after infection). A similar reduction in AOE expression in the lung was also observed in mice infected with hMPV, a paramyxovirus that causes a significant proportion of lower respiratory tract infections in young infants and children (22) (Figure E4).

To determine whether levels of AOE detected in the BAL reflected changes in the AOE in airway epithelium, a major target of RSV infection, we performed Western blot analysis of SOD 1, 2, and 3 in proteins isolated from airway epithelial cells of infected mice. We found a significant decrease of SOD 1 and 3 in epithelial proteins of RSV-infected mice compared with epithelial proteins from control mice (Figure 2). On the other hand, SOD 2 levels were similar in epithelial proteins of RSV-infected and control mice, suggesting that the reduction of such enzymes observed in Western blots of infected BAL samples may reflect a nonepithelial source/cell target of such enzymes after RSV infection (*see* DISCUSSION).

RSV Infection Decreases Lung AOE Activities

To determine whether changes in AOE protein expression resulted in changes in their activities in response to RSV infection, BAL was collected from groups of RSV-infected or sham-inoculated mice at Days 1, 3, 5, and 9 after infection, and total SOD, catalase, GST, and GPx enzymatic activity were assessed by biochemical assays. There was a significant reduction of all AOE activities in RSV-infected mice compared with control animals (Figure 3). In particular, in RSV-infected mice, total SOD and GPx activities decreased significantly at Days 1 (86 and 59%, respectively) and 3 (52 and 46%, respectively), compared with sham-inoculated mice, with levels returning to those in control mice by Day 9. In addition, catalase and GST activities were significantly lower in RSV-infected mice compared with control mice at all tested time points, but different from our findings with SOD and GPx, they did not return to control levels by Day 9 (76, 63, 37, and 50% reduction for catalase and 75, 59, 50, and 48% reduction for GST at Days 1, 3, 5, and 9 after infection). Overall, these results indicate that RSV significantly reduces antioxidant defenses of the airways.

Global Proteomic Analysis of AOE Expression in BAL

In recent years, proteomic analysis has advanced our knowledge of BAL proteins and their degradation products present at the alveolar level. These proteins may be plasma derived or locally produced and are released under normal or pathological conditions by inflammatory, immune, and tissue-resident cells (23). Thus, with the intent to gain a more global insight into the lung antioxidant response in the course of a viral infection, we investigated differential protein expression in BAL of RSV-infected mice compared with control uninfected animals by 2DE. Comparison of SYPRO Ruby-stained 2DE gels of RSV-infected and uninfected BAL proteins showed significant changes in the protein spot profile, as shown in the master gel images of 2DE BAL proteins from control (Figure 4A) and RSV-infected mice (Figure 4B) at Day 3 after infection. Overall, more than 1,300 protein spots with pH range 3 to 10 and relative molecular masses range of 10 to 250 kD were detected on our 2DE. BAL protein spots found to be significantly different in expression level between RSV-infected and control mice (either increased or decreased) were excised from the gels, trypsinized, and analyzed

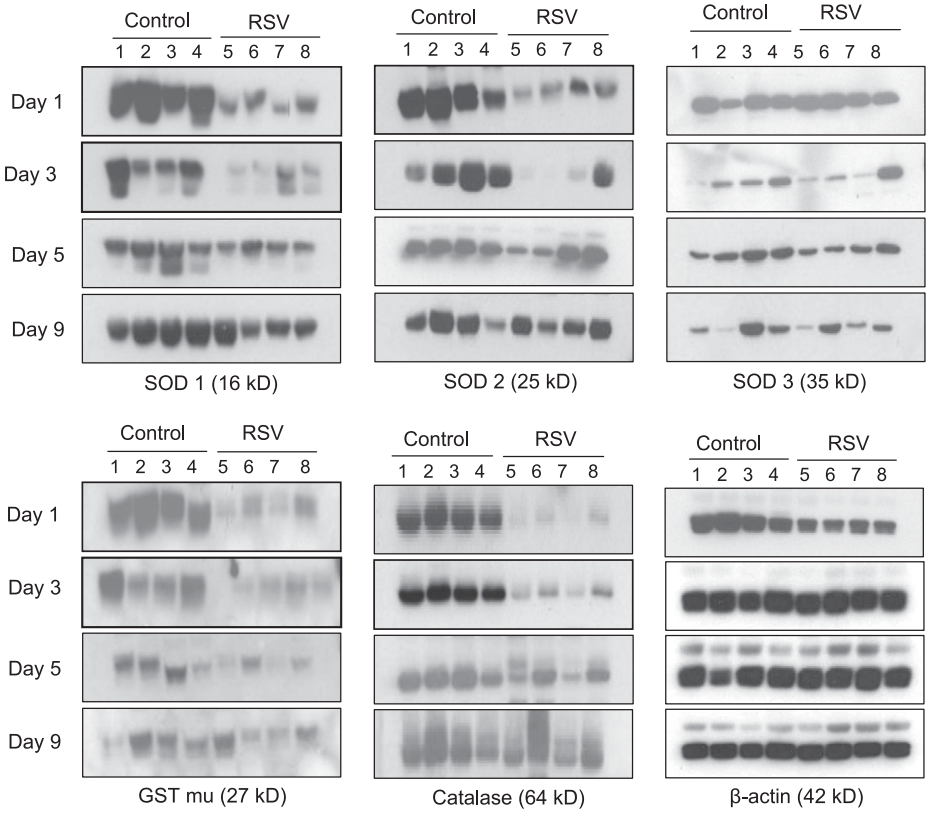

Figure 1. Antioxidant enzymes are reduced in bronchoalveolar lavage (BAL) of respiratory syncytial virus (RSV)-infected mice. Groups of mice were infected with RSV or sham inoculated with saline (Control) and BAL was collected at Days 1, 3, 5, and 9. BAL proteins were resolved on 10% sodium dodecyl sulfate–polyacrylamide gel electrophoresis and Western blots were performed using antibodies against superoxide dismutase (SOD) 1, SOD 2, SOD 3, catalase, and glutathione S-transferase (GST)-mu. Membranes were stripped and reprobed for β-actin as an internal control for protein integrity and loading. Lanes 1 to 4 are BAL from four control and 5 to 8 from four RSV-infected mice at each time point. Densitometric analysis of Western blot band intensities is presented in Figure E1. The figure is representative of three independent experiments, each experiment with four mice per group at each time point.

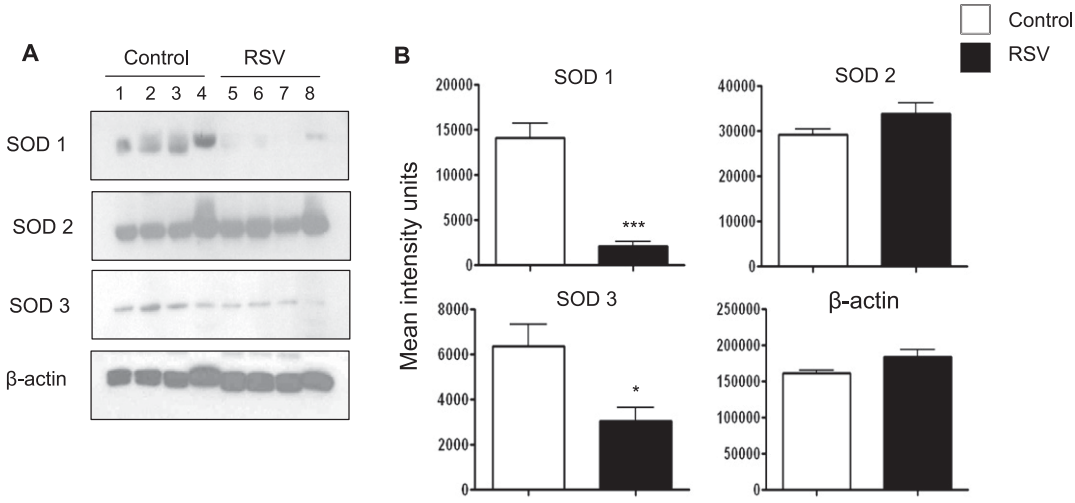

Figure 2. Superoxide dismutase (SOD) 1, SOD 2, and SOD 3 in conductive airway epithelial cells. (*A*) Proteins of conductive airway epithelial cells were obtained by lysis-lavage from respiratory syncytial virus (RSV)-infected or control mice (Day 1 after infection). Proteins were analyzed by Western blot for content of SOD 1, SOD 2, and SOD 3 as in Figure 1. (*B*) Densitometric analysis of Western blot band intensities was performed using Alpha Ease software, version 2200 (2.2d) (Alpha Innotech Co., San Leandro, CA). Bands in RSV-infected samples were normalized to uninfected control sample background and are presented as mean ± SEM of n = 4. *$P < 0.05$; ***$P < 0.001$ relative to control mice.0x(105)

by MALDI-TOF-MS. Among the spots that we were able to identify with high probability score there were several antioxidant enzymes that were decreased in the BAL of RSV-infected mice compared with control mice. We found reduced expression of several other AOE, including peroxiredoxin enzymes (listed with their corresponding spot number in Figure 4C), in addition to catalase, SOD 1, GPx 1, and GST-mu (whose change in expression is better shown in Figure E2). Table 1 summarizes all antioxidant proteins whose expression in BAL changed during the course of RSV infection. Most of the AOE levels were significantly reduced as early as Day 1 (with the exception of peroxiredoxin 2), and they were significantly lower throughout the acute phase of RSV infection, compared with control mice, to return to basal or slightly above basal levels by Day 25 after infection. Thioredoxin 1 was the only AOE substantially unchanged in infected mice compared with control mice. These results confirm and extend our findings by Western blots, indicating that RSV significantly diminishes antioxidant defenses in the lung.

RSV Infection Modifies the Expression of Transcription Factor Nrf2 in Mouse Lung Nuclear Extracts

Recent findings have demonstrated that Nrf2 is a crucial transcription factor that binds to antioxidant responsive element (ARE) sequences and regulates the expression of antioxidant and phase 2 metabolizing enzymes in response to oxidative stress (12) (24, 25). To examine the effect of RSV infection on Nrf2 activation, we performed Western blot analysis of mouse lung nuclear extracts. Groups of BALB/c mice were infected with RSV or sham inoculated, and nuclear extracts were obtained from lungs at 12, 24, 48, and 72 hours after infection. There was a significant decrease of Nrf2 nuclear abundance in

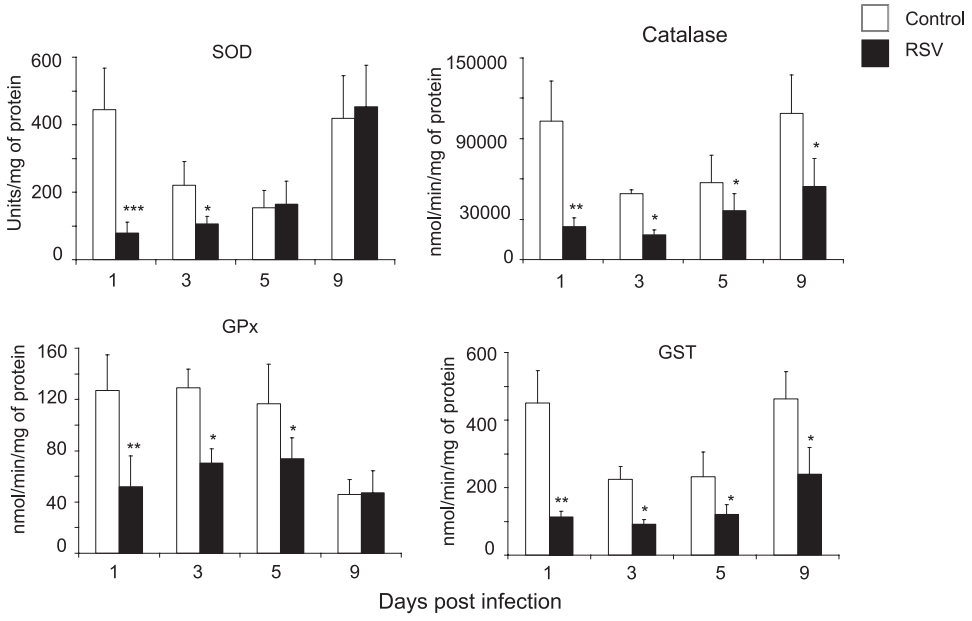

Figure 3. Respiratory syncytial virus (RSV) infection inhibits antioxidant enzyme activity in the lung. Specific biochemical assays were used to determine total superoxide dismutase (SOD), catalase, glutathione peroxidase (GPx), and glutathione S-transferase (GST) activity in bronchoalveolar lavage of groups of mice that were RSV infected or sham inoculated as in Figure 1. The figure is representative of three independent experiments, each experiment with four to five mice per group at each time point. Data are presented as mean ± SEM of four mice per group at each time point. *$P < 0.05$; **$P < 0.01$ and ***$P < 0.001$ relative to control mice.

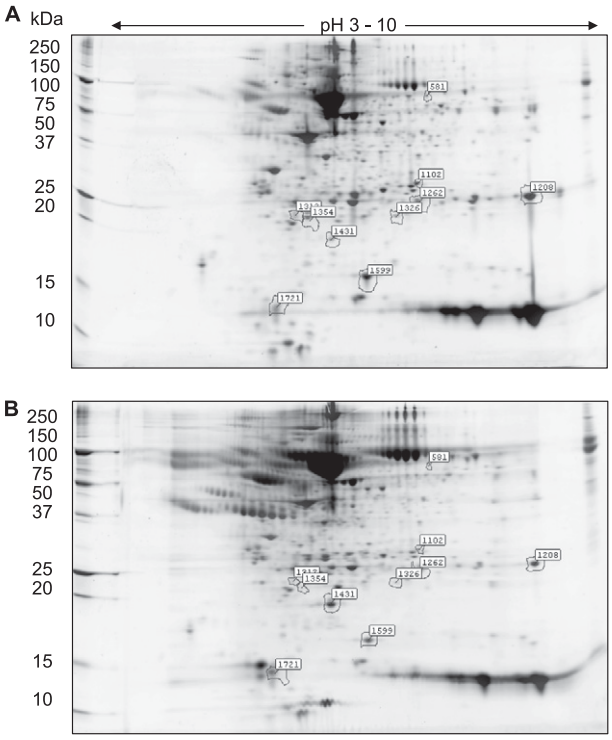

C

Spot No.	Antioxidant protein
1354	1-Cys peroxiredoxin
581	Catalase
1326	GPx 1
1208	GST mu1
1262	GST mu2
1102	GST omega 1
1312	Peroxiredoxin 6
1431	Prdx 2
1599	SOD 1
1721	Thioredoxin 1

Figure 4. Two-dimensional gel electrophoresis (2DE) of bronchoalveolar lavage (BAL) proteins reveals a global reduction in antioxidant enzyme expression after respiratory syncytial virus (RSV) infection. SYPRO Ruby–stained 2DE of BAL from (*A*) control and (*B*) RSV-infected mouse at Day 3 after infection Desalted and albumin-depleted proteins (200 μl at 1 mg/ml concentration) were fractionated over immobilized pH gradients from 3 to 10 in the horizontal dimension, followed by sodium dodecyl sulfate–polyacrylamide gel electrophoresis in the vertical dimension. *Left,* migration of molecular mass standards (kDa). The spot volumes were normalized based on the total spot volume for each gel, and the control and RSV-infected samples were compared. The numbers indicate differentially expressed spots identified by tryptic peptide mass fingerprinting and listed in *C*.

RSV-infected mice compared with control mice at 12 hours and 24 hours after infection (average percentage change of Nrf2 in RSV over control is 61 and 97% at 12 and 24 hours, respectively) (Figure 5), with nuclear levels in RSV-infected mice still below control at 48 and 72 hours after infection (data not shown). These results suggest that decreased AOE expression after RSV infection could be due to reduced basal activation of Nrf2 in the airways of mice.

Oxidative Stress Markers and AOE in Children with RSV Infection

We have previously shown that RSV is a potent inducer of ROS in airway epithelial cells *in vitro* (8) and causes significant oxidative stress damage *in vivo*, as demonstrated by the increase of lipid peroxidation markers F_2 8-isoprostane, MDA, and 4-hydroxynonenal in the lung of experimentally infected mice (10). These data along with the findings presented herein showing a global down-regulation of the lung antioxidant capacity as a consequence of RSV infection prompted us to conduct a study in children to determine whether the virus is capable of inducing oxidative stress damage in naturally acquired infections. Thus, we measured the levels of F_2 8-isoprostane and MDA in NPS of children with RSV-proven infections of increasing clinical severity, from milder URTI to bronchiolitis without or with hypoxia (demographics of the study population described in Table 2). The group of children with hypoxic bronchiolitis

TABLE 1. DIFFERENTIAL EXPRESSION OF ANTIOXIDANT ENZYMES IN BAL OF MICE BY TWO-DIMENSIONAL GEL ELECTROPHORESIS

	Fold Change in RSV BAL Compared to Control				
AOE	Day 1	Day 3	Day 5	Day 9	Day 25
1-Cys peroxiredoxin protein	−1.0	−6.1	—	−4.1	—
Catalase	—	−2.5	−2.1	—	—
Cu/Zn SOD 1	−2.3	−3.4	−2.0	−2.0	—
Glutathione peroxidase 1	−1.8	−2.3	—	1.3	—
Glutathione S-transferase	—	—	—	−6.0	—
Glutathione S-transferase omega 1	−6.8	−3.6	−2.3	−2.0	1.3
Glutathione S-transferase, alpha 4	−2.2	—	—	—	—
Glutathione S-transferase, mu 1	—	−4.0	−7.0	−1.7	1.4
Glutathione S-transferase, mu 2	—	−4.3	—	3.4	−1.3
Glutathione-disulfide reductase	—	—	—	3	—
Nonselenium glutathione peroxidase	−2.6	—	−4.2	−1.3	1.2
Peroxiredoxin 6	—	−3.1	−3.9	−4.1	1.3
Peroxiredoxin 2	2.7	2.4	−2.1	1.7	—
Thioredoxin 1	—	1.5	—	—	1.1

Definition of abbreviations: AOE = antioxidant enzymes; BAL = bronchoalveolar lavage; RSV = respiratory syncytial virus; SOD = superoxide dismutase; 2DE = two-dimensional gel electrophoresis.

Shown are fold changes of spot volume/intensity in RSV-infected over control mice. Listed AOE protein spots were identified based on high-probability from peptide mass fingerprinting in MALDI-TOF-MS (Expectation score). — indicates a protein spot that was not excised from the 2DE gel for mass fingerprinting.

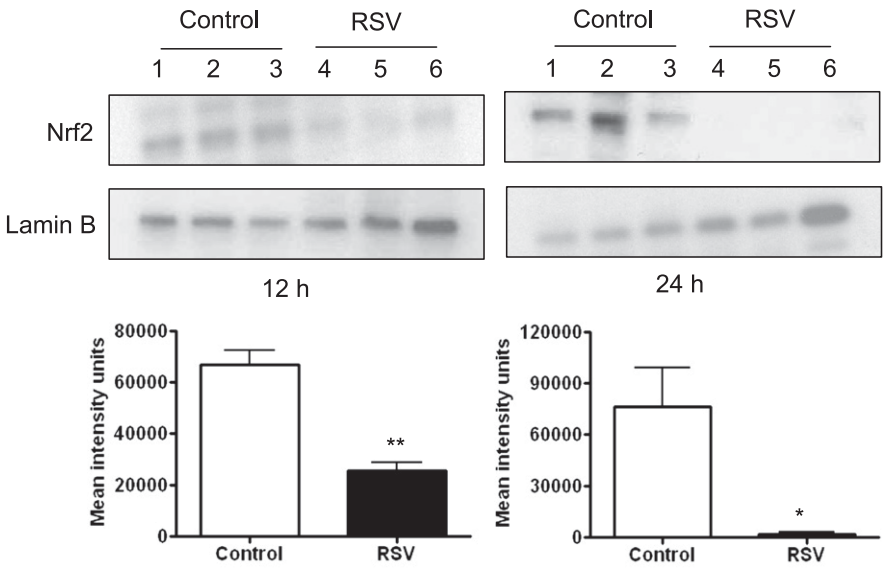

Figure 5. Respiratory syncytial virus (RSV) infection is associated with decreased levels of nuclear Nrf2 in the lung. Mice were infected with RSV or sham inoculated and lungs were harvested at 12 and 24 hours to isolate nuclear proteins. Equal amounts of nuclear proteins were analyzed by Western blot using anti-Nrf2 antibody. Membranes were stripped and reprobed for Lamin B, as control for equal loading of the samples. Lanes 1 to 3 are lung nuclear proteins from control and 4 to 6 from RSV-infected mice at each time point. The figure is representative of three independent experiments, each experiment with four to five mice per group at each time point. Densitometric analysis of Western blot band intensities was performed using Alpha Ease software presented as mean ± SEM of n = 3. *$P < 0.05$; **$P < 0.01$ relative to control mice.

included also three subjects who required intubation and VS because of respiratory failure. As shown in Figure 6A, concentration of F_2 8-isoprostane in NPS was slightly increased in subjects with mild bronchiolitis compared with those with URTI, but the difference was not statistically significant. However, subjects with hypoxic bronchiolitis had significantly more F_2 8-isoprostane in NPS than did subjects with URTI alone ($P < 0.01$) or with nonhypoxic bronchiolitis ($P < 0.001$). A similar trend was observed for MDA concentrations in a smaller number of NPS samples that were tested (Figure 6B).

To determine whether natural RSV infection along with an oxidative stress response may cause reduction of antioxidant defenses as we observed in experimentally infected mice, we measured levels of SOD 1, 2, and 3, catalase, and GST-mu in NPS of infected children by Western blot (Figure 7). For this analysis, infants on VS (i.e., those with most severe illness) were included in a separate group. SOD 1 levels were lower in infants with bronchiolitis, hypoxic bronchiolitis, and VS compared with those with URTI alone. The VS group showed also significantly lower levels of SOD 3, catalase, and GST-mu compared with the other illness groups. SOD 2 levels were similar in all illness groups.

To further investigate the spectrum of AOE changes in NPS samples from RSV-infected children, NPS proteins from the four groups described above were separated by high-resolution 2DE followed by MALDI-TOF-MS. We found that the antioxidant protein spots corresponding to SOD 1 and catalase were clearly present in URTI and bronchiolitis but significantly decreased in patients with hypoxic bronchiolitis and patients on VS, in agreement with the data of the Western blot analysis. Peroxiredoxin 1 expression was also significantly lower in children with bronchiolitis with hypoxia and VS compared with those with URTI and bronchiolitis (Figure E3).

DISCUSSION

Free radicals and ROS have been shown to function as cellular signaling molecules influencing a variety of molecular and biochemical processes, including expression of proinflammatory mediators, such as cytokines and chemokines (reviewed in Reference 4). However, excessive ROS formation can lead to a condition of oxidative stress, which has been implicated in the pathogenesis of several acute and chronic airway diseases, such

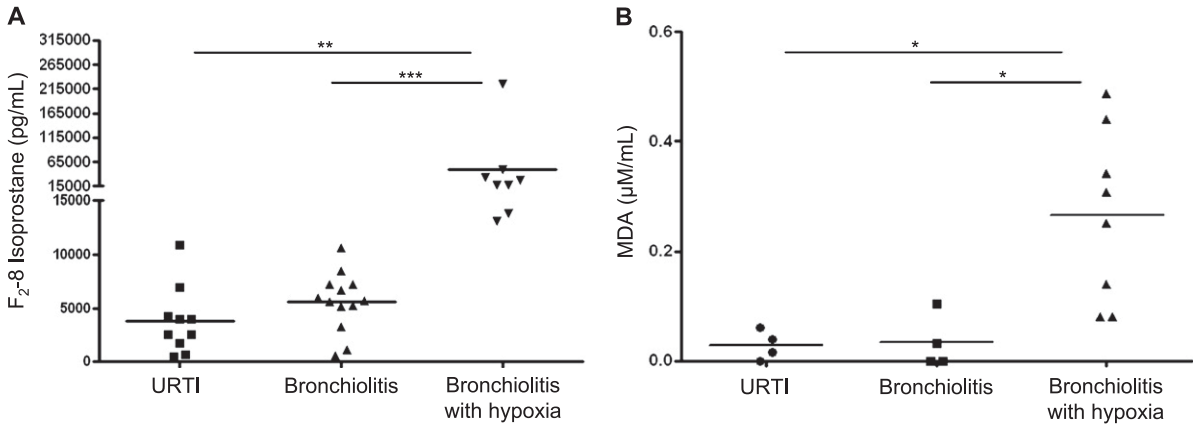

Figure 6. Concentrations of the oxidative stress markers in nasopharyngeal secretions (NPS) of infants with naturally acquired respiratory syncytial virus (RSV) infections. NPS collected from infants and young children with RSV-proven upper respiratory tract infections (URTI) and bronchiolitis were tested for (*A*) F2-isoprostane or (*B*) malondialdehyde (MDA) concentrations. Horizontal lines indicate the mean concentration. **$P < 0.01$ and ***$P < 0.001$ compared with URTI.

TABLE 2. CHARACTERISTICS OF STUDY PATIENTS WITH RESPIRATORY SYNCYTIAL VIRUS INFECTION, BY ILLNESS GROUP

Study Patient Characteristics	URTI Alone	Bronchiolitis	Hypoxic Bronchiolitis
No. of subjects	10	13	8
Age, mean months	6.4	6.3	9.7
Boys:girls	5:5	8:5	4:4
Race			
White	0	4	2
Black	0	2	4
Hispanic	9	5	2
Others	1	2	0

Definition of abbreviations: URTI = upper respiratory tract infection.

as asthma and COPD (reviewed in References 26 and 27). Inducible ROS generation has been shown after stimulation with a variety of molecules and infection with certain viruses, such as HIV, hepatitis B, influenza, and rhinovirus (reviewed in Reference 28). We have recently shown that RSV infection of airway epithelial cells induces ROS production, in part through an NAD(P)H oxidase-dependent mechanism, inducing oxidative stress *in vitro* (11) and *in vivo* (10), and that antioxidant treatment blocks transcription factor activation and chemokine gene expression *in vitro* (8, 9, 29) and ameliorates RSV-induced clinical illness *in vivo* (10), indicating a central role of ROS in RSV-induced cellular signaling and lung disease. Although there is increasing evidence that generation of oxidative stress is linked to the pathogenesis of a variety of acute and chronic inflammatory lung diseases, little is known regarding the role of oxidative stress in viral-induced lung diseases and the effect of respiratory viruses on AOE expression and/or activity. In the present study, we investigated whether RSV-induced lung oxidative stress *in vivo*, defined as a disruption of the prooxidant–antioxidant balance in favor of the former, could be due to an impairment of the antioxidant defense systems and whether increased oxidative stress could play a role in RSV-associated lung disease severity. Our results show that RSV infection induces a significant decrease in the expression of most AOE involved in maintaining cellular oxidant–antioxidant balance in mice and children, with the exception of SOD 2, for which levels are reduced in the BAL of infected mice but not in epithelial cell proteins of the conductive airways or in NPS of infected children, suggesting that airway epithelial cells may not be the only cellular source of the lung antioxidant response measured in BAL of mice. Other tissue resident cells, such as alveolar macrophages, which are early targets of RSV infection (30), could contribute to the observed BAL findings.

Similar to RSV, hMPV, a recently identified paramyxovirus, induces a progressive decrease of AOE expression levels in airway epithelial cells (31) and in the lung of infected mice as showed herein (Figure E4). In other studies, total lung SOD and catalase activities have been shown to be reduced in mice after influenza infection (32), supporting the knowledge that oxidative stress plays a significant role in the pathogenesis of influenza-induced pneumonia (33, 34). On the other hand, rhinovirus infection of bronchial epithelial cells has been shown to induce ROS formation (35) and to increase SOD 1 expression and total SOD activity at early time points of infection, with no changes in SOD 2, catalase, and GPx (36), although AOE expression/activity was investigated only at 6 hours after infection. Regarding other noninfectious conditions, an increase in antioxidant defenses has been shown to occur in certain pulmonary diseases with significant oxidant burden, such as

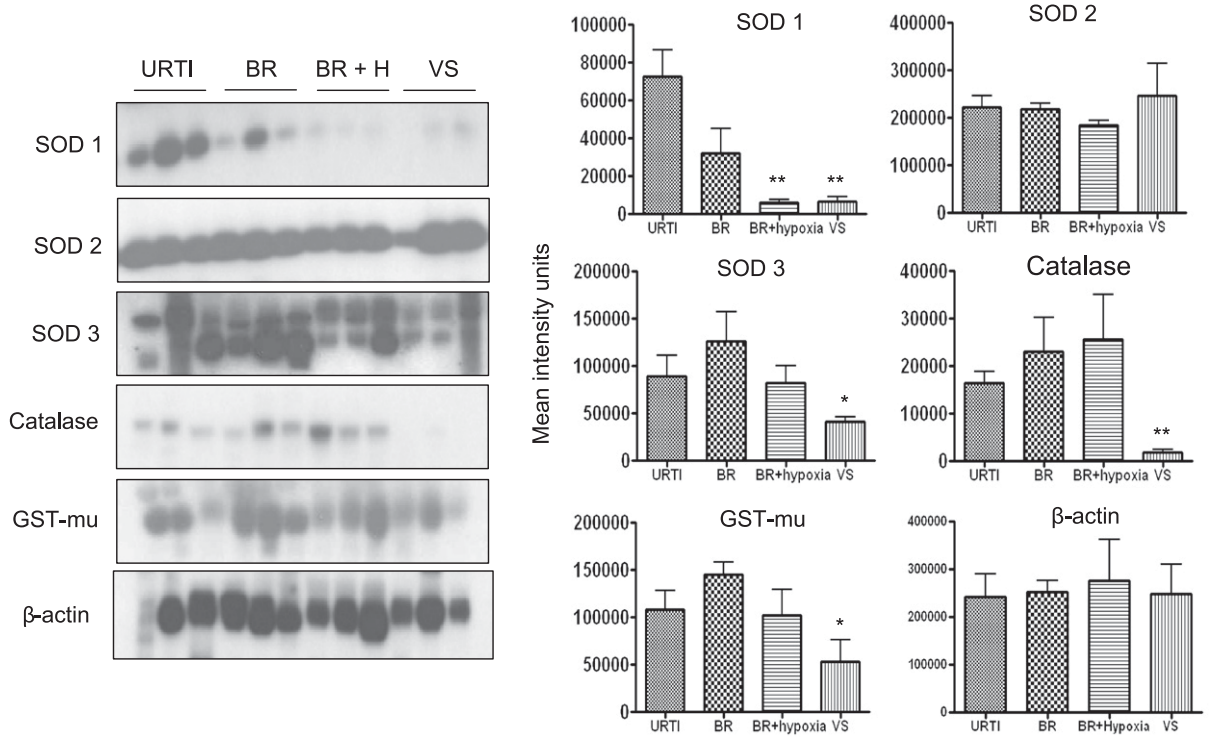

Figure 7. Antioxidant enzyme expression in nasopharyngeal secretions (NPS) of infants with naturally acquired respiratory syncytial virus (RSV) infections. (*A*) Western blot analysis of superoxide dismutase (SOD) 1, SOD 2, and SOD 3, catalase, and glutathione S-transferase (GST)-mu in NPS of children with upper respiratory tract infections (URTI), bronchiolitis (BR), bronchiolitis with hypoxia (BR + H), and patients on ventilatory support (VS). β-actin was used as a control for protein integrity and equal loading of the samples. Densitometric analysis of Western blot band intensities was performed using Alpha Ease software. *$P < 0.05$; **$P < 0.01$, compared with URTI.

exposure to hyperoxia (37), ozone (38), and cigarette smoke (39), although decreased antioxidant expression and/or activity has been reported in other respiratory acute and chronic inflammatory disease, such as asthma and COPD (40–43). Reduced SOD and catalase activity has been shown in airway epithelial cells and/or bronchoalveolar lavage obtained from patients with asthma (40–42). Similarly, decreased catalase and GST expression has been found in the lungs of COPD patients in association with chronic smoke exposure (43). Low dietary intake of antioxidants, including vitamins C and E, has been associated with worse symptoms in children with asthma (44).

The mechanism leading to decreased expression/activity of AOE is not clear. SOD 3 and catalase expression has been shown to be negatively regulated in response to cytokine stimulation, such as interleukin-1, tumor necrosis factor-α, and interferon-γ (45). Furthermore, oxidative stress can lead to SOD and catalase inactivation, as it has been shown in the BAL of patients with asthma (42). Nrf2 is a central transcription factor regulating the expression of a variety of cytoprotective genes involved in detoxification of xenobiotics and in counteracting cellular oxidative stress, including inducible AOE genes (reviewed in Reference 46). In this study, we have observed that RSV infection leads to a progressive decrease in the nuclear protein levels of Nrf2, suggesting a potential mechanism for down-regulation of AOE gene expression. Reduced nuclear levels of Nrf2 can occur as a result of various mechanisms, including decreased expression or increased degradation or through increased nuclear export (47). As Nrf2 positively regulates its own gene transcription, there are reduced Nrf2 mRNA levels in airway epithelial cells at a late time point of RSV infection, as we recently published (11). However, it is likely that other mechanisms contribute to the decreased Nrf2 nuclear levels at the earlier time points of infection. A recent study has shown that the Nrf2-ARE pathway plays a protective role in the murine airways against RSV-induced injury and oxidative stress (48). More severe RSV disease, including higher viral titers, augmented inflammation, and enhanced mucus production and epithelial injury, were found in $Nrf2^{-/-}$ mice compared with $Nrf2^{+/+}$ mice. Significant down-regulation of Nrf2 mRNA expression has been observed in pulmonary macrophages of aged smokers and patients with COPD (49), and functional polymorphisms in the Nrf2 gene promoter, leading to reduced gene transcription, are associated with the severity of COPD (50) and increased risk of acute lung injury after trauma (51).

In our initial study of NPS obtained from children with RSV infection, we found a significant increase in markers of oxidative injury and a significant decrease in AOE expression, which correlated with the severity of lung disease. In previous studies of patients with RSV infection we have shown that concentration of certain inflammatory mediators and cytokines in NPS, many of which are of epithelial origin, correlate with their concentration in the lower airway (52). We therefore speculate that ROS or oxidative stress marker production measured in the NPS samples may reflect the events occurring in the lower airways. Although our study was performed in a relatively small cohort of RSV-infected subjects, it included a balanced representation of the spectrum of disease that is caused by this pathogen in infancy. Since viral culture or real-time PCR for other viral pathogens in samples that were positive for RSV antigen were not performed, the potential effect of single RSV versus dual infections on oxidative stress responses and AOE expression cannot be answered at this point. Also, our data in mice suggest that infections caused by other viral respiratory pathogens, which are known to cause bronchiolitis in infants, may also result in a similar inhibition of AOE expression. To unequivocally answer this question there is a need for larger clinical studies. In this regard, we are currently enrolling infants in a prospective study in which patients with a broad spectrum of disease severity caused by RSV or by other viral agents will be tested.

Other important aspects in future studies of RSV infections compared with those caused by other pathogens include the actual profile of AOE that are altered in expression, either decreased or increased in severe versus milder forms of infection, the ability of each pathogen to trigger the generation of ROS, and the "magnitude" and type of oxidative damage in the airways, including the presence of other lipid peroxidation products or protein modifications, which characterize the biological targets of ROS formation. Also, the known developmental process of the AOE system that starts during fetal life and is characterized by a certain degree of immaturity in the neonatal period and early infancy may contribute to the severity of RSV infections that occur during this vulnerable period of life (53). All these factors are likely to contribute to the oxidative-mediated pathogenesis of viral bronchiolitis and perhaps to the relative greater effect of a pathogen (for example RSV) compared with others. With even broader implications, generation of such an oxidative stress environment in the airways, along with the impaired antioxidant response that we describe as result of paramyxovirus infections, may induce critical chemical modifications of bystander antigens and their immunogenicity. Such a possibility has been suggested by studies of aldehyde-mediated carbonylation of protein allergens resulting in enhanced Th2 responses, perhaps via enhanced immune priming (54).

In conclusion, our findings suggest that virus-induced oxidative damage *in vivo* is the result of an imbalance between ROS production and airway antioxidant defenses. Based on our findings in this work as well as our previous published data in the experimental mouse model of RSV infection in which antioxidants were used (10), we suggest that modulation of AOE expression and/or blocking of oxidative stress response may represent potential pharmacological approaches to prevent or treat viral-induced lung inflammation and its long-term consequences.

Author Disclosure: Y.M.H. does not have a financial relationship with a commercial entity that has an interest in the subject of this manuscript. P.D.J. does not have a financial relationship with a commercial entity that has an interest in the subject of this manuscript. D.L.E. does not have a financial relationship with a commercial entity that has an interest in the subject of this manuscript. H.S. does not have a financial relationship with a commercial entity that has an interest in the subject of this manuscript. A.K. does not have a financial relationship with a commercial entity that has an interest in the subject of this manuscript. A.C. received grant support from the Department of Defense and the Flight Attendant Medical Research Institute. R.P.G. received grant support from the Department of Defense, the Flight Attendant Medical Research Institute, and NASA.

Acknowledgment: The authors thank Drs. Alan Buckpitt and Asa Wheelock, University of California Davis, for training in the lysis-lavage technique, and Mrs. Cynthia Tribble for her assistance in manuscript submission.

References

1. Nair H, Nokes DJ, Gessner BD, Dherani M, Madhi SA, Singleton RJ, O'Brien KL, Roca A, Wright PF, Bruce N, *et al.* Global burden of acute lower respiratory infections due to respiratory syncytial virus in young children: a systematic review and meta-analysis. *Lancet* 2010; 375:1545–1555.
2. Leader S, Kohlhase K. Respiratory syncytial virus-coded pediatric hospitalizations, 1997 to 1999. *Pediatr Infect Dis J* 2002;21:629–632.
3. Gabbita SP, Robinson KA, Stewart CA, Floyd RA, Hensley K. Redox regulatory mechanisms of cellular signal transduction. *Arch Biochem Biophys* 2000;376:1–13.
4. Allen RG, Tresini M. Oxidative stress and gene regulation. *Free Radic Biol Med* 2000;28:463–499.
5. MacNee W, Rahman I. Is oxidative stress central to the pathogenesis of chronic obstructive pulmonary disease? *Trends Mol Med* 2001;7:55–62.
6. Rahman I, Morrison D, Donaldson K, MacNee W. Systemic oxidative stress in asthma, COPD, and smokers. *Am J Respir Crit Care Med* 1996;154:1055–1060.

7. Hull J, Vervaart P, Grimwood K, Phelan P. Pulmonary oxidative stress response in young children with cystic fibrosis. *Thorax* 1997; 52:557–560.
8. Casola A, Burger N, Liu T, Jamaluddin M, Brasier AR, Garofal RP. Oxidant tone regulates RANTES gene transcription in airway epithelial cells infected with Respiratory Syncytial Virus: role in viral-induced Interferon Regulatory Factor activation. *J Biol Chem* 2001;276:19715–19722.
9. Liu T, Castro S, Brasier AR, Jamaluddin M, Garofalo RP, Casola A. Reactive oxygen species mediate virus-induced STAT activation: role of tyrosine phosphatases. *J Biol Chem* 2004;279:2461–2469.
10. Castro SM, Guerrero-Plata A, Suarez-Real G, Adegboyega PA, Colasurdo GN, Khan AM, Garofalo RP, Casola A. Antioxidant treatment ameliorates respiratory syncytial virus-induced disease and lung inflammation. *Am J Respir Crit Care Med* 2006;174:1361–1369.
11. Hosakote YM, Liu T, Castro SM, Garofalo RP, Casola A. Respiratory syncytial virus induces oxidative stress by modulating antioxidant enzymes. *Am J Respir Cell Mol Biol* 2009;41:348–357.
12. Jaiswal AK. Nrf2 signaling in coordinated activation of antioxidant gene expression. *Free Radic Biol Med* 2004;36:1199–1207.
13. Hosakote, Y, Esham, D, Casola A, and Garofalo, RP. Oxidative injury in the lungs is associated with inhibition of antioxidant gene expression in RSV infection [abstract]. E-Pediatric Academic Societies 2010:2735.6. Available from: http://www.abstracts2view.com/pasall/view.php?nu=PAS10L1_2375.
14. Ueba O. Respiratory syncytial virus: I. concentration and purification of the infectious virus. *Acta Med Okayama* 1978;32:265–272.
15. Patel JA, Kunimoto M, Sim TC, Garofalo R, Eliott T, Baron S, Ruuskanen O, Chonmaitree T, Ogra PL, Schmalstieg F. Interleukin-1 alpha mediates the enhanced expression of intercellular adhesion molecule-1 in pulmonary epithelial cells infected with respiratory syncytial virus. *Am.J.Resp.Cell Mol.* 1995;13:602–609.
16. Guerrero-Plata A, Casola A, Garofalo RP. Human metapneumovirus induces a profile of lung cytokines distinct from that of respiratory syncytial virus. *J Virol* 2005;79:14992–14997.
17. Bohrer H, Qiu F, Zimmermann T, Zhang Y, Jllmer T, Mannel D, Bottiger BW, Stern DM, Waldherr R, Saeger HD, *et al.* Role of NFkB in the mortality of sepsis. *J Clin Invest* 1997;100:972–985.
18. Haeberle HA, Nesti F, Dieterich HJ, Gatalica Z, Garofalo RP. Perflubron reduces lung inflammation in respiratory syncytial virus infection by inhibiting chemokine expression and nuclear factor-kappaB Activation. *Am J Respir Crit Care Med* 2002;165:1433–1438.
19. Wheelock AM, Zhang L, Tran MU, Morin D, Penn S, Buckpitt AR, Plopper CG. Isolation of rodent airway epithelial cell proteins facilitates in vivo proteomics studies of lung toxicity. *Am J Physiol Lung Cell Mol Physiol* 2004;286:L399–L410.
20. Berndt P, Hobohm U, Langen H. Reliable automatic protein identification from matrix-assisted laser desorption/ionization mass spectrometric peptide fingerprints. *Electrophoresis* 1999;20:3521–3526.
21. Zhang W, Chait BT. ProFound: an expert system for protein identification using mass spectrometric peptide mapping information. *Anal Chem* 2000;72:2482–2489.
22. Kahn JS. Human metapneumovirus: a newly emerging respiratory pathogen. *Curr Opin Infect Dis* 2003;16:255–258.
23. Magi B, Bini L, Perari MG, Fossi A, Sanchez JC, Hochstrasser D, Paesano S, Raggiaschi R, Santucci A, Pallini V, *et al.* Bronchoalveolar lavage fluid protein composition in patients with sarcoidosis and idiopathic pulmonary fibrosis: a two-dimensional electrophoretic study. *Electrophoresis* 2002;23:3434–3444.
24. Rangasamy T, Cho CY, Thimmulappa RK, Zhen L, Srisuma SS, Kensler TW, Yamamoto M, Petrache I, Tuder RM, Biswal S. Genetic ablation of Nrf2 enhances susceptibility to cigarette smoke-induced emphysema in mice. *J Clin Invest* 2004;114:1248–1259.
25. Chan JY, Kwong M. Impaired expression of glutathione synthetic enzyme genes in mice with targeted deletion of the Nrf2 basic-leucine zipper protein. *Biochim Biophys Acta* 2000;1517:19–26.
26. Folkerts G, Kloek J, Muijsers RB, Nijkamp FP. Reactive nitrogen and oxygen species in airway inflammation. *Eur J Pharmacol* 2001;429: 251–262.
27. Ciencewicki J, Trivedi S, Kleeberger SR. Oxidants and the pathogenesis of lung diseases. *J Allergy Clin Immunol* 2008;122:456–468.
28. Schwarz KB. Oxidative stress during viral infection: a review. *Free Radic Biol Med* 1996;21:641–649.
29. Indukuri H, Castro SM, Liao SM, Feeney LA, Dorsch M, Coyle AJ, Garofalo RP, Brasier AR, Casola A. Ikkepsilon regulates viral-induced interferon regulatory factor-3 activation via a redox-sensitive pathway. *Virology* 2006;353:155–165.
30. Haeberle H, Takizawa R, Casola A, Brasier AR, Dieterich H-J, van Rooijen N, Gatalica Z, Garofalo RP. Respiratory syncytial virus-induced activation of NF-kB in the lung involves alveolar macrophages and Toll-like receptor 4-dependent pathways. *J Infect Dis* 2002;186:1199–1206.
31. Bao X, Sinha M, Liu T, Hong C, Luxon BA, Garofalo RP, Casola A. Identification of human metapneumovirus-induced gene networks in airway epithelial cells by microarray analysis. *Virology* 2008;374:114–127.
32. Kumar P, Khanna M, Srivastava V, Tyagi YK, Raj HG, Ravi K. Effect of quercetin supplementation on lung antioxidants after experimental influenza virus infection. *Exp Lung Res* 2005;31:449–459.
33. Akaike T, Noguchi Y, Ijiri S, Setoguchi K, Suga M, Zheng YM, Dietzschold B, Maeda H. Pathogenesis of influenza virus-induced pneumonia: involvement of both nitric oxide and oxygen radicals. *Proc Natl Acad Sci USA* 1996;93:2448–2453.
34. Suliman HB, Ryan LK, Bishop L, Folz RJ. Prevention of influenza-induced lung injury in mice overexpressing extracellular superoxide dismutase. *Am J Physiol Lung Cell Mol Physiol* 2001;280: L69–L78.
35. Biagioli MC, Kaul P, Singh I, Turner RB. The role of oxidative stress in rhinovirus induced elaboration of IL-8 by respiratory epithelial cells. *Free Radic Biol Med* 1999;26:454–462.
36. Kaul P, Singh I, Turner RB. Effect of rhinovirus challenge on antioxidant enzemes in respiratory epithelial cells. *Free Radic Res* 2002;36: 1085–1089.
37. Erzurum SC, Danel C, Gillissen A, Chu CS, Trapnell BC, Crystal RG. In vivo antioxidant gene expression in human airway epithelium of normal individuals exposed to 100% O2. *J Appl Physiol* 1993;75: 1256–1262.
38. Boehme DS, Hotchkiss JA, Henderson RF. Glutathione and GSH-dependent enzymes in bronchoalveolar lavage fluid cells in response to ozone. *Exp Mol Pathol* 1992;56:37–48.
39. Gilks CB, Price K, Wright JL, Churg A. Antioxidant gene expression in rat lung after exposure to cigarette smoke. *Am J Pathol* 1998;152: 269–278.
40. Smith LJ, Shamsuddin M, Sporn PH, Denenberg M, Anderson J. Reduced superoxide dismutase in lung cells of patients with asthma. *Free Radic Biol Med* 1997;22:1301–1307.
41. De Raeve HR, Thunnissen FB, Kaneko FT, Guo FH, Lewis M, Kavuru MS, Secic M, Thomassen MJ, Erzurum SC. Decreased Cu,Zn-SOD activity in asthmatic airway epithelium: correction by inhaled corticosteroid in vivo. *Am J Physiol* 1997;272:L148–L154.
42. Ghosh S, Janocha AJ, Aronica MA, Swaidani S, Comhair SA, Xu W, Zheng L, Kaveti S, Kinter M, Hazen SL, *et al.* Nitrotyrosine proteome survey in asthma identifies oxidative mechanism of catalase inactivation. *J Immunol* 2006;176:5587–5597.
43. Tomaki M, Sugiura H, Koarai A, Komaki Y, Akita T, Matsumoto T, Nakanishi A, Ogawa H, Hattori T, Ichinose M. Decreased expression of antioxidant enzymes and increased expression of chemokines in COPD lung. *Pulm Pharmacol Ther* 2007;20:596–605.
44. Burns JS, Dockery DW, Neas LM, Schwartz J, Coull BA, Raizenne M, Speizer FE. Low dietary nutrient intakes and respiratory health in adolescents. *Chest* 2007;132:238–245.
45. Chung-man HJ, Zheng S, Comhair SA, Farver C, Erzurum SC. Differential expression of manganese superoxide dismutase and catalase in lung cancer. *Cancer Res* 2001;61:8578–8585.
46. Kensler TW, Wakabayashi N, Biswal S. Cell survival responses to environmental stresses via the Keap1-Nrf2-ARE pathway. *Annu Rev Pharmacol Toxicol* 2007;47:89–116.
47. Kaspar JW, Niture SK, Jaiswal AK. Nrf2:INrf2 (Keap1) signaling in oxidative stress. *Free Radic Biol Med* 2009;47:1304–1309.
48. Cho HY, Imani F, Miller-Degraff L, Walters D, Melendi GA, Yamamoto M, Polack FP, Kleeberger SR. Antiviral activity of Nrf2 in a murine model of respiratory syncytial virus (RSV) disease. *Am J Respir Crit Care Med* 2009;179:138–150.
49. Suzuki M, Betsuyaku T, Ito Y, Nagai K, Nasuhara Y, Kaga K, Kondo S, Nishimura M. Down-regulated NF-E2-related factor 2 in pulmonary macrophages of aged smokers and patients with chronic obstructive pulmonary disease. *Am J Respir Cell Mol Biol* 2008; 39:673–682.
50. Hua CC, Chang LC, Tseng JC, Chu CM, Liu YC, Shieh WB. Functional haplotypes in the promoter region of transcription factor

Nrf2 in chronic obstructive pulmonary disease. *Dis Markers* 2010;28: 185–193.
51. Marzec JM, Christie JD, Reddy SP, Jedlicka AE, Vuong H, Lanken PN, Aplenc R, Yamamoto T, Yamamoto M, Cho HY, *et al.* Functional polymorphisms in the transcription factor NRF2 in humans increase the risk of acute lung injury. *FASEB J* 2007;21:2237–2246.
52. Garofalo RP, Patti J, Hintz KA, Hill V, Ogra PL, Welliver RC. Macrophage inflammatory protein 1-alpha, and not T-helper type 2 cytokines, is associated with severe forms of bronchiolitis. *J Infect Dis* 2001;184:393–399.
53. Davis JM, Auten RL. Maturation of the antioxidant system and the effects on preterm birth. *Semin Fetal Neonatal Med* 2010;15:191–195.
54. Moghaddam A, Olszewska W, Wang B, Tregoning JS, Helson R, Sattentau QJ, Openshaw PJ. A potential molecular mechanism for hypersensitivity caused by formalin-inactivated vaccines. *Nat Med* 2006;12:905–907.

Am J Physiol Lung Cell Mol Physiol 303: L991–L1000, 2012.
First published September 28, 2012; doi:10.1152/ajplung.00192.2012.

Antioxidant mimetics modulate oxidative stress and cellular signaling in airway epithelial cells infected with respiratory syncytial virus

Yashoda M. Hosakote,[1] Narayana Komaravelli,[1] Nicolas Mautemps,[1] Tianshuang Liu,[1] Roberto P. Garofalo,[1,2,3] and Antonella Casola[1,2,3]

[1]*Department of Pediatrics, University of Texas Medical Branch, Galveston, Texas;* [2]*Department of Microbiology and Immunology, University of Texas Medical Branch, Galveston, Texas; and* [3]*Sealy Center for Molecular Medicine, University of Texas Medical Branch, Galveston, Texas*

Submitted 22 June 2012; accepted in final form 20 September 2012

Hosakote YM, Komaravelli N, Mautemps N, Liu T, Garofalo RP, Casola A. Antioxidant mimetics modulate oxidative stress and cellular signaling in airway epithelial cells infected with respiratory syncytial virus. *Am J Physiol Lung Cell Mol Physiol* 303: L991–L1000, 2012. First published September 28, 2012; doi:10.1152/ajplung.00192.2012.—Respiratory syncytial virus (RSV) is one of the most common causes of bronchiolitis and pneumonia among infants and young children worldwide. In previous investigations, we have shown that RSV infection induces rapid generation of reactive oxygen species (ROS), which modulate viral-induced cellular signaling, and downregulation of antioxidant enzyme (AOE) expression, resulting in oxidative stress in vitro and in vivo, which plays a pathogenetic role in RSV-induced lung disease. In this study, we determined whether pharmacological intervention with synthetic catalytic scavengers could reduce RSV-induced proinflammatory gene expression and oxidative cell damage in an in vitro model of infection. Treatment of airway epithelial cells (AECs) with the salen-manganese complexes EUK-8 or EUK-189, which possess superoxide dismutase, catalase, and glutathione peroxidase activity, strongly reduced RSV-induced ROS formation by increasing cellular AOE enzymatic activity and levels of the lipid peroxidation products F_2-8-isoprostane and malondialdehyde, which are markers of oxidative stress. Treatment of AECs with AOE mimetics also significantly inhibited RSV-induced cytokine and chemokine secretion and activation of the transcription factors nuclear factor-κB and interferon regulatory factor-3, which orchestrate proinflammatory gene expression. Both EUKs were able to reduce viral replication, when used at high doses. These results suggest that increasing antioxidant cellular capacities can significantly impact RSV-associated oxidative cell damage and cellular signaling and could represent a novel therapeutic approach in modulating virus-induced lung disease.

respiratory syncytial virus; airway epithelial cells; antioxidant enzyme mimetics; oxidative stress

RESPIRATORY SYNCYTIAL VIRUS (RSV) is the one of the most important causes of viral upper and lower respiratory tract infections (LRTI) in infants and young children. RSV is so ubiquitous in nature that it will infect 100% of children before the age of two. The number of children hospitalized each year in the United States with viral LRTI has recently been estimated at >200,000, with 500 deaths per year in children under age 5 years (24). Although the mechanisms of RSV-induced airway disease and associated long-term consequences remain incompletely defined, the lung inflammatory response is thought to play a fundamental role. Oxidative stress has been shown to play an important role in the pathogenesis of both acute and chronic lung inflammatory diseases (reviewed in Refs. 27, 29, and 33). Reactive oxygen species (ROS) are highly unstable molecules produced by the pulmonary epithelial and endothelial cells involved in many forms of tissue damage, including the damage caused to cellular components such as lipids, proteins, and DNA (reviewed in Refs. 1 and 11). We have previously shown that RSV infection of AECs induces ROS production, which is involved in transcription factor activation and chemokine gene expression (6, 26). We have also shown that rapid generation of ROS is associated with oxidative stress and lung damage in infected cells in both animals and children (8, 16, 17). Antioxidant treatment significantly ameliorates RSV-induced oxidative stress, clinical disease, and pulmonary inflammation in a mouse model of infection, suggesting a causal relationship between increased ROS production and lung disease (8). RSV infection leads to a significant decrease in the expression and activity of antioxidant enzymes (AOEs) in AECs, in lungs of RSV-infected mice, as well as in children with severe RSV-induced LRTI (16, 17), suggesting that oxidative damage associated with RSV infection results from an imbalance between ROS production and antioxidant cellular defenses.

The use of recombinant superoxide dismutase (SOD) and SOD mimetics has been explored as therapeutics in a variety of disease models either in vitro or in vivo. A number of SOD mimetics based around organo-manganese complexes have been developed. They include metalloporphyrin-based compounds, such as AEOL10113 and -10150, cyclic polyamine-based molecules, such as M40403 and -40419, and the salen compounds, such as EUK-8, -134 and -189, the latter ones possessing also significant catalase and peroxidase activity (reviewed in Ref. 3). Although EUKs have been used in a variety of disease models, there is no reported literature about their use in models of viral infections. Recently, we have shown that treatment of A549 cells with EUK-134 significantly inhibits RSV-induced interleukin (IL)-8 and regulated on activation normal T cell expressed and secreted (RANTES) secretion (17). In the present study, we found that EUK-8 and EUK-189 treatment of AECs significantly restored intracellular catalase and glutathione peroxidase (GPx) enzyme activities, which are significantly diminished by RSV infection, leading to reduced viral-induced ROS production and generation of lipid peroxidation markers, such as isoprostane and malondialdehyde (MDA). In addition, EUK administration significantly reduced secretion of a variety of proinflammatory molecules in response to RSV infection. At high concentration,

Address for reprint requests and other correspondence: A. Casola, Dept. of Pediatrics, 301 Univ. Blvd., Galveston, TX 77555-0366 (e-mail: ancasola@utmb.edu).

both EUK-8 and -189 reduced viral replication, indicating that EUKs could represent a novel therapeutic approach to restore the prooxidant/antioxidant balance in favor of the latter, in the context of RSV infection, leading to reduced cellular oxidative stress, proinflammatory mediator secretion, and reduced viral replication.

MATERIALS AND METHODS

Materials. Eukarion compounds (salen-manganese complexes) EUK-8 and EUK-189 were kindly provided by Susan Doctrow (Boston University, School of Medicine). 2′,7′-Dichlorodihydro-fluorescein diacetate (DCF-DA) was from Invitrogen (Molecular Probes, Eugene, OR); 3-amino-9-ehtyl carbazole was from Sigma (St. Louis, MO).

RSV preparation. The RSV long strain was grown in Hep-2 cells and purified by centrifugation on discontinuous sucrose gradients as described elsewhere (39). The virus titer of the purified RSV pools was 8–9 $\log_{10}$ plaque-forming units (PFU)/ml using a methylcellulose plaque assay. No contaminating cytokines were found in these sucrose-purified viral preparations (31). Lipopolysaccharide (LPS), assayed using the limulus hemocyanin agglutination assay, was not detected. Virus pools were separated into aliquots, quick-frozen on dry ice/alcohol, and stored at −70°C until used.

Cell culture and infection of epithelial cells with RSV. A549 cells, a human alveolar type II-like epithelial cell line (American Type Culture Collection, Manassas, VA), and small alveolar epithelial (SAE) cells (Clonetics, San Diego, CA), normal human AECs derived from terminal bronchioli, were grown according to the manufacturer's instructions. A549 and SAE were maintained in F12K and small airway epithelial cell (SAEC) growth medium, respectively, containing 10% (vol/vol) FBS, 10 mM glutamine, 100 IU/ml penicillin, and 100 μg/ml streptomycin for F12K medium and 7.5 mg/ml bovine pituitary extract, 0.5 mg/ml hydrocortisone, 0.5 μg/ml human epidermal growth factor, 0.5 mg/ml epinephrine, 10 mg/ml transferrin, 5 mg/ml insulin, 0.1 μg/ml retinoic acid, 0.5 μg/ml triiodothyronine, 50 mg/ml gentamicin, and 50 mg/ml BSA for SAEC medium. When SAE were used for RSV infection, they were changed to basal medium, not supplemented with growth factors, 6 h before and throughout the length of the experiment. At around 80–90% confluency, cell monolayers were infected with RSV at multiplicity of infection (MOI) of three (unless otherwise stated), as previously described (13). An equivalent amount of a 30% sucrose solution was added to uninfected A549 and SAE cells, as a control.

For the catalytic scavenger experiment, cells were treated with EUK-8 or EUK-189 either 1 h before and throughout the infection or at different times postinfection. Because EUKs were diluted in ethanol, equal amounts of ethanol were added to untreated cells, as control. Total number of cells and cell viability, following antioxidant treatment, were measured by trypan blue exclusion. There was no significant change in cell viability with both compounds at all doses tested.

Luciferase assay. Logarithmically growing A549 cells were transfected in triplicate in 24-well plate dishes with Cignal Antioxidant Response Reporter from Qiagen, an optimized luciferase reporter construct that monitors both increases and decreases in the transcriptional activity of NF-E2-related factor 1 and NF-E2-related factor 2 (Nrf2), using Fugene 6 (Roche Diagnostic, Indianapolis, IN). Reporter gene plasmid (0.5 μg/well) and β-galactosidase (0.05 μg/well) expression plasmid were premixed with FuGene 6 and added to the cells in 1 ml of regular medium. The next morning, cells were infected with RSV in the presence or absence of EUKs and harvested at 24 h postinfection to independently measure luciferase and β-galactosidase reporter activity, as previously described (7). Luciferase activity was normalized to the internal control β-galactosidase activity. Results are expressed in arbitrary units. All experiments were performed at least two to three times.

Determination of lactate dehydrogenase activity. Lactate dehydrogenase (LDH) activity in the medium, an index of cellular damage, was measured by a colorimetric LDH release assay using a commercially available kit (catalog no. 10008882; Cayman Chemical). The assay was carried out according to the kit's instructions.

Antiviral assay in the presence of EUKs. A549 cells were seeded into 48-well plates at 5×10^4 cells/well. Cells were treated with EUKs in triplicate wells for 1 h and infected with RSV at a MOI of 0.01 PFU/cell. Following adsorption of virus for 1 h at 37°C and 5% CO_2, viral inoculum was aspirated, the cells were washed three times with minimal essential medium (MEM), and then MEM with 2% FBS was added. Control or EUK-treated and infected cells were then incubated at 37°C and 5% CO_2 for 24 h. RSV titers were determined by using polyclonal antibodies and a horseradish peroxidase (HRP) staining method, as previously described (23). Briefly, medium was aspirated, and the cells were fixed for 20 min using methanol and 2% H_2O_2. Cells were then incubated for 30 min with anti-RSV polyclonal antibody (Biogenesis, Kingston, NH) followed by HRP-conjugated anti-guinea pig secondary antibody (Zymed, San Francisco, CA). Plaques were visualized by the addition of 3-amino-9-ethyl-carbazole substrate and enumerated by light microscopy.

Quantitative real-time PCR. RNA samples were quantified by using a Nanodrop Spectrophotometer (Nanodrop Technologies), and quality was analyzed on RNA Nano or Pico chip using the Agilent 2100 Bioanalyzer (Agilent Technologies). Synthesis of cDNA was performed with 1 μg of total RNA in a 20-μl reaction by using the reagents in the Taqman Reverse Transcription Reagents Kit from ABI (Applied Biosystems no. N8080234). The reaction conditions were as follows: 25°C 10 min, 48°C 30 min, 95°C 5 min. Quantitative real-time PCR amplifications (performed in triplicate) were done with 1 μl of cDNA in a total volume of 25 μl by use of the Faststart Universal SYBR Green Master Mix (Roche Applied Science no. 04913850001). The final concentration of the primers was 300 nM. 18S RNA was used as housekeeping gene for normalization. PCR assays were run in the ABI Prism 7500 Sequence Detection System with the following conditions: 50°C 2 min, 95°C 10 min and then 95°C 15 s, 60°C 1 min for 40 cycles. RSV N-specific RT primer contained a tag sequence from the bacterial chloroamphenicol resistance gene to generate the cDNA, because of self-priming exhibited by RSV RNA. Duplicate cycle threshold (C_T) values were analyzed in Microsoft Excel by the comparative C_T ($\Delta\Delta C_T$) method as described by the manufacturer (Applied Biosystems). The amount of target ($2^{-\Delta\Delta CT}$) was obtained by normalizing to endogenous reference (18S) sample. RSV N dT+Tag (RT primer): CTGCGATGAGTGGCAGGC-TTTTTTTTTTTTTAACTYAAAGCTC Cmr Tag. For PCR assay, RSV Tag (R primer): CTGCGATGAGTGGCAGGC. RSV N forward primer: ACTACAGTGTATTAGACTTRACAGCAGAAG.

Measurement of intracellular ROS. A549 cells were grown in 96-well tissue culture plates and infected with RSV. At different times postinfection, cells were washed with Hanks' balanced salt solution (HBSS) and loaded with 10 μM 2,7 DCF-DA in HBSS medium containing 25 mM HEPES, pH 7.4, for 30 min at 37°C. The cells were then washed two times, and fluorescence intensity was determined at 485 nm excitation and 590 nm emission, using an automated fluorescence reader (Molecular Devices, Sunnyvale, CA).

Measurement of lipid peroxidation products. Measurement of F_2-8-isoprostane was performed using a competitive enzyme immunoassay from Cayman Chemical (Ann Arbor, MI) according to the manufacturer's instructions. Measurement of the lipid peroxidation marker MDA was carried out using a lipid peroxidation kit from Calbiochem/EMD Chemicals.

Western blotting. Nuclear extracts of uninfected and infected cells were prepared using hypotonic/nonionic detergent lysis, according to the protocol of Schreiber et al. (35). To prevent contamination with cytoplasmic proteins, isolated nuclei were purified by centrifugation through 1.7 M sucrose buffer for 30 min, at 12,000 rpm, before nuclear protein extraction, as previously described (5). Total cell

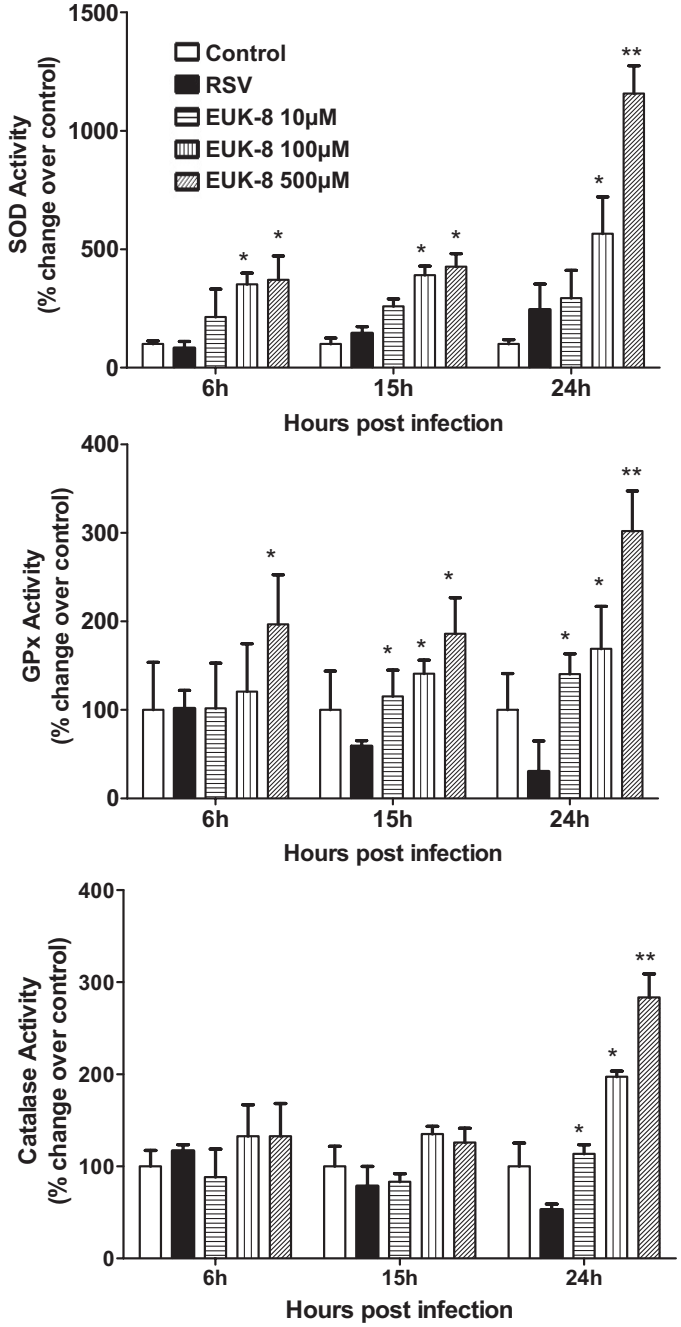

Fig. 1. Effect of EUK treatment on total superoxide dismutase (SOD), catalase, and glutathione peroxidase (GPx) activity in respiratory syncytial virus (RSV)-infected cells. Total lysates were prepared from uninfected and RSV-infected treated or untreated with different doses of EUK-8 at 6, 15, and 24 h postinfection to measure total SOD, catalase, and GPx enzyme activities. Data are expressed as %change over control. Results are representative of two independent experiments. $*P < 0.05$ and $**P < 0.01$ compared with RSV-infected cells.

lysates were prepared from uninfected and infected A549 cells by adding ice-cold lysis buffer (50 mM Tris·HCl, pH 7.4, 150 mM NaCl, 1 mM EGTA, 0.25% sodium deoxycholate, 1 mM Na_3VO_4, 1 mM NaF, 1% Triton X-100, and 1 μg/ml of aprotinin, leupeptin, and pepstatin). After incubation on ice for 10 min, the lysates were collected, and detergent-insoluble materials were removed by centrifugation at 4°C at 14,000 *g*. Proteins (10–20 μg/sample) were then boiled in 2× Laemmli buffer and resolved on SDS-PAGE. Proteins were transferred onto Hybond-polyvinylidene difluoride membrane (Amersham, Piscataway, NJ), and nonspecific binding sites were blocked by immersing the membrane in Tris-buffered saline-Tween (TBST) containing 5% skim milk powder or 5% BSA for 30 min. After a short wash in TBST, membranes were incubated with the primary antibody for 1 h or overnight at 4°C, depending on the antibody used, followed by HRP-conjugated secondary antibody (Sigma) diluted 1:10,000 in TBST for 30 min at room temperature. After being washed, proteins were detected using an enhanced chemiluminescence system (Amersham Life Science) and visualized through autoradiography. Antibodies used for Western blot assay are goat anti-RSV (Ab D SeroTec) and rabbit anti-p65, anti-Ser^{536} p65, and anti-IRF-3 (Cell Signaling Technology, Danvers, MA).

Biochemical assays. Catalase, GPx, and SOD activities were determined using specific kits (catalog nos. 707002, 703102, and 706002, respectively, for catalase, GPx, and SOD; Cayman Chemical), according to the manufacturer's instructions, as previously described (17).

Bio-Plex. Cell-free supernatant from EUK-8 and EUK-189-treated and virus- and mock-infected A549 and SAE cells were collected at 24 h postinfection to measure the production of cytokines and chemokines. Samples were tested for multiple cytokines using the Bio-Plex Cytokine Human Multi-Plex panel (Bio-Rad Laboratories, Hercules, CA) according to the manufacturer's instructions. IL-8 and RANTES were also quantified by enzyme-linked immunosorbent assay following the manufacturer's protocol (DuoSet; R&D Systems, Minneapolis, MN).

Statistics. A two-tailed Student's *t*-test using 95% confidence levels was used when comparison of two groups was performed, whereas one-way ANOVA was used for multiple group comparison. Significance is designated by the following: $*P < 0.05$ and $**P < 0.01$.

RESULTS

Antioxidant mimetic treatment increases total SOD, catalase, and GPx enzyme activities in RSV-infected A549 cells. In recent investigations, we have shown that RSV infection of AECs induces a significant decrease in SOD 1, SOD 3, catalase, and glutathione *S*-transferase (GST) expression with a concomitant increase of SOD 2. Total SOD activity was

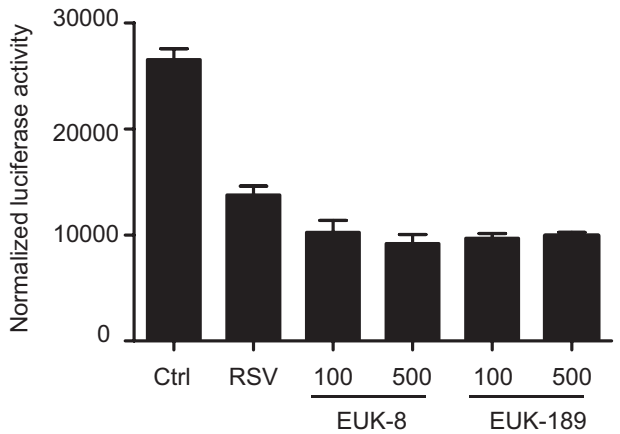

Fig. 2. Effect of EUK treatment on NF-E2-related factor 2-dependent gene transcription. A549 cells were transiently transfected with an airway epithelial cell-luciferase reporter plasmid and β-galactosidase control plasmid. The next day, cells were infected with RSV in the presence or absence of either EUK-8 or -189, at 100 or 500 μM concentration, and harvested at 24 h postinfection to measure luciferase activity. Uninfected plates served as controls. For each plate, luciferase was normalized to the β-galactosidase activity. Data are expressed as means ± SE of normalized luciferase activity. Data are representative of two independent experiments performed in triplicates.

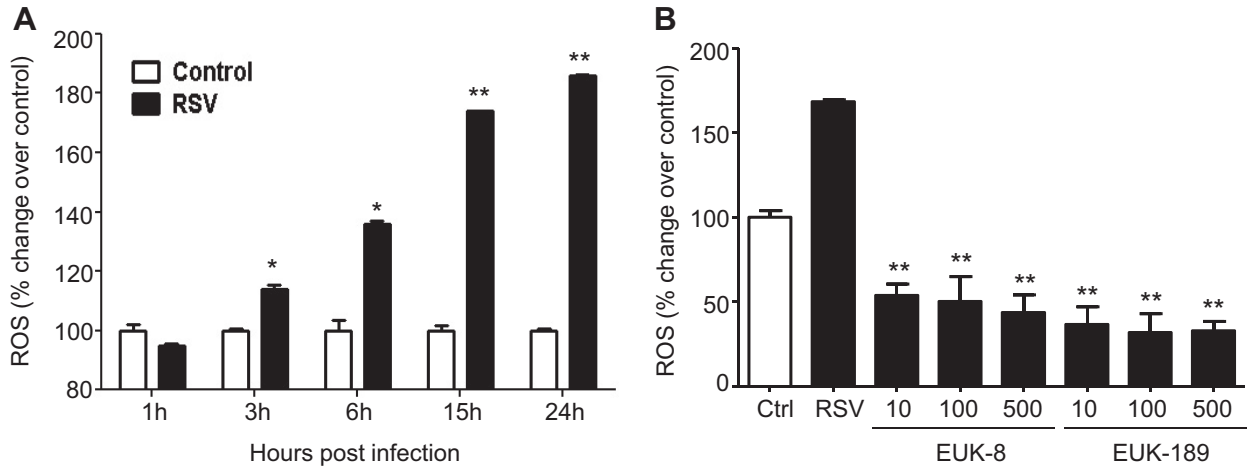

Fig. 3. Effect of EUK treatment on RSV-induced reactive oxygen species (ROS) formation and cellular oxidative stress. *A*: A549 cells were infected with RSV and, at various time points after infection, cells were loaded with 2′,7′-dichlorodihydro-fluorescein diacetate (DCF-DA), and fluorescence was measured in control and infected cells. $*P < 0.05$ and $**P < 0.01$ compared with control cells. *B*: A549 cells were treated with different μM concentrations of EUK-8 and EUK-189, infected with RSV for 24 h, and harvested to measure DCF-DA fluorescence. Ctrl, control, uninfected cells. Mean fluorescence intensity is reported as % increase over control. Results are representative of two independent experiments. $*P < 0.05$ and $**P < 0.01$ compared with untreated RSV-infected cells.

increased, but catalase, GPx, and GST activities, needed to detoxify H_2O_2 produced by SOD, were decreased following RSV infection (17). In this study, we tested whether treatment with the antioxidant mimetics EUK-8 and -189, which possess significant catalase and peroxidase activity in addition to SOD, could restore AOE capacity in RSV-infected AECs and thereby exert a protective effect against RSV-induced oxidative stress.

A549 cells were treated 1 h before infection and throughout the length of infection with increasing concentration of EUK and infected with RSV. Cells were harvested at a different time postinfection to measure AOE activity in the presence or absence of EUK treatment. RSV infection induced a progressive increase in SOD activity with a concomitant decrease in catalase and peroxidase activity (Fig. 1). EUK-8 treatment further increased SOD activity but, more importantly, reversed the loss of catalase and peroxidase activity observed in response to RSV infection, with the highest dose of EUK-8 increasing the latter two AOE activities above values of uninfected cells (Fig. 1). Similar results were obtained in cells treated with EUK-189 (data not shown).

Transcription of many oxidative stress-inducible genes, including AOEs, is regulated in part through *cis*-acting antioxidant responsive element (ARE) sequences. Nrf2 is an important redox-responsive protein that binds to ARE promoter elements to induce gene transcription (19). We have recently shown that RSV infection decreases nuclear levels of Nrf2 in AECs (17), as well as in the lungs of infected mice (16), and reduces ARE-dependent gene transcription (12). To determine whether changes in AOE activity observed with EUK treatment affected Nrf2-dependent gene transcription and endogenous AOE expression, we performed reporter gene assays. A549 cells were transfected with an artificial ARE-driven promoter, linked to the luciferase reporter gene, and infected with RSV in the presence or absence of EUKs. As previously shown, RSV infection induced a substantial decrease in Nrf2-driven gene transcription, demonstrated by the decrease in

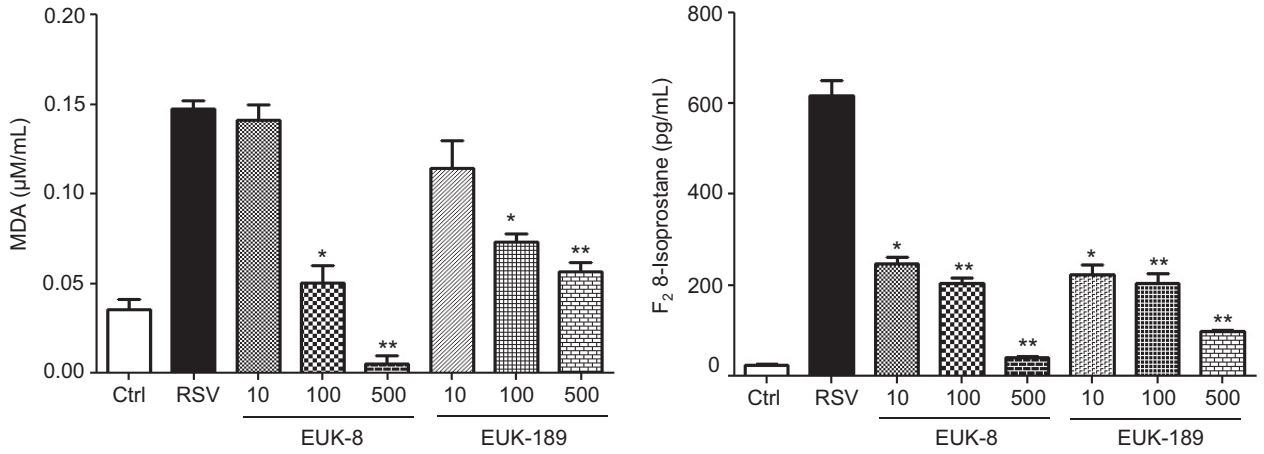

Fig. 4. Effect of EUK treatment on RSV-induced lipid peroxidation. A549 cells were treated with different μM concentrations of EUK-8 and EUK-189 and infected with RSV. Cell supernatants were harvested at 24 h postinfection to measure F_2-isoprostanes and malondialdehyde (MDA). Results are expressed as means ± SE. Results are representative of two independent experiments run in triplicate. $*P < 0.05$ and $**P < 0.01$ compared with untreated RSV-infected cells.

luciferase activity, which was not rescued by EUK treatment (Fig. 2). In addition, we did not observe a significant increase in endogenous AOE protein levels in cells infected with RSV and treated with EUK (data not shown), suggesting that the increased AOE activities in EUK-treated cells are not due to an increase in the endogenous enzymes.

Effects of antioxidant mimetics on RSV-induced ROS formation and cellular oxidative stress. To determine whether EUK treatment could reduce RSV-induced ROS production and cellular oxidative stress, A549 cells were treated with different concentrations of the two antioxidant mimetics either 1 h before and throughout the length of infection, or at a different time postinfection Cells were harvested at 24 h postinfection to measure ROS generation and concentration of the lipid peroxidation markers MDA and F_2-8-isoprostane. As previously reported (6), RSV infection of AECs induced a time-dependent increase in ROS generation, starting between 1 and 3 h postinfection (Fig. 3*A*), which was significantly reduced by pretreatment with both EUK-8 and EUK-189, in a dose-dependent manner (Fig. 3*B*). In agreement with the observed reduction in ROS production, EUK pretreatment of AECs significantly decreased the elevated cellular levels of the lipid peroxidation

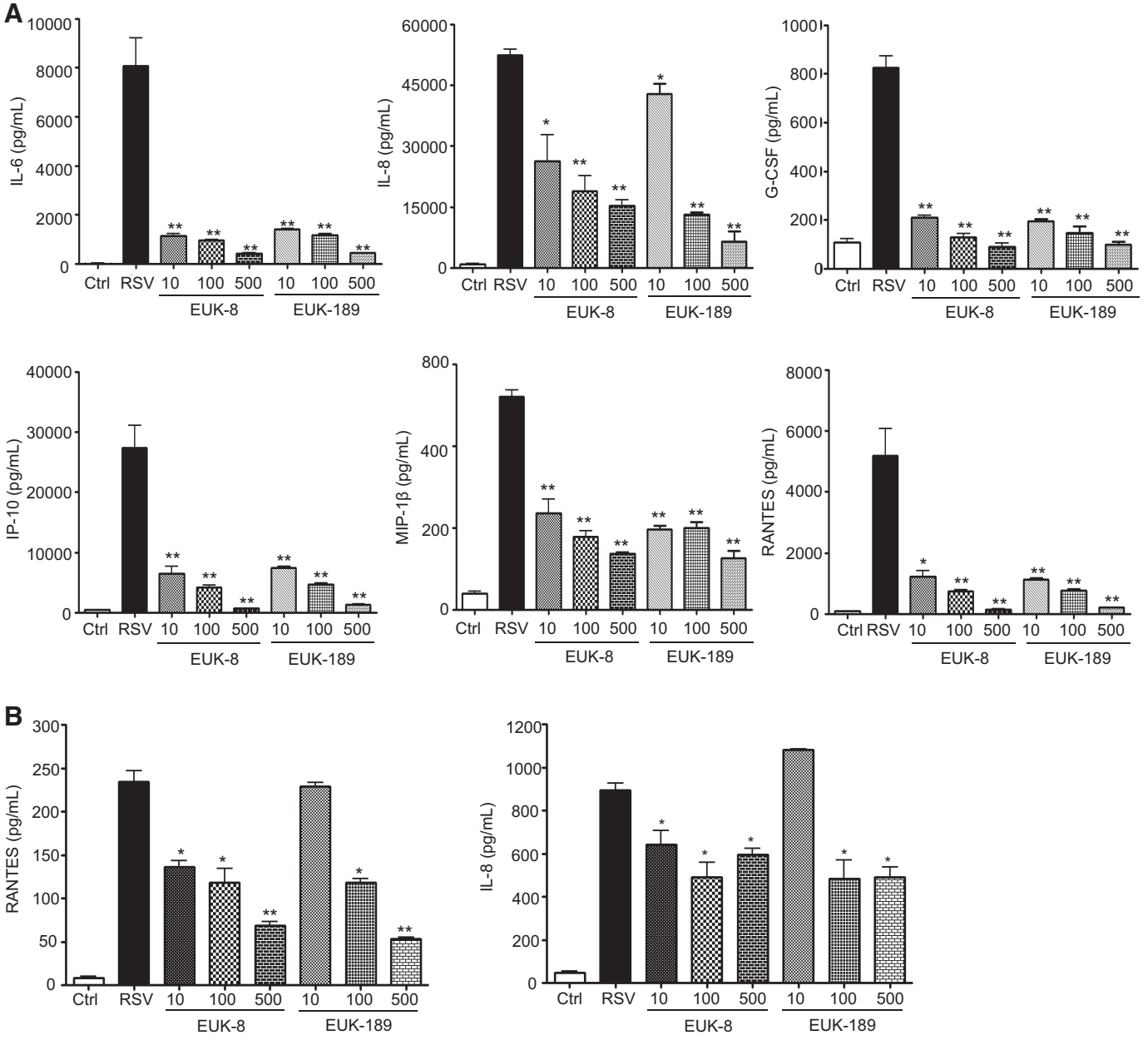

Fig. 5. Effect of EUK treatment on RSV-induced cytokine and chemokine production. A549 cells (*A*) or small alveolar epithelial (SAE) cells (*B*) were infected with RSV in the absence or presence of different μM concentrations of EUK-8 and EUK-189. Cell supernatants from uninfected and RSV-infected, treated or untreated, were assayed at 24 h postinfection for cytokine and chemokine secretion by Bio-Plex. IL, interleukin; G-CSF, granulocyte colony-stimulating factor; IP-10, interferon-induced protein-10; MIP-1β, macrophage inflammatory protein-1β; RANTES, regulated on activation normal T cell expressed and secreted. Results are expressed as means ± SE. Results are representative of two independent experiments run in triplicate. $^*P < 0.05$ and $^{**}P < 0.01$ compared with untreated RSV-infected cells.

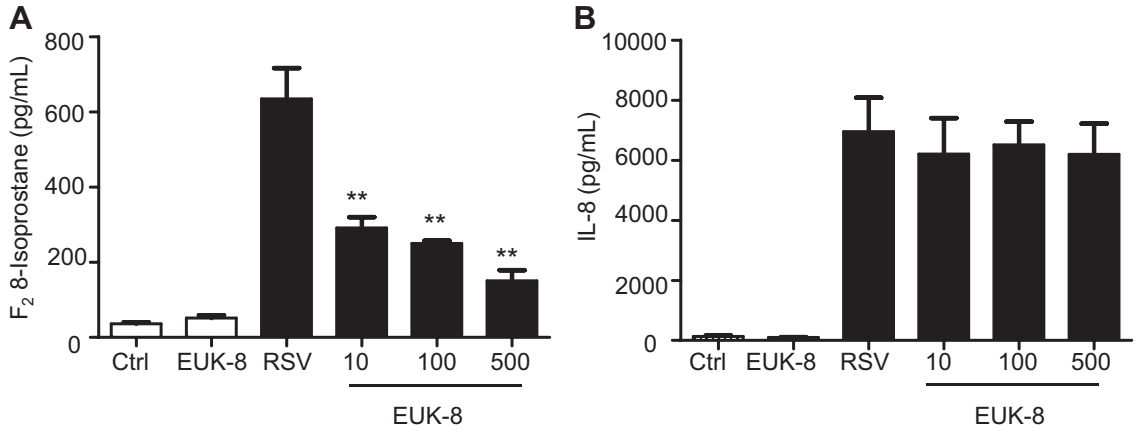

Fig. 6. Effect of EUK postinfection treatment on RSV-induced lipid peroxidation and IL-8 secretion. A549 cells were treated with different μM concentrations of EUK-8 at 3 h postinfection and harvested at 24 h postinfection to measure 8-isoprostane (*A*) and IL-8 (*B*). Results are expressed as means ± SE. Results are representative of two independent experiments run in triplicate. $^{**}P < 0.01$ compared with untreated RSV-infected cells.

markers MDA and 8-isoprostane generated in response to RSV infection (Fig. 4), indicating that antioxidant mimetic pretreatment can effectively counteract viral-induced cellular oxidative stress. EUK treatment was still effective, leading to a significant reduction in 8-isoprostane generation, even after RSV infection was established (see Fig. 6*A*).

Effects of antioxidant mimetics on RSV-induced cellular signaling. Because ROS generation plays a key role in RSV-induced cellular signaling, leading to transcription factor activation and expression of proinflammatory mediators (6, 20, 26), we investigated the effect of EUK treatment on viral-induced cytokine and chemokine secretion. A549 cells were treated either 1 h before and throughout the length of infection or at a different time postinfection with increasing concentrations of EUK-8 and -189 and infected with RSV. Cell supernatants were collected to measure levels of various cytokines and chemokines by Bio-Plex assay. As shown in Fig. 5*A*, EUK pretreatment caused a dose-dependent decrease in several cytokines, such as IL-6 and granulocyte colony-stimulating factor, and chemokines, such as IL-8, RANTES, macrophage inflammatory protein-1β (MIP-1β), and interferon-induced protein-10. Similar results were obtained in SAE cells, normal human AECs derived from cadaveric donor, which we have previously shown to behave very similarly to A549 cells in terms of chemokine/cytokine gene expression and transcription factor and signaling pathway activation after RSV infection (2, 6, 13, 16, 30, 32, 41) (Fig. 5*B*). On the other hand, administration of EUKs, when infection was already established, was not able to reduce proinflammatory mediator production, as shown for IL-8 in Fig. 6*B*.

Cytokine and chemokine gene expression in AECs infected by RSV is orchestrated by activation of two key transcription factors, nuclear factor (NF)-κB and interferon regulatory factor (IRF)-3. A number of RSV-inducible inflammatory and immunoregulatory genes require NF-κB for their transcription and/or are dependent on an intact NF-κB signaling pathway (4, 38), and IRF-3 is necessary for viral induction of RANTES transcription and gene expression (25). We have previously shown that treatment of AECs with the antioxidant butylated hydroxyanisole blocks RSV-induced IRF-3 nuclear translocation and DNA binding to the RANTES interferon-stimulated responsive element (6), an event required for RSV-induced RANTES gene transcription. We have also shown that the antioxidants *N*-acetylcysteine or dimethyl sulfoxide significantly reduce RSV-dependent serine phosphorylation of the NF-κB subunit p65,

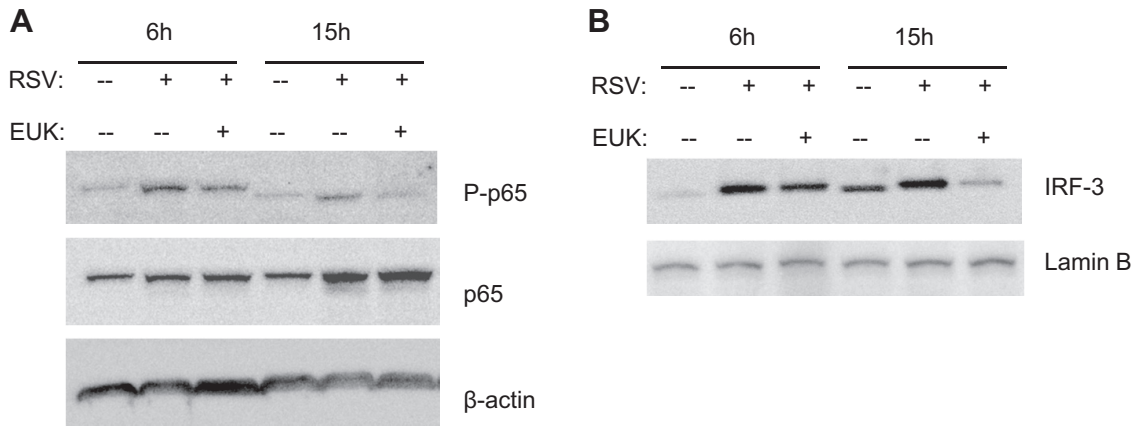

Fig. 7. Effect of EUK treatment on RSV-induced interferon regulatory factor (IRF)-3 and p65 activation. Total cell lysates (*A*) or nuclear extracts (*B*) were prepared from A549 cells, control and infected with RSV for 6 and 15 h, in the absence or presence of 100 μM EUK-8 and assayed for p65 phosphorylation and IRF-3 nuclear levels, respectively, by Western blot. Membranes were stripped and reprobed for either β-actin or lamin b as a control for equal loading of the samples. Blot is representative of two independent experiments with similar results.

resulting in the inhibition of RSV-induced expression of several NF-κB-dependent genes, without affecting its nuclear translocation (20). To determine whether EUK treatment was able to modulate viral-induced NF-κB and IRF-3 activation, A549 cells were pretreated with 100 μM EUK-8, infected with RSV, and harvested at 6 and 15 h postinfection to prepare either total cell lysates or nuclear extracts. IRF-3 nuclear levels or cellular levels of p65 serine phosphorylation were assessed by Western blot. As shown in Fig. 7, EUK-8 pretreatment significantly reduced activation of both transcription factors, in particular at the 15-h time point of infection. Taken together, these results indicate that increasing antioxidant cellular defenses can effectively modulate the strong proinflammatory cellular response induced by RSV infection.

Effects of antioxidant mimetics on viral replication. To determine whether antioxidant mimetic treatment of A549 cells affected viral replication, we used several approaches, including quantification of viral gene transcription, direct cell-based plaque immunostaining (23) and viral antigen detection, and determination of released infectious particles in the cell supernatants. As shown in Fig. 8*A*, there was no significant difference in the number of RSV N gene copies between untreated and EUK-pretreated cells at any given concentration. To further characterize the antiviral activity of EUKs, we assessed the expression of RSV proteins by Western blot. A549 cells were pretreated with different concentrations of EUKs and infected with RSV. At 24 h postinfection, cell extracts were prepared, and RSV proteins were detected by Western blot using a polyclonal antibody, as described previously (23). In RSV-infected cells, viral proteins, including G, N, P, and M, were expressed at comparable levels in untreated and EUK-treated cells using concentrations of 10 and 100 μM, whereas significant lower (EUK-189) or almost no expression (EUK-8) of RSV proteins was detected in infected cells treated with 500 μM of both compounds (Fig. 8*B*). A similar result was observed when the number of plaques was detected by direct immunostaining of infected cells (Fig. 8*C*). In addition, both 100 and 500 μM concentrations of EUK-8 significantly reduced virus infectious particle release from AECs, as shown by the decreased viral titers in cell supernatants (Fig. 8*D*). The reduction in viral replication was not due to cellular toxicity, as shown by LDH release assay in Fig. 9. Taken together, these results suggest that EUKs impair viral replication at a step

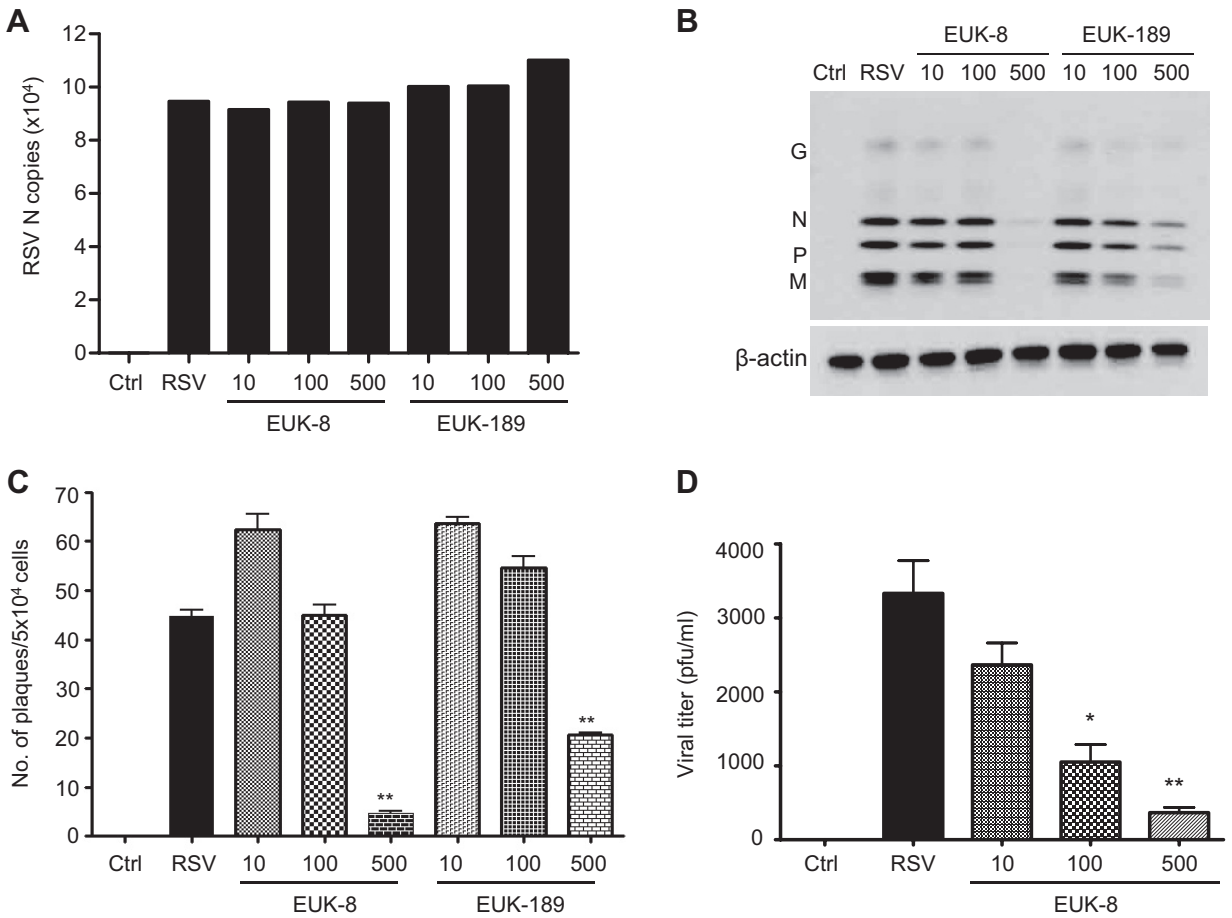

Fig. 8. Effect of EUK treatment on viral replication. A549 cells were treated with different μM concentrations of EUK-8 and EUK-189, followed by infection with RSV. Cells were harvested at 24 h postinfection to prepare either total RNA to measure RSV N gene copies by real-time PCR (*A*) or total cell lysates to detect RSV proteins by Western blot. Membrane was stripped and reprobed with β-actin as a control for equal loading of the samples (*B*). Figures are representative of two independent experiments with similar results. A549 cells were treated with different μM concentrations of EUK-8 and EUK-189 followed by infection with RSV at a multiplicity of infection of 0.01. Viral replication was determined 24 h postinfection by either direct immunostaining (*C*) or by titration of viral infectious particles released in the cell supernatants by plaque assay (*D*). Data are representative of two independent experiments with similar results. $^{*}P < 0.05$ and $^{**}P < 0.01$ compared with untreated RSV-infected cells.

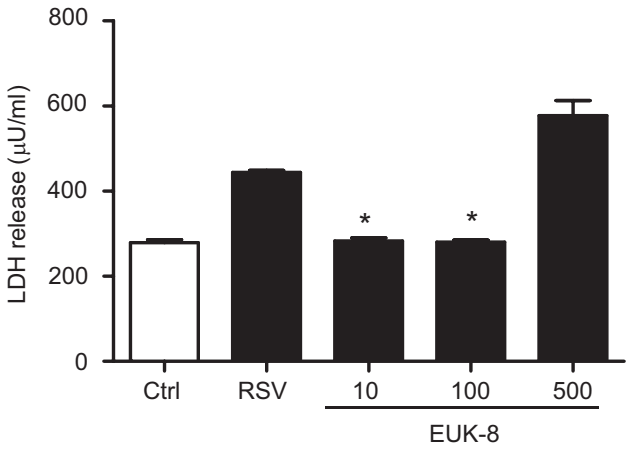

Fig. 9. Effect of EUK treatment on RSV-induced lactate dehydrogenase (LDH) release. A549 cells were infected with RSV in the absence or presence of different μM concentrations of EUK-8. Cell supernatants from uninfected and RSV infected, treated or untreated, were assayed at 24 h postinfection for LDH activity. Results are expressed as means ± SE. Results are representative of two independent experiments run in triplicate. *$P < 0.05$ compared with untreated, RSV-infected cells.

subsequent to virus cellular binding and entry, and after initiation of viral gene transcription.

DISCUSSION

Free radicals and ROS have been shown to function as cellular signaling molecules influencing a variety of molecular and biochemical processes, including expression of proinflammatory mediators, such as cytokines and chemokines (reviewed in Ref. 1). However, excessive ROS formation can lead to a condition of oxidative stress, which has been implicated in the pathogenesis of several acute and chronic airway diseases, such as asthma and chronic obstructive pulmonary disease (reviewed in Refs. 9 and 10). Inducible ROS generation has been shown following stimulation with a variety of molecules and infection with certain viruses like human immunodeficiency virus, hepatitis B, influenza, and rhinovirus (reviewed in Ref. 36). In the past few years, we have shown that RSV infection of AECs induces ROS production, in part through an NAD(P)H oxidase-dependent mechanism, inducing oxidative stress in vitro (17) and in vivo (8), which correlates with severity of disease (16), and that antioxidant treatment blocks transcription factor activation and chemokine gene expression in vitro (6, 18, 26) and ameliorates RSV-induced clinical illness in vivo (8), indicating a central role of ROS in RSV-induced cellular signaling and lung disease. RSV infection leads to a significant decrease in the expression and activity of AOEs in AECs, lungs of RSV-infected mice, as well as in children with severe RSV-induced LRTI (16, 17), likely because of decreased activation of Nrf2 (16, 17), which regulates basal and inducible expression of AOE genes (19), suggesting that oxidative damage associated with RSV infection results from an imbalance between ROS production and antioxidant cellular defenses.

Based on this strong supportive evidence that RSV-induced intracellular ROS formation regulates the expression of proinflammatory mediators and that oxidative stress likely represents an important pathogenetic mechanism of RSV-induced lung disease, antioxidant intervention would represent a rational approach for treatment of RSV LRTI. Two complementary approaches could be used to affect the outcome of RSV-associated LRTI. The first would be to increase airway antioxidant defenses by modulation of AOE expression/activity, and the second would be by enhancing nonenzymatic defenses through pharmacological intervention with molecules able to scavenge/detoxify ROS. Approaches that combine scavenging ROS by administration of antioxidant compounds or compounds able to increase lung antioxidant defenses, such as AOE mimetics or Nrf2 inducers, together with inhibitors of viral replication would likely be the most effective in modulating severe lung disease associated with RSV infection.

In the past few years, several classes of synthetic antioxidant mimetics have been generated and tested as a potential therapeutic approach to oxidant-related lung damage. The salen class of AOE mimetics includes compounds that have mainly SOD activity as well as compounds that, in addition, exhibit catalase and peroxidase activity. These molecules have been shown to be effective in preventing lung injury in animal models of oxidative stress, as well as to protect against damage of other organs, such as heart, kidney, and liver (reviewed in Ref. 22). EUK-8 administration has been shown to ameliorate LPS-induced lung injury in a porcine model of endotoxemia (14, 15) and to mitigate lung radiation injury (34). In this study, we found that pretreatment of AECs with EUK-8 and -189 effectively restored catalase and GPx enzyme activities, which were significantly decreased in response to RSV infection, leading to reduced viral-induced ROS production and generation of the lipid peroxidation markers isoprostanes and MDA, as well as reduced activation of the ROS-dependent signaling pathway involved in NF-κB and IRF-3 activation and proinflammatory gene expression. Administration of EUKs when infection was fully established was effective primarily in reducing cellular oxidative stress, but not in blocking ROS-dependent cellular signaling. This is the first report of the effect of EUKs on oxidative stress in a model of viral infection. We had previously reported that treatment of epithelial cells with EUK-134, which is similar to EUK-8 and -189, but not EUK-163, which lacks catalase or peroxidase activity, significantly inhibited RSV-induced IL-8 and RANTES secretion (17). This suggests that enhancement of cellular SOD activity alone in response to RSV infection cannot modulate ROS-mediated signaling and subsequent viral-induced gene expression, whereas increasing the levels of catalase and/or peroxidase activity is beneficial in reducing proinflammatory gene expression.

In addition, both EUKs were able to significantly reduce viral replication, which also represents a novel finding for this type of antioxidant compounds. We and others did not observe a similar effect when AECs were treated with other classes of antioxidants, such as *N*-acetylcysteine or dimethyl sulfoxide (20, 28). These initial studies suggest that EUK antiviral activity might affect different steps of the viral replication cycle, from viral protein synthesis to viral assembly and release. Cytoskeletal proteins, such as actin, play an important role in various stages of RSV replication (21), and their function is known to be affected by ROS production (37); therefore, it is possible that changes in specific ROS species, following EUK administration, lead to alteration in cytoskeletal structures, affecting ultimately viral replication. A previous report on administration of SOD 1 and 2 in a rodent model of RSV infection showed a significant reduction in lung viral titers, supporting the concept that increased SOD expression/activity can indeed be associated with antiviral activity

(40). These results, together with our previous finding that antioxidant treatment attenuates symptoms and pathology in RSV infection (8), warrant further investigation of AOE mimetics as a novel therapeutic approach to modulate viral-induced pulmonary disease. Antioxidant supplementation would be successful only if available at the site of infection/inflammation; therefore, route of administration, bioavailability, and tissue distribution are all important parameters that will need to be taken into consideration when planning future therapeutic intervention.

ACKNOWLEDGMENTS

We thank Susan Doctrow for the generous gift of the EUKs and Cynthia Tribble for assistance in manuscript editing and submission.

GRANTS

This work was supported by National Institutes of Health Grants AI-062885 and N01 HV-00245; by Department of Defense Grant W81XWH1010146; and by Flight Attendant Medical Research Institute Clinical Innovator Awards to A. C (no. 072147) and R. P. G (no. 42253).

DISCLOSURES

No conflicts of interest, financial or otherwise are declared by the authors.

AUTHOR CONTRIBUTIONS

Author contributions: Y.M.H., N.K., N.M., T.L., and A.C. performed experiments; Y.M.H. and A.C. analyzed data; Y.M.H. and A.C. prepared figures; R.P.G. and A.C. conception and design of research; R.P.G. and A.C. interpreted results of experiments; R.P.G. and A.C. edited and revised manuscript; R.P.G. and A.C. approved final version of manuscript; A.C. drafted manuscript.

REFERENCES

1. **Allen RG, Tresini M.** Oxidative stress and gene regulation. *Free Rad Biol Med* 28: 463–499, 2000.
2. **Bao X, Liu T, Spetch L, Kolli D, Garofalo RP, Casola A.** Airway epithelial cell response to human metapneumovirus infection. *Virology* 368: 91–101, 2007.
3. **Batinic-Haberle I, Reboucas JS, Spasojevic I.** Superoxide dismutase mimics: chemistry, pharmacology, and therapeutic potential. *Antioxid Redox Signal* 13: 877–918, 2010.
4. **Bitko V, Velazquez A, Yank L, Yang YC, Barik S.** Transcriptional induction of multiple cytokines by human respiratory syncytial virus requires activation of NF-kB and is inhibited by sodium salicylate and aspirin. *Virology* 232: 369–378, 1997.
5. **Brasier AR, Spratt H, Wu Z, Boldogh I, Zhang Y, Garofal RP, Casola A, Pashmi J, Haag A, Luxon B, Kurosky A.** Nuclear heat shock response and novel nuclear domain 10 reogranization in respiratory syncytial virus-infected A549 cells identified by high resolution 2D gel electrophoresis. *J Virol* 78: 11461–11476, 2004.
6. **Casola A, Burger N, Liu T, Jamaluddin M, Brasier AR, Garofal RP.** Oxidant tone regulates RANTES gene transcription in airway epithelial cells infected with respiratory syncytial virus: role in viral-induced interferon regulatory factor activation. *J Biol Chem* 276: 19715–19722, 2001.
7. **Casola A, Garofalo RP, Jamaluddin M, Vlahopoulos S, Brasier AR.** Requirement of a novel upstream response element in RSV induction of interleukin-8 gene expression: stimulus-specific differences with cytokine activation. *J Immunol* 164: 5944–5951, 2000.
8. **Castro SM, Guerrero-Plata A, Suarez-Real G, Adegboyega PA, Colasurdo GN, Khan AM, Garofalo RP, Casola A.** Antioxidant treatment ameliorates respiratory syncytial virus-induced disease and lung inflammation. *Am J Respir Crit Care Med* 174: 1361–1369, 2006.
9. **Ciencewicki J, Trivedi S, Kleeberger SR.** Oxidants and the pathogenesis of lung diseases. *J Allergy Clin Immunol* 122: 456–468, 2008.
10. **Folkerts G, Kloek J, Muijsers RB, Nijkamp FP.** Reactive nitrogen and oxygen species in airway inflammation. *Eur J Pharmacol* 429: 251–262, 2001.
11. **Gabbita SP, Robinson KA, Stewart CA, Floyd RA, Hensley K.** Redox regulatory mechanisms of cellular signal transduction. *Arch Biochem Biophys* 376: 1–13, 2000.
12. **Garofalo R, Kolli D, Casola A.** Respiratory syncytial virus infection: mechanisms of redox control and novel therapeutic opportunities. *Antioxid Redox Signal* Sep 7 [Epub ahead of print] 2012.
13. **Garofalo RP, Sabry M, Jamaluddin M, Yu RK, Casola A, Ogra PL, Brasier AR.** Transcriptional activation of the interleukin-8 gene by respiratory syncytial virus infection in alveolar epithelial cells: Nuclear translocation of the RelA transcription factor as a mechanism producing airway mucosal inflammation. *J Virol* 70: 8773–8781, 1996.
14. **Gonzalez PK, Zhuang J, Doctrow SR, Malfroy B, Benson PF, Menconi MJ, Fink MP.** EUK-8, a synthetic superoxide dismutase and catalase mimetic, ameliorates acute lung injury in endotoxemic swine. *J Pharmacol Exp Ther* 275: 798–806, 1995.
15. **Gonzalez PK, Zhuang J, Doctrow SR, Malfroy B, Benson PF, Menconi MJ, Fink MP.** Role of oxidant stress in the adult respiratory distress syndrome: evaluation of a novel antioxidant strategy in a porcine model of endotoxin-induced acute lung injury. *Shock* 6, *Suppl* 1: S23–S26, 1996.
16. **Hosakote YM, Jantzi PD, Esham DL, Spratt H, Kurosky A, Casola A, Garofalo RP.** Viral-mediated inhibition of antioxidant enzymes contributes to the pathogenesis of severe respiratory syncytial virus bronchiolitis. *Am J Respir Crit Care Med* 183: 1550–1560, 2011.
17. **Hosakote YM, Liu T, Castro SM, Garofalo RP, Casola A.** Respiratory syncytial virus induces oxidative stress by modulating antioxidant enzymes. *Am J Respir Cell Mol Biol* 41: 348–357, 2009.
18. **Indukuri H, Castro SM, Liao SM, Feeney LA, Dorsch M, Coyle AJ, Garofalo RP, Brasier AR, Casola A.** Ikkepsilon regulates viral-induced interferon regulatory factor-3 activation via a redox-sensitive pathway. *Virology* 353: 155–165, 2006.
19. **Jaiswal AK.** Nrf2 signaling in coordinated activation of antioxidant gene expression. *Free Radic Biol Med* 36: 1199–1207, 2004.
20. **Jamaluddin M, Tian B, Boldogh I, Garofalo RP, Brasier AR.** Respiratory syncytial virus infection induces a reactive oxygen species-MSK1-phospho-Ser-276 RelA pathway required for cytokine expression. *J Virol* 83: 10605–10615, 2009.
21. **Kallewaard NL, Bowen AL, Crowe JE Jr.** Cooperativity of actin and microtubule elements during replication of respiratory syncytial virus. *Virology* 331: 73–81, 2005.
22. **Kinnula VL, Crapo JD.** Superoxide dismutases in the lung and human lung diseases. *Am J Respir Crit Care Med* 167: 1600–1619, 2003.
23. **Lai SH, Stein DA, Guerrero-Plata A, Liao SL, Ivanciuc T, Hong C, Iversen PL, Casola A, Garofalo RP.** Inhibition of respiratory syncytial virus infections with morpholino oligomers in cell cultures and in mice. *Mol Ther* 16: 1120–1128, 2008.
24. **Leader S, Kohlhase K.** Respiratory syncytial virus-coded pediatric hospitalizations, 1997 to 1999. *Pediatr Infect Dis J* 21: 629–632, 2002.
25. **Lin R, Heylbroeck C, Genin P, Pitha PM, Hiscott J.** Essential role of interferon regulatory factor 3 in direct activation of RANTES chemokine transcription. *Mol Cell Biol* 19: 959–966, 1999.
26. **Liu T, Castro S, Brasier AR, Jamaluddin M, Garofalo RP, Casola A.** Reactive oxygen species mediate virus-induced STAT activation: role of tyrosine phosphatases. *J Biol Chem* 279: 2461–2469, 2004.
27. **MacNee W.** Oxidative stress and lung inflammation in airways disease. *Eur J Pharmacol* 429: 195–207, 2001.
28. **Mastronarde JG, Monick MM, Hunninghake GW.** Oxidant tone regulates IL-8 production in epithelium infected with respiratory syncytial virus. *Am J Respir Cell Mol Biol* 13: 237–244, 1995.
29. **Morcillo EJ, Estrela J, Cortijo J.** Oxidative stress and pulmonary inflammation: pharmacological intervention with antioxidants. *Pharmacol Res* 40: 393–404, 1999.
30. **Olszewska-Pazdrak B, Casola A, Saito T, Alam R, Crowe SE, Mei F, Ogra PL, Garofalo RP.** Cell-specific expression of RANTES, MCP-1, and MIP-1alpha by lower airway epithelial cells and eosinophils infected with respiratory syncytial virus. *J Virol* 72: 4756–4764, 1998.
31. **Patel JA, Kunimoto M, Sim TC, Garofalo R, Eliott T, Baron S, Ruuskanen O, Chonmaitree T, Ogra PL, Schmalstieg F.** Interleukin-1 alpha mediates the enhanced expression of intercellular adhesion molecule-1 in pulmonary epithelial cells infected with respiratory syncytial virus. *Am J Respir Cell Mol* 13: 602–609, 1995.
32. **Pazdrak K, Olszewska-Pazdrak B, Liu B, Takizawa R, Brasier AR, Garofalo RP, Casola A.** MAP-kinase activation is involved in post-transcriptional regulation of RSV-induced RANTES gene expression. *Am J Physiol Lung Cell Mol Physiol* 283: L364–L372, 2002.
33. **Rahman I, Morrison D, Donaldson K, MacNee W.** Systemic oxidative stress in asthma, COPD, and smokers. *Am J Respir Crit Care Med* 154: 1055–1060, 1996.

34. **Rosenthal RA, Fish B, Hill RP, Huffman KD, Lazarova Z, Mahmood J, Medhora M, Molthen R, Moulder JE, Sonis ST, Tofilon PJ, Doctrow SR.** Salen Mn complexes mitigate radiation injury in normal tissues. *Anticancer Agents Med Chem* 11: 359–372, 2011.
35. **Schreiber E, Matthias P, Muller MM, Schaffner W.** Rapid detection of octamer binding proteins with 'mini-extracts', prepared from a small number of cells (Abstract). *Nucleic Acids Res* 17: 6419, 1989.
36. **Schwarz KB.** Oxidative stress during viral infection: a review. *Free Rad Biol Med* 21: 641–649, 1996.
37. **Taulet N, Delorme-Walker VD, Dermardirossian C.** Reactive oxygen species regulate protrusion efficiency by controlling actin dynamics. *PLoS ONE* 7: e41342, 2012.
38. **Tian B, Zhang Y, Luxon B, Garofalo RP, Casola A, Sinha M, Brasier AR.** Identification of NF-kB dependent gene networks in respiratory syncytial virus-infected cells. *J Virol* 76: 6800–6814, 2002.
39. **Ueba O.** Respiratory syncytial virus. I. Concentration and purification of the infectious virus. *Acta Med Okayama* 32: 265–272, 1978.
40. **Wyde PR, Moore DK, Pimentel DM, Gilbert BE, Nimrod R, Panet A.** Recombinant superoxide dismutase (SOD) administered by aerosol inhibits respiratory syncytial virus infection in cotton rats. *Antiviral Res* 31: 173–184, 1996.
41. **Zhang Y, Luxon B, Casola A, Garofalo RP, Jamaluddin M, Brasier AR.** Expression of RSV-induced chemokine gene networks in lower airway epithelial cells revealed by cDNA microarrays. *J Virol* 75: 9044–9058, 2001.

Free Radical Biology and Medicine 88 (2015) 391–403

Contents lists available at ScienceDirect

Free Radical Biology and Medicine

journal homepage: www.elsevier.com/locate/freeradbiomed

Respiratory syncytial virus infection down-regulates antioxidant enzyme expression by triggering deacetylation-proteasomal degradation of Nrf2

Narayana Komaravelli [a], Bing Tian [b], Teodora Ivanciuc [a], Nicholas Mautemps [a], Allan R. Brasier [b,c], Roberto P. Garofalo [a], Antonella Casola [a,c,*]

[a] Department of Pediatrics, University of Texas Medical Branch at Galveston, TX 77555, USA
[b] Department of Internal Medicine, University of Texas Medical Branch at Galveston, TX 77555, USA
[c] Department of Sealy Center for Molecular Medicine, University of Texas Medical Branch at Galveston, TX 77555, USA

ARTICLE INFO

Article history:
Received 23 January 2015
Received in revised form
21 May 2015
Accepted 27 May 2015
Available online 11 June 2015

Keywords:
Respiratory syncytial virus
ROS
Oxidative stress
Antioxidant enzymes
Nrf2
Acetylation
Proteasome

ABSTRACT

Respiratory syncytial virus (RSV) is the most important cause of viral acute respiratory tract infections and hospitalizations in children, for which no vaccine or treatment is available. RSV infection in cells, mice, and children leads to rapid generation of reactive oxygen species, which are associated with oxidative stress and lung damage, due to a significant decrease in the expression of airway antioxidant enzymes (AOEs). Oxidative stress plays an important role in the pathogenesis of RSV-induced lung disease, as antioxidants ameliorate clinical disease and inflammation in vivo. The aim of this study is to investigate the unknown mechanism(s) of virus-induced inhibition of AOE expression. RSV infection is shown to induce a progressive reduction in nuclear and total cellular levels of the transcription factor NF-E2-related factor 2 (Nrf2), resulting in decreased binding to endogenous AOE gene promoters and decreased AOE expression. RSV induces Nrf2 deacetylation and degradation via the proteasome pathway in vitro and in vivo. Histone deacetylase and proteasome inhibitors block Nrf2 degradation and increase Nrf2 binding to AOE endogenous promoters, resulting in increased AOE expression. Known inducers of Nrf2 are able to increase Nrf2 activation and subsequent AOE expression during RSV infection in vitro and in vivo, with significant amelioration of oxidative stress. This is the first study to investigate the mechanism(s) of virus-induced inhibition of AOE expression. RSV-induced inhibition of Nrf2 activation, due to deacetylation and proteasomal degradation, could be targeted for therapeutic intervention aimed to increase airway antioxidant capacity during infection.

1. Introduction

Respiratory syncytial virus (RSV) is the single most important virus causing acute respiratory tract infections in children, with an estimated 40–90% of children with bronchiolitis and 25–50% of children with viral pneumonia infected with RSV [1]. It is also a major cause of severe respiratory morbidity and mortality in the elderly [2], being responsible for 64 million clinical infections and 160 thousand deaths annually worldwide [3]. In addition to acute morbidity, RSV infection has been linked to both the development and the severity of asthma. No vaccine or effective treatment is currently available for RSV. In a series of in vitro and in vivo studies, over the past few years, we have discovered that in the course of RSV infection, reactive oxygen species (ROS) are rapidly generated, and they are associated with cellular oxidative damage, indicated by an increase in lipid peroxidation, lung inflammation, and clinical disease [4–6]. RSV-induced ROS formation also controls inducible expression of chemokine and other inflammatory genes in response to infection [7,8]. Antioxidant treatment significantly ameliorates RSV-induced clinical disease and pulmonary inflammation in a mouse model of infection, suggesting a casual relationship between increased ROS production and lung disease [6]. We found that the expression and/or activity of the antioxidant enzymes (AOEs) superoxide dismutase (SOD), catalase,

Abbreviations: AEC, Airway epithelial cell; AOE, Antioxidant enzyme; ARE, Antioxidant response element; BHA, Butylated hydroxyanisole; ChIP, Chromatin immunoprecipitation; GCLC, Glutamyl cysteine ligase-catalytic; GPX1, Glutathione peroxidase 1; HDAC, Histone deacetylase; IP, Immunoprecipitation; Keap1, Kelch-like-ECH-associated protein 1; NQO1, NAD(P)H:quinone oxidoreductase 1; Nrf2, Nuclear factor erythroid 2-related factor 2; QgPCR, Quantitative genomic PCR; ROS, Reactive oxygen species; RSV, Respiratory syncytial virus; SAEC, Small airway epithelial cell; SOD1, Superoxide dismutase 1; tBHQ, t-Butylhydroquinone; TSA, Trichostatin A; Ub, Ubiquitin

* Corresponding author at: Department of Pediatrics, University of Texas Medical Branch at Galveston, TX 77555, USA. Fax: +1 409 772 1761.
E-mail address: ancasola@utmb.edu (A. Casola).

http://dx.doi.org/10.1016/j.freeradbiomed.2015.05.043
0891-5849/

glutathione peroxidase (GPx), and glutathione S-transferase (GST) were dramatically decreased in RSV-infected human airway epithelial cells (AECs)[4]. Similar decreases in AOE expression were also observed in the lungs of RSV-infected mice and in nasopharyngeal secretions (NPS) of children with severe RSV-induced lower respiratory tract infections [5], suggesting that oxidative damage associated with RSV infection results from an imbalance between ROS production and antioxidant cellular defenses. Transcription of many oxidative-stress-inducible genes is regulated in part through *cis*-acting antioxidant responsive element (ARE) sequences. This element has been identified in the regulatory regions of genes encoding detoxification enzymes, such as NQO1 (NADPH:quinone oxidoreductase), as well as many AOEs, including SOD1, catalase, heme oxygenase 1, GST, and glutathione-generating enzymes such as glutamate cysteine ligase (GCLC) (reviewed in [9]). NF-E2-related factor 2 (Nrf2) is an important redox-responsive protein that helps protect cells from oxidative stress and injury (reviewed in [10]). It is a basic leucine zipper transcription factor that is normally bound in the cytosol to a cytoskeleton-associated inhibitor called Keap1 (Kelch-like-ECH associated protein 1). Electrophile-induced release of Nrf2 is proposed to involve covalent modifications of Keap1 and/or Nrf2 in the cytoplasm. Such modifications include oxidation of key cysteine residues in Keap1, phosphorylation of Nrf2, and switching of Cullin-3-dependent ubiquitination from Nrf2 to Keap1, leading to the degradation of Keap1 and the stabilization and activation of Nrf2. The released Nrf2 then translocates to the nucleus and binds to ARE sites to promote gene transcription [10]. During activation, Nrf2 also undergoes different type of post-translational modifications, including phosphorylation, which regulates nuclear translocation and export [11], as well as acetylation, which is important for stabilization of Nrf2 binding to DNA once activated [12].

The aim of our study was to investigate the unexplored mechanism(s) leading to virus-induced decreased expression of AOE. Our data show that RSV infection induces a progressive reduction in nuclear and total cellular levels of Nrf2, resulting in decreased binding to the ARE site of endogenous AOE gene promoter, with a subsequent decrease in their expression. RSV induces Nrf2 deacetylation, ubiquitination, and degradation via the proteasome pathway both in vitro and in vivo. Histone deacetylase (HDAC) and proteasome inhibitors block Nrf2 degradation and increase Nrf2 binding to endogenous promoter ARE sites, resulting in increased AOE expression. Known inducers of Nrf2 are able to increase Nrf2 activation and subsequent AOE expression during RSV infection in AECs, as well as in an animal model of infection, with significant amelioration of oxidative stress, which is an important pathogenic component of virus-induced lung disease, adding additional support to the concept that therapeutic strategies aimed to increase airway antioxidant capacity by increasing Nrf2 activity could be beneficial in RSV infection.

2. Materials and methods

2.1. Materials

BHA, tBHQ, and TSA were purchased from Sigma, MO, USA. MG132 and lactacystin were purchased from Calbiochem, CA, USA.

2.2. RSV preparation

The RSV Long strain was grown in Hep-2 cells and purified by centrifugation on discontinuous sucrose gradients as described elsewhere [13]. The virus titer of the purified RSV pools was 8–9 $\log_{10}$ plaque forming units (PFU)/mL using a methylcellulose plaque assay. No contaminating cytokines were found in these sucrose-purified viral preparations [14]. LPS, assayed using the limulus hemocyanin agglutination assay, was not detected. Virus pools were aliquoted, quick-frozen on dry ice/alcohol, and stored at −80 °C until used.

2.3. Cell culture and infection of epithelial cells with RSV

A549 cells, a human alveolar type II like the epithelial cell line (American Type Culture Collection, Manassas, VA) and small alveolar epithelial cells (SAECs) (from Clonetics, now part of Lonza Inc., San Diego, CA), normal human AECs derived from terminal bronchioli, were grown according to the manufacturer's instructions. RSV infection in A549 cells was done in F12K medium containing 2% FBS. When SAECs were used for RSV infection, they were changed to basal medium, not supplemented with growth factors, 6 h before and throughout the length of the experiment. At 80% to 90% confluence, cell monolayers were infected with RSV at a multiplicity of infection (MOI) of 3. An equivalent amount of 30% sucrose solution was added to uninfected A549 and SAECs, as a control.

For tBHQ and TSA experiments, cells were pretreated with the compounds for 1 h and then infected in their presence for the duration of the experiment. In selected experiments, tBHQ was also added at different time points after infection. For proteasome inhibitor experiments, MG132 or lactacystin were added 10 h post-infection (p.i.). Equal amounts of diluent were added to uninfected and infected cells as control. Total number of cells and cell viability, following various treatments, were measured by trypan blue exclusion. There was no significant change in cell viability with any compounds tested. Similarly, there was no effect of either compound on viral replication, tested by plaque assay.

2.4. Reporter gene assay

Logarithmically growing A549 cells were transfected in triplicate with Cat # 336841 Cignal Antioxidant Response Reporter from Qiagen (Maryland), an optimized luciferase reporter construct containing the NQO1 ARE promoter sequence, together with β-galactosidase expression plasmid. Cells were infected with RSV in the presence or absence of specific inhibitors and harvested 24 h p.i. to measure luciferase and β-galactosidase reporter activity independently, as previously described [15]. Luciferase activity was normalized to the internal control β-galactosidase activity. Results are expressed in arbitrary units.

2.5. Western blot

Nuclear extracts of uninfected and infected cells were prepared using hypotonic/nonionic detergent lysis, according to the Schaffner protocol [16]. To prevent contamination with cytoplasmic proteins, isolated nuclei were purified by centrifugation through 1.7 M sucrose buffer A for 30 min, at 12,000 rpm, before nuclear protein extraction, as previously described [16,17]. Total cell lysates of uninfected and infected cells were prepared as previously described [16]. Equal amount of proteins (10 to 20 μg) were separated by SDS-PAGE and transferred onto polyvinylidene difluoride membrane. Nonspecific binding was blocked by immersing the membrane in Tris-buffered saline-Tween (TBST) blocking solution containing 5% skim milk powder. After a short wash in TBST, the membranes were incubated with the primary antibody overnight at 4 °C, followed by the appropriate secondary antibody diluted in TBST for 1 h at room temperature. Proteins were detected using enhanced-chemiluminescence assay. Densitometric analysis of band intensities was performed using UVP VisionWorksLS Image Acquisition and Analysis Software 8.0 RC 1.2 (UVP, Upland, CA). The primary antibodies used for Western blots

were anti-Nrf2 (H-300, sc-13032), anti-HDAC1(H-51, sc-7872), -HDAC2 (H-54, sc-7899), and -HDAC3 (H-99, sc-11417) from Santa Cruz Biotechnology Inc, CA, anti-SOD1 (SOD100, Stressgen Bioreagents, MI), anti-lamin B (GWB5CD4D4, GenWay Biotech), and anti-β-actin (A1978 Sigma, MO).

2.6. Immunoprecipitation

Portions of 250 μg of total cell lysate or 200 μg of nuclear extracts from RSV-infected A549 or SAECs were immunoprecipitated using 5 μg of anti-Nrf2 antibody and protein A/G agarose beads (Santa Cruz Biotechnology Inc, sc-2003). Complexes were eluted in 2 × SDS PAGE buffer and subjected to Western blot analysis using anti-ubiquitin (SC-8017, Santa Cruz Biotechnology Inc, CA) or anti-acetyl lysine (ab21623, Abcam, MA) antibodies.

2.7. HDAC activity

Nuclear extracts prepared from A549 cells and SAECs uninfected or infected with RSV were assayed for HDAC activity using a commercially available kit (10011563, Cayman, Ann Arbor, MI) according to the manufacturer's instructions.

2.8. 8-Isoprostane assay

Measurements of F_2 8-isoprostane were performed using Cat 516351 competitive enzyme immunoassay from Cayman Chemical (Ann Arbor, MI).

2.9. Quantitative reverse transcriptase PCR (Q-RT-PCR)

Total RNA was extracted using a Cat # AM1910 ToTALLY RNA kit from Ambion (Austin, TX). RNA samples were quantified using a Nanodrop spectrophotometer (Nanodrop Technologies) and quality was analyzed using the Agilent 2100 bioanalyzer (Agilent Technologies, Santa Clara, CA). Synthesis of cDNA was performed with 1 μg of total RNA in a 20 μl reaction using the reagents in the #N8080234 Taqman Reverse Transcription Reagents Kit from Applied Biosystems, according to manufacturer's instructions. Q-PCR amplification was done using 1 μl of cDNA in a total volume of 25 μl using the Faststart Universal SYBR green Master Mix (Roche Applied Science #04913850001). The final concentration of the primers was 300 nM. 18 S RNA was used as housekeeping gene for normalization. PCR assays were run in the ABI Prism 7500 sequence detection system. Duplicate CT values were analyzed in Microsoft Excel using the comparative CT (ΔΔCT) method as described by the manufacturer (Applied Biosystems). The amount of target ($2^{-\Delta\Delta CT}$) was obtained by normalizing to the endogenous reference (18S) sample. Primer sequences are available upon request.

2.10. Two-step chromatin immunoprecipitation (XChIP) and quantitative genomic PCR (Q-gPCR)

For XChIP we used a Cat # 53008 & 53032 ChIP-IT Express kit from Active Motif (Carlsbad, CA) and followed manufacturer's instructions with slight modifications. Briefly, A549 cells on a 10 cm plate were washed three times with PBS and fixed with freshly prepared 2 mM Cat # 20593 disuccinimidyl gluterate (DSG) (Thermo Scientific, Rockford, IL). After three washes with PBS, cells were fixed with freshly prepared formaldehyde for 1 min and neutralized with glycine for 5 min at room temperature. Cells were harvested and disrupted using a Dounce homogenizer to isolate nuclei. Nuclei were sheared by sonication to obtain DNA fragments from 200 to 1500 base pairs (bp). Portions of 20 micrograms of sheared chromatin were immunoprecipitated with 5 μg of ChIP grade anti-Nrf2 (sc-722X), -CBP (sc-369X), -or HDAC1 (sc-7872X) antibody from Santa Cruz Biotechnology, CA, USA, and magnetic beads conjugated with protein G at 4 °C overnight. Immunoprecipitation with IgG antibody was used as negative control. Chromatin was reverse cross-linked, eluted from magnetic beads, and purified using a Cat # 28106 PCR purification kit (Qiagen GmbH, Hilden). Q-gPCR was done by SyBR green-based real time PCR using the following primers spanning the SOD1 gene promoter ARE site: forward-AAAGCATCCATCTTGGGGCG and reverse-AACCTTCTTTTCACGGGGGC, or the catalase promoter ARE site: forward-AACGGCCGCGTCCCAG and reverse-CTCTCCGAAGGAGGCCTGAA. Total input chromatin DNA for immunoprecipitation was included as positive control for PCR amplification.

2.11. In vivo studies

Female BALB/c mice 10–12 weeks old were purchased from Harlan (Houston, TX) and were housed under pathogen-free conditions in the animal research facility of the University of Texas Medical Branch (UTMB), Galveston, TX, in accordance with the National Institutes of Health and UTMB institutional guidelines for animal care. Experiments were performed with a minimum of 4–6 animals/group. Under light anesthesia, mice were inoculated intranasally with 10^7 PFU of sucrose-purified RSV (Long strain) in a final volume of 50 μl/dose diluted in phosphate-buffered saline (PBS). Control animals (mock infected, defined as sham) received PBS treated in a similar manner. Mice were treated by gavage with 250 mg/kg body weight of BHA or corn oil (diluents for BHA) two days prior to RSV infection and during the first two days of infection. Bronchoalveolar lavages were prepared by flushing the lungs twice via the trachea with 1 mL of ice-cold PBS. BAL fluid supernatant were collected 48 h p.i. following centrifugation (5 min at 5000 rpm), and stored at -80 °C prior to 8-isoprostane assay. Lung samples from all groups were harvested 48 h p.i. to assess mRNA levels of SOD1 and catalase by Q-RT-PCR and Nrf2 nuclear levels by Western blot. Mice were given intranasal proteasome inhibitor MG-132 at 10 μg/dose, or an appropriate volume of vehicle, 1 h before infection. Lungs samples from all groups were harvested 48 h p.i. to assess mRNA levels of SOD1 and catalase by Q-RT-PCR, and Nrf2 nuclear levels by Western blot.

2.12. Statistical analysis

All results are expressed as mean ± SEM. Data were analyzed using the GraphPad Prism 5 software. Results were compared among treatment groups by either one-way ANOVA analysis followed by Tukey's post hoc test or two-way ANOVA analysis followed by the Bonferroni post-test. Significance was accepted at $p < 0.05$. To streamline figures, all significant results were reported as $p < 0.05$, although in many instances significance was well below that threshold.

3. Results

3.1. RSV infection down-regulates Nrf2-dependent gene transcription

To determine whether Nrf2 activation was affected by RSV infection, nuclear proteins isolated from A549 cells infected for various lengths of time were subjected to Western blot analysis. After an initial modest increase in nuclear translocation, around 6 h p.i., there was a progressive, time-dependent decrease in Nrf2 nuclear amounts in infected cells at 15 h and later to levels below that of uninfected cells (Fig. 1A, left panel). To confirm our findings in A549 cells, which are a widely accepted model for studying RSV–epithelial cell interactions of the lower airways, a similar

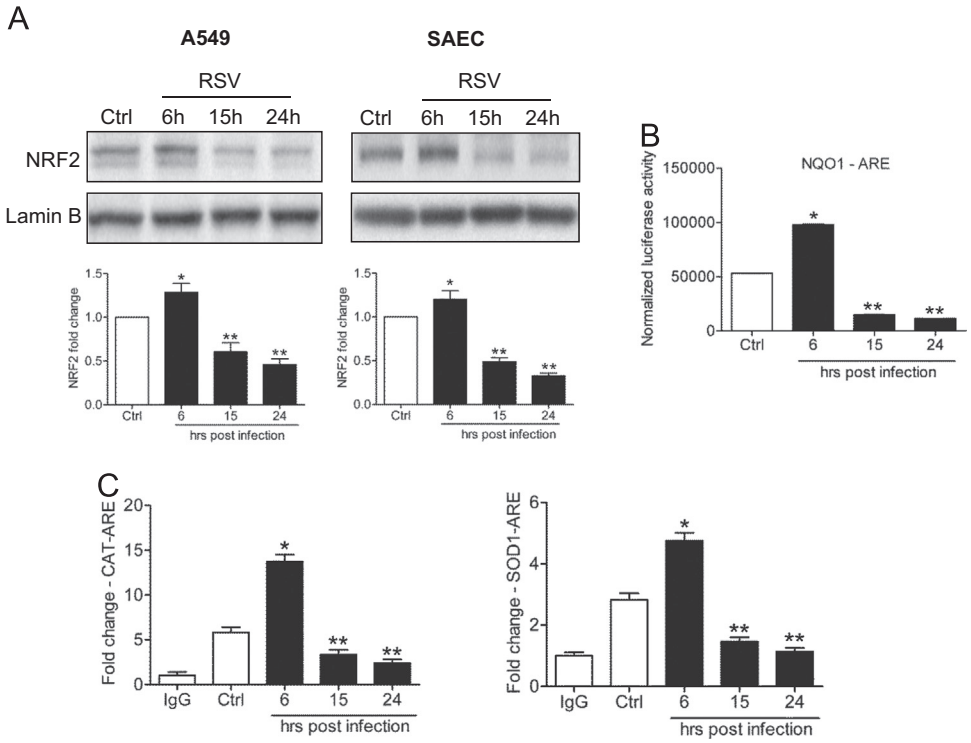

Fig. 1. RSV infection down-regulates Nrf2 dependent gene transcription. (A) Nuclear proteins isolated from A549 cells (left panel) and SAECs (right panel) uninfected or infected with RSV for 6, 15, and 24 h were subjected to Western blot analysis using anti-Nrf2 antibody. For loading controls, membranes were stripped and re-probed with anti-lamin B antibody. The blots are representative of three independent experiments. Densitometric analysis of Nrf2 band intensity is shown after normalization to lamin B. The groups were analyzed by one-way ANOVA followed by Tukey's post hoc test. Data are shown as mean ± SEM. $^{*}P < 0.05$ relative to uninfected cells, $^{**}P < 0.05$ relative to uninfected and 6 h infected cells. Open bars represent uninfected (control, Ctrl) and solid bars represent RSV-infected cells. (B) A549 cells were transiently transfected with an ARE-driven luciferase reporter plasmid, infected with RSV for various lengths of time, and harvested to measure luciferase activity. Data are representative of three independent experiments. The groups were analyzed by one-way ANOVA followed by Tukey's post hoc test. Data are shown as mean ± SEM. $^{*}P < 0.05$ relative to uninfected cells, $^{**}P < 0.05$ relative to uninfected and 6 h infected cells. (C) ChIP-QgPCR analysis of Nrf2 occupancy of endogenous ARE promoter sites. Chromatin DNA from A549 cells uninfected or infected with RSV for 6, 15, and 24 h was immunoprecipitated using anti-Nrf2 antibody or IgG as negative control. QgPCR was performed using primers spanning the ARE binding site of the catalase (left) and SOD1 (right) gene promoter. Total input chromatin DNA for immunoprecipitation was included as positive control for QgPCR amplification. Fold change was calculated compared to IgG control. Data are representative of three independent experiments. The groups were analyzed by one-way ANOVA followed by Tukey's post hoc test. Data are shown as mean ± SEM $^{*}P < 0.05$ relative to uninfected cells, $^{**}P < 0.05$ relative to uninfected and 6 h infected cells.

experiment was performed in SAECs, normal human airway epithelial cells derived from bronchioli, which represent a major target of RSV infection, as shown in post mortem studies by us [18] and others [19]. In SAECs infected with RSV we observed an identical response, associated with decreased Nrf2 nuclear levels at 15 and 24 h p.i. (Fig. 1A, right panel). The reduction in nuclear translocation was associated with reduced Nrf2-dependent gene transcription, demonstrated by reporter gene assay. A549 cells were transiently transfected with a synthetic ARE-driven promoter, linked to a luciferase reporter gene, and infected with RSV for 6, 15, and 24 h. Nrf2-dependent gene transcription increased at 6 h p.i., but then significantly decreased at subsequent times p.i. to values below that of uninfected cells (Fig. 1B), correlating with a time-dependent decrease in Nrf2 target genes, including NQO1 and the AOEs SOD1, catalase, GPX1, and GCLC (Supplementary Material, Fig. 1A). To investigate the mechanism, we measured Nrf2 occupancy of the ARE sites of SOD1 and catalase by XChIP. Nrf2 binding to both promoters was reduced at 15 and 24 h p.i., quantitated by Q-gPCR (Fig. 1C). A similar result was obtained for the NQO1 gene (Supplementary Material, Fig. 1B).

In a parallel set of experiments, AECs were treated with a known pro-oxidative stimulus, hydrogen peroxide, to investigate the effect on Nrf2 activation. Differently from what occurs in the context of RSV infection, hydrogen peroxide induced a sustained increase in Nrf2 nuclear levels, up to 15 h post-treatment, investigated by Western blot analysis, with levels returning to basal conditions by 24 h (Supplementary Material, Fig. 2A). The increase in Nrf2 activation was paralleled by an increase in the Nrf2 target genes catalase and SOD1 (Supplementary Material, Fig. 2B).

3.2. RSV infection induces Nrf2 degradation

To determine whether an RSV-induced decrease in Nrf2 nuclear levels corresponded to a decrease in total cellular levels, whole cell lysates from A549 and SAECs infected with RSV for various lengths of time were subjected to Western blot analysis. Both A549 cells (Fig. 2A, left panel) and SAECs (Fig. 2A, right panel) showed significantly lower levels of Nrf2 at 15 and 24 h p.i., compared with uninfected controls and with early time points of infection, suggesting that RSV induces Nrf2 degradation, possibly through the proteasome pathway. Treatment of A549 cells with the specific proteasome inhibitor lactacystin restored Nrf2 cellular levels (Fig. 2B), indicating that Nrf2 degradation associated with RSV infection occurs through the proteasome. To investigate whether RSV induced changes in Nrf2 ubiquitination, total cell lysates of either A549 cells or SAECs infected with RSV for 6 and 15 h were immunoprecipitated with anti-Nrf2 antibody and subjected to Western blot analysis using an anti-ubiquitin antibody. RSV infection was associated with increased Nrf2 ubiquitination compared with uninfected cells (Fig. 2C), suggesting that this is an important mechanism(s) targeting Nrf2 to proteasome degradation.

Treatment of AECs with proteasome inhibitors not only led to increased Nrf2 cellular levels, but also restored Nrf2 function, as MG132, another proteasome inhibitor, and lactacystin treatment were associated with increased ARE-dependent gene

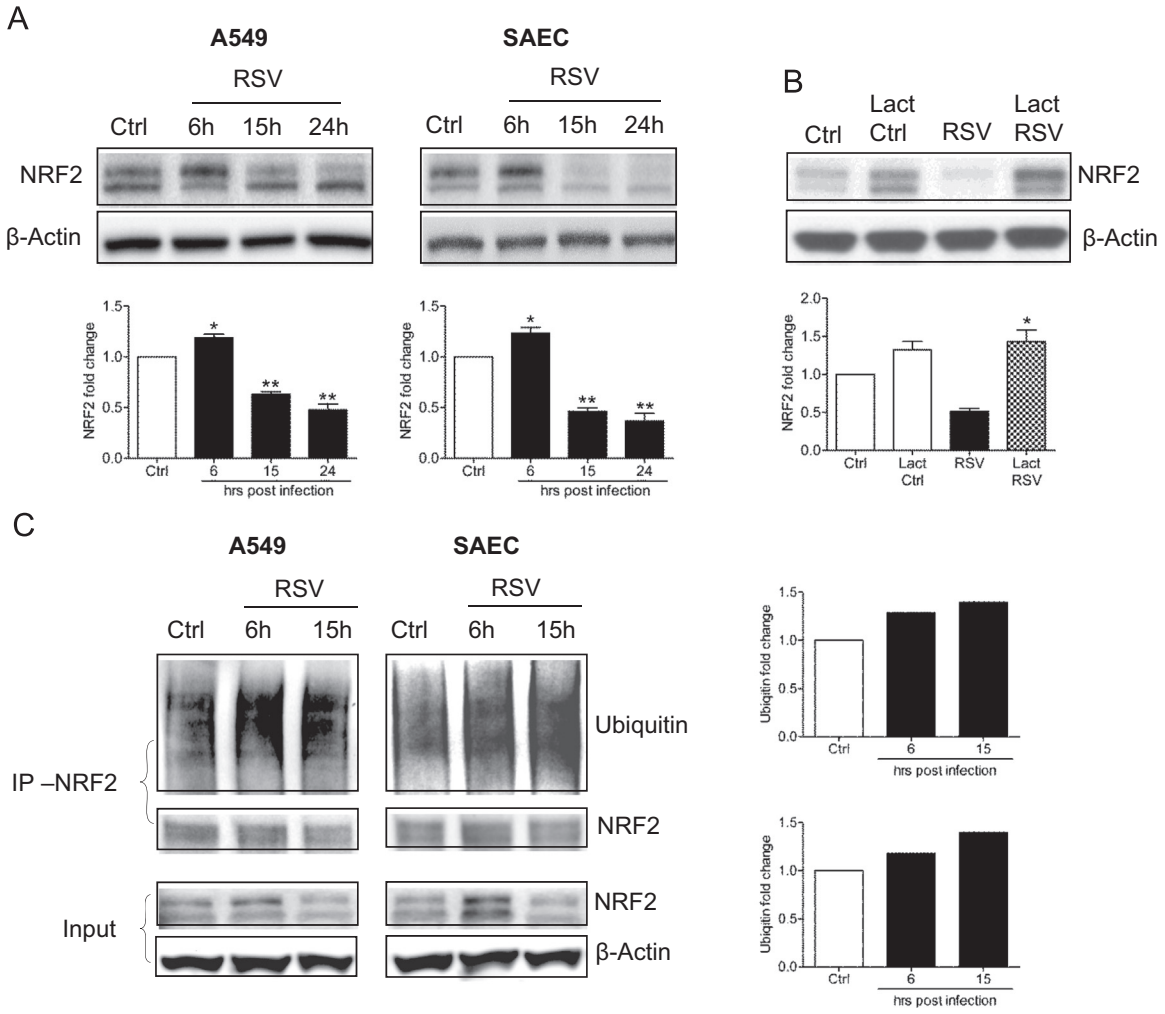

Fig. 2. RSV infection is associated with proteasome-dependent Nrf2 degradation. (A) Total cell lysates prepared from A549 cells (left panel) and SAECs (right panel) uninfected or infected with RSV for 6, 15, and 24 h were subjected to Western blot analysis using anti-Nrf2 antibody. For loading controls, membranes were stripped and reprobed using anti-β-actin antibody. The blots are representative of three independent experiments. Densitometric analysis of Nrf2 band intensity is shown after normalization to β-actin. Open bars represent uninfected (Ctrl) and solid bars represent RSV-infected cells. The groups were analyzed by one-way ANOVA followed by Tukey's post hoc test. Data are shown as mean ± SEM. $^{*}P < 0.05$ relative to uninfected cells, $^{**}P < 0.05$ relative to uninfected and 6 h infected cells. (B) Total cell lysates prepared from A549 cells uninfected or infected with RSV for 18 h in the presence or absence of 10 μM lactacystin (Lact) were subjected to Western blot analysis using anti-Nrf2 antibody. For loading controls, membranes were stripped and reprobed with anti-β-actin antibody. The blots are representative of three independent experiments. Densitometric analysis of Nrf2 band intensity is shown after normalization to β-actin. The groups were analyzed by two-way ANOVA followed by a Bonferroni post-test. Data are shown as mean ± SEM. $^{*}P < 0.05$ relative to untreated RSV-infected cells. (C) Total cell lysates prepared from A549 cells (left panel) and SAECs (right panel), uninfected or infected with RSV for 6 and 15 h, were immunoprecipitated using anti-Nrf2 antibody and immune complexes analyzed by Western blots using anti-ubiquitin antibody. Membranes were stripped and reprobed with anti-Nrf2 antibody to determine the level of immunoprecipitated Nrf2. The lower panel shows Nrf2 Western blot of input proteins and β-actin as internal control. Blots are representative of two independent experiments.

transcription, shown by reporter gene assays (Fig. 3A) and NQO1 and AOE gene expression, analyzed by Q-RT-PCR (Fig. 3B), as well as increased Nrf2 binding to the endogenous SOD1 and catalase ARE sites, assessed by XChIP (Fig. 3C). From these data, we conclude that proteasome inhibition can restore Nrf2 expression and function in the context of RSV infection.

3.3. *RSV infection is associated with Nrf2 deacetylation*

Acetylation is a post-translational modification important for stabilization of Nrf2 binding to DNA once activated [12]. To determine whether RSV infection could modulate Nrf2 acetylation, total cell lysates from A549 cells were immunoprecipitated with anti-Nrf2 antibody and subjected to Western blot analysis using anti-acetyl-lysine antibody. RSV infection was associated with a significant decrease in basal Nrf2 acetylation, both in A549 (Fig. 4A, left panel) and in SAECs (Fig. 4A, right panel), starting as early as 6 h p.i. (data shown represent 15 h p.i.). Treatment of AECs with the HDAC inhibitor Trichostatin A (TSA) significantly restored Nrf2 acetylation, leading to increased Nrf2 cellular levels as well (Fig. 4A, input). RSV infection up-regulated nuclear HDAC activity, starting 6 h p.i. and continuing up to 24 h p.i., both in A549 (Fig. 4B, left panel) and in SAECs (Fig. 4B, right panel). In addition, RSV infection was associated with a significant reduction of binding of the transacetylase CBP to the ARE site of the SOD1 gene promoter, starting around 15 h p.i., after an initial increase in binding at early time points of infection, as determined by XChIP assay (Fig. 4C). Increasing CBP expression by transient transfection was able to rescue ARE-driven reporter gene activity in viral-infected cells (Fig. 4D), supporting the idea that Nrf2 deacetylation could be the result of unbalanced HDAC and acetylation activity.

Inhibition of HDAC activity was able to restore nuclear levels of Nrf2 during viral infection, as shown by Western blot analysis of nuclear fractions from A549 cells (Fig. 5A, left panel) and SAECs (Fig. 5A, right panel), and importantly, it was also associated with an overall increase in Nrf2 cellular levels, assessed by Western blot

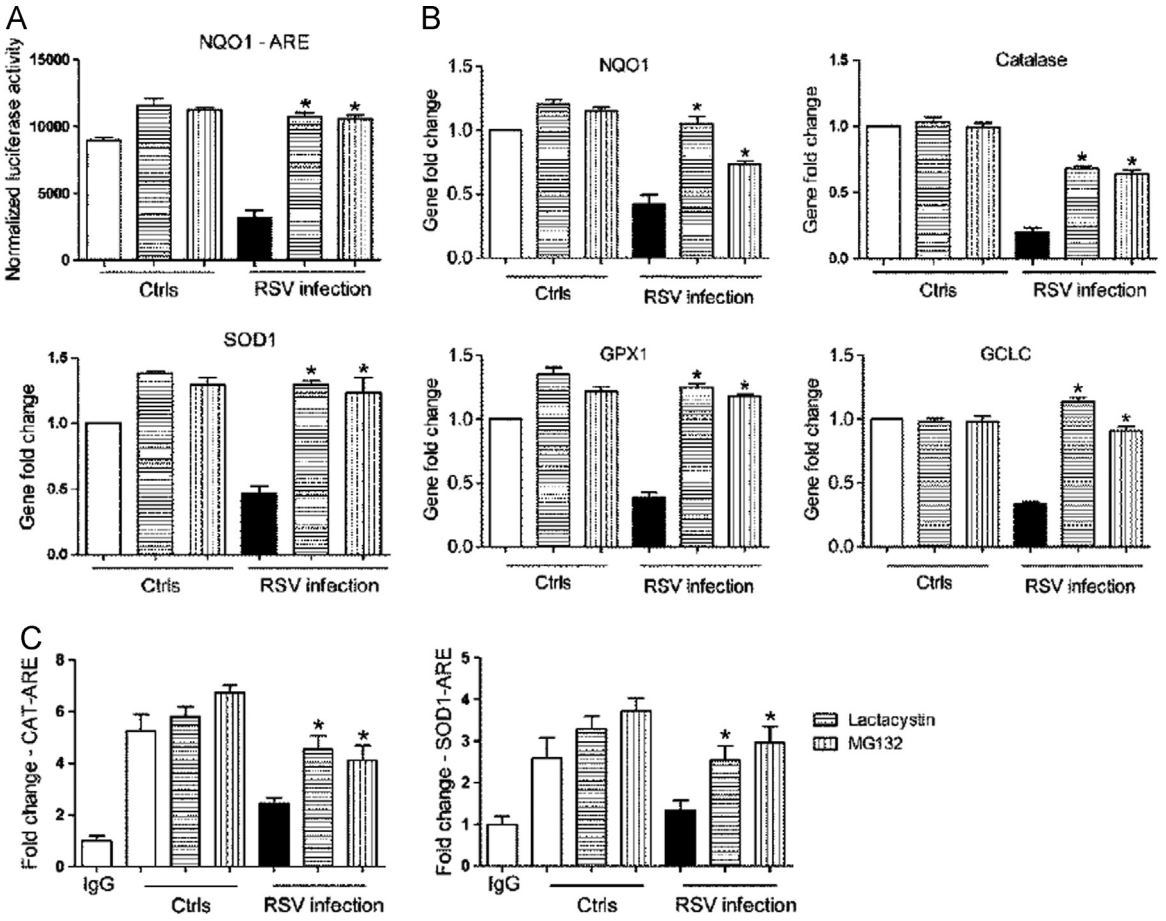

Fig. 3. Blocking Nrf2 degradation restores ARE-dependent gene expression. (A) A549 cells were transiently transfected with the ARE-luciferase reporter plasmid. Cells uninfected and infected with RSV for 18 h in the presence or absence of either 10 μM lactacystin or MG132 were harvested to measure luciferase activity. Data are representative of three independent experiments. The groups were analyzed by two-way ANOVA followed by a Bonferroni post-test. Data are shown as mean ± SEM. $^*P < 0.05$ relative to RSV-infected untreated cells. (B) A549 cells, uninfected or infected with RSV for 18 h in the presence or absence of either 10 μM lactacystin or MG132, were harvested to prepare total RNA. NQO1, Catalase, SOD1, GPX1, and GCLC gene expression were quantified by real-time PCR. Data are representative of three independent experiments. The groups were analyzed by two-way ANOVA followed by a Bonferroni post-test. Data are shown as mean ± SEM. $^*P < 0.05$ relative to RSV-infected untreated cells. (C) Chromatin DNA from A549 cells uninfected or infected with RSV for 18 h in the presence or absence of either 10 μM lactacystin or MG132 was immunoprecipitated using anti-Nrf2 antibody or IgG as negative control. QgPCR was performed using primers spanning the ARE binding site of the catalase (left panel) or SOD1 (right panel) gene promoter. Total input chromatin DNA for immunoprecipitation was included as a positive control for QgPCR amplification. Fold change was calculated compared with IgG control. Data are representative of three independent experiments. The groups were analyzed by one-way ANOVA followed by Tukey's post hoc test. Data are shown as mean ± SEM. $^*P < 0.05$ relative to untreated RSV-infected cells.

analysis of total cell lysates from A549 cells (Fig. 5B, left panel) and SAECs (Fig. 5B, right panel).

Inhibition of HDAC activity was also able to restore ARE-dependent gene transcription, as shown by reporter gene assay in A549 cells transiently transfected with the ARE-driven promoter and infected with RSV in the presence or absence of TSA (Fig. 5C), leading to increased expression of Nrf2 target genes assessed by Q-RT-PCR, both in A549 (Fig. 5D, upper panel, and Supplementary Material, Fig. 3A) and SAECs (Fig. 5D, lower panel, and Supplementary Material, Fig. 3B). Increased AOE expression was associated with a significant increase of Nrf2 occupancy of the catalase and SOD1 promoter ARE sites (Fig. 5E), supporting the finding that inhibition of HDAC can rescue Nrf2 activation in the context of RSV infection.

3.4. HDAC1 and 2 play an important role in RSV-induced inhibition of Nrf2 activation

Human HDACs are classified, based on the sequence similarity and cofactor dependency, into three groups [20]. TSA is a broad specific inhibitor and it blocks both Class I and II HDAC activity [21]. As shown before, TSA treatment in AECs infected with RSV infection was able to rescue Nrf2 activation. On the other hand, the HDAC Class III specific inhibitor Ex-527 [22] did not have a significant effect, indicating that this class of HDAC proteins were not involved in RSV-induced Nrf2 inhibition (data not shown). Since HDAC Class II proteins are present predominantly in skeletal muscle, heart, brain, and thymus [23,24], we first investigated the role of HDAC class I proteins, specifically HDAC1, 2, and 3, in RSV-induced Nrf2 deacetylation, as they are known to modulate activation of other transcription factors such as nuclear factor (NF)-κB and signal transducer and activator of transcription [25,26]. We first determined whether there was any change in HDAC expression. A549 cells were infected with RSV and harvested at different time points after infection to prepare nuclear proteins, and HDAC1, 2, and 3 levels were assessed by Western blot analysis. There was no difference in nuclear levels of any of the three HDAC proteins (Supplementary Material, Fig. 4), indicating that change in total HDAC activity was not due to an increase in their nuclear amounts. We then inhibited their expression using specific siRNAs. A549 were transfected with either scrambled or siRNAs selectively targeting HDAC1, 2, or 3, infected with RSV, and harvested to prepare either nuclear extracts or total RNA. Western blot analysis showed that Nrf2 nuclear levels in HDAC1 and 2 siRNA transfected cells

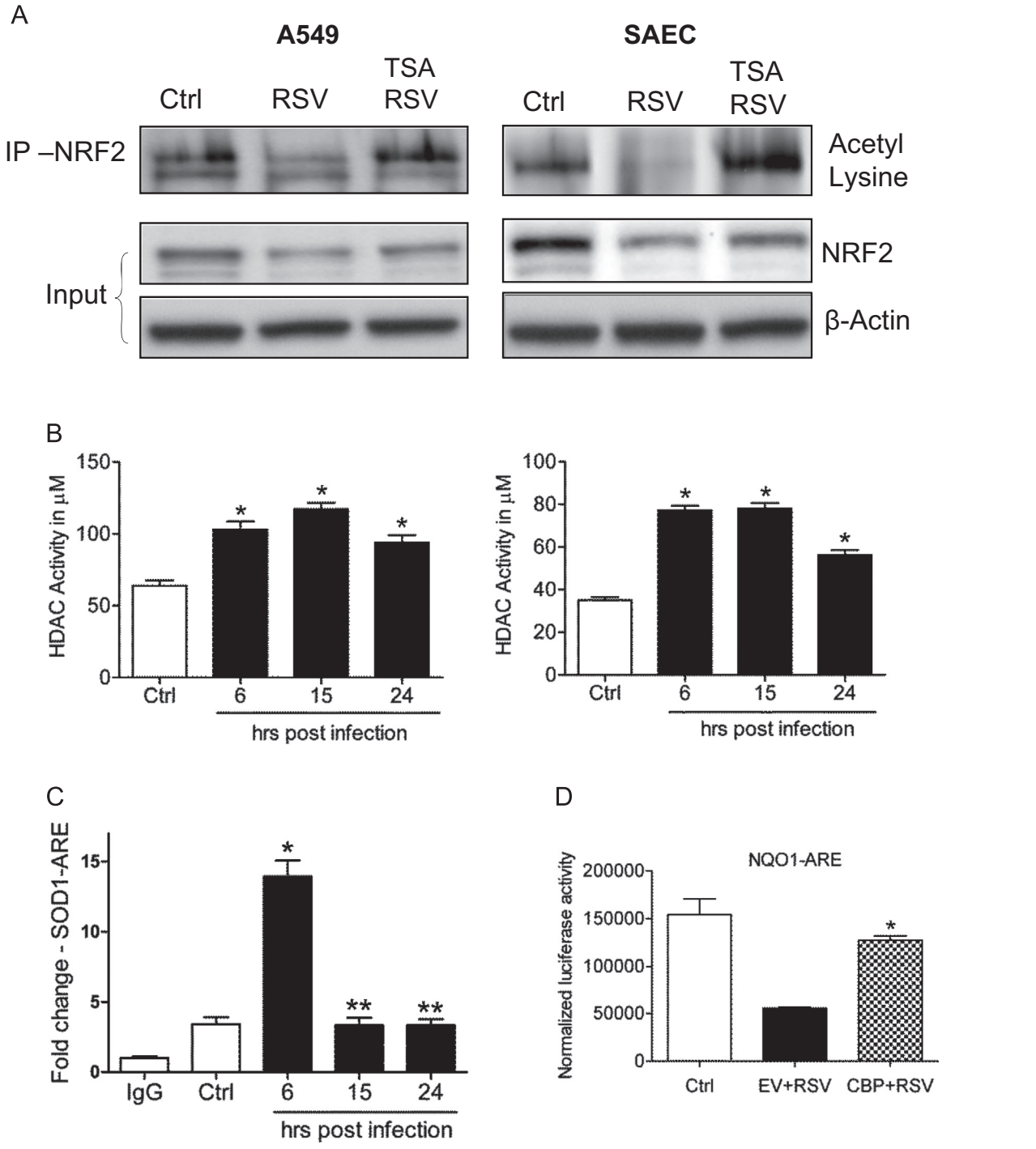

Fig. 4. RSV infection induces Nrf2 deacetylation. (A) Total cell lysates from A549 (left panel) and SAECs (right panel) uninfected or infected with RSV for 15 h in the presence or absence of 250 nM TSA were immunoprecipitated using anti-Nrf2 antibody and subjected to Western blot using anti-acetyl lysine antibody. The lower panel shows Nrf2 Western blot for input of the IP. β-actin was used as loading control. (B) HDAC activity in nuclear extracts prepared from A549 (left panel) and SAECs (right panel) uninfected and infected with RSV for 6, 15, and 24 h was analyzed using an HDAC activity assay kit (Cayman). Data are representative of three independent experiments. The groups were analyzed by one-way ANOVA followed by Tukey's post hoc test. Data are shown as mean ± SEM. $^{*}P < 0.05$ relative to uninfected cells. (C) Chromatin DNA from A549 cells uninfected or infected with RSV for 6, 15, and 24 h was immunoprecipitated using anti-CBP antibody or IgG as a negative control. QgPCR was performed using primers spanning the ARE binding site of the SOD1 promoter. Total input chromatin DNA for immunoprecipitation was included as a positive control for QgPCR amplification. Fold change was calculated compared with IgG control. Data are representative of three independent experiments. The groups were analyzed by one-way ANOVA followed by Tukey's post hoc test. Data are shown as mean ± SEM. $^{*}P < 0.05$ relative to uninfected cells, $^{**}P < 0.05$ relative to uninfected and 6 h infected cells. (D) A549 cells, transiently co-transfected with the ARE-luciferase reporter plasmid and CBP expression plasmid or empty vector (EV), were infected with RSV for 18 h and harvested to measure luciferase activity. Data are representative of three independent experiments. The groups were analyzed by one-way ANOVA followed by Tukey's post hoc test. Data are shown as mean ± SEM. $^{*}P < 0.05$ relative to EV-transfected RSV-infected cells.

were significantly higher than those of scramble transfected ones following infection with RSV, with HDAC1 siRNA being the most effective in restoring Nrf2 activation to levels comparable of that of uninfected cells (Fig. 6A and B), while no significant change was observed in HDAC3 siRNA transfected cells (Fig. 6C). In agreement with these findings, mRNA levels of the Nrf2 target genes NQO1 and AOEs were significantly higher in RSV-infected cells transfected with siRNA for HDAC1 and 2, but not HDAC3, compared

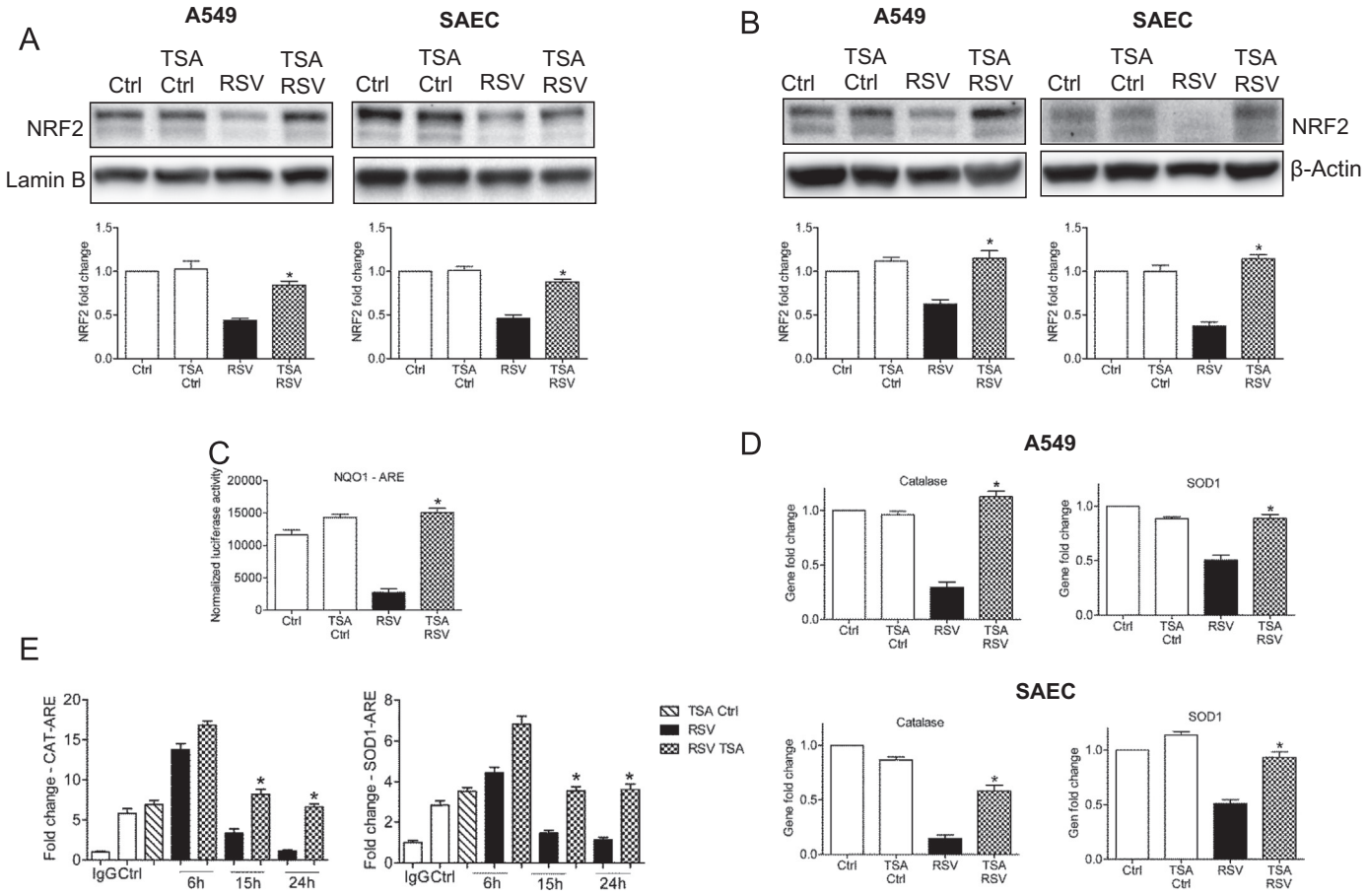

Fig. 5. Blocking HDAC activity restores Nrf2-dependent gene transcription. Nuclear protein (A) or total cell lysates (B) prepared from A549 cells (left panel) and SAECs (right panel) uninfected or infected with RSV for 18 h in the presence or absence of 250 nM TSA were subjected to Western blot analysis using anti-Nrf2 antibody. For loading controls, membranes were stripped and reprobed using either anti-lamin B or β-actin antibody. The blots are representative of three independent experiments. Densitometric analysis of Nrf2 band intensity is shown after normalization to the appropriate internal control. The groups were analyzed by two-way ANOVA followed by a Bonferroni post-test. Data are shown as mean ± SEM. $^{*}P < 0.05$ relative to untreated RSV-infected cells. (C) A549 cells were transiently transfected with the ARE-luciferase reporter plasmid. Cells uninfected or infected with RSV for 18 h in the presence or absence of 250 nM TSA were harvested to measure luciferase activity. The groups were analyzed by two-way ANOVA followed by a Bonferroni post-test. Data are shown as mean ± SEM. $^{*}P < 0.05$ relative to untreated RSV-infected cells. (D) A549 cells (upper panel) and SAECs (lower panel) uninfected or infected with RSV for 18 h in the presence or absence of 250 nM TSA were harvested to prepare total RNA. Catalase and SOD1 gene expression was quantified by real-time PCR. Data are representative of three independent experiments. The groups were analyzed by two-way ANOVA followed by a Bonferroni post-test. Data are shown as mean ± SEM. $^{*}P < 0.05$ relative to untreated RSV-infected cells. (E) Chromatin DNA from A549 cells uninfected or infected with RSV for 6, 15, and 24 h in the presence or absence of 250 nM TSA was immunoprecipitated using an anti-Nrf2 antibody or IgG as a negative control. QgPCR was performed using primers spanning the ARE binding site of the catalase (left) and SOD1 (right) gene promoters. Total input chromatin DNA for immunoprecipitation was included as a positive control for QgPCR amplification. Fold change was calculated compared with IgG control. Data are representative of three independent experiments. The groups were analyzed by one-way ANOVA followed by Tukey's post hoc test. Data are shown as mean ± SEM. $^{*}P < 0.05$ relative to untreated RSV-infected cells.

with scrambled (Fig. 6D and Supplementary Material, Fig. 5). To determine whether HDAC1 was binding to the ARE site of the SOD1 gene promoter, we performed XChIP/Q-gPCR. HDAC1 occupancy of the SOD1 ARE site was significantly lower in RSV-infected cells at 6 h p.i., below levels of uninfected cells; however, it increased significantly at 15 h p.i. (Fig. 6E). Treatment of infected cells with TSA resulted in a significant inhibition of HDAC1 recruitment to the SOD1 ARE site (Fig. 6E), in agreement with the previously observed changes in Nrf2 activation.

3.5. *Nrf2 is deacetylated and degraded through the proteasome in vivo*

To determine whether deacetylation and proteasome degradation played a role in virus-induced inhibition of Nrf2 activation in vivo, we performed confirmatory experiments in our mouse model of RSV infection. Nuclear proteins isolated from lungs of mice either sham-inoculated or infected with RSV for 48 h were tested for HDAC activity and Nrf2 acetylation, as described for the in vitro experiments. Similar to our findings in AECs, RSV infection was associated with increased HDAC activity (Fig. 7A), as well as a significant decrease in basal Nrf2 acetylation, along with reduced Nrf2 nuclear levels (Fig. 7B).

To determine whether inhibition of proteasome activity could restore Nrf2 expression and ARE-dependent gene expression, mice were treated with MG132 1 h prior to viral infection and harvested to prepare nuclear extract or extract total RNA at 48 h p.i. Mice infected with RSV and treated with MG132 showed significantly increased Nrf2 nuclear levels, compared with untreated infected mice (Fig. 7C). Proteasome inhibition was also able to significantly increase SOD1 expression during RSV infection, while there was only a modest rescue of catalase expression (Fig. 7D).

3.6. *Nrf2 inducers ameliorate oxidative stress during RSV infection in vitro and in vivo*

Among the compounds known to stimulate ARE-driven transcription [27], butylated hydroxynanisole (BHA) and its metabolite *tert*-butylhydroquinone (tBHQ) have been shown to increase HO-1, NQO1, and Nrf2 protein expression in both primary and cultured

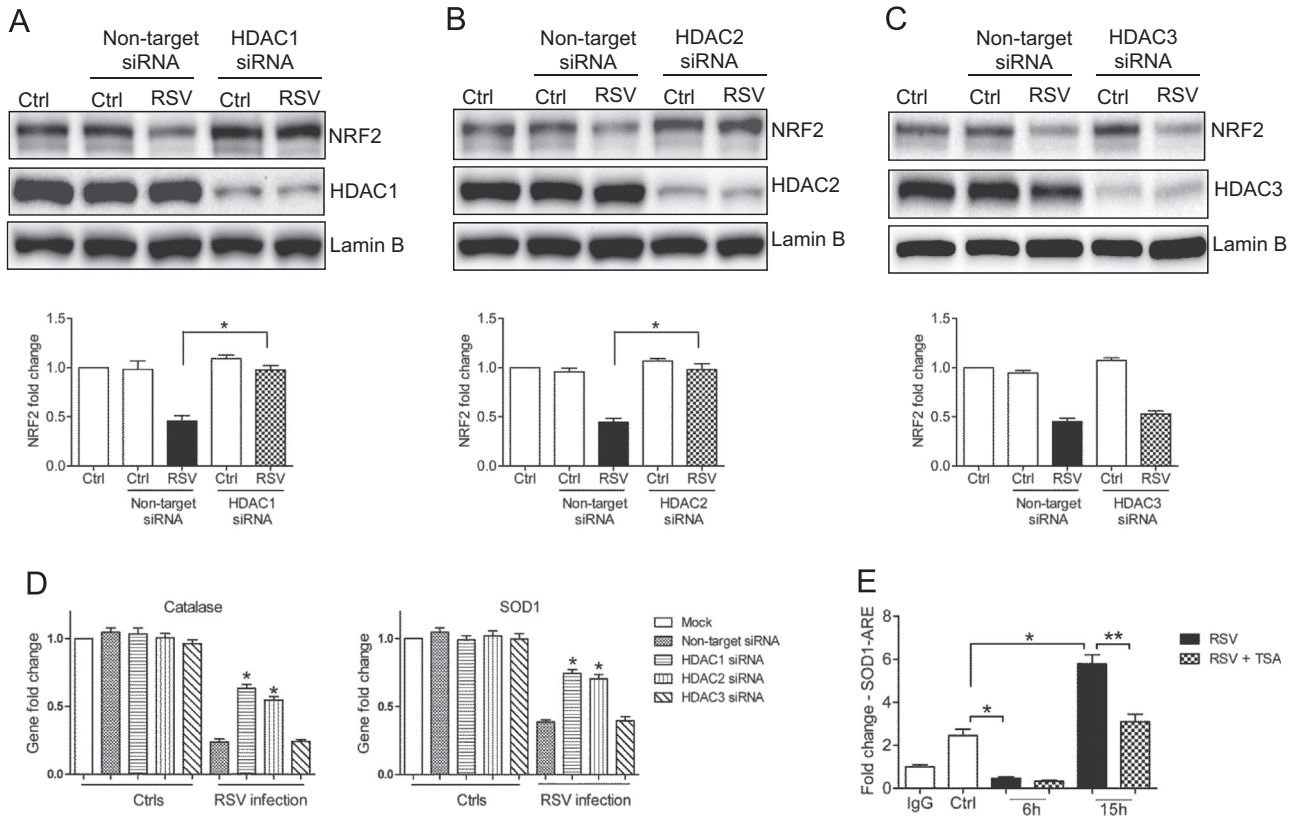

Fig. 6. Blocking HDAC1 and 2 expression restores Nrf2 activation. Nuclear protein prepared from A549 cells transfected with nontarget siRNA or (A) HDAC1 or (B) HDAC2 or (C) HDAC3 siRNA, uninfected or infected with RSV for 18 h, was subjected to Western blot analysis with anti-Nrf2 antibody. Membranes were stripped and reprobed with anti-HDAC1/2/3 and anti-lamin B antibodies for loading control. The blots are representative of three independent experiments. Densitometric analysis of Nrf2 band intensity is shown after normalization to lamin B. The groups were analyzed by two-way ANOVA followed by a Bonferroni post-test. Data are shown as mean ± SEM. $^{*}P < 0.05$ relative to nontarget siRNA-transfected RSV-infected cells. (D) A549 cells transfected with nontarget siRNA or siRNAs for HDAC1, 2, or 3, uninfected or infected with RSV for 18 h, were harvested to prepare total RNA. Catalase (left panel) and SOD1 (right panel) gene expression were quantified by real-time PCR. Data are representative of three independent experiments. The groups were analyzed by two-way ANOVA followed by a Bonferroni post-test. Data are shown as mean ± SEM. $^{*}P < 0.05$ relative to nontarget siRNA-transfected RSV-infected cells. (E) Chromatin DNA from A549 cells uninfected or infected with RSV for 6 and 15 h in the presence or absence of 250 nM TSA was immunoprecipitated using anti-HDAC1 antibody or IgG as a negative control. QgPCR was performed using primers spanning the ARE binding site of the SOD1 promoter. Total input chromatin DNA for immunoprecipitation was included as a positive control for QgPCR amplification. Fold change was calculated compared to IgG control. Data are representative of three independent experiments. The groups were analyzed by one-way ANOVA followed by Tukey's post hoc test. Data are shown as mean ± SEM. $^{*}P < 0.05$ relative to uninfected cells, $^{**}P < 0.05$ relative to untreated RSV-infected cells.

cells [28]. Since BHA was effective in decreasing RSV-induced oxidative stress [6], we investigated whether tBHQ treatment could rescue Nrf2 activity following viral infection [28]. A549 cells were transiently transfected with the ARE-driven reporter plasmid and infected with RSV in the presence or absence of tBHQ. RSV infection was associated with a significant decrease in reporter gene activity, compared with uninfected cells, which was restored close to levels of uninfected cells by tBHQ treatment (Comp: Fig. 8 about here.). AOE gene and protein expression, as well as Nrf2 nuclear levels, were also significantly increased in RSV-infected cells by tBHQ treatment (Fig. 8B and C and Supplementary Material, Figs. 6A and 6B), indicating that Nrf2 inducers can restore ARE-dependent gene expression following RSV infection. Treatment of AECs with tBHQ up to 6 h p.i. was able to restore Nrf2 activation and ARE-dependent gene expression in response to RSV infection (Supplementary Material, Figs. 6C and 6D), but not at later time points of infection (data not shown). Restoration of AOE cellular capacity was paralleled by significant reduction of RSV-induced oxidative stress, as shown by a significant decrease of the oxidative marker 8-isoprostane in virus-infected tBHQ-treated cells (Fig. 8D). The effect of tBHQ treatment on Nrf2 activation was not due to changes in HDAC activity (Fig. 8E).

As tBHQ treatment of AECs was able to restore Nrf2 activation, we tested whether BHA (precursor of tBHQ) had a similar effect in the airways of infected mice. Lungs of mice either sham-inoculated or infected with RSV for 48 h in the presence or absence of BHA (250 mg/kg) were harvested to prepare bronchoalveolar lavages (BALs), nuclear extracts, or total RNA. Mice infected with RSV showed significantly reduced Nrf2 nuclear levels, compared with sham-inoculated mice, and in most of the infected mice, BHA treatment was able to restore Nrf2 activation to levels close to that in uninfected mice (Fig. 9A), as well as the expression of the Nrf2 target genes catalase and SOD1 (Fig. 9B). In addition, there was a very significant reduction in RSV-induced lung oxidative stress in BHA-treated mice, as indicated by a significant reduction of 8-isoprostane levels in BALs, compared with untreated, infected mice (Fig. 9C), supporting our previous finding that BHA treatment has a positive impact on RSV-induced lung disease.

4. Discussion

Since its isolation, RSV has been identified as a leading cause of epidemic respiratory infections in infants and children worldwide [2]. No efficacious treatment or vaccine exists yet for RSV and immunity is incomplete, resulting in repeated attacks of acute respiratory tract illness through adulthood [2]. Several recent studies have directly or indirectly indicated an important role of ROS produced by epithelial and inflammatory cells and subsequent oxidative stress in the pathogenesis of acute and chronic lung

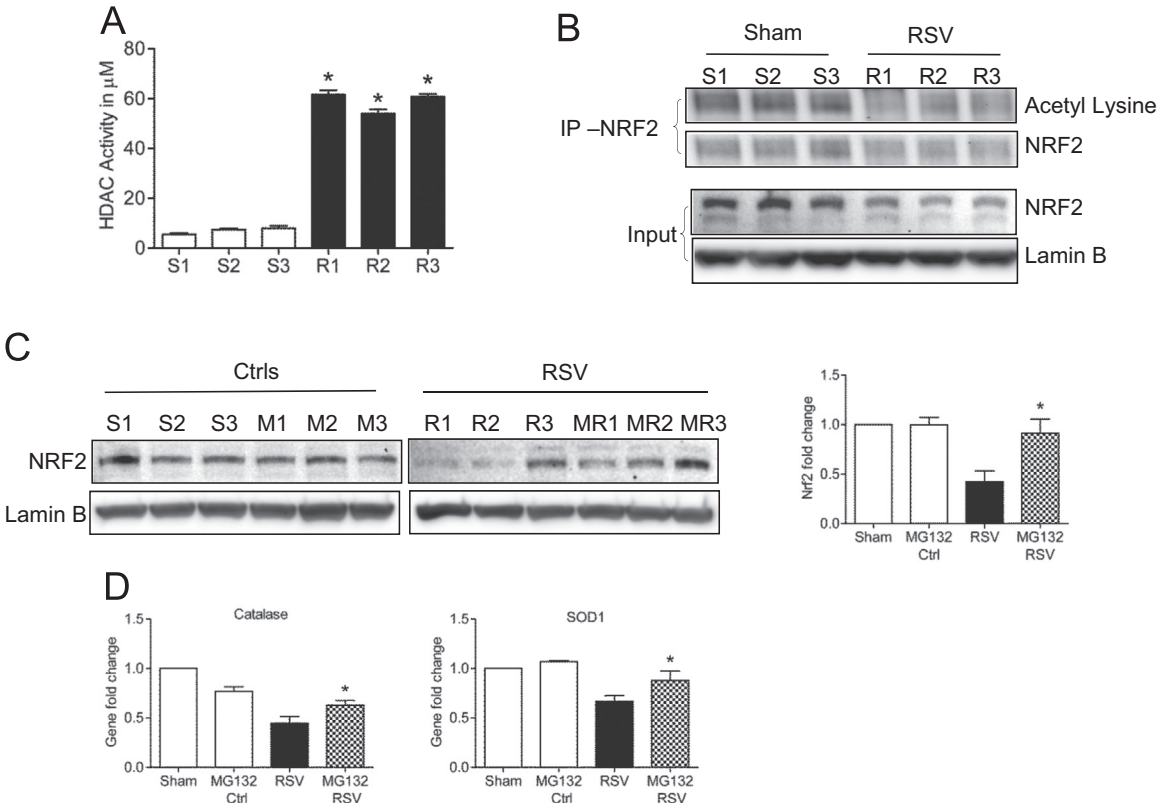

Fig. 7. Nrf2 is deacetylated and degraded through the proteasome pathway in vivo. Nuclear protein isolated from lungs of mice that were either sham inoculated (S1–S3) or infected with RSV (R1–R3) for 48 h was (A) analyzed for HDAC activity by using HDAC activity assay kit. Data are representative of three independent experiments. The groups were analyzed by one-way ANOVA followed by Tukey's post hoc test. Data are shown as mean ± SEM. $^*P < 0.05$ relative to sham inoculated mice. Nuclear protein was (B) immunoprecipitated using anti-Nrf2 antibody and subjected to Western blot using anti-acetyl lysine antibody. Lower panel shows Nrf2 Western blot for input of the IP. Lamin B was used as a loading control. (C) Nuclear protein prepared from lungs of mice that were either sham inoculated or infected with RSV for 48 h in the presence or absence of MG132 was subjected to Western blot analysis using anti-Nrf2 antibody. S1–S3: sham inoculated mice;, M1–M3: sham inoculated, MG132 treated mice; R1–R3: RSV infected mice;, and MR1–MR3: MG132 treated, RSV infected mice. For loading controls, membranes were stripped and reprobed with anti-lamin B antibody. The blots are representative of three independent experiments. Densitometric analysis of Nrf2 band intensity is shown after normalization to lamin B. The groups were analyzed by two-way ANOVA followed by a Bonferroni post-test. Data are shown as mean ± SEM. $^*P < 0.05$ relative to untreated RSV-infected mice. (D) Catalase (left panel) and SOD1 (right panel) gene expression were quantified by q-RT-PCR. Data are representative of three independent experiments. The groups were analyzed by two-way ANOVA followed by a Bonferroni post-test. Data are shown as mean ± SEM. $^*P < 0.05$ relative to untreated RSV-infected mice.

inflammatory diseases such as acute respiratory distress, cystic fibrosis, asthma, and COPD [29–32]. We and others have shown that infection with RSV, the recently identified human metapneumovirus (hMPV), and influenza can all induce ROS formation [7,33–36] and that inhibiting ROS production by administering antioxidants or recombinant SODs significantly decreases lung injury and improves clinical disease in RSV- and influenza-infected animals, suggesting that ROS play a significant role in the pathogenesis of virus-induced pneumonia [37,38]. Although increased antioxidant defenses have been reported in certain pulmonary diseases resulting from exposure to hyperoxia [39], ozone [40], and cigarette smoke [41], our recent studies and data presented here show that RSV infection induces a significant decrease in the expression of most AOEs involved in maintaining the cellular oxidant–antioxidant balance, leading to cellular oxidative stress, both in vitro and in vivo.

AOE gene transcription is regulated through binding of Nrf2 to the ARE site located in the gene promoters [10]. Several viruses have been shown to induce ARE-dependent responses by activating Nrf2. Among them, hepatitis B and C viruses, human cytomegalovirus, and the Kaposi's sarcoma-associated herpes virus, which can all induce ROS formation (reviewed in [34]), have been shown to activate Nrf2 in infected cells, leading to the induction of cytoprotective genes, as a mechanism to protect infected cells from oxidative damage [42–46]. Similarly, Marburg virus, an important cause of human hemorrhagic fever, blocks Keap1 activation, leading to the expression of AOE genes to ensure survival of infected cells [47]. In our study, we found that RSV infection of AECs induces transient Nrf2 activation, demonstrated by increased Nrf2 binding to the ARE of the AOE gene promoter and activation of ARE-dependent gene transcription at 6 h p.i., followed, however, by a progressive decrease in Nrf2 activation, starting at 15 h p.i., to levels below the ones found in uninfected cells (Fig. 1), with a kinetics that mirrors the progressive decrease in AOE expression observed in RSV-infected cells [4].

Reduced nuclear levels of Nrf2 can occur as a result of various mechanisms, including decreased expression, increased degradation, or increased nuclear export [9]. Our results show that RSV infection is associated with increased Nrf2 ubiquitination and degradation through a proteasomal pathway, based on our observation that the proteasomal inhibitors MG132 and Lactacystin restore Nrf2 expression and binding to the ARE site of the AOE gene promoters, restoring ARE-dependent gene transcription and AOE gene expression to that of uninfected cells (Figs. 2 and 3). Nrf2 degradation through the proteasome pathway also occurred in vivo, as MG132 treatment in mice was able to restore Nrf2 nuclear levels in lungs of mice infected with RSV; however, it had a modest impact in restoring AOE gene expression, in particular on catalase (Fig. 7). A possible explanation of these findings is that MG132 affects activation of other signaling molecules, which in turn could be important in regulating AOE gene expression. For example, MG132 inhibits NF-κB activation [48], and NF-κB seems

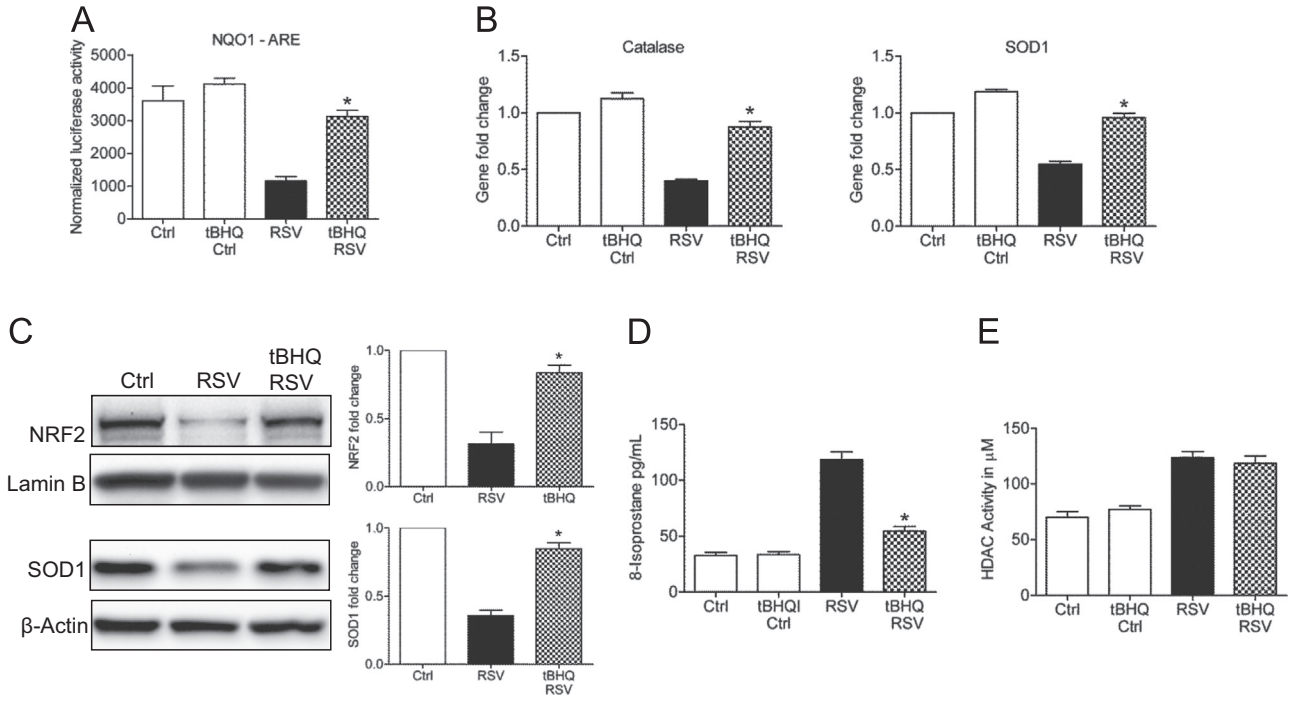

Fig. 8. Nrf2 modulation restores ARE-dependent gene transcription and ameliorates oxidative stress during RSV infection. (A) A549 cells were transiently transfected with the ARE-luciferase reporter plasmid, uninfected or infected with RSV for 1 8 h in the presence or absence of 25 μM tBHQ, and harvested to measure luciferase activity. Data are representative of three independent experiments. The groups were analyzed by two-way ANOVA followed by a Bonferroni post-test. Data are shown as mean ± SEM. $^{*}P < 0.05$ relative to untreated RSV-infected cells. (B) SAECs, uninfected or infected with RSV for 18 h in the presence or absence of 25 μM tBHQ, were harvested to prepare total RNA. Catalase (left panel) and SOD1 (right panel) gene expression were quantified by real-time PCR. Data are presented as fold changes and are representative of three independent experiments. The groups were analyzed by two-way ANOVA followed by a Bonferroni post-test. Data are shown as mean ± SEM. $^{*}P < 0.05$ relative to untreated RSV-infected cells. (C) SAECs were infected with RSV for 18 h in the presence or absence of 25 μM tBHQ. Nuclear protein and total cell lysates were subjected to Western blot analysis using anti-Nrf2 or SOD1 antibodies. For loading controls, membranes were stripped and reprobed using anti-lamin B antibody for nuclear fractions or anti-β-actin antibody for total cell lysates. The blots are representative of three independent experiments. Densitometric analysis of Nrf2 and SOD1 band intensity is shown after normalization to the appropriate internal control. The groups were analyzed by two-way ANOVA followed by a Bonferroni post-test. Data are shown as mean ± SEM. $^{*}P < 0.05$ relative to untreated RSV-infected cells. (D) The oxidative stress marker 8-isoprostane was measured by competitive enzyme immunoassay from the supernatant of SAECs uninfected or infected with RSV for 18 h in the presence or absence of 25 μM tBHQ. Data are representative of three independent experiments. The groups were analyzed by two-way ANOVA followed by a Bonferroni post-test. Data are shown as mean ± SEM. $^{*}P < 0.05$ relative to untreated RSV-infected cells. (E) HDAC activity in nuclear extracts prepared from SAECs uninfected and infected with RSV for 18 h in the presence or absence of 25 μM tBHQ were analyzed using an HDAC activity assay kit. Data are representative of three independent experiments. The groups were analyzed by two-way ANOVA followed by a Bonferroni post-test. Data are shown as mean ± SEM.

to play an important role in transcriptional response to oxidative stress, including the expression of catalase and glutathione peroxidase [49]. Although stabilization of Nrf2 by proteasome inhibition and subsequent transcriptional activation of its downstream genes, by preventing Nrf2 degradation, have been shown in different cell types and disease conditions (reviewed in [50]), suggesting that proteasome inhibition could be a promising therapeutic strategy for oxidative-stress-damage-associated diseases, it does not seem to have a beneficial effect in the context of RSV, at least in a mouse model of infection [51]. Treatment of RSV-infected mice with bortezomib, an FDA-approved proteasome inhibitor, resulted in increased pulmonary inflammation and disease compared with untreated infected animals. Whether Nrf2 ubiquitination in response to RSV infection occurs through Keap1 remains to be established, as we observed it both in SAE and A549 cells, which carry a Keap1 mutation that greatly reduces its repressor activity [52].

RSV-induced decrease in Nrf2 activation could be restored by treatment of AECs with the Nrf2 inducer tBHQ, shown by restoration of Nrf2 nuclear levels, ARE-dependent gene transcription, and AOE expression, which resulted in a significant decrease of cellular oxidative stress (Fig. 8). Administration of tBHQ was also able to restore Nrf2 activation in vivo, as indicated by a significant increase of Nrf2 nuclear levels in lung extracts of RSV-infected mice, which were dramatically decreased by the infection (Fig. 9), as we have previously described [5]. The Nrf2-ARE pathway has been shown to play a protective role in the murine airways against RSV-induced injury and oxidative stress. More severe RSV disease, with higher viral titers, augmented inflammation, and enhanced mucus production and epithelial injury, was found in *Nrf2*-/- mice compared with *Nrf2*+/+ mice [53]. Similarly, lack of Nrf2 expression resulted in increased influenza virus replication [54], while treatment of AECs with the Nrf2 inducer sulforaphane or Nrf2 overexpression led to significant inhibition of viral replication and oxidative stress [54,55].

Post-translational modifications, such as phosphorylation and acetylation, are important regulators of transcription factor activation, regulating multiple steps of activation, from nuclear translocation to DNA binding to transcriptional activity. Nrf2 has been shown to be acetylated by p300/CBP [56]. Acetylation promotes DNA binding of Nrf2 and enhances gene transcription, although not of all Nrf2 target genes [56]. It also regulates Nrf2 cellular distribution, as deacetylating conditions result in relocalization of Nrf2 to the cytoplasmic compartment [12]. As a dynamic and reversible process, acetylation of Nrf2 is determined by the relative activities of HATs and histone deacetylases. Our results show that RSV infection was associated with increased deacetylase activity and reduced recruitment of CBP to the ARE site of AOE gene promoters, resulting in Nrf2 deacetylation both in vitro and in vivo (Figs. 4 and 7). CBP overexpression could rescue ARE-dependent gene transcription and treatment of infected cells with the HDAC inhibitor TSA led to restoration of Nrf2 acetylation,

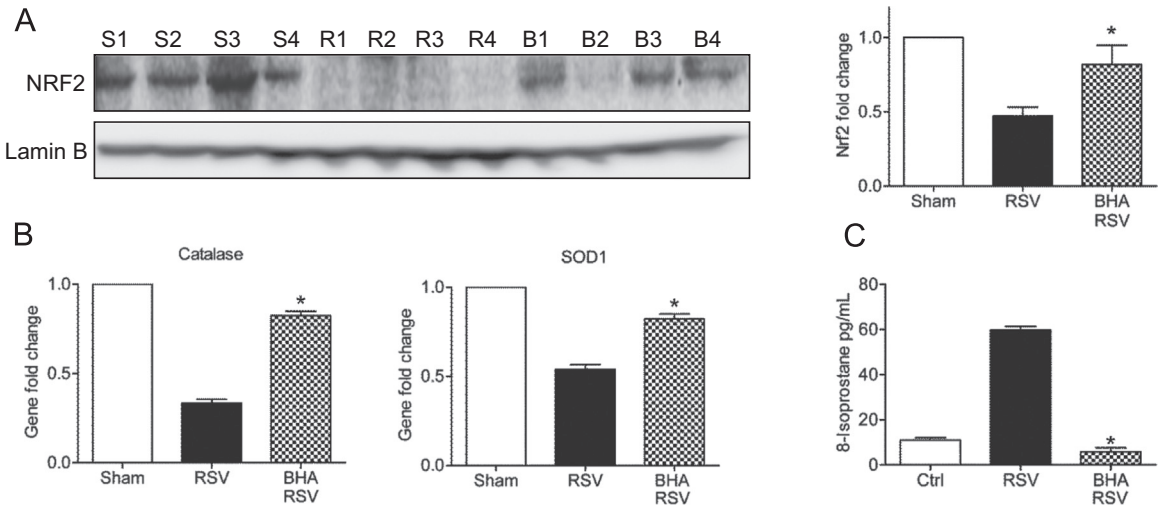

Fig. 9. BHA treatment restores Nrf2 expression and ameliorates oxidative stress in vivo during RSV infection. (A) Nuclear protein isolated from lungs of mice that were either sham inoculated or infected with RSV for 48 h in the presence or absence of BHA were subjected to Western blot analysis with anti-Nrf2 antibody. S1–S4: sham inoculated mice; R1–R4: RSV-infected mice; and B1––B4: BHA-treated and RSV- infected mice. For loading controls, membranes were stripped and reprobed with anti-lamin B antibody. The blots are representative of three independent experiments. Densitometric analysis of Nrf2 band intensity is shown after normalization to lamin B. The groups were analyzed by one-way ANOVA followed by Tukey's post hoc test. Data are shown as mean ± SEM. $^*P < 0.05$ relative to untreated RSV-infected mice. (B) Catalase (left panel) and SOD1 (right panel) gene expression were quantified by q-RT-PCR. Data are representative of three independent experiments. The groups were analyzed by one-way ANOVA followed by Tukey's post hoc test. Data are shown as mean ± SEM. $^*P < 0.05$ relative to untreated RSV-infected mice. (C) The oxidative stress marker 8-isoprostane was measured by competitive enzyme immunoassay in BAL of mice sham inoculated or infected with RSV for 48 h in the presence or absence of BHA. Data are representative of three independent experiments. The groups were analyzed by one-way ANOVA followed by Tukey's post hoc test. Data are shown as mean ± SEM. $^*P < 0.05$ relative to untreated RSV-infected mice.

suggesting that RSV infection is associated with an unbalanced acetylation/deacetylation environment at the ARE transcription sites. HDAC inhibition was able to restore Nrf2 nuclear levels and Nrf2 binding to the ARE site of AOE gene promoters, therefore restoring ARE-dependent gene transcription and gene expression in RSV-infected cells (Fig. 5). Importantly, HDAC inhibition was also associated with increased Nrf2 cellular levels (Fig. 5), suggesting that blocking RSV-induced Nrf2 deacetylation might indeed protect Nrf2 against degradation by retaining it in the nucleus, bound to its cognate promoter site. Although HDAC class III (sirtuins) have been shown to play a role in Nrf2 deacetylation [12], we could not demonstrate a significant role of this class of HDAC in RSV-induced inhibition of Nrf2 activation. On the other hand, Class I HDAC1 and 2 seem to be important in regulating Nrf2 function in infected cells, as inhibition of their expression was associated with restoration of Nrf2 nuclear levels and Nrf2-dependent gene expression both in A549 and SAECs (Fig. 6). Although we did observe an increase in HDAC activity, there was no induction of HDAC 1 or 2 expression in RSV-infected cells (Supplementary Material, Fig. 4). Induction of global HDAC activity has been reported in other disease models, such as cardiac hypertrophy and ischemia–reperfusion injury, as well as rheumatoid arthritis [57,58]. HDAC1 and 2 activity is regulated at multiple levels (reviewed in [59]). Both proteins are active within a complex of proteins, the better characterized being Sin3, NuRD (nucleosome remodeling and deacetylating), and Co-REST, which are necessary for modulating HDAC deacetylase activity and DNA binding, together with other proteins that mediate the recruitment of HDACs to gene promoters. A second way of regulating HDAC activity is via post-translational modifications. Both activity and complex formation are regulated by phosphorylation. HDAC1 and HDAC2 are phosphorylated at a low level in resting cells, and hyperphosphorylation leads to a significant increase in deacetylase activity. It is possible that RSV infection leads to modification of either or both of these important regulatory elements of HDAC activation. HDAC inhibitors are currently being developed as a new class of anticancer agents, many of which have already entered clinical trials, and our findings suggest that they could represent an attractive novel treatment for virus-induced lung inflammation.

In conclusion, RSV-induced respiratory disease is associated with increased ROS generation and oxidative stress that are likely to play a key role in initiating and amplifying lung injury and inflammation. Compounds that stimulate ARE-driven transcription, as well as possibly HDAC inhibitors, could hold great potential for modulating RSV-induced oxidative stress and the associated lung damage.

Acknowledgments

This project was supported by R01 AI062885, R21 AI111042, R21 AI103565, P01 AI07924602, P30 ES006676, and W81XWH1010146-DoD. We acknowledge Tianshuang Liu and Yinghong Ma for their technical assistance and Cynthia Tribble for manuscript editing and submission.

Appendix A. Supplementary material

Supplementary data associated with this article can be found in the online version at http://dx.doi.org/10.1016/j.freeradbiomed.2015.05.043.

References

[1] C.B. Hall, G.A. Weinberg, M.K. Iwane, A.K. Blumkin, K.M. Edwards, M.A. Staat, et al., The burden of respiratory syncytial virus infection in young children, N Engl J Med **360** (2009) 588–598.
[2] C.B. Hall, Respiratory syncytial virus and parainfluenza virus, N Engl J Med **344** (2001) 1917–1928.
[3] A.R. Falsey, P.A. Hennessey, M.A. Formica, C. Cox, E.E. Walsh, Respiratory syncytial virus infection in elderly and high-risk adults, N Engl J Med **352** (2005) 1749–1759.
[4] Y.M. Hosakote, T. Liu, S.M. Castro, R.P. Garofalo, A. Casola, Respiratory syncytial virus induces oxidative stress by modulating antioxidant enzymes, Am J Respir Cell Mol Biol **41** (2009) 348–357.
[5] Y.M. Hosakote, P.D. Jantzi, D.L. Esham, H. Spratt, A. Kurosky, A. Casola, et al.,

Viral-mediated inhibition of antioxidant enzymes contributes to the pathogenesis of severe respiratory syncytial virus bronchiolitis, Am J Respir Crit Care Med **183** (2011) 1550–1560.
[6] S.M. Castro, A. Guerrero-Plata, G. Suarez-Real, P.A. Adegboyega, G.N. Colasurdo, A.M. Khan, et al., Antioxidant Treatment Ameliorates Respiratory Syncytial Virus-induced Disease and Lung Inflammation, Am J Respir Crit Care Med **174** (2006) 1361–1369.
[7] A. Casola, N. Burger, T. Liu, M. Jamaluddin, A.R. Brasier, R.P. Garofalo, Oxidant tone regulates RANTES gene transcription in airway epithelial cells infected with Respiratory Syncytial Virus: role in viral-induced Interferon Regulatory Factor activation, J Biol Chem **276** (2001) 19715–19722.
[8] T. Liu, S. Castro, A.R. Brasier, M. Jamaluddin, R.P. Garofalo, A. Casola, Reactive oxygen species mediate virus-induced STAT activation: role of tyrosine phosphatases, J Biol Chem **279** (2004) 2461–2469.
[9] J.W. Kaspar, S.K. Niture, A.K. Jaiswal, Nrf2:INrf2 (Keap1) signaling in oxidative stress, Free Radic Biol Med **47** (2009) 1304–1309.
[10] A.K. Jaiswal, Nrf2 signaling in coordinated activation of antioxidant gene expression, Free Radic Biol Med **36** (2004) 1199–1207.
[11] D.A. Bloom, A.K. Jaiswal, Phosphorylation of Nrf2 at Ser40 by protein kinase C in response to antioxidants leads to the release of Nrf2 from INrf2, but is not required for Nrf2 stabilization/accumulation in the nucleus and transcriptional activation of antioxidant response element-mediated NAD(P)H:quinone oxidoreductase-1 gene expression, J Biol Chem **278** (2003) 44675–44682.
[12] Y. Kawai, L. Garduno, M. Theodore, J. Yang, I.J. Arinze, Acetylation-deacetylation of the transcription factor Nrf2 (nuclear factor erythroid 2-related factor 2) regulates its transcriptional activity and nucleocytoplasmic localization, J Biol Chem **286** (2011) 7629–7640.
[13] O. Ueba, Respiratory syncytial virus: I. concentration and purification of the infectious virus, Acta Med Okayama **32** (1978) 265–272.
[14] J.A. Patel, M. Kunimoto, T.C. Sim, R. Garofalo, T. Eliott, S. Baron, et al., Interleukin-1 alpha mediates the enhanced expression of intercellular adhesion molecule-1 in pulmonary epithelial cells infected with respiratory syncytial virus, Am J Resp Cell Mol **13** (1995) 602–609.
[15] A. Casola, R.P. Garofalo, M. Jamaluddin, S. Vlahopoulos, A.R. Brasier, Requirement of a novel upstream response element in RSV induction of interleukin-8 gene expression: stimulus-specific differences with cytokine activation, J Immunol **164** (2000) 5944–5951.
[16] E. Schreiber, P. Matthias, M.M. Muller, W. Schaffner, Rapid detection of octamer binding proteins with"mini-extracts', prepared from a small number of cells, Nucleic Acids Res **17** (1989) 6419.
[17] X. Bao, T. Liu, Y. Shan, K. Li, R.P. Garofalo, A. Casola, Human metapneumovirus glycoprotein G inhibits innate immune responses, PLoS Pathog **4** (2008) e1000077.
[18] T.P. Welliver, R.P. Garofalo, Y. Hosakote, K.H. Hintz, L. Avendano, K. Sanchez, et al., Severe human lower respiratory tract illness caused by respiratory syncytial virus and influenza virus is characterized by the absence of pulmonary cytotoxic lymphocyte responses, J Infect Dis **195** (2007) 1126–1136.
[19] J.E. Johnson, R.A. Gonzales, S.J. Olson, P.F. Wright, B.S. Graham, The histopathology of fatal untreated human respiratory syncytial virus infection, Mod Pathol **20** (2007) 108–119.
[20] I.V. Gregoretti, Y.M. Lee, H.V. Goodson, Molecular evolution of the histone deacetylase family: functional implications of phylogenetic analysis, J Mol Biol **338** (2004) 17–31.
[21] M. Dokmanovic, C. Clarke, P.A. Marks, Histone deacetylase inhibitors: overview and perspectives, Mol Cancer Res **5** (2007) 981–989.
[22] M. Gertz, F. Fischer, G.T. Nguyen, M. Lakshminarasimhan, M. Schutkowski, M. Weyand, et al., Ex-527 inhibits Sirtuins by exploiting their unique NAD+-dependent deacetylation mechanism, Proc Natl Acad Sci U S A **110** (2013) E2772–E2781.
[23] E. Verdin, F. Dequiedt, H.G. Kasler, Class II histone deacetylases: versatile regulators, Trends Genet **19** (2003) 286–293.
[24] X.J. Yang, S. Gregoire, Class II histone deacetylases: from sequence to function, regulation, and clinical implication, Mol Cell Biol **25** (2005) 2873–2884.
[25] S. Spange, T. Wagner, T. Heinzel, O.H. Kramer, Acetylation of non-histone proteins modulates cellular signalling at multiple levels, Int J Biochem Cell Biol **41** (2009) 185–198.
[26] S. Khochbin, A. Verdel, C. Lemercier, D. Seigneurin-Berny, Functional significance of histone deacetylase diversity, Curr Opin Genet Dev **11** (2001) 162–166.
[27] W. Hur, N.S. Gray, Small molecule modulators of antioxidant response pathway, Curr Opin Chem Biol **15** (2011) 162–173.
[28] Y.S. Keum, Y.H. Han, C. Liew, J.H. Kim, C. Xu, X. Yuan, et al., Induction of heme oxygenase-1 (HO-1) and NAD[P]H: quinone oxidoreductase 1 (NQO1) by a phenolic antioxidant, butylated hydroxyanisole (BHA) and its metabolite, tert-butylhydroquinone (tBHQ) in primary-cultured human and rat hepatocytes, Pharm Res **23** (2006) 2586–2594.
[29] V. Lucidi, G. Ciabattoni, S. Bella, P.J. Barnes, P. Montuschi, Exhaled 8-iso-prostane and prostaglandin E(2) in patients with stable and unstable cystic fibrosis, Free Radic Biol Med **45** (2008) 913–919.
[30] W. MacNee, Oxidative stress and lung inflammation in airways disease, Eur J Pharmacol **429** (2001) 195–207.
[31] I. Rahman, D. Morrison, K. Donaldson, W. MacNee, Systemic oxidative stress in asthma, COPD, and smokers, Am J Respir Crit Care Med **154** (1996) 1055–1060.
[32] E.J. Morcillo, J. Estrela, J. Cortijo, Oxidative stress and pulmonary inflammation: pharmacological intervention with antioxidants, Pharmacol Res **40** (1999) 393–404.
[33] X. Bao, M. Sinha, T. Liu, C. Hong, B.A. Luxon, R.P. Garofalo, et al., Identification of human metapneumovirus-induced gene networks in airway epithelial cells by microarray analysis, Virology **374** (2008) 114–127.
[34] A.M. Choi, K. Knobil, S.L. Otterbein, D.A. Eastman, D.B. Jacoby, Oxidant stress responses in influenza virus pneumonia: gene expression and transcription factor activation, Am J Physiol **271** (1996) L383–L391.
[35] D.B. Jacoby, A.M. Choi, Influenza virus induces expression of antioxidant genes in human epithelial cells, Free Radic Biol Med **16** (1994) 821–824.
[36] M. Jamaluddin, B. Tian, I. Boldogh, R.P. Garofalo, A.R. Brasier, Respiratory syncytial virus infection induces a reactive oxygen species-MSK1-phospho-Ser-276 RelA pathway required for cytokine expression, J Virol **83** (2009) 10605–10615.
[37] T. Akaike, M. Ando, T. Oda, T. Doi, S. Ljiri, S. Araki, et al., Dependence on O2 generation by xanthine oxidase of pathogenesis of influenza virus infection in mice, J Clin Invest **85** (1990).
[38] T. Akaike, Y. Noguchi, S. Ijiri, K. Setoguchi, M. Suga, Y.M. Zheng, et al., Pathogenesis of influenza virus-induced pneumonia: involvement of both nitric oxide and oxygen radicals, Proc Natl Acad Sci U S A **93** (1996) 2448–2453.
[39] S.C. Erzurum, C. Danel, A. Gillissen, C.S. Chu, B.C. Trapnell, R.G. Crystal, In vivo antioxidant gene expression in human airway epithelium of normal individuals exposed to 100% O2, J Appl Physiol **75** (1993) 1256–1262.
[40] D.S. Boehme, J.A. Hotchkiss, R.F. Henderson, Glutathione and GSH-dependent enzymes in bronchoalveolar lavage fluid cells in response to ozone, Exp Mol Pathol **56** (1992) 37–48.
[41] C.B. Gilks, K. Price, J.L. Wright, A. Churg, Antioxidant gene expression in rat lung after exposure to cigarette smoke, Am J Pathol **152** (1998) 269–278.
[42] S. Schaedler, J. Krause, K. Himmelsbach, M. Carvajal-Yepes, F. Lieder, K. Klingel, et al., Hepatitis B virus induces expression of antioxidant response element-regulated genes by activation of Nrf2, J Biol Chem **285** (2010) 41074–41086.
[43] D. Burdette, M. Olivarez, G. Waris, Activation of transcription factor Nrf2 by hepatitis C virus induces the cell-survival pathway, J Gen Virol **91** (2010) 681–690.
[44] A.V. Ivanov, O.A. Smirnova, O.N. Ivanova, O.V. Masalova, S.N. Kochetkov, M. G. Isaguliants, Hepatitis C virus proteins activate Nrf2/ARE pathway by distinct ROS-dependent and independent mechanisms in HUH7 cells, PLoS ONE **6** (2011) e24957.
[45] J. Lee, K. Koh, Y.E. Kim, J.H. Ahn, S. Kim, Up-regulation of Nrf2 Expression by Human Cytomegalovirus Infection Protects Host Cells from Oxidative Stress, J Gen Virol **94** (2013) 1658–1668.
[46] O. Gjyshi, V. Bottero, M.V. Veettil, S. Dutta, V.V. Singh, L. Chikoti, et al., Kaposi's sarcoma-associated herpesvirus induces Nrf2 during de novo infection of endothelial cells to create a microenvironment conducive to infection., PLoS Pathog **10** (2014) e1004460.
[47] A. Page, V.A. Volchkova, S.P. Reid, M. Mateo, A. Bagnaud-Baule, K. Nemirov, et al., Marburgvirus Hijacks Nrf2-Dependent Pathway by Targeting Nrf2-Negative Regulator Keap1, Cell Rep (2014).
[48] M. Karin, M. Delhase, The I kappa B kinase (IKK) and NF-kappa B: key elements of proinflammatory signalling, Semin Immunol **12** (2000) 85–98.
[49] L.Z. Zhou, A.P. Johnson, T.A. Rando, NF kappa B and AP-1 mediate transcriptional responses to oxidative stress in skeletal muscle cells, Free Radic Biol Med **31** (2001) 1405–1416.
[50] W. Cui, Y. Bai, P. Luo, L. Miao, L. Cai, Preventive and therapeutic effects of MG132 by activating Nrf2-ARE signaling pathway on oxidative stress-induced cardiovascular and renal injury, Oxid Med Cell Longev **2013** (2013) 306073.
[51] C. Lupfer, K.M. Patton, M.K. Pastey, Treatment of human respiratory syncytial virus infected Balb/C mice with the proteasome inhibitor bortezomib (Velcade, PS-341) results in increased inflammation and mortality, Toxicology **268** (2010) 25–30.
[52] A. Singh, V. Misra, R.K. Thimmulappa, H. Lee, S. Ames, M.O. Hoque, et al., Dysfunctional Keap1-Nrf2 interaction in non-small-cell lung cancer, PLoS Med **3** (2006) e420.
[53] H.Y. Cho, F. Imani, L. Miller-Degraff, D. Walters, G.A. Melendi, M. Yamamoto, et al., Antiviral Activity of Nrf2 in a Murine Model of Respiratory Syncytial Virus (RSV) Disease, Am J Respir Crit Care Med (2008).
[54] M.J. Kesic, S.O. Simmons, R. Bauer, I. Jaspers, Nrf2 expression modifies influenza A entry and replication in nasal epithelial cells, Free Radic Biol Med **51** (2011) 444–453.
[55] B. Kosmider, E.M. Messier, W.J. Janssen, P. Nahreini, J. Wang, K.L. Hartshorn, et al., Nrf2 protects human alveolar epithelial cells against injury induced by influenza A virus, Respir Res **13** (2012) 43.
[56] Z. Sun, Y.E. Chin, D.D. Zhang, Acetylation of Nrf2 by p300/CBP augments promoter-specific DNA binding of Nrf2 during the antioxidant response, Mol Cell Biol **29** (2009) 2658–2672.
[57] T.A. McKinsey, Therapeutic potential for HDAC inhibitors in the heart, Annu Rev Pharmacol Toxicol **52** (2012) 303–319.
[58] J. Gillespie, S. Savic, C. Wong, A. Hempshall, M. Inman, P. Emery, et al., Histone deacetylases are dysregulated in rheumatoid arthritis and a novel histone deacetylase 3-selective inhibitor reduces interleukin-6 production by peripheral blood mononuclear cells from rheumatoid arthritis patients, Arthritis Rheum **64** (2012) 418–422.
[59] A.J. de Ruijter, A.H. van Gennip, H.N. Caron, S. Kemp, A.B. van Kuilenburg, Histone deacetylases (HDACs): characterization of the classical HDAC family, Biochem J **370** (2003) 737–749.

JVI Journals.ASM.org

Role of Hydrogen Sulfide in Paramyxovirus Infections

Hui Li,[a] Yinghong Ma,[a] Oliver Escaffre,[b] Teodora Ivanciuc,[a] Narayana Komaravelli,[a] John P. Kelley,[a] Ciro Coletta,[c] Csaba Szabo,[c] Barry Rockx,[b,f] Roberto P. Garofalo,[a,d,e] Antonella Casola[a,d,e]

Department of Pediatrics,[a] Department of Pathology,[b] Department of Anesthesiology,[c] and Sealy Centers for Vaccine Development[d] and Molecular Medicine,[e] University of Texas Medical Branch at Galveston, Galveston, Texas, USA; Department of Rare and Emerging Viral Infections and Response, Center for Infectious Disease Control, National Institute for Public Health and the Environment, Bilthoven, The Netherlands[f]

ABSTRACT

Hydrogen sulfide (H_2S) is an endogenous gaseous mediator that has gained increasing recognition as an important player in modulating acute and chronic inflammatory diseases. However, its role in virus-induced lung inflammation is currently unknown. Respiratory syncytial virus (RSV) is a major cause of upper and lower respiratory tract infections in children for which no vaccine or effective treatment is available. Using the slow-releasing H_2S donor GYY4137 and propargylglycin (PAG), an inhibitor of cystathionine-γ-lyase (CSE), a key enzyme that produces intracellular H_2S, we found that RSV infection led to a reduced ability to generate and maintain intracellular H_2S levels in airway epithelial cells (AECs). Inhibition of CSE with PAG resulted in increased viral replication and chemokine secretion. On the other hand, treatment of AECs with the H_2S donor GYY4137 reduced proinflammatory mediator production and significantly reduced viral replication, even when administered several hours after viral absorption. GYY4137 also significantly reduced replication and inflammatory chemokine production induced by human metapneumovirus (hMPV) and Nipah virus (NiV), suggesting a broad inhibitory effect of H_2S on paramyxovirus infections. GYY4137 treatment had no effect on RSV genome replication or viral mRNA and protein synthesis, but it inhibited syncytium formation and virus assembly/release. GYY4137 inhibition of proinflammatory gene expression occurred by modulation of the activation of the key transcription factors nuclear factor κB (NF-κB) and interferon regulatory factor 3 (IRF-3) at a step subsequent to their nuclear translocation. H_2S antiviral and immunoregulatory properties could represent a novel treatment strategy for paramyxovirus infections.

IMPORTANCE

RSV is a global health concern, causing significant morbidity and economic losses as well as mortality in developing countries. After decades of intensive research, no vaccine or effective treatment, with the exception of immunoprophylaxis, is available for this infection as well as for other important respiratory mucosal viruses. This study identifies hydrogen sulfide as a novel cellular mediator that can modulate viral replication and proinflammatory gene expression, both important determinants of lung injury in respiratory viral infections, with potential for rapid translation of such findings into novel therapeutic approaches for viral bronchiolitis and pneumonia.

Hydrogen sulfide (H_2S) is an endogenous gaseous transmitter that participates in the regulation of the respiratory system's physiological functions and pathophysiological alterations, including chronic obstructive pulmonary disease (COPD), asthma, pulmonary fibrosis, and hypoxia-induced pulmonary hypertension, as it regulates lung functions such as airway constriction, pulmonary circulation, cell proliferation/apoptosis, fibrosis, oxidative stress, and inflammation (reviewed in reference 1). H_2S is produced endogenously in mammals, including humans, by three enzymes: cystathionine-γ-lyase (CSE), cystathionine-β-synthase (CBS), and 3-mercaptopyruvate sulfurtransferase (MST) (2–4). Sulfide salts such as sodium hydrosulfide (NaHS) and sodium sulfide (Na_2S) have been widely used to study the biological effects of hydrogen sulfide in many cells, tissues, and animals. These salts generate a large burst of H_2S over a short time period, when used in cell culture. GYY4137 is a novel water-soluble H_2S donor that releases H_2S slowly over a period of hours (5). H_2S donors have been used to demonstrate how therapeutic H_2S administration exerts significant effects on various animal models of inflammation, reperfusion injury, and circulatory shock (6). There are no studies investigating the role of H_2S generation in pathophysiology of viral infections or the use of H_2S donors as a pharmacological intervention for virus-induced diseases.

Respiratory tract infections are a leading cause of morbidity and mortality worldwide. Paramyxoviruses, which include respiratory syncytial virus (RSV) and human metapneumovirus (hMPV), represent a major cause of pediatric upper and lower respiratory tract infections (7, 8). These viruses are associated with bronchiolitis, pneumonia, flu-like syndromes, as well as asthma exacerbations and represent a substantial public health problem for the community. Nipah virus (NiV) is a zoonotic emerging pathogen that also belongs to the *Paramyxoviridae* family and can cause severe and often fatal respiratory disease and/or encephalitis in humans (9). No vaccine or effective treatment is available for

Received 30 January 2015 **Accepted** 27 February 2015

Accepted manuscript posted online 4 March 2015

Citation Li H, Ma Y, Escaffre O, Ivanciuc T, Komaravelli N, Kelley JP, Coletta C, Szabo C, Rockx B, Garofalo RP, Casola A. 2015. Role of hydrogen sulfide in paramyxovirus infections. J Virol 89:5557–5568. doi:10.1128/JVI.00264-15.

Editor: S. R. Ross

Address correspondence to Antonella Casola, ancasola@utmb.edu.

doi:10.1128/JVI.00264-15

RSV, hMPV, or NiV, with the exception of immunoprophylaxis for RSV. Our previous studies have shown that these viruses induce the expression of a variety of proinflammatory genes, including cytokines and chemokines, in airway epithelial cells (AECs), the main target of infection (10–12), which are likely to play a major role in disease pathogenesis. Cytokine and chemokine gene expression in virus-infected cells is orchestrated by the activation of two key transcription factors, nuclear factor κB (NF-κB) and interferon regulatory factor 3 (IRF-3). A number of virus-inducible inflammatory and immunoregulatory genes require NF-κB for their transcription and/or are dependent on an intact NF-κB signaling pathway (13, 14), and IRF-3 is necessary for viral induction of RANTES transcription and gene expression (15, 16).

To address the role of H_2S generation/administration in viral infections, we used an *in vitro* model of RSV infection of AECs. We found that RSV infection led to decreased expression of CSE, a reduced ability to generate cellular H_2S, as well as increased H_2S degradation. Inhibition of H_2S generation by using PAG was associated with increased generation of virus infectious particles as well as increased proinflammatory mediator secretion, suggesting an important role of endogenous H_2S in controlling viral replication and proinflammatory gene expression. GYY4137 treatment of both A549 (a lung carcinoma cell line retaining features of type II alveolar epithelial cells) and primary small alveolar epithelial (SAE) cells significantly reduced virus-induced proinflammatory mediator release, and it significantly inhibited viral replication at a step subsequent to viral adsorption. GYY4137 administration blocked RSV replication without significantly reducing viral mRNA synthesis, viral genome replication, and viral protein synthesis, indicating that it affects steps involved in viral assembly and/or release. It also resulted in significant inhibition of syncytium formation, indicating a modulatory effect on virus-induced cellular fusion.

GYY4137 treatment of AECs infected with RSV did not affect the initial step of virus-induced activation of IRF-3 and NF-κB, as shown by the lack of changes in their nuclear translocation; however, it significantly reduced IRF-3 and NF-κB binding to the endogenous promoter of proinflammatory genes, resulting in an inhibition of chemokine gene transcription, indicating an important effect of H_2S on cellular signaling, independent of its antiviral activity.

MATERIALS AND METHODS

Materials. GYY4137 [morpholin-4-ium-4-methoxyphenyl(morpholino) phosphinodithioate], a novel water-soluble, slow-releasing H_2S compound, and DL-propargylglycin (PAG), an inhibitor of the H_2S-generating enzyme cystathionine-γ-lyase (CSE), were purchased from Sigma-Aldrich (St. Louis, MO, USA). Solutions were prepared freshly in culture medium and filtered through a 0.2-μm filter before treatment. Sulfidefluor-7-acetoxymethyl ester (SF7-AM), a fluorescent probe that allows direct, real-time visualization of endogenous H_2S produced in live human cells (17), was generously provided by Christopher J. Chang (Department of Chemistry, University of California, Berkeley). An SF7-AM stock solution was prepared in dimethyl sulfoxide (DMSO) and diluted in serum-free medium at least a thousandfold.

Virus preparation. The RSV Long strain was grown in HEp-2 cells and purified by centrifugation on discontinuous sucrose gradients, as described previously (18, 19), and titers of viral pools in PFU/ml were determined by using a methylcellulose plaque assay, as described previously (20). No contaminating cytokines or lipopolysaccharide (LPS), tested by the *Limulus* hemocyanin agglutination assay, was found in these virus preparations. Virus pools were aliquoted, quick-frozen on dry ice-alcohol, and stored at −80°C until use.

hMPV strain CAN97-83 was obtained from the Centers for Disease Control and Prevention (CDC), Atlanta, GA, with permission from Guy Boivin at the Research Center in Infectious Diseases, Regional Virology Laboratory, Laval University, Quebec City, Canada; propagated on LLC-MK2 cells; and purified on sucrose cushions, as previously described (21). Titers of virus pools in PFU/ml were determined by immunostaining, as previously described (21).

The Nipah virus Bangladesh strain (NiV-B) was obtained from the Special Pathogens Branch of the Centers for Disease Control and Prevention (Atlanta, GA). The virus was propagated on Vero cells, as previously described (10). Titers of virus pools were determined by a 50% tissue culture infective dose ($TCID_{50}$) assay, as previously described (10). All infectious work with NiV was performed in a class II biological safety cabinet in a biosafety level 4 (BSL4) laboratory at the Galveston National Laboratory.

Cell culture and viral infection. A549 cells, a human alveolar type II-like epithelial cell line (American Type Culture Collection, Manassas, VA), and small alveolar epithelial (SAE) cells (Clonetics, San Diego, CA), derived from terminal bronchioli of cadaveric donors, were grown in F12K medium and SAE cell growth medium, respectively, containing 10% (vol/vol) fetal bovine serum (FBS), 10 mM glutamine, 100 IU/ml penicillin, and 100 μg/ml streptomycin for F12K medium and 7.5 mg/ml bovine pituitary extract (BPE), 0.5 mg/ml hydrocortisone, 0.5 μg/ml human epidermal growth factor (hEGF), 0.5 mg/ml epinephrine, 10 mg/ml transferrin, 5 mg/ml insulin, 0.1 μg/ml retinoic acid, 0.5 μg/ml triiodothyronine, 50 mg/ml gentamicin, and 50 mg/ml bovine serum albumin (BSA) for SAE cell medium. When SAE cells were used for RSV infection, they were changed to basal medium, not supplemented with growth factors, 6 h prior to and throughout the experiment. Confluent cell monolayers were infected with RSV or hMPV at multiplicity of infection (MOI) of 1, as previously described (22), unless otherwise stated. NiV infection was performed at an MOI of 0.01 (10). For PAG experiments, cells were seeded into 6-well or 24-well plates, infected with RSV for 1 h at 37°C in 5% CO_2, and then treated with PAG after the viral inoculum was removed. For GYY4137 experiments, cells were seeded into 6-well or 24-well plates and treated either prior to infection, but not throughout the duration of infection, or at different times postinfection (p.i.), after the viral inoculum was removed. There was no effect of either compound on uninfected-cell viability, as assessed by trypan blue exclusion, or on basal cellular mediator secretion.

Methylene blue assay. H_2S production was measured by use of a colorimetric methylene blue assay, as previously described (23). Briefly, cells were homogenized, incubated at 37°C for 5 min, and then cooled on ice for 10 min. L-Cysteine (1 and 3 mmol/liter) and pyridoxal 5-phosphate (2 mmol/liter) were added and incubated for 1 h at 37°C. Zinc acetate (1%) and 10% trichloroacetic acid solutions were used to terminate the reaction. After the addition of *N*,*N*-dimethylphenylendiamine sulfate and $FeCl_3$ for 15 min, the optical absorbance of the solutions was measured at 650 nm.

SF7-AM fluorescence assay. A549 cells were grown in eight-well Lab-Tek II glass chamber slides (Thermo Scientific, Pittsburgh, PA, USA) and incubated with 5 μM SF7-AM probe at 37°C for 30 min. After washing with culture medium, A549 cells were infected with RSV and treated with GYY4137, as described above. Confocal fluorescence imaging studies were performed with a Zeiss 710 laser scanning microscope with a 20× water objective lens, with Zen 2009 software (Carl Zeiss). SF7-AM was excited by using a 488-nm argon laser, and emission was collected by using a Meta detector at wavelengths of between 500 and 650 nm. Cells were imaged at 37°C with 5% CO_2 throughout the experiment. Image analysis was performed by using Metamorph software (Carl Zeiss), and fluorescence was quantified by using the mean pixel intensity after setting a common threshold for all images.

Luciferase assay. A549 cells were transiently transfected by using a NF-κB- or interferon-stimulated responsive element (ISRE)-driven luciferase reporter plasmid containing five repeats of the NF-κB site of the IgG promoter or three repeats of the RANTES ISRE promoter, respectively, linked to the luciferase reporter gene, using Fugene 6 (Roche Diagnostic Corp., Indianapolis, IN), as previously described (16, 24). A total of 0.5 μg of the reporter gene plasmid and 0.05 μg of β-galactosidase expression plasmid/well were premixed with Fugene 6 and added to the cells in regular medium. The next day, cells were infected with RSV for 1 h, followed by treatment with GYY4137, and harvested at either 15 or 24 h p.i. to independently measure luciferase and β-galactosidase reporter activities, as previously described (24). Luciferase activity was normalized to the activity of the internal control β-galactosidase. Results are expressed in arbitrary units.

Determination of lactate dehydrogenase activity. Lactate dehydrogenase (LDH) activity in the medium, an index of cellular damage, was measured by a colorimetric assay using a commercially available kit (Cayman Chemical, MI, USA) according to the manufacturer's instructions.

Quantitative real-time PCR. Total RNA was extracted by using a ToTALLY RNA kit (catalog number AM1910; Ambion, Austin, TX). RNA samples were quantified by using a NanoDrop spectrophotometer (Thermo Fisher Scientific Inc., Wilmington, DE), and quality was analyzed on an RNA Nano or Pico chip by using the Agilent 2100 bioanalyzer (Agilent Technologies). Synthesis of cDNA was performed with 1 μg of total RNA in a 20-μl reaction mixture by using the TaqMan Reverse Transcription Reagents kit from ABI (catalog number N8080234; Applied Biosystems). The reaction conditions were as follows: 25°C for 10 min, 48°C for 30 min, and 95°C for 5 min. Quantitative real-time PCR amplification (performed in triplicate) was done with 1 μl of cDNA in a total volume of 25 μl by using Faststart Universal SYBR green master mix (catalog number 04913850001; Roche Applied Science). The final concentration of the primers was 300 nM. 18S RNA was used as a housekeeping gene for normalization. PCR assays were run with the ABI Prism 7500 sequence detection system with the following conditions: 50°C for 2 min, 95°C for 10 min, and then 95°C for 15 s and 60°C for 1 min for 40 cycles. The RSV N-specific reverse transcriptase (RT) primer contained a tag sequence from the bacterial chloramphenicol resistance (Cm^r) gene to generate the cDNA, because of self-priming exhibited by RSV RNA. Duplicate cycle threshold (C_T) values were analyzed in Microsoft Excel by the comparative C_T ($\Delta\Delta C_T$) method according to the manufacturer's instructions (Applied Biosystems). The amount of target ($2^{-\Delta\Delta CT}$) was obtained by normalization to the endogenous reference (18S) sample. To detect RSV N transcripts, we used RT primer 5′-CTGCGATGAGTGGCAGGC TTTTTTTTTTTTTAACTCAAAGCTC-3′; the tag is underlined. For PCR assays, we used RSV tag reverse primer CTGCGATGAGTGGCAGGC and forward primer ACTACAGTGTATTAGACTTRACAGCAGAAG. To detect the genome minus strand, we used RSV N RT primer 5′-CTGCGAT GAGTGGCAGGCACTACAGTGTATTAGACTTRACAGCAGAA G-3′. For PCR assays, we used RSV tag primer CTGCGATGAGTGGC AGGC and primer RSV P GCATCTTCTCCATGRAATTCAGG.

Western blotting. Nuclear extracts of uninfected and infected cells were prepared by using hypotonic/nonionic detergent lysis, according to a protocol described previously by Schreiber et al. (25). To prevent contamination with cytoplasmic proteins, isolated nuclei were purified by centrifugation through 1.7 M sucrose buffer for 30 min at 12,000 rpm, before nuclear protein extraction, as previously described (26). Total cell lysates were prepared from uninfected and infected A549 cells by the addition of ice-cold lysis buffer (50 mM Tris-HCl [pH 7.4], 150 mM NaCl, 1 mM EGTA, 0.25% sodium deoxycholate, 1 mM Na_3VO_4, 1 mM NaF, 1% Triton X-100, and 1 μg/ml of aprotinin, leupeptin, and pepstatin). After incubation on ice for 10 min, the lysates were collected, and detergent-insoluble materials were removed by centrifugation at 4°C at 14,000 × *g*. Proteins (10 to 20 μg per sample) were then boiled in 2× Laemmli buffer and resolved on SDS-PAGE gels. Proteins were transferred onto a Hybond polyvinylidene difluoride membrane (Amersham, Piscataway, NJ), and nonspecific binding sites were blocked by immersing the membrane in Tris-buffered saline–Tween (TBST) containing 5% skim milk powder or 5% bovine serum albumin for 30 min. After a short wash in TBST, membranes were incubated with the primary antibody for 1 h at room temperature or overnight at 4°C, depending on the antibody used, followed by incubation with horseradish peroxidase (HRP)-conjugated secondary antibody (Sigma, St. Louis, MO), diluted 1:10,000 in TBST, for 30 min at room temperature. After washing, proteins were detected by using an enhanced chemiluminescence system (RPN 2016; Amersham, GE Healthcare, United Kingdom) and visualized by autoradiography. Antibodies used for Western blot assays were goat anti-RSV polyclonal antibody from Ab D SeroTec; rabbit anti-p65, anti-Ser536, or anti-Ser276 p65 from Cell Signaling Technology Inc., Danvers, MA; and rabbit anti-IRF-3 from Santa Cruz Biotechnology, Santa Cruz, CA.

Bio-Plex assay. Cell-free supernatants were tested for multiple cytokines and chemokines by using the Bio-Plex Cytokine Human multiplex panel (Bio-Rad Laboratories, Hercules, CA), according to the manufacturer's instructions. Interleukin-8 (IL-8) and RANTES were also quantified by an enzyme-linked immunosorbent assay (ELISA) according to the manufacturer's protocol (DuoSet; R&D Systems, Minneapolis, MN). Prior to analysis, NiV samples were inactivated on dry ice by gamma radiation (5 megarads).

Chromatin immunoprecipitation and quantitative genomic PCR. For chromatin immunoprecipitation (ChIP) assays, we used a ChIP-It express kit from Active Motif (Carlsbad, CA) according to the manufacturer's instructions, with some modifications. Briefly, A549 cells in a 10-cm plate were washed three times with phosphate-buffered saline (PBS) and fixed with freshly prepared 2 mM disuccinimidyl glutarate (DSG) for 45 min at room temperature. After three washes with PBS, cells were fixed with freshly prepared formaldehyde for 10 min and neutralized with glycine for 5 min at room temperature. Cells were harvested and disrupted by using a Dounce homogenizer to isolate nuclei. Nuclei were sheared by sonication to obtain DNA fragments of 200 to 1,500 bp. Twenty micrograms of sheared chromatin was immunoprecipitated with 5 μg of ChIP-grade anti-NF-κB (catalog number sc-722X) or anti-IRF-3 (catalog number sc-369X) antibodies from Santa Cruz Biotechnology and magnetic beads conjugated with protein G at 4°C overnight. Immunoprecipitation with IgG antibody was used as a negative control. Chromatin was reverse cross-linked, eluted from magnetic beads, and purified by using a Qiagen PCR purification kit (Qiagen, USA). Quantitative genomic PCR (Q-gPCR) was done by SYBR green-based real-time PCR using primers spanning the IL-8 gene NF-κB promoter site (forward primer AGGTTTGCCCTGAGGGGATG and reverse primer GGAGTGCTCCG GTGGCTTTT) or primers spanning the RANTES gene ISRE promoter site (forward primer AGCGGCTTCCTGCTCTCTGA and reverse primer CAGCTCAGGCTGGCCCTTTA). Total input chromatin DNA for immunoprecipitation was included as a positive control for PCR amplification.

Statistical analysis. Statistical analyses were performed with the InStat 3.05 Biostatistics package from GraphPad, San Diego, CA. To ascertain differences between two groups, Student's *t* test was used, and if more than two groups were compared, one-way analysis of variance was performed, followed by Tukey's *post hoc* test. *P* values of <0.05 were considered statistically significant. When indicated, values of measurements are expressed as means ± standard errors of the means (SEM) in the figures.

RESULTS

RSV infection affects H_2S generation in airway epithelial cells. Of the three H_2S-generating enzymes CSE, CBS, and MST, CSE represents the major source of H_2S in lung tissue, and it uses cysteine as the main substrate. Sulfide:quinone oxidoreductase (SQOR) is a membrane-bound enzyme that catalyzes the first step in the mitochondrial metabolism of H_2S (27). To determine whether RSV induced changes in H_2S-generating and -metabolizing enzymes in AECs, A549 cells were infected for 6, 15, and 24 h

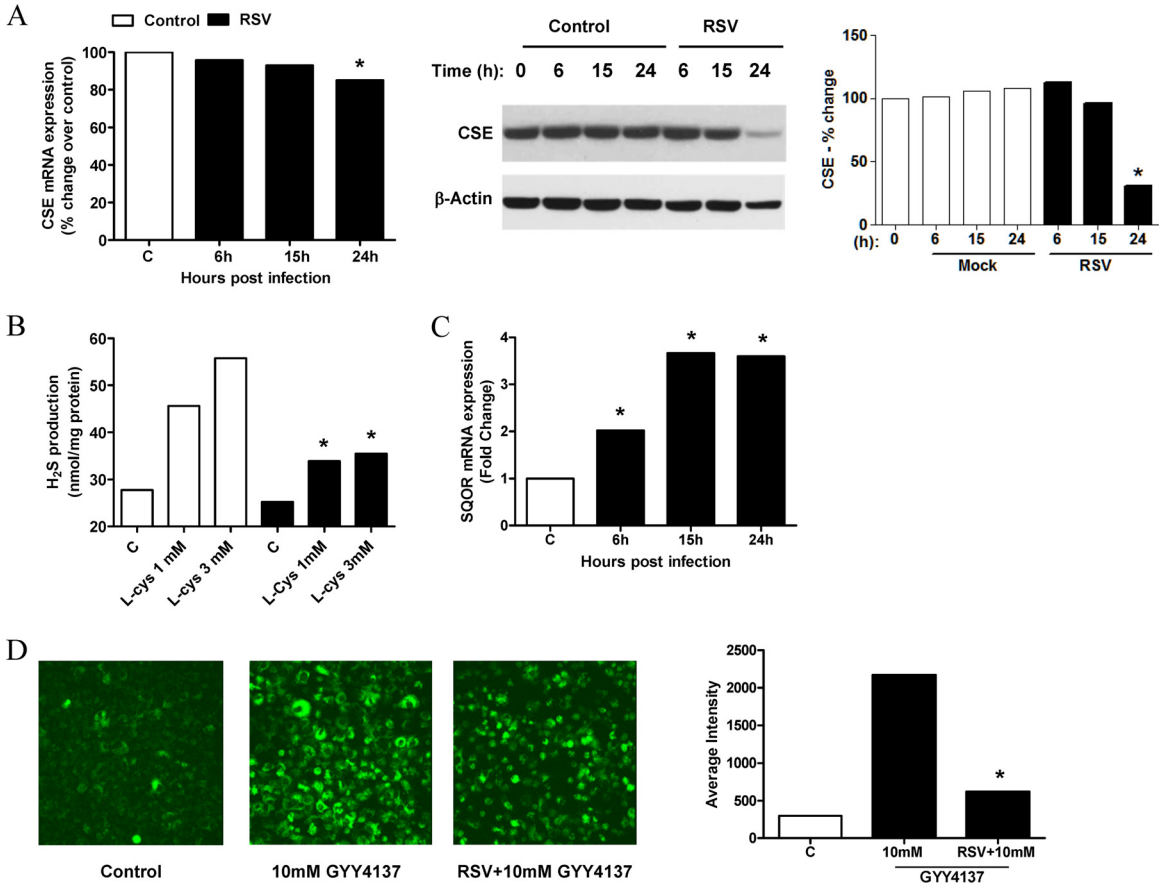

FIG 1 Effect of RSV infection on H_2S production in airway epithelial cells. A549 cells were infected with RSV for 6, 15, and 24 h and harvested to prepare total RNA or total cell lysates. (A and C) CSE (A, left) and SQOR (C) mRNA levels in uninfected and RSV-infected cells were measured by reverse transcriptase quantitative PCR (qRT-PCR). CSE cellular levels were also measured by Western blotting of total cell lysates. The membrane was stripped and reprobed for β-actin to determine equal loading of the samples (A, middle). Densitometric analysis of CSE band intensity, normalized to β-actin, was performed by using Alpha Ease software version 2200 (2.2d) (Alpha Innotech Co., San Leandro, CA) (A, right). Results are representative of data from three independent experiments. *, $P < 0.05$ compared to uninfected cells. (B) A549 cells were infected with RSV for 15 h and harvested to prepare total cell lysates. H_2S production in uninfected and RSV-infected cells was determined by a methylene blue colorimetric assay. Results are representative of data from three independent experiments. *, $P < 0.05$ compared to uninfected cells. (D) A549 cells were incubated with 5 μM the fluorescent probe SF7-AM and infected with RSV for 1 h. Medium or 10 mM GYY4137 was added to uninfected or infected cells and incubated for 15 h. (Left) Images of uninfected and untreated cells (control) and uninfected or infected cells treated with 10 mM GYY4137. (Right) Average fluorescence intensity quantified by confocal microscopy using Zeiss Metamorph software. Results are representative of data from three independent experiments. *, $P < 0.05$ compared to uninfected, treated cells.

and harvested for extraction of total RNA and measurement of CSE, CBS, and SQOR mRNA levels by real-time PCR. We found that CSE mRNA and protein expression levels were decreased by RSV infection only at later time points (Fig. 1A), while there was no significant change in the CBS mRNA level (data not shown). On the other hand, there was a significant time-dependent increase in the SQOR mRNA expression level in RSV-infected cells compared to uninfected cells (Fig. 1C). To investigate whether RSV modulated the capacity of airway epithelial cells to generate H_2S, A549 cells were infected for 15 h and harvested to prepare total cell lysates. H_2S production was then measured by a methylene blue assay. There was a significant reduction in H_2S generation in RSV-infected cells, compared to uninfected cells, when cysteine was supplied at 1 and 3 mM concentrations as the CSE substrate (Fig. 1B). When A549 cells were treated with the slow-releasing H_2S donor GYY4137, there was a significant increase in the intracellular level of H_2S detected by the fluorescent probe SF7-AM, which was significantly lower in infected cells, suggesting an increase in H_2S degradation following RSV infection (Fig. 1D).

CSE inhibition enhances RSV-induced chemokine production and viral replication. To examine the effect of CSE inhibition on virus-induced cellular responses, A549 cells were infected with RSV for 1 h and then treated with different concentrations of DL-propargylglycin (PAG). Cell supernatants were harvested at 24 h p.i. to measure virus-induced chemokine secretion. PAG administration significantly increased the levels of production of several cytokines and chemokines in response to RSV infection in a dose-dependent manner (Fig. 2A). PAG treatment of A549 cells also resulted in a significant increase in viral infectious-particle formation (3- to 4-fold increase), assessed by a plaque assay (Fig. 2B), indicating a role of endogenous H_2S production in viral replication and proinflammatory cellular responses.

Effect of H_2S treatment on RSV-induced proinflammatory mediator production. To investigate the effect of increasing intracellular H_2S levels on viral responses, we determined levels of cytokine and chemokine secretion in A549 cells infected with RSV in the presence or absence of GYY4137, a slow-releasing H_2S donor. A549 cells were infected with RSV for 1 h, followed by incubation with

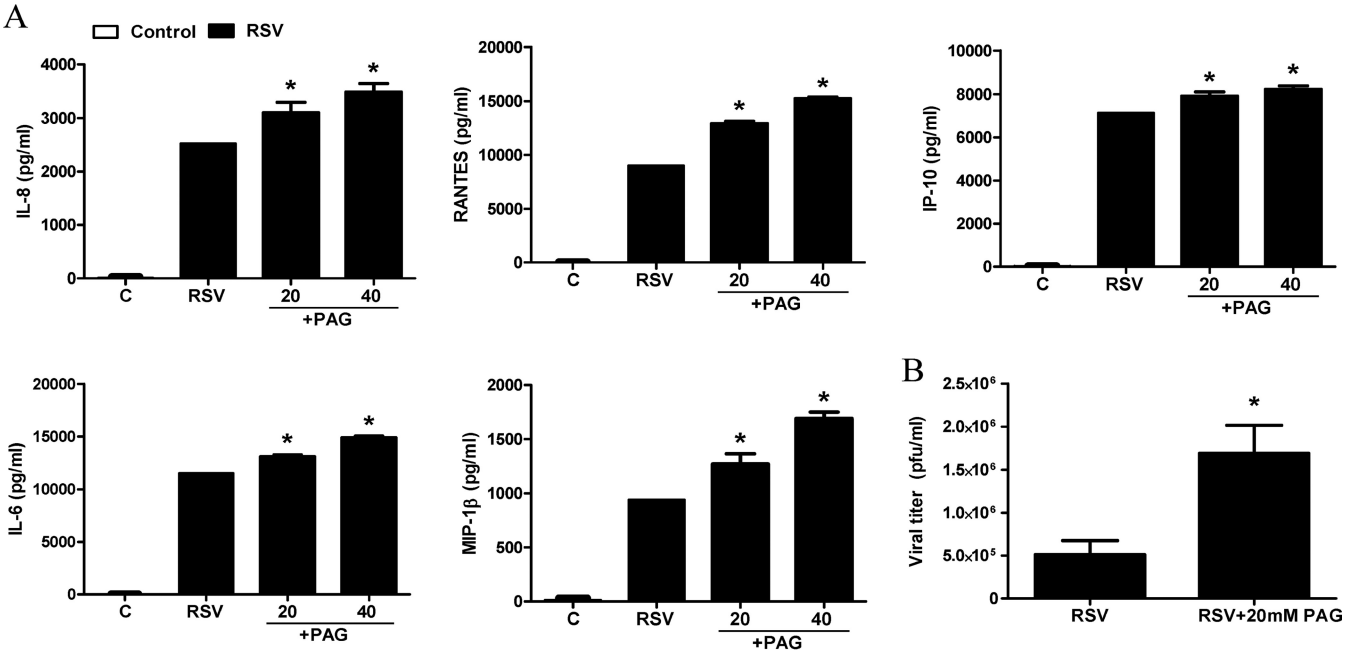

FIG 2 Effect of CSE inhibition on RSV-induced cytokine and chemokine production and viral replication. A549 cells were infected with RSV for 1 h and then incubated in the presence or absence of 20 or 40 mM PAG. (A) Cell supernatants from uninfected and RSV-infected cells, treated or untreated, were assayed at 24 h p.i. for cytokine and chemokine secretion by a Bio-Plex assay. Results are expressed as means ± standard errors. Results are representative of data from three independent experiments run in triplicate. (B) Cells were treated as described above for panel A and harvested at 24 h p.i. to determine viral titers by a plaque assay. *, $P < 0.05$ compared to untreated RSV-infected cells.

different concentrations of GYY4137, and harvested to collect the cell supernatant at 24 h p.i. to measure proinflammatory mediator release by ELISAs and Bio-Plex assays. RSV-induced secretion of several cytokines and chemokines, such as IL-6, IL-8, RANTES, macrophage inflammatory protein 1β (MIP-1β), and interferon-induced protein 10, was decreased by GYY4137 treatment in a dose-dependent manner (Fig. 3A). To investigate possible GYY4137 cytotoxicity, supernatants of uninfected or infected and treated or untreated A549 cells were harvested and tested for LDH release. There was no enhanced cellular damage; on the contrary, we observed a protective effect against virus-induced cytotoxicity in response to GYY4137 treatment (Fig. 3B). Inhibition of proinflammatory secretion, following RSV infection, by GYY4137 administration was also confirmed in SAE cells, normal human AECs, which we have shown to behave very similarly to A549 cells in terms of chemokine/cytokine gene expression and transcription factor and signaling pathway activation in response to RSV infection (12, 19, 22, 28–31) (Fig. 4).

Effects of H_2S treatment on RSV replication. To determine whether increasing intracellular H_2S levels affect viral replication, A549 cells were treated with different concentrations of GYY4137 either 1 h prior to RSV adsorption, until adsorption but not during infection, or 1 h after RSV adsorption and throughout infection and harvested at 24 p.i. to measure viral titers by a plaque assay. There was no change in viral titers when GYY4137 was given before infection (data not shown), while there was a significant decrease in RSV replication when GYY4137 was added after adsorption, in particular with the highest dose of the H_2S donor, in the order of a several-log reduction (Fig. 5, left), indicating significant antiviral activity of H_2S administration. To investigate whether this effect was reproducible if GYY4137 was administered several hours after infection, A549 cells were treated at 3 and 6 h p.i. and harvested to measure viral titers. We observed a significant decrease in RSV replication with both treatments, although the decrease was somewhat less striking than that with administration at 1 h p.i. (Fig. 5, middle and right), indicating that GYY4137 can affect viral replication when infection is already established.

H_2S treatment affects virus particle release and syncytium formation. To further investigate how H_2S treatment affected viral replication, we used several approaches, including quantification of viral gene transcription, genome replication, viral antigen detection, and viral particle release. GYY4137 administration did not decrease the number of RSV genome copies and N gene copies; on the contrary, they were somewhat increased at all concentrations tested (Fig. 6A and B). Viral protein expression, assessed by a Western blot assay of total cell lysates, was not significantly affected by GYY4137 treatment at any of the doses tested (Fig. 6C). When viral titers were assessed separately on cell supernatants and cell pellets, we found that GYY4137 administration dramatically reduced the number of infectious virus particles present in the cell supernatant, with a much less robust effect on those associated with the cell pellet (Fig. 6D, left versus right), suggesting that H_2S treatment affects viral replication in part at the level of virus assembly but mostly at the level of virus release. When viral replication was assessed in a multicycle replication system, this resulted in a significant inhibition of the cell-associated virus content in addition to the almost complete absence of virus in the cell supernatant of infected cells treated with the higher dose of GYY4173 (Fig. 6E). To determine whether the reduction in viral titers in cell supernatants was due to fewer virus particles released or to a loss of infectivity, we performed a Western blot analysis of viral proteins in supernatants from cells infected in the absence or presence of GYY4173. We found clear decreases in the levels of most of the

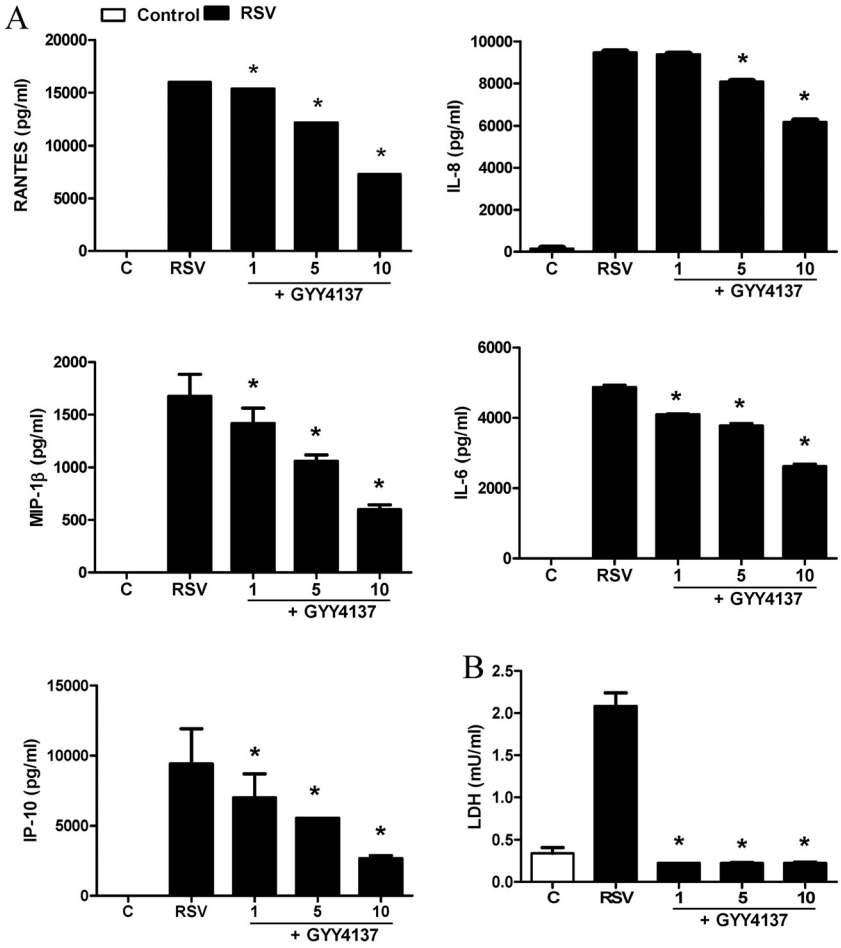

FIG 3 Effect of H_2S donor treatment on RSV-induced cytokine and chemokine production in A549 cells. Cells were infected with RSV for 1 h and then incubated in the presence or absence of GYY4137 at 1, 5, and 10 mM for 24 h. Cell supernatants were assayed for cytokine and chemokine secretion by an ELISA or a Bio-Plex assay (A) and for cytotoxicity by an LDH release assay (B). Results are expressed as means ± standard errors and are representative of data from at least three independent experiments run in triplicate for the experiments described above for panel A. *, $P < 0.05$ compared to untreated RSV-infected cells.

viral proteins, with the exception of the G protein, which represents in good part a secreted protein (Fig. 6F). Moreover, we observed a striking reduction in cellular syncytium formation, suggesting that GYY4137 treatment can significantly affect virus-induced cellular fusion (Fig. 6G).

Effect of GYY4137 on RSV-induced cellular signaling. Cytokine and chemokine gene expression in A549 cells infected by RSV is orchestrated by the activation of the two key transcription factors NF-κB and IRF-3. To determine whether changes in RSV-induced cytokine and chemokine production observed with GYY4137 treatment affected NF-κB- and IRF-3-dependent gene transcription, we performed reporter gene assays. Cells were transiently transfected with either a NF-κB- or IRF-driven luciferase reporter plasmid and then treated with GYY4137 after 1 h of viral adsorption and harvested at 24 h p.i. to measure luciferase activity. RSV infection significantly enhanced both IRF-3- and NF-κB-dependent gene transcription, which was significantly inhibited by GYY4137 treatment in a dose-dependent manner (Fig. 7A and B), consistent with the observed reduction in IL-8 and RANTES secretion.

To determine whether GYY4137 treatment was able to modulate virus-induced NF-κB and IRF-3 activation, A549 cells were infected with RSV for 1 h, incubated with or without GYY4137, and harvested at 15 and 24 h p.i. to prepare either total cell lysates or nuclear extracts. NF-κB and IRF-3 nuclear levels or cellular levels of phosphorylated serine in p65, the major NF-κB subunit activated in response to RSV infection (22), were assessed by Western blotting. Nuclear translocation of both transcription factors was not changed by GYY4137 treatment compared to RSV infection alone (Fig. 7C); however, there was a significant decrease in RSV-induced p65 Ser276 and Ser536 phosphorylation (Fig. 7D), two important posttranslational modifications that affect NF-κB transcriptional activity (32). In addition, GYY4137 treatment significantly reduced p65 and IRF occupancy of their cognate binding site on the IL-8 and RANTES endogenous promoters, assessed by a two-step chromatin immunoprecipitation (XChIP) and genomic PCR (Q-gPCR) assay (Fig. 7E). Taken together, these results indicate that increasing cellular H_2S levels by using a slow-releasing donor can effectively modulate the strong proinflammatory cellular response induced by RSV infection through blocking IRF- and NF-κB-dependent gene transcription.

Effects of H_2S treatment on chemokine production and viral replication induced by other paramyxoviruses. To investigate whether GYY4137 had similar antiviral and anti-inflammatory

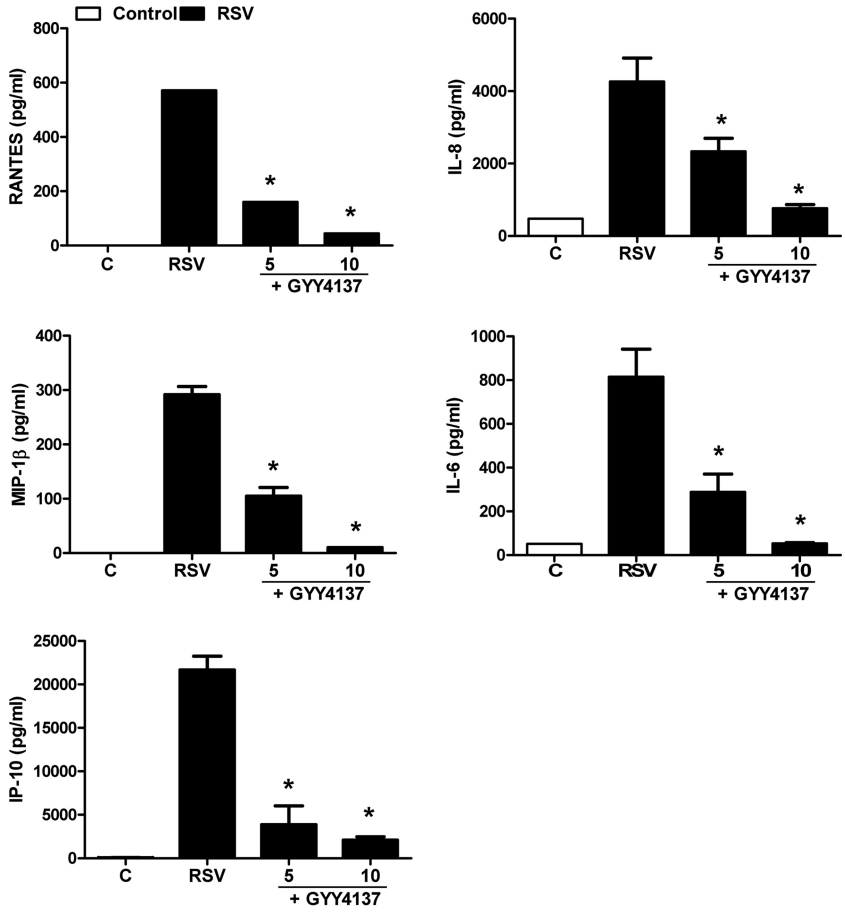

FIG 4 Effect of H_2S donor treatment on RSV-induced cytokine and chemokine production in SAE cells. Cells were infected with RSV for 1 h and then incubated in the presence or absence of GYY4137 at 5 and 10 mM for 24 h. Cell supernatants were assayed for cytokine and chemokine secretion by an ELISA or a Bio-Plex assay. Results are expressed as means ± standard errors and are representative of data from three independent experiments run in triplicate. *, $P < 0.05$ compared to untreated RSV-infected cells.

effects on other paramyxoviruses, we measured chemokine secretion and viral replication in A549 cells in response to hMPV infection. A549 cells were infected with hMPV for 1 h and incubated in the presence or absence of GYY4137 for a total of 24 h. Cell supernatants were collected to measure levels of IL-8 and RANTES induction by an ELISA, while viral titers were determined by immunostaining. hMPV-induced IL-8 and RANTES secretion was significantly decreased by GYY4137 treatment in a dose-dependent manner (Fig. 8A). Similarly, viral replication was also significantly reduced by GYY4137 treatment (Fig. 8B). A similar experiment was conducted by using a model of SAE cells infected with NiV-B. Similarly to RSV and hMPV, GYY4137 treatment led to a significant reduction of virus-induced cytokine and chemokine secretion (Fig. 9A) and inhibi-

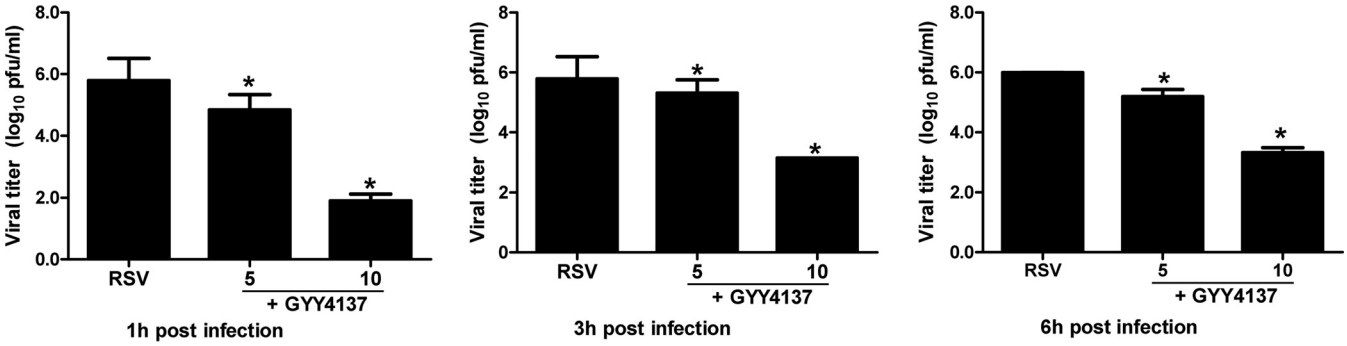

FIG 5 Effect of H_2S donor treatment on RSV replication. A549 cells were infected with RSV for 1, 3, or 6 h and then incubated in the presence or absence of GYY4137 at 5 and 10 mM for 24 h. Cells were harvested to determine viral titers by a plaque assay. Results are expressed as means ± standard errors and are representative of data from five independent experiments run in triplicate. *, $P < 0.05$ compared to untreated RSV-infected cells.

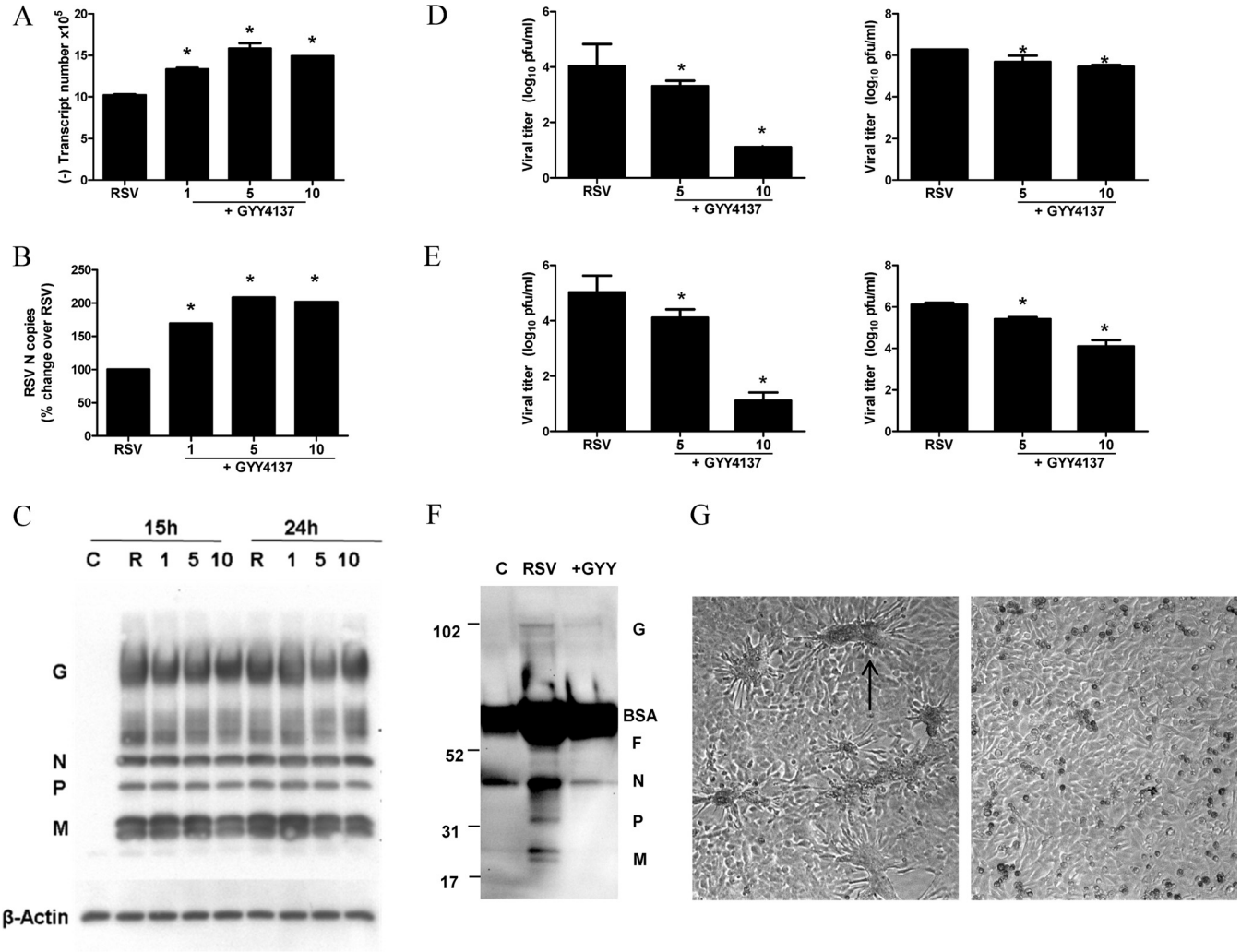

FIG 6 Effect of H_2S donor treatment on different steps of viral replication. A549 cells were infected with RSV for 1 h and then incubated in the presence or absence of GYY4137 for 24 h. (A to C) Cells were harvested to prepare either total RNA to measure viral genome copy numbers (A) or RSV N gene copy numbers (B) by qRT-PCR or total cell lysates to measure viral protein expression by Western blotting (C). The membrane was stripped and reprobed with β-actin as a control for equal loading of the samples. Data are representative of data from three independent experiments with similar results. (D) A549 cells were infected with RSV for 1 h and then incubated in the presence or absence of GYY4137 at 5 and 10 mM for 24 h. Cell supernatants (left) and cell pellets (right) were harvested separately to determine viral titers by a plaque assay. Results are expressed as means ± standard errors and are representative of data from three independent experiments run in triplicate. *, $P < 0.05$ compared to untreated RSV-infected cells. (E) HEp-2 cells were infected with RSV at an MOI of 0.01 in the presence or absence of GYY4137 at 5 and 10 mM for 48 h. Cell supernatants (left) and cell pellets (right) were harvested separately to determine viral titers by a plaque assay. Results are expressed as means ± standard errors and are representative of two independent experiments run in triplicate. *, $P < 0.05$ compared to untreated RSV-infected cells. (F) A549 cells were infected with RSV for 1 h and then incubated in the presence or absence of GYY4137 for 24 h. Cell supernatants were harvested to measure viral protein expression by Western blotting. Data are representative of data from two independent experiments with similar results. (G) Light microscopy photograph (magnification, ×20) of HEp-2 cells infected with RSV at an MOI of 0.01 for 48 h in the presence (right) or absence (left) of GYY4137 at 10 mM. The arrow indicates one of the many syncytia present in the cell monolayer as a result of viral infection.

tion of viral replication (Fig. 9B). In addition, GYY4137 treatment inhibited syncytium formation in response to both hMPV and NiV infection (data not shown), suggesting that GYY4137 has a broad antiviral effect on paramyxoviruses.

DISCUSSION

In this study, we investigated the role of H_2S in airway epithelial cell responses to viral infection. Paramyxoviruses, in particular RSV and hMPV, are a primary cause of severe lower respiratory tract infections in children as well as in other populations, leading to increased morbidity and mortality, for which there is no vaccine or treatment besides supportive measures. The virus-induced lung inflammatory response, triggered by the secretion of cytokines and chemokines from virus-infected airway-resident cells such as AECs and alveolar macrophages, plays an important role in disease pathogenesis. We and others have shown that modulation of the inflammatory response is associated with an amelioration of clinical illness in animal models of RSV infection (33–36), making it an important target for the development of effective treatment strategies.

H_2S is an important endogenous gaseous mediator that has recently been the focus of intense investigation, leading to sup-

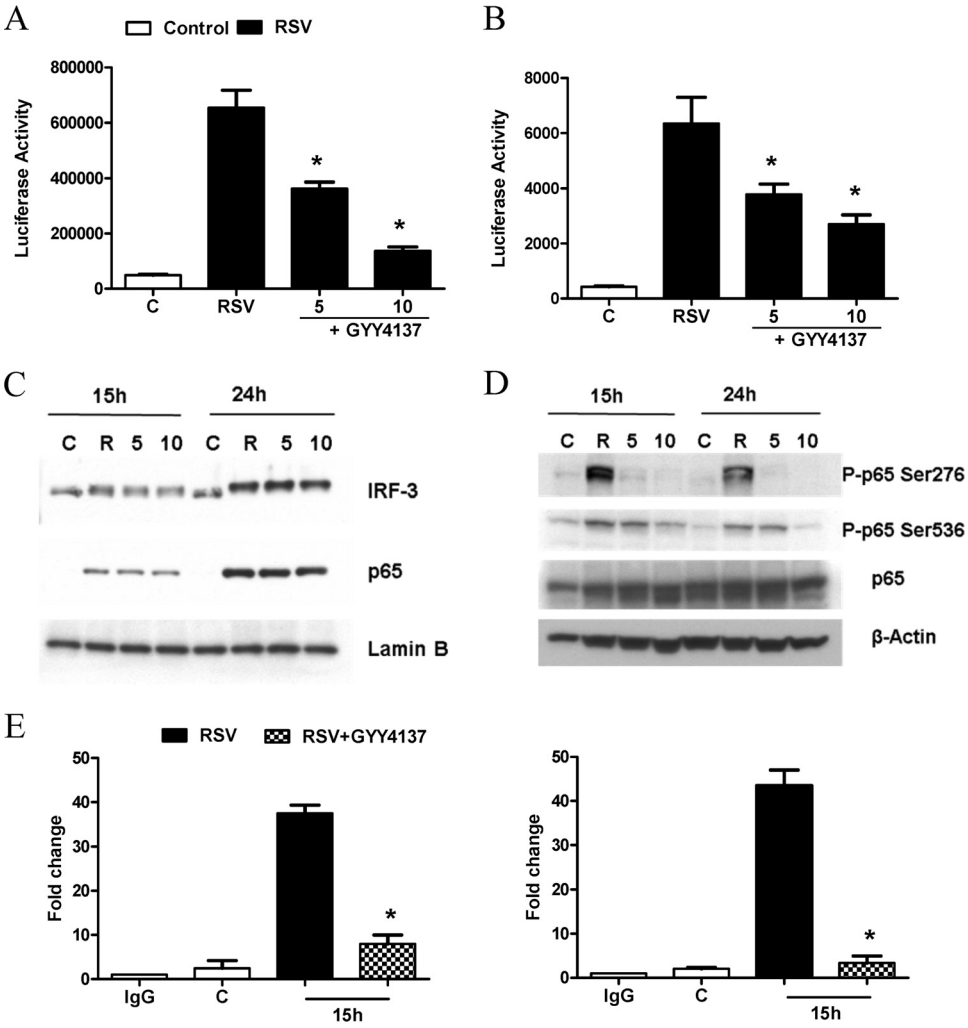

FIG 7 Effect of H_2S donor treatment on virus-induced signaling. (A and B) A549 cells were transiently transfected with an ISRE-driven (A) or NF-κB-driven (B) reporter gene plasmid, infected with RSV for 1 h, and then treated with 5 and 10 mM GYY4137. Cells were harvested at 15 or 24 h p.i. to measure luciferase and β-galactosidase reporter activities. Luciferase activity was normalized to the activity of the internal control β-galactosidase. Results are representative of data from three independent experiments run in triplicate. Data are expressed as means ± standard errors for normalized luciferase activity. *, $P < 0.05$ relative to untreated, RSV-infected cells. (C) A549 cells were infected with RSV for 1 h, followed by GYY4137 treatment at different concentrations, and harvested at 15 and 24 h p.i. to prepare either total cell lysates or nuclear extracts. IRF-3 and p65 nuclear translocation was assessed by Western blotting of nuclear extracts. Membranes were stripped and reprobed with lamin B to determine equal loading of the samples. (D) Total Ser276 and Ser536 p65 phosphorylation levels were determined by Western blotting of total cell lysates. The membrane was stripped and reprobed for total p65 and β-actin to determine equal loading of the samples. Data are representative of data from three independent experiments with similar results. (E) Chromatin DNA from uninfected and RSV-infected A549 cells in the presence or absence of GYY4137 for 15 h was immunoprecipitated by using an anti-NF-κB antibody (left), an anti-IRF-3 antibody (right), or IgG as a negative control. Q-gPCR was performed by using primers spanning either the NF-κB-binding site of the IL-8 promoter or the ISRE-binding site of the RANTES promoter. Total input chromatin DNA for immunoprecipitation was included as positive control for Q-gPCR amplification. The fold change was calculated compared to the IgG control. Results are representative of data from two independent experiments. *, $P < 0.05$ relative to untreated, RSV-infected cells.

portive evidence that it plays an important role in vasoactive, cytoprotective, anti-inflammatory, and antioxidant cellular responses (reviewed in reference 37). Our study shows for the first time that H_2S has a protective role in RSV infection by modulating both inflammatory gene expression and viral replication. AECs infected with RSV displayed a decreased ability to generate H_2S and enhanced degradation of H_2S released by the donor GYY4137, indicating that viral infection leads to changes in H_2S cellular homeostasis. Endogenous H_2S production appears to play an important role in modulating virus-induced chemokine secretion and viral replication, as both were significantly enhanced by treatment of AECs with the CSE inhibitor PAG, while increased H_2S cellular levels, as a result of the administration of GYY4137, were associated with a significant reduction of proinflammatory mediator production and, most importantly, a striking reduction of late-stage viral replication.

GYY4137 administration resulted in a strong inhibition of viral replication at a step subsequent to viral adsorption. It dramatically reduced the amount of infectious virus present in the cell supernatant, with a much less robust effect on cell-associated virus, without having a significant effect on viral gene transcription, protein synthesis, or genome replication. These findings suggest that

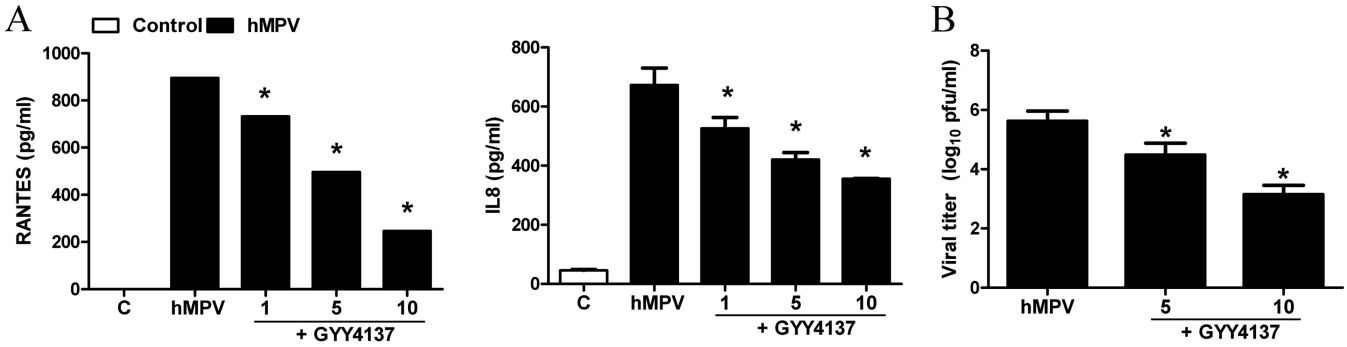

FIG 8 Effect of H_2S donor treatment on hMPV-induced chemokine production and viral replication. A549 cells were infected with hMPV for 1 h, followed by treatment with different millimolar concentrations of GYY4137. (A) Cell supernatants from uninfected and hMPV-infected cells, treated or untreated, were assayed at 24 h p.i. for cytokine and chemokine secretion by a Bio-Plex assay. Results are expressed as means ± standard errors. Results are representative of data from two independent experiments run in triplicate. *, $P < 0.05$ compared to untreated hMPV-infected cells. (B) Viral replication was determined at 24 h postinfection by titration of viral infectious particles released into the cell supernatants by a plaque assay. Results are representative of data from two independent experiments run in triplicate. *, $P < 0.05$ compared to untreated hMPV-infected cells.

H_2S treatment inhibits viral replication in part at the level of virus assembly but mostly at the level of virus release, which in part explains the increases in cellular viral mRNA and genomic RNA levels observed with H_2S treatment. To produce progeny virions, ribonuclear protein complexes, which form cytoplasmic inclusions and contain newly synthesized genomic RNA together with several viral proteins translated in the cytoplasm, have to be assembled with the surface glycoproteins that have trafficked to the cell surface through the secretory pathway and are then released to form mature infectious virus (reviewed in reference 38). The apical recycling endosome (ARE) has been implicated in RSV protein trafficking and membrane scission, and downregulation of specific proteins such as myosin Vb or Rab11 disrupts virion formation and results in diminished numbers of viral progeny. To date, it is not known whether H_2S, or any other endogenous gaseous transmitters, modulates ARE functions. The final step in viral assembly and budding involves a membrane scission event to separate the assembled viral particle from the host cell membrane, which often involves multivesicular body formation and the endosomal sorting complex required for transport (ESCRT) protein system, with membrane scission being performed by the ATPase Vps4 (38). In the case of RSV, budding is unaffected by the inhibition of Vps4, suggesting that RSV uses a novel mechanism for this final step of replication. Some evidence suggests that surface glycoproteins, both F and G, could actively contribute to the budding process leading to RSV egress from infected cells (38). Although we did not detect significant changes in the levels of expression of most viral proteins, we have not investigated whether H_2S treatment could affect their routing to the cell membrane. Changes in the cellular localization of the F protein, for example, could explain the changes observed in syncytium formation and assembly/release following H_2S treatment.

Endogenous H_2S production and exogenous H_2S administration have been associated with both proinflammatory and anti-inflammatory effects in various models of disease (reviewed in reference 39). In the context of acute pancreatitis and in burn injury, for example, H_2S seems to play a proinflammatory role, while in other pathologies, such as asthma, COPD, LPS-induced inflammation, and ischemia reperfusion, it displays anti-inflammatory properties. In models of lung injury, administration of H_2S donors has often been associated with an anti-inflammatory effect. For example, in a mouse model of hyperoxia, treatment with NaHS was associated with reduced lung permeability and inflammation, due to decreased levels production of proinflammatory mediators such as IL-1β, monocyte chemoattractant protein 1 (MCP-1), and MIP-2 and increased levels of anti-inflam-

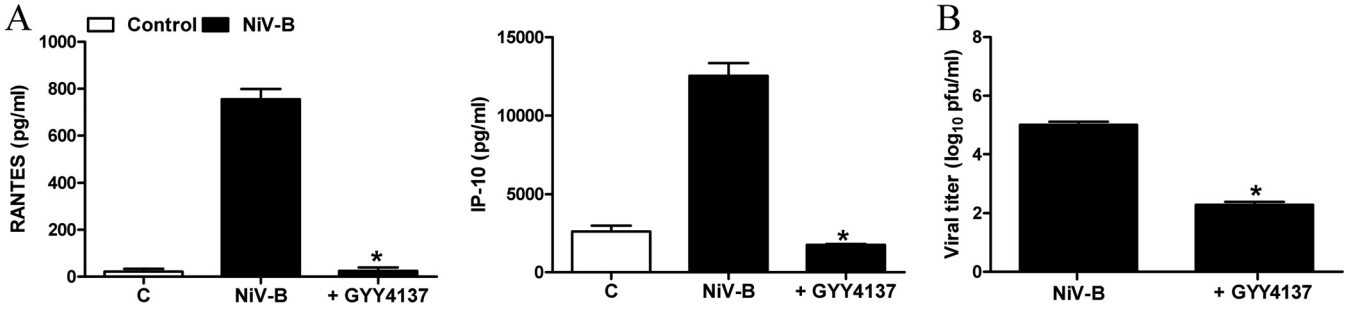

FIG 9 Effect of H_2S donor treatment on NiV-induced chemokine production and viral replication. SAE cells were infected with NiV at an MOI of 0.1 for 1 h, followed by treatment with a 5 mM concentration of GYY4137. (A) Cell supernatants from uninfected and NiV-infected cells, treated or untreated, were assayed at 24 h p.i. for cytokine and chemokine secretion by a Bio-Plex assay. Results are expressed as means ± standard errors. Results are representative of data from two independent experiments run in triplicate. *, $P < 0.05$ compared to untreated NiV-infected cells. (B) Viral replication was determined at 24 h postinfection by titration of viral infectious particles released into cell supernatants by a plaque assay. Results are representative of data from two independent experiments run in triplicate. *, $P < 0.05$ compared to untreated NiV-infected cells.

matory cytokine expression (40). Similar results were obtained in other models of acute lung injury, such as the one associated with hemorrhagic shock or with bleomycin treatment (41, 42).

Recent studies have established that H_2S is indeed a biologically relevant signaling molecule, similar to the other gaseous mediators nitric oxide and carbon monoxide (reviewed in reference 43). In several models of inflammatory diseases, the inhibition of proinflammatory mediator expression was paralleled by the inhibition of NF-κB activation. NaHS administration inhibited NF-κB activation in a mouse model of hemorrhagic shock as well as in a rat model of acute lung injury. Similarly, H_2S donor treatment in a rat model of bleomycin-induced pulmonary inflammation and fibrosis led to the inhibition of activation of the NF-κB subunit p65 (44). *In vitro*, NaHS and GYY4137 have been shown to inhibit LPS-induced NF-κB activation in cultured macrophages (5). Garlic compounds such as diallyl sulfide, a possible H_2S donor, can also downregulate NF-κB activation (41). GYY4137 treatment of AECs infected with RSV did not change primary virus-induced activation of IRF-3 and NF-κB, as shown by the lack of changes in their nuclear translocation, in agreement with the absence of differences due to GYY4137 treatment in viral RNA generation, the major trigger of cellular signaling in RSV-infected cells through the activation of the virus-sensing cytosolic receptor RIG-I (45). GYY4137 treatment, however, significantly reduced IRF-3 and NF-κB binding to RANTES and IL-8 endogenous promoters, indicating a direct effect of H_2S on cellular signaling. An important mechanism by which H_2S can modulate cellular signaling is through its direct and indirect antioxidant activity (reviewed in reference 43). Administration of H_2S has been shown to increase cellular glutathione levels, and it has also been associated with increased activation of Nrf2, a transcription factor that regulates oxidative stress by affecting the gene expression of several key antioxidant enzymes (43). Inducible phosphorylation on distinct serine residues, including Ser276 and Ser536, has been shown to regulate NF-κB transcriptional activity without modification of nuclear translocation or DNA-binding affinity (32). We have recently shown that the inhibition of RSV-induced reactive oxygen species (ROS) formation by treatment of AECs with antioxidants significantly reduces RSV-dependent NF-κB serine phosphorylation, resulting in the inhibition of RSV-induced expression of several NF-κB-dependent genes without affecting nuclear translocation (46). Our finding that H_2S treatment significantly reduced p65 Ser276 and Ser536 phosphorylation suggests that modulation of ROS cellular levels could be a major mechanism by which H_2S affects virus-induced cellular signaling.

In conclusion, we have shown that modulation of cellular H_2S significantly impacts cellular responses and viral replication in an *in vitro* model of RSV infection. Our finding that H_2S donor treatment also affects replication and proinflammatory mediator production in a model of hMPV and NiV infection suggests that H_2S possesses broad antiviral activity against paramyxoviruses. We are currently investigating the effect of H_2S donor treatment in the context of other nonparamyxovirus infections to determine the potential antiviral spectrum of these compounds. We are also determining the role of endogenous H_2S production in RSV infection *in vivo*, taking advantage of knockout mice available for the enzymes CSE and CBS. Indeed, preliminary studies indicate that CSE is an important modulator of disease and airway hyperresponsiveness as well as lung inflammation triggered by RSV infection (A. Casola, unpublished data), similar to what was recently reported for allergic airway inflammation triggered by ovalbumin sensitization in mice (47). Of interest is the observation that premature infants, who are at high risk of developing severe bronchiolitis following RSV and other respiratory viral infections, have very low tissue CSE activity compared to full-term infants (48). We are also evaluating the efficacy of H_2S donors in a mouse model of RSV infection to determine whether their administration has therapeutic potential for the prevention and treatment of virus-induced lung disease.

ACKNOWLEDGMENTS

This project was supported by grants R01 AI062885, R21 AI111042, R21 AI103565, P01 AI07924602, GM107846, P30 ES006676, and W81XWH1010146-DoD; the UTMB John Sealy Memorial Endowment Fund (A.C.); and a UTMB Center for Tropical Diseases postdoctoral fellowship (O.E.).

We thank Kimberly Palkowetz and Tianshuang Liu for technical assistance and Cynthia Tribble for manuscript submission.

REFERENCES

1. **Chen Y, Wang R.** 2012. The message in the air: hydrogen sulfide metabolism in chronic respiratory diseases. Respir Physiol Neurobiol **184:**130–138. http://dx.doi.org/10.1016/j.resp.2012.03.009.
2. **Wang P, Zhang G, Wondimu T, Ross B, Wang R.** 2011. Hydrogen sulfide and asthma. Exp Physiol **96:**847–852. http://dx.doi.org/10.1113/expphysiol.2011.057448.
3. **Wang R.** 2012. Physiological implications of hydrogen sulfide: a whiff exploration that blossomed. Physiol Rev **92:**791–896. http://dx.doi.org/10.1152/physrev.00017.2011.
4. **Wang R.** 2011. Signaling pathways for the vascular effects of hydrogen sulfide. Curr Opin Nephrol Hypertens **20:**107–112. http://dx.doi.org/10.1097/MNH.0b013e3283430651.
5. **Li L, Whiteman M, Guan YY, Neo KL, Cheng Y, Lee SW, Zhao Y, Baskar R, Tan CH, Moore PK.** 2008. Characterization of a novel, water-soluble hydrogen sulfide-releasing molecule (GYY4137): new insights into the biology of hydrogen sulfide. Circulation **117:**2351–2360. http://dx.doi.org/10.1161/CIRCULATIONAHA.107.753467.
6. **Szabo C.** 2007. Hydrogen sulphide and its therapeutic potential. Nat Rev Drug Discov **6:**917–935. http://dx.doi.org/10.1038/nrd2425.
7. **Hall CB, Weinberg GA, Iwane MK, Blumkin AK, Edwards KM, Staat MA, Auinger P, Griffin MR, Poehling KA, Erdman D, Grijalva CG, Zhu Y, Szilagyi P.** 2009. The burden of respiratory syncytial virus infection in young children. N Engl J Med **360:**588–598. http://dx.doi.org/10.1056/NEJMoa0804877.
8. **Williams JV, Harris PA, Tollefson SJ, Halburnt-Rush LL, Pingsterhaus JM, Edwards KM, Wright PF, Crowe JE, Jr.** 2004. Human metapneumovirus and lower respiratory tract disease in otherwise healthy infants and children. N Engl J Med **350:**443–450. http://dx.doi.org/10.1056/NEJMoa025472.
9. **Escaffre O, Borisevich V, Rockx B.** 2013. Pathogenesis of Hendra and Nipah virus infection in humans. J Infect Dev Ctries **7:**308–311. http://dx.doi.org/10.3855/jidc.3648.
10. **Escaffre O, Borisevich V, Carmical JR, Prusak D, Prescott J, Feldmann H, Rockx B.** 2013. Henipavirus pathogenesis in human respiratory epithelial cells. J Virol **87:**3284–3294. http://dx.doi.org/10.1128/JVI.02576-12.
11. **Garofalo RP, Haeberle H.** 2000. Epithelial regulation of innate immunity to respiratory syncytial virus. Am J Respir Cell Mol Biol **23:**581–585. http://dx.doi.org/10.1165/ajrcmb.23.5.f204.
12. **Bao X, Liu T, Spetch L, Kolli D, Garofalo RP, Casola A.** 2007. Airway epithelial cell response to human metapneumovirus infection. Virology **368:**91–101. http://dx.doi.org/10.1016/j.virol.2007.06.023.
13. **Bitko V, Velazquez A, Yank L, Yang Y-C, Barik S.** 1997. Transcriptional induction of multiple cytokines by human respiratory syncytial virus requires activation of NF-kB and is inhibited by sodium salicylate and aspirin. Virology **232:**369–378. http://dx.doi.org/10.1006/viro.1997.8582.
14. **Tian B, Zhang Y, Luxon B, Garofalo RP, Casola A, Sinha M, Brasier AR.**

2002. Identification of NF-kB dependent gene networks in respiratory syncytial virus-infected cells. J Virol **76:**6800–6814. http://dx.doi.org/10.1128/JVI.76.13.6800-6814.2002.
15. **Lin R, Heylbroeck C, Genin P, Pitha PM, Hiscott J.** 1999. Essential role of interferon regulatory factor 3 in direct activation of RANTES chemokine transcription. Mol Cell Biol **19:**959–966.
16. **Casola A, Garofalo RP, Haeberle H, Elliott TF, Lin A, Jamaluddin M, Brasier AR.** 2001. Multiple *cis* regulatory elements control RANTES promoter activity in alveolar epithelial cells infected with respiratory syncytial virus. J Virol **75:**6428–6439. http://dx.doi.org/10.1128/JVI.75.14.6428-6439.2001.
17. **Lin VS, Lippert AR, Chang CJ.** 2013. Cell-trappable fluorescent probes for endogenous hydrogen sulfide signaling and imaging H2O2-dependent H2S production. Proc Natl Acad Sci U S A **110:**7131–7135. http://dx.doi.org/10.1073/pnas.1302193110.
18. **Ueba O.** 1978. Respiratory syncytial virus. I. concentration and purification of the infectious virus. Acta Med Okayama **32:**265–272.
19. **Olszewska-Pazdrak B, Casola A, Saito T, Alam R, Crowe SE, Mei F, Ogra PL, Garofalo RP.** 1998. Cell-specific expression of RANTES, MCP-1, and MIP-1alpha by lower airway epithelial cells and eosinophils infected with respiratory syncytial virus. J Virol **72:**4756–4764.
20. **Kisch AL, Johnson KM.** 1963. A plaque assay for respiratory syncytial virus. Proc Soc Exp Biol Med **112:**583–589.
21. **Kolli D, Bao X, Liu T, Hong C, Wang T, Garofalo RP, Casola A.** 2011. Human metapneumovirus glycoprotein G inhibits TLR4-dependent signaling in monocyte-derived dendritic cells. J Immunol **187:**47–54. http://dx.doi.org/10.4049/jimmunol.1002589.
22. **Garofalo RP, Sabry M, Jamaluddin M, Yu RK, Casola A, Ogra PL, Brasier AR.** 1996. Transcriptional activation of the interleukin-8 gene by respiratory syncytial virus infection in alveolar epithelial cells: nuclear translocation of the RelA transcription factor as a mechanism producing airway mucosal inflammation. J Virol **70:**8773–8781.
23. **Asimakopoulou A, Panopoulos P, Chasapis CT, Coletta C, Zhou Z, Cirino G, Giannis A, Szabo C, Spyroulias GA, Papapetropoulos A.** 2013. Selectivity of commonly used pharmacological inhibitors for cystathionine beta synthase (CBS) and cystathionine gamma lyase (CSE). Br J Pharmacol **169:**922–932. http://dx.doi.org/10.1111/bph.12171.
24. **Casola A, Garofalo RP, Jamaluddin M, Vlahopoulos S, Brasier AR.** 2000. Requirement of a novel upstream response element in RSV induction of interleukin-8 gene expression: stimulus-specific differences with cytokine activation. J Immunol **164:**5944–5951. http://dx.doi.org/10.4049/jimmunol.164.11.5944.
25. **Schreiber E, Matthias P, Muller MM, Schaffner W.** 1989. Rapid detection of octamer binding proteins with 'mini-extracts', prepared from a small number of cells. Nucleic Acids Res **17:**6419. http://dx.doi.org/10.1093/nar/17.15.6419.
26. **Brasier AR, Spratt H, Wu Z, Boldogh I, Zhang Y, Garofalo RP, Casola A, Pashmi J, Haag A, Luxon B, Kurosky A.** 2004. Nuclear heat shock response and novel nuclear domain 10 reorganization in respiratory syncytial virus-infected A549 cells identified by high-resolution two-dimensional gel electrophoresis. J Virol **78:**11461–11476. http://dx.doi.org/10.1128/JVI.78.21.11461-11476.2004.
27. **Jackson MR, Melideo SL, Jorns MS.** 2012. Human sulfide:quinone oxidoreductase catalyzes the first step in hydrogen sulfide metabolism and produces a sulfane sulfur metabolite. Biochemistry **51:**6804–6815. http://dx.doi.org/10.1021/bi300778t.
28. **Casola A, Burger N, Liu T, Jamaluddin M, Brasier AR, Garofalo RP.** 2001. Oxidant tone regulates RANTES gene transcription in airway epithelial cells infected with respiratory syncytial virus: role in viral-induced interferon regulatory factor activation. J Biol Chem **276:**19715–19722. http://dx.doi.org/10.1074/jbc.M101526200.
29. **Zhang Y, Luxon B, Casola A, Garofalo RP, Jamaluddin M, Brasier AR.** 2001. Expression of respiratory syncytial virus-induced chemokine gene networks in lower airway epithelial cells revealed by cDNA microarrays. J Virol **75:**9044–9058. http://dx.doi.org/10.1128/JVI.75.19.9044-9058.2001.
30. **Pazdrak K, Olszewska-Pazdrak B, Liu B, Takizawa R, Brasier AR, Garofalo RP, Casola A.** 2002. MAPK activation is involved in posttranscriptional regulation of RSV-induced RANTES gene expression. Am J Physiol Lung Cell Mol Physiol **283:**L364–L372. http://dx.doi.org/10.1152/ajplung.00331.2001.
31. **Hosakote YM, Jantzi PD, Esham DL, Spratt H, Kurosky A, Casola A, Garofalo RP.** 2011. Viral-mediated inhibition of antioxidant enzymes contributes to the pathogenesis of severe respiratory syncytial virus bronchiolitis. Am J Respir Crit Care Med **183:**1550–1560. http://dx.doi.org/10.1164/rccm.201010-1755OC.
32. **Zhong H, Voll RE, Ghosh S.** 1998. Phosphorylation of NF-kappa B p65 by PKA stimulates transcriptional activity by promoting a novel bivalent interaction with the coactivator CBP/p300. Mol Cell **1:**661–671. http://dx.doi.org/10.1016/S1097-2765(00)80066-0.
33. **Haeberle HA, Kuziel WA, Dieterich HJ, Casola A, Gatalica Z, Garofalo RP.** 2001. Inducible expression of inflammatory chemokines in respiratory syncytial virus-infected mice: role of MIP-1alpha in lung pathology. J Virol **75:**878–890. http://dx.doi.org/10.1128/JVI.75.2.878-890.2001.
34. **Haeberle HA, Casola A, Gatalica Z, Petronella S, Dieterich HJ, Ernst PB, Brasier AR, Garofalo RP.** 2004. IkappaB kinase is a critical regulator of chemokine expression and lung inflammation in respiratory syncytial virus infection. J Virol **78:**2232–2241. http://dx.doi.org/10.1128/JVI.78.5.2232-2241.2004.
35. **Bennett BL, Garofalo RP, Cron SG, Hosakote YM, Atmar RL, Macias CG, Piedra PA.** 2007. Immunopathogenesis of respiratory syncytial virus bronchiolitis. J Infect Dis **195:**1532–1540. http://dx.doi.org/10.1086/515575.
36. **Castro SM, Guerrero-Plata A, Suarez-Real G, Adegboyega PA, Colasurdo GN, Khan AM, Garofalo RP, Casola A.** 2006. Antioxidant treatment ameliorates respiratory syncytial virus-induced disease and lung inflammation. Am J Respir Crit Care Med **174:**1361–1369. http://dx.doi.org/10.1164/rccm.200603-319OC.
37. **Kimura H.** 2014. Production and physiological effects of hydrogen sulfide. Antioxid Redox Signal **20:**783–793. http://dx.doi.org/10.1089/ars.2013.5309.
38. **El Najjar F, Schmitt AP, Dutch RE.** 2014. Paramyxovirus glycoprotein incorporation, assembly and budding: a three way dance for infectious particle production. Viruses **6:**3019–3054. http://dx.doi.org/10.3390/v6083019.
39. **Whiteman M, Winyard PG.** 2011. Hydrogen sulfide and inflammation: the good, the bad, the ugly and the promising. Expert Rev Clin Pharmacol **4:**13–32. http://dx.doi.org/10.1586/ecp.10.134.
40. **Li HD, Zhang ZR, Zhang QX, Qin ZC, He DM, Chen JS.** 2013. Treatment with exogenous hydrogen sulfide attenuates hyperoxia-induced acute lung injury in mice. Eur J Appl Physiol **113:**1555–1563. http://dx.doi.org/10.1007/s00421-012-2584-5.
41. **Kalayarasan S, Sriram N, Sudhandiran G.** 2008. Diallyl sulfide attenuates bleomycin-induced pulmonary fibrosis: critical role of iNOS, NF-kappaB, TNF-alpha and IL-1beta. Life Sci **82:**1142–1153. http://dx.doi.org/10.1016/j.lfs.2008.03.018.
42. **Xu DQ, Gao C, Niu W, Li Y, Wang YX, Gao CJ, Ding Q, Yao LN, Chai W, Li ZC.** 2013. Sodium hydrosulfide alleviates lung inflammation and cell apoptosis following resuscitated hemorrhagic shock in rats. Acta Pharmacol Sin **34:**1515–1525. http://dx.doi.org/10.1038/aps.2013.96.
43. **Li L, Rose P, Moore PK.** 2011. Hydrogen sulfide and cell signaling. Annu Rev Pharmacol Toxicol **51:**169–187. http://dx.doi.org/10.1146/annurev-pharmtox-010510-100505.
44. **Cao H, Zhou X, Zhang J, Huang X, Zhai Y, Zhang X, Chu L.** 2014. Hydrogen sulfide protects against bleomycin-induced pulmonary fibrosis in rats by inhibiting NF-kappaB expression and regulating Th1/Th2 balance. Toxicol Lett **224:**387–394. http://dx.doi.org/10.1016/j.toxlet.2013.11.008.
45. **Liu P, Jamaluddin M, Li K, Garofalo RP, Casola A, Brasier AR.** 2007. Retinoic acid-inducible gene I mediates early antiviral response and Toll-like receptor 3 expression in respiratory syncytial virus-infected airway epithelial cells. J Virol **81:**1401–1411. http://dx.doi.org/10.1128/JVI.01740-06.
46. **Jamaluddin M, Tian B, Boldogh I, Garofalo RP, Brasier AR.** 2009. Respiratory syncytial virus infection induces a reactive oxygen species-MSK1-phospho-Ser-276 RelA pathway required for cytokine expression. J Virol **83:**10605–10615. http://dx.doi.org/10.1128/JVI.01090-09.
47. **Benetti LR, Campos D, Gurgueira SA, Vercesi AE, Guedes CE, Santos KL, Wallace JL, Teixeira SA, Florenzano J, Costa SK, Muscara MN, Ferreira HH.** 2013. Hydrogen sulfide inhibits oxidative stress in lungs from allergic mice in vivo. Eur J Pharmacol **698:**463–469. http://dx.doi.org/10.1016/j.ejphar.2012.11.025.
48. **Vina J, Vento M, Garcia-Sala F, Puertes IR, Gasco E, Sastre J, Asensi M, Pallardo FV.** 1995. L-cysteine and glutathione metabolism are impaired in premature infants due to cystathionase deficiency. Am J Clin Nutr **61:**1067–1069.

American Journal of Respiratory Cell and Molecular Biology/AJRCMB

Hydrogen Sulfide: Antiviral and Anti-inflammatory Endogenous Gasotransmitter in the Airways Role in Respiratory Syncytial Virus Infection

Journal:	*American Journal of Respiratory Cell and Molecular Biology*
Manuscript ID	Red-2015-0385OC.R1
Manuscript Type:	OC - Original Contribution
Date Submitted by the Author:	16-May-2016
Complete List of Authors:	Ivanciuc, Teodora; University of Texas Medical Branch, Pediatrics Sbrana, Elena; University of Texas Medical Branch, Pathology Ansar, Maria; University of Texas Medical Branch, Pediatrics Bazhanov, Nikolay; University of Texas Medical Branch, Pediatrics Szabo, Csaba; University of Texas Medical Branch, Anesthesiology Casola, Antonella; University of Texas Medical Branch, Pediatrics Garofalo, Roberto; University of Texas Medical Branch,
Subject Category:	10.06 Host Defenses to Microbial Pathogens < MICROBIOLOGY AND PULMONARY INFECTIONS
Keywords:	paramyxovirus, lung injury, airway hyperresponsiveness, cystathionine-γ-lyase (CSE), antiviral

HYDROGEN SULFIDE: ANTIVIRAL AND ANTI-INFLAMMATORY ENDOGENOUS GASOTRANSMITTER IN THE AIRWAYS.

ROLE IN RESPIRATORY SYNCYTIAL VIRUS INFECTION

Teodora Ivanciuc[1], Elena Sbrana[2], Maria Ansar[1], Nikolay Bazhanov[1], Csaba Szabo[3], Antonella Casola[1, 2, 4, 5 *], Roberto P. Garofalo[1, 2, 4, 5*]

[1]Dept. of Pediatrics, [2] Dept. of Microbiology, [3]Dept. of Anesthesiology, [4]Sealy Center for Vaccine Development and [5] Sealy Center for Molecular Medicine, University of Texas Medical Branch, Galveston, TX

Correspondence and requests for reprints should be addressed to Antonella Casola, M.D., and Roberto P. Garofalo, M.D., Department of Pediatrics, University of Texas Medical Branch, 301 University Blvd., Galveston, TX 77555-0369. E-mail: ancasola@utmb.edu and rpgarofa@utmb.edu

T.I. contributed to the conception of the manuscript, performed experiments, literature review, and drafting of the manuscript; E.S. performed experiments and contributed to the revision of the manuscript; M.A. performed experiments and literature review; N.B. performed experiments and literature review; C.S. contributed to the conception of the manuscript, literature review and review of the manuscript; A.C. contributed to the conception of the manuscript, drafting of the manuscript, literature review, and final manuscript review; R.P.G. contributed to the conception of the manuscript, literature review, drafting of the manuscript, and final manuscript review.

This project was supported by NIH R01 AI079246, R21 AI109088, R21 AI103565, P01 AI062885, Department of Defense W81XWH1010146, and UTMB John Sealy Memorial Endowment Fund.

Running head: Hydrogen sulfide and RSV lung disease

Descriptor: 10.6

Manuscript word count: 4,048

AT A GLANCE COMMENTARY

Scientific Knowledge on the Subject:

H_2S is an endogenous gasotransmitter that functions as a biologically relevant signaling molecule in mammals. H_2S is involved in various pathophysiological conditions of the respiratory system, including smooth muscle contractility.

What this Study Adds to the Field:

This study identifies H_2S as a novel molecule that can modulate viral replication and airway inflammatory responses, both important determinants of lung injury in RSV infection, with the potential for rapid translation of such findings into novel therapeutic approaches for viral bronchiolitis and pneumonia.

ABSTRACT

Rationale: Hydrogen sulfide (H_2S) is an endogenous gaseous transmitter whose role in the pathophysiology of several lung diseases has been increasingly appreciated. Our recent studies *in vitro* have shown for the first time that H_2S has an important antiviral and anti-inflammatory activity in respiratory syncytial virus (RSV) infection, the leading cause of bronchiolitis and viral pneumonia in children. **Objectives:** To evaluate the therapeutic potential of GYY4137, a novel slow-releasing H_2S donor, for prevention and treatment of RSV-induced lung disease, as well as to investigate the role of endogenous H_2S in a mouse model of RSV infection. **Methods:** 10-12 week-old BALB/c mice treated with GYY4137 or C57BL/6J mice genetically deficient in the cystathionine γ-lyase enzyme (CSE KO), the major H_2S generating enzyme in the lung, were infected with RSV and assessed for viral replication, clinical disease, airway hyperresponsiveness (AHR) and inflammatory responses. **Measurements and Main Results:** Our results show that intranasal delivery of GYY4137 to RSV-infected mice significantly reduced viral replication and markedly improved clinical disease parameters and pulmonary dysfunction compared to vehicle treated controls. The protective effect of H_2S donor was associated with significant reduction of viral-induced proinflammatory mediators and lung cellular infiltrates. Furthermore, CSE $^{-/-}$ mice showed significantly enhanced RSV-induced lung disease and viral replication compared to wild type animals. **Conclusions:** Overall our results indicate that H_2S exerts a novel antiviral and anti-inflammatory activity in the context of RSV infection and represents a potential novel pharmacological approach to ameliorate viral-induced lung disease.

Keywords: paramyxovirus, lung injury, airway hyperresponsiveness, cystathionine-γ-lyase (CSE), antiviral Manuscript word count: 243

INTRODUCTION

Hydrogen sulfide (H_2S) is an endogenous gaseous transmitter, which participates in the regulation of physiological functions of the respiratory system including smooth muscle contractility, pulmonary circulation, cell proliferation/apoptosis, oxidative stress, and inflammation [reviewed in (1)]. As such, impaired H_2S production in human and experimental animal models has been implicated in the pathogenesis of chronic obstructive pulmonary disease, asthma, pulmonary fibrosis and hypoxia-induced pulmonary hypertension. H_2S is produced endogenously in mammals, including humans, by three enzymes: cystathionine-γ-lyase (CSE), cystathionine-β-synthase (CBS), and 3-mercaptopyruvate sulfurtransferase (MST) (2-4). Sulfide salts such as sodium hydrosulfide (NaHS) and sodium sulfide (Na_2S) have been widely used to study the biological effects of hydrogen sulfide in many cells, tissues and animals. These salts generate a large burst of H_2S over a short time period, when used in cell culture. GYY4137 is a novel water-soluble H_2S donor that releases H_2S slowly over a period of hours (5). H_2S donors have been used to demonstrate how therapeutic H_2S administration exert significant effects in various animal models of inflammation, reperfusion injury and circulatory shock (6), however, their role in the context of viral infections is largely unknown.

We have recently shown, for the first time, that modulation of intracellular H_2S significantly impacts cellular responses and viral replication in an *in vitro* model of respiratory viral infections caused by respiratory syncytial virus (RSV) and other paramyxoviruses (7). Treatment of both A549 cells and primary small alveolar epithelial cells with the H_2S donor GYY4137 significantly reduced viral-induced proinflammatory mediators release and it significantly inhibited replication not only of RSV but of other paramyxoviruses as well, such as human metapneumovirus and Nipah virus (7). Based on the observations from our *in vitro*

studies, we used an *in vivo* model of RSV infection to address the role of H_2S in RSV-induced lung disease. In the present study, we found that GYY4137 administration significantly attenuated RSV-induced body weight loss, clinical illness and AHR. H_2S-donor treatment also significantly reduced pulmonary cytokine and chemokine production and neutrophil recruitment to the lung, following RSV infection. To further explore the role of endogenous H_2S production in an experimental model of RSV infection, we used C57BL/6J mice genetically deficient in cystathionine γ-lyase enzyme ($CSE^{-/-}$), which exhibit a profound depletion of H_2S in peripheral tissues including the lungs (8). We found that endogenous H_2S modulates viral replication and disease severity in mice experimentally infected with RSV. These data suggest that endogenous H_2S plays a central role in protection against RSV infection and that treatment with slow-releasing H_2S donors could provide a novel approach for prevention and/or treatment of viral-induced pulmonary diseases.

METHODS

RSV Preparation. The RSV Long strain was grown in Hep-2 cells and purified by centrifugation on discontinuous sucrose gradients, as described (9, 10), and viral pools were titered in plaque forming units (PFU)/mL using a methylcellulose plaque assay, as described (11). UV-inactivated RSV was generated by exposing RSV to UV radiation (UVG-54 Entela, CA) for 30 min.

H_2S Donor. GYY4137 (morpholin-4-ium 4 methoxyphenyl(morpholino) phosphinodithioate) was purchased from Cayman Chemical (Ann Arbor, MI). GYY4137 was freshly prepared daily in phosphate buffered saline prior to mice delivery.

Ethic Statement. All procedures involving mice in this study were carried out in accordance with the recommendations in the Guide for the Care and Use of Laboratory Animals of the National Institutes of Health. The protocol was approved by the Institutional Animal Care and Use Committee of the University of Texas Medical Branch at Galveston (Protocol: 9001002). The mice were sacrificed by an intraperitoneal injection of ketamine and xylazine and exsanguinated via the femoral vessels.

Mice and Infection Protocol. 10-12 weeks female BALB/c mice were purchased from Harlan (Houston, TX). 10-12 weeks male and female C57BL/6J mice (wild type, WT) used in this work were purchased from The Jackson Laboratory (Bar Harbor, Maine). CSE KO mice on C57BL/6J background were generously provided by Dr. Solomon Snyder, Johns Hopkins University, Baltimore, MD. Under light anesthesia, mice were infected intranasally (i.n.) with 50 μl of RSV diluted in phosphate-buffered saline (PBS, at dose 10^7 PFU) or mock inoculated using the same volume of control buffer. In some experiments BALB/c mice were inoculated with either RSV dose 10^6 for measurements of cytokines and chemokines, or 10^5 PFU for pulmonary function testing. GYY4137 administration was performed via i.n. at different doses and timing of RSV infection. Cystathionine γ-lyase (CSE) deficient (CSE KO) mice were used to examine the role of endogenous H_2S in the pathogenesis of RSV infection. Both genders CSE KO and WT age-matched mice were used. WT and CSE KO mice were inoculated i.n. with 10^7 PFU of RSV, in a total volume of 50 μl, under light anesthesia. As mock treatment, all mice were inoculated with an equivalent volume of PBS. Daily determination of body weight and illness score, bronchoalveolar lavage (BAL) differential cell counts, lung neutrophil counts by flow cytometry

analysis, cytokines, chemokines and type I IFNs measurements, lung viral titration, pulmonary histopathology and pulmonary function testing were performed as previously described (12, 13). CSE and CBS mRNA expression in lung tissue was analyzed by real-time PCR as described before (7, 8). Real-time visualization of H_2S generation in the lung was performed using the azide-based probe sulfidefluor-7 acetoxymethyl ester (SF-7AM)(7). Briefly, mice received one dose of GYY4137 or PBS and one hour later were injected intratracheally with SF-7AM (100 μl; 10 μM). Thirty minutes later lungs were excised and imaged ex vivo in a UPV Small Animal Imaging System (Upland, CA) and analyzed using the Living Image software.

Statistical Analysis. The data were evaluated using ANOVA and two-tailed unpaired Student's *t*-test for samples with unequal variances to determine significant difference between each set of two groups (GraphPad Prism 5.02; GraphPad Software, Inc., San Diego, CA). Results are expressed as mean ± standard error of the mean for each experimental group unless otherwise stated. $p<0.05$ value was selected to indicate significance. All experiments were repeated at least three times, data in figures are shown from a representative experiment.

RESULTS

GYY4137 Treatment Ameliorates Viral-Induced Disease and Pulmonary Function in Response to RSV Infection. We have previously shown that RSV infection inhibits endogenous H_2S generation in airway epithelial cells, to a large extent by reducing expression of the H_2S-generating enzyme CSE (7). In our initial experiments *in vivo*, we found that infection of mice also resulted in reduced expression of both CBS and CSE in the lung (Figure ES1, panel A). Thus, to determine whether treatment with an H_2S donor could ameliorate RSV-induced disease,

we initially assessed the effect of different GYY4137 treatment protocols on body weight loss. Release of H_2S can be directly measured in airway epithelial cells *in vitro* by the SF7-AM fluorescence probe (7) and we confirmed that this also occurs in the lung (Fig. ES1, panel B). In the first protocol, animals were treated with various doses of GYY4137, ranging from 50 to 200 mg/kg, 1h prior to, 6h and 24h after infection. As shown in Figure 1A, mice inoculated with RSV alone progressively lost weight during the first three days of infection, with a peak of 15-20% loss by day 3 post-infection (p.i.). Treatment with GYY4137 at any given dose consistently attenuated RSV-induced body weight loss, starting at day 2 p.i. Treatment with additional doses of the GYY4137 in the following 2-3 days of infection did not result in further clinical benefit, with some signs of toxicity (ruffled fur) at the 200 mg/kg dose (data not shown).

We then determined whether the 50 mg/kg dose was effective if treatment was initiated after infection. The dose of 50 mg/kg GYY4137 was administered to mice as follows: (a) three doses, one at 2, 6 and 24h p.i., (b) two doses, one at 6 and the other at 24 h p.i. and (c) one single dose 24 h after infection. Mice treated with three or two doses of GYY4137 after RSV infection exhibited significantly attenuated body weight loss compared with vehicle-treated mice, although to a lesser extent than when the compound was administered prior to infection (Figure 1B). When GYY4137 was administered at 24 h p.i. mice exhibited similar body weight loss compared to vehicle-treated infected mice (Figure 1B). As the pretreatment protocol was the most effective in modulating RSV-induced disease, all subsequent experiments were performed using the dose of 50mg/kg given 1h before, 6h and 24h after infection.

A positive effect of H_2S-donor administration was also observed on other clinical parameters of RSV infection that constitute the viral-induced illness score (see Methods for details). Typically, the peak of illness severity coincides with the peak of RSV-induced body

weight loss and occurs between day 2 and 4 of infection (14). We observed a highly statistically significant difference in total illness score for GYY4137-treated versus vehicle-treated RSV-infected mice (Figure 1C), indicating that this treatment is effective in modulating RSV-induced clinical disease.

We and others have previously shown that RSV infection induces AHR in response to methacholine challenge (12, 15). To determine the effect of GYY4137 on pulmonary function, RSV-infected or mock-infected mice were assessed for AHR in response to methacholine challenge by whole-body plethysmography (Buxco Electronics, Inc. Sharon, CT), at day 5 after infection. Aerosolized methacholine elicited significantly increased AHR in vehicle-treated mice infected with RSV, compared with all other groups. A significant difference was observed between vehicle- and GYY4137-treated RSV-infected animals, as GYY4137 strongly attenuated RSV-induced AHR at higher doses of methacholine (i.e., 25 and 50 mg/ml) (Figure 1D). Indeed, compared to the vehicle-treated RSV-infected group, GYY4137-treated RSV-infected mice showed approximately a two-fold reduction in Penh values at dose of 50 mg/ml. GYY4137 treatment did not alter baseline Penh values or AHR to methacholine in mock-infected animals. The protective effect of GYY4137 on lung function was confirmed by analysis of airway resistance using the Flexivent system (Scireq, Montreal, Quebec, Canada). As shown in Figure 1E, RSV-infected mice treated with GYY4137 exhibited lung resistance values similar to those measured in mock-infected animals. No differences in lung resistance were observed between vehicle- and GYY4137-treated mock-infected mice. Overall, these data indicate that slow-releasing H_2S donors significantly ameliorated clinical disease and lung function during RSV infection.

Treatment with GYY4137 Reduces Viral Replication. We have recently shown for the first time that GYY4137 has an important antiviral activity *in vitro* against several members of the *Paramixoviridae* family (7). To determine whether H_2S donors administration altered RSV replication in the lung, mice were treated with 50 mg/kg GYY4137 or control vehicle, starting 1 h prior to infection as described above, and sacrificed at day 5 p.i., when peak viral titer occurs (14). A reduction ranging between 0.81-0.91 log of in RSV peak titer was consistently observed across four independent experiments in GYY-treated animals (Figure 2A). Higher concentration of GYY4137 (i.e., 100 and 200 mg/kg body weight) did not show any greater antiviral effect (data not shown). The observed effect of H_2S donor on RSV replication in the lung appeared to be independent of the known antiviral activity of IFN-γ as concentrations of this cytokine in BAL samples were comparable at day 5 and 7 in infected mice treated with GYY4137 or vehicle control (data not shown). We then tested whether GYY4137 treatment could reduce viral replication when administered after RSV infection. For that, groups of mice were infected with RSV and treated with three doses (2h, 6h and 24h after infection), two doses (6 h and 24 h after infection), or one dose (24 h after infection) of GYY4137 (50mg/kg) or vehicle. Results of these experiments showed that administration of GYY4137 up to 6h p.i. (in first two protocols) was effective in reducing RSV viral titer in the lung, although to a lesser extent than observed in the pretreatment protocol, while administration at the later 24h time point was no longer effective in reducing viral replication (Figure 2B).

GYY4137 Treatment Decreases Pulmonary Inflammation in RSV-Infected Mice. Next, we investigated whether GYY4137 administration could modulate RSV-induced lung inflammation. GYY4137 or vehicle-treated mice (1h prior, 6h and 24h p.i.) were infected with RSV or mock

inoculated and sacrificed at day 1, 3, 5 and 7 p.i. to collect BAL samples for total and differential cell count, and at day 7 p.i. for lung histopathology. A significant attenuation of total cell influx by GYY4137 treatment was observed in RSV-infected mice, compared with vehicle alone, at day 1 and 3 p.i. (Figure 3A), but not at subsequent days (data not shown). While macrophages are the predominant cell type recovered from the BAL of uninfected mice, following RSV infection neutrophils become the predominant inflammatory cell in BAL and lung during the first few days of infection (16). GYY4137 administration significantly reduced neutrophil recruitment into the airways, both in BAL fluid (Figure 3A) and lung tissue (Figure 3B) with a concomitant increase in the macrophage population. To further investigate histological changes in response to H_2S donor, lung tissue from GYY4137- and vehicle-treated mock- and RSV-infected mice was harvested at day 7 p.i. and subjected to H&E staining. Lung histopathology analysis showed no airway inflammation in mock-infected GYY4137- or vehicle-treated animals (Figure 3C, upper panels). RSV-infected vehicle-treated mice had increased cellular infiltration in the perivascular and peribronchial spaces, which was greatly reduced by GYY4137-treatment (Figure 3C, lower panels and Figure 3D, expressed as pathology score).

GYY4137 Inhibits Production of Proinflammatory Mediators. RSV is a potent inducer of cytokines and chemokines, which have been shown to play an important role in viral-mediated lung inflammation and disease severity [Reviewed in (17)]. In our mouse model, the peak of chemokine production occurs during the first two days of infection (18). Thus, to determine whether H_2S donor treatment was able to modulate RSV-induced pro-inflammatory mediator secretion, we measured cytokine, chemokine and type I IFN levels in BAL samples collected at day 1 p.i. In RSV-infected mice, GYY4137 treatment significantly decreased the production of

the pro-inflammatory cytokines IL-1α, IL-1β, IL-6, and TNF-α, as well as other cytokines such as granulocyte-macrophage colony-stimulating factor (GM-CSF) and granulocyte-colony stimulating factor (G-CSF)(Figure 4A). Similar results were observed with the release of the chemokines RANTES, MIP-1α, MIP-1β, MCP-1, and KC (Figure 4B), and the secretion of both IFN-α and -β, which were all reduced by GYY4137 treatment (Figure 4C).

We have shown that GYY4137-mediated inhibition of RSV-induced cellular signaling and expression of proinflammatory genes in airway epithelial cells is a process distinct from its ability to inhibit viral replication (7). To determine whether this finding was true *in vivo*, mice were inoculated with UV-treated RSV (which was non-replicating as assessed in HEp-2 cells by a plaque assay) and treated with GYY4137 or control vehicle, and BAL samples were collected to measure concentration of cytokines and chemokines. As expected, UV-RSV induced secretion of cytokines known to be also released by cells such as alveolar macrophages that do not require viral replication, including IL-1β, IL-6, TNF-α, MCP-1, MIP-1β and RANTES (13, 19). As shown in Figure 5, treatment of UV-RSV inoculated mice with GYY4137 significantly reduced levels of these cytokines in BAL, suggesting that H_2S exerted immunomodulatory and anti-inflammatory activities in the lung, which are distinct from its inhibitory activity on viral replication.

CSE Deficiency Exacerbates Disease Severity, Airway dysfunction and Pulmonary Inflammation in RSV Infection. To further determine whether endogenous H_2S had a protective effect in RSV-induced lung disease, we investigated body weight loss, AHR, viral replication, cytokine/chemokine secretion and lung histologic changes in RSV-infected mice lacking CSE, a key enzyme in the biosynthesis of H_2S in peripheral tissue, including the lung (8).

CSE-deficient mice exhibit a profound depletion of H_2S in peripheral tissues (8). In our experiments, CSE KO mice exhibited enhanced body weight loss at the peak of the clinical disease and a delayed recovery to baseline weight compared with WT infected animals (Figure 6A). No differences in body weight loss were observed between WT and KO mock-infected mice. While no differences in baseline Penh values were observed between the WT and CSE KO animals, RSV-infected CSE KO mice exhibited a significantly enhanced sensitivity to methacholine challenge, demonstrated by greater Penh values at most of the doses tested, compared to WT infected mice (Figure 6B, left panel). Additional studies of lung mechanical properties in artificially ventilated mice showed no differences in total lung respiratory resistance between the CSE KO and WT animals at low concentrations of methacholine, however, there was a significant increase in lung resistance in CSE KO RSV-infected mice at the higher concentrations (Figure 6B, right panel). Since we have recently shown that CSE inhibition *in vitro* is associated with enhanced viral replication (7), we assessed viral titers in RSV-infected CSE KO and WT mice at day 5 p.i. We observed a 50% increase in viral titer in CSE KO mice, compared to WT (Figure 6C), indicating that endogenous H_2S plays an important role in controlling RSV replication.

To determine whether treatment with an H_2S releasing compound could rescue the exacerbated disease in CSE deficient mice, GYY4137 was used at dose 50 mg/kg 1h before, 6h and 24h after infection. Similarly to our observation in BALB/c mice, GYY4137 treatment of WT control mice (on C57BL/6 background) attenuated RSV-induced body weight loss at day 1 and 2 post-infection, with faster recovery at later time points. Moreover, GYY4137 treatment rescued body weight loss in RSV-infected CSE deficient mice when compared with vehicle treated CSE deficient littermates (Figure 6D). The protective effect of GYY4137 in CSE

deficient mice was also observed in studies of lung function as AHR in response to methacholine was significantly decreased in RSV-infected CSE deficient mice treated with GYY4137 (Figure 6E). To investigate whether the lack of CSE affected RSV-induced pro-inflammatory response, BAL samples collected at day 1 p.i. from CSE KO and WT mice were assessed for cytokines and chemokine levels by multi-plex detection assay. We found that in the absence of CSE, RSV infection induced significantly higher levels of the cytokines TNF-α, IL-6, IL-13 and IL-12 (p40), compared to WT-infected mice (Figure 7A). A similar effect was observed with the release of chemokines MIP-1α, MIP-1β (Figure 7A), with a trend towards increased secretion for RANTES and MCP-1 (data not shown). Levels of IFN-γ and IL-4 measured in BAL samples at day 5 post-infection by high sensitive ELISA were not statistically different in WT and CSE KO mice after infection with RSV (Figure 7B).

Finally, lung samples were harvested at day 7 p.i. and lung sections were stained with H&E. Lung histopathology analysis showed no airway inflammation in mock-infected WT and CSE KO mice, however, pulmonary perivascular and peribrochial inflammation, vasculitis and alveolitis were significantly increased in the CSE KO mice compared to WT animals in response to infection (Figure 7C). Overall, these data indicate a role of CSE and endogenous H_2S production in viral replication and inflammatory cellular responses in mice experimentally infected with RSV.

DISCUSSION

Lung inflammation, which is initiated by secretion of cytokines and chemokines from infected tissue-resident cells of the respiratory mucosa plays an important role in the pathogenesis of RSV infection. Indeed, we and others have shown that modulation of the inflammatory response is

associated with amelioration of clinical illness in animal models of RSV infection (12, 20-22). Recent studies have also pointed to an important correlation between the amount and kinetics of viral replication in the airways and the clinical outcome of RSV infections. Infants with greater RSV quantities in the respiratory tract secretions have been shown to be at greater risk for prolonged hospitalization, intensive care unit stay and mechanical ventilation (23, 24), while those with slower clearance of the virus have greater disease severity (25). This clinical and experimental evidence is important as new approaches to treat RSV infections are being developed, possibly with combined spectrum of anti-inflammatory and antiviral activities. In that regard, our discovery of H_2S as an endogenous biochemical pathway that can modulate inflammation as well as viral replication is of particular interest.

For several hundred years, hydrogen sulfide (H_2S) has been known to exist in animal tissues as a noxious gas. As H_2S is typically formed by commensal bacteria, it was not regarded as physiologically significant. However, recent studies have established that H_2S is indeed a biologically relevant signaling molecule in mammals [reviewed in (26)]. H_2S acts as a messenger molecule, and together with the volatile substances nitric oxide (NO) and carbon monoxide (CO) it is defined as a gasotransmitter, playing physiological roles in a variety of functions such as synaptic transmission, vascular tone, angiogenesis, inflammation and cellular signaling (1). We have recently shown for the first time that levels of intracellular H_2S modulates cellular responses and viral replication in an *in vitro* model of paramyxovirus infection (7), including RSV. Herein, we provide evidence that H_2S has a protective role in RSV infection *in vivo* as well, by modulating both inflammatory responses and viral replication. Indeed, our study shows that treatment of mice with an H_2S donor reduced RSV peak titer in the lung and ameliorated clinical disease, including AHR. These effects were associated with a reduction in BAL and lung

neutrophilia and overall lung pathology in RSV-infected H_2S-treated mice compared to RSV-infected untreated mice. The observed effect of the H_2S donor GYY4137 on RSV replication in the lung appeared to be independent of the known antiviral activity of IFN-γ (similar concentrations of this cytokine in mice treated or not with GYY4137) and IFN type I, which levels were in fact reduced in BAL samples of RSV-infected animals treated with GYY4137. The latter observation is not particularly surprising given the modest antiviral activity against RSV of endogenously-produced IFN type I in mice (27), rather its contribution to the pathogenesis of airway inflammation (28). Moreover, our data show that administration of GYY4137 up to 6h after viral inoculation was effective in reducing RSV titer in the lung, a quite remarkable finding given the limitation of the mouse model in which the intranasal inoculation of virus results in its very rapid spread to the lower airways.

These findings were further supported by the evidence that: 1) RSV infection, similarly to our observations in epithelial cells, causes a time-dependent reduction in the expression of H_2S-generating enzymes CSE and CBS; 2) CSE-deficient mice had increased RSV replication, greater disease and inflammatory mediator production compared to CSE-competent mice; and 3) anti-viral activity and lung function (AHR) could be rescued in CSE-deficient mice by treatment with GYY4137. In humans, CSE expression and activity are developmentally regulated as demonstrated by studies in premature infants, newborns and infants in the first year of life, in which this enzyme has been measured and found to be delayed in maturation (29, 30). These findings are of particular relevance in relation to natural RSV infections, which cause the most severe disease during the first year of life, when the endogenous H_2S tone would likely be reduced or in premature infants with smaller airways.

Although the mechanism(s) leading to increased AHR in the experimental mouse model of RSV infection are not fully understood, RSV-infected CSE-deficient mice showed increased AHR to methacholine challenge compared to WT-infected mice. Moreover, the H_2S donor GYY4137 significantly reduced AHR in RSV-infected BALB/c mice, further suggesting that the H_2S pathway in the lung is critical in relaxing airway smooth muscle and controlling viral-mediated airway reactivity. In this regard, some studies have shown that H_2S relaxes vascular smooth muscle by increasing K_{ATP} channel currents and hyperpolarizing cell membrane (31), or by K_{ATP} channel-independent mechanisms, such as inhibition of Ca^{2+} release through the inositol-1,4,5-triphosphate receptor ($InsP_3$) (32). In our mouse models of infection, treatment with the H_2S donor significantly decreased airway neutrophilia and secretion of inflammatory cytokines, which may contribute to RSV-induced AHR (12). Some limited studies have investigated the role of H_2S in the pathogenesis of asthma. In one study of Wu *et al*. (33), serum level of H_2S was significantly lower in patients with asthma, compared to healthy controls, and significantly correlated with severity of acute exacerbations and changes in FEV1. In a mouse model of OVA-mediated allergic inflammation, CSE deficiency was associated with increased Th2 cytokines and enhanced AHR after OVA challenge, whereas exogenous H_2S supplementation was able to reduce it (34). In this regard, we did not observe any significant difference in Th1 or Th2 cytokines in CSE deficient mice compared to WT controls following RSV infection. In chronic diseases of the lung data from the literature suggest a correlation of serum H_2S level with COPD severity, as defined by lung function and airway inflammation (35, 36). Serum H_2S level was significantly higher in patients with stable COPD than that in patients with acute exacerbation of COPD (AECOPD). In patients with stable COPD, serum H_2S levels were significantly lower in those with stage III obstruction, versus than stage I. This correlated

positively with the percentage of predicted forced expiratory volume in one second (FEV1) value.

Overall, our results support the notion that the antiviral activity of H_2S appears to be largely independent of its anti-inflammatory properties. In airway epithelial cells, inhibition of RSV-induced cellular signaling and expression of proinflammatory genes by GYY4137 treatment occurs separately from its ability to inhibit viral replication (7). Similarly, treatment with GYY4137 significantly reduced cytokine and chemokine production in mice inoculated with UV-inactivated RSV (i.e. non-replicating). Endogenous H_2S production and exogenous H_2S administration have been associated to both pro-inflammatory and anti-inflammatory effects in various models of disease [reviewed in (37)]. In the context of acute pancreatitis and in burn injury, for example, H_2S seems to play a pro-inflammatory role, while in other pathologies such as asthma, COPD, LPS-induced inflammation, and ischemia reperfusion it displays anti-inflammatory properties. In models of lung injury, administration of H_2S donors has been often associated with an anti-inflammatory effect. For example, in a mouse model of hyperoxia, treatment with NaHS was associated with reduced lung permeability and inflammation, due to decreased production of proinflammatory mediators such as IL-1β, MCP-1, and MIP-2, and increased anti-inflammatory cytokine expression (38). Similar results were obtained in other models of acute lung injury, such as the one associated with hemorrhagic shock or with bleomycin treatment (39, 40). In the only study investigating the anti-inflammatory effect of H_2S administration in the course of a viral infection, GYY4137 suppressed Coxsackie B3-induced secretion of pro-inflammatory cytokines, an effect associated with suppression of activation of the NF-κB signaling pathway (41).

In summary, our results establish for the first time a critical protective role of the H_2S pathway in the development of disease, viral replication and airway inflammation in an *in vivo* model of RSV infection, shedding insight into a new potential therapeutic approach for this important respiratory pathogen, and possibly other significant respiratory viral infections, by targeting the endogenous CSE/H_2S pathway.

REFERENCES

ACKNOWLEDGMENTS

The authors would like to thank Kimberly Palkowetz and Yinghong Ma for technical assistance and Cynthia Tribble for manuscript editing and submission.

FIGURE LEGENDS

Figure 1. GYY4137 treatment attenuates RSV-induced disease and pulmonary lung function. **(A)** GYY4137 dose response in *vivo*. Mice were treated i.n. with different doses of GYY4137 (50 mg, 100mg, and 200mg/kg body weight) or an appropriate volume of vehicle (PBS) 1h before, 6h and 24h after infection. Mice were inoculated with either RSV or PBS. **(A)** Mice were monitored daily and body weight was calculated based on the original weight before the infection. Data are expressed as mean ± SEM (n = 3-4 mice/group). **(B)** Disease parameters - BALB/c mice were infected with 10^6 PFU RSV and treated with GYY4137 or vehicle as follows: (1) three doses, at 2h and at 6h and 24h after infection, (2) two doses, one at 6h and one at 24h after infection, (3) one dose, at 24h before infection. Data are expressed as mean ± SEM (n = 4 mice/group). *$p<0.05$ compared with PBS/RSV at days 1, 2, and 3 p.i. **(C, D, E)** Mice were treated i.n. with GYY4137 (50 mg/kg body weight) or an appropriate volume of vehicle

(PBS) 1h before, 6h and 24h after infection. Mice were inoculated with RSV or PBS. **(C)** Clinical illness scores of GYY4137 RSV (open squares) and RSV vehicle (solid squares) were measured from day 1 to day 7 p.i. (data shown for the 50 mg/kg dose). GYY4137/RSV infected mice were assigned illness score 0 starting with day 3 post-infection (data shown as n.d, not detected). Sham (mock) infected mice treated with either vehicle or GYY4137 received a healthy illness score 0 throughout the course of the experiment (data not shown). **(D)** Unrestrained, whole-body plethysmography (Buxco Electronics, Inc. Sharon, CT) was used to measure the Enhanced Pause (Penh) to evaluate AHR. Baseline and post-methacholine challenge Penh values were determined at day 5 after infection. Penh values are presented as mean ± SEM (n = 4-6 mice/group). **(E)** Airway resistance (day 5 p.i.) measured in mechanically ventilated mice by the Flexivent system. Data are means ± SEM (n = 3 mice/group). *p<0.05, **p<0.001, and ***p<0.0001 compared with PBS/RSV group.

Figure 2. GYY4137 treatment reduces viral replication in RSV infected mice. **(A)** Mice were treated with GYY4137 or vehicle and infected with either RSV or PBS and harvested at day 5 p.i. to determine viral replication by plaque assay, expressed as pfu/g of lung tissue. The bar graph represents mean ± SEM (n = 4 mice/group), *p<0.001 compared with PBS/RSV group. (B) Mice were infected with 10^6 PFU RSV and treated with GYY4137 after infection as indicated. Data are expressed as mean ± SEM (n = 4 mice/group). At day 5 post-infection, virus titer in the lung was determined by plaque assay. *p<0.05 compared with PBS/RSV group.

Figure 3. GYY4137 reduces airway neutrophilia and lung inflammation after infection. Mice were treated i.n. with GYY4137 (50 mg/kg body weight) or an appropriate volume of vehicle

(PBS) 1h before, 6h and 20h after infection. Mice were inoculated with either RSV or PBS as described in Material and Methods. BAL and lungs were collected at different time points after infection to determine differential cell counts by hematoxylin and eosin staining in BAL (**A**) and neutrophils ($CD11b^+Gr1^+$) recruitment to the lung (**B**) by flow cytometry analysis after staining with specific antibodies. **(C)** Lung samples were harvested at day 7 post-infection, fixed for slide preparation and H&E stained. Representative stained lung tissue sections from the indicated treatment. **(D)** Pathology score of prepared slides (scored as described in Materials and Methods). The bar graph represents mean ± SEM (n = 3-4 mice/group). *p<0.05, **p<0.001, and ***p<0.0001 compared with PBS/RSV mice.

Figure 4. GYY4137 inhibits proinflammatory mediator secretion in response to RSV infection. Mice were treated with GYY4137 or vehicle, RSV at the dose of 10^6 PFU or sham-infected and harvested at day 1 p.i. to collect BAL samples to measure cytokines **(A)** and chemokines **(B)** by multi-Plex Cytokine detection system, and type I IFN by ELISA **(C)**. The bar graph represents mean ± SEM (n = 4-6 mice/group). *p<0.05; **p<0.001; ***p<0.0001 compared with PBS/RSV group.

Figure 5. Effect of GYY4137 on cytokines/chemokine secretion in response to UV-inactivated RSV. Mice were treated i.n. with GYY4137 or vehicle and inoculated with either UV-inactivated 10^7 PFU RSV or mock-infected. BAL was collected at day 1 p.i. to measure cytokines and chemokines by a multi-Plex Cytokine detection system. The bar graph represents mean ± SEM (n = 4 mice/group). **p<0.001; ***p<0.0001 compared with PBS/UV-RSV group.

Figure 6. CSE-deficient mice have increased disease severity, viral replication and lung inflammation. C57BL/6 (WT) and CSE $^{-/-}$ (CSE KO) mice were infected i.n. with 10^7 PFU of RSV or PBS. **(A)** Mice were monitored daily and body weight was calculated based on the original weight before the infection. Data are expressed as mean ± SEM (n = 3-4 mice/group). **(B) Left panel:** Unrestrained, whole-body plethysmography (Buxco Electronics, Inc. Sharon, CT) was used to measure the Enhanced Pause (Penh) to evaluate AHR. Baseline and post-methacholine challenge Penh values were determined at day 1 p.i. Data are expressed as means ± SEM (n = 3-4 mice/group). **Right panel:** Airway resistance (day 1 p.i.) was measured in mechanically ventilated mice by the Flexivent system. Data are expressed as means ± SEM (n = 3-4 mice/group). **(C)** Viral replication. At day 5 p.i., lungs were excised and viral titers were determined by plaque assay. The bar graph represents mean ± SEM (n = 3-4 mice/group). **(D, E)** C57BL/6 (WT) and CSE $^{-/-}$ (CSE KO) mice were given GYY4137 or vehicle at dose 50mg/kg 1h before, 6h and 24h after infection. Mice were infected i.n. with 10^7 PFU of RSV or PBS. **(D)** Mice were monitored daily and body weight was calculated based on the original weight before the infection. Data are expressed as mean ± SEM (n = 2-3mice/group). *p<0.05 CSE KO GYY4137/RSV vs. CSE KO PBS/RSV and WT GYY4137/RSV vs. WTPBS/RSV at day 1 post-infection; CSE KO GYY4137/RSV vs.. CSE KO PBS/RSV and CSE KO PBS/RSV vs. WT PBS/RSV at day 2 post-infection, WT GYY4137/RSV vs. WT PBS/RSV and CSE KO PBS/RSV vs. WT PBS/RSV at day 4 post-infection. **(E)** Unrestrained, whole-body plethysmography (Buxco Electronics, Inc. Sharon, CT) was used to measure the Enhanced Pause (Penh) to evaluate AHR. Baseline and post-methacholine challenge Penh values were determined at day 5 p.i. Data are expressed as means ± SEM (n = 2-3 mice/group).).*p<0.05 compared with

WT/RSV, WT/GYY4137/RSV groups and between CSE KO/RSV and CSEKO/GYY4137/RSV mice.

Figure 7. Effect of CSE-defieincy on cytokines, chemokines production and pulmonary inflammation after infection. C57BL/6 (WT) and CSE $^{-/-}$ (CSE KO) mice were infected i.n. with 10^7 PFU of RSV or PBS. **(A)** Mice were infected with RSV or mock-infected and sacrificed at day 1 p.i. to collect BAL samples. Cytokine/chemokine production was measured by a multi-Plex Cytokine detection system. The bar graph represents mean ± SEM (n = 3-4 mice/group. **(B)** BAL was collected at day 5 after infection to measure INF-γ and IL-4 by ELISA. Data are expressed as mean ± SEM (n = 4 mice/group)**. (C)** Pathology score of lungs harvested at day 7 p.i., fixed and H&E stained. The bar graph represents mean ± SEM (n = 3-4 mice/group). *p<0.05 compared with WT/RSV group.

Figure ES1. H_2S expression in lung tissue. (A) Effect of RSV infection on CSE and CBS gene expression in lungs of mock or RSV-infected mice. BALB/c mice were either inoculated with PBS (sham-infected) or infected with $5x10^6$ pfu of RSV and harvested at different days post-infection to isolate total RNA from lungs. CSE and CBS mRNA levels in sham and viral-infected mice were measured by qRT-PCR. The bar graph represents mean ± SEM (n = 4 mice/group). * p<0.05 compared to sham. **(B)** Hydrogen sulfide expression in the lungs by ex vivo imaging using a novel fluorescent probe (SF-7AM). SF-7AM probe was delivered to vehicle or GYY4137 treated mice as described in Methods section. Left panels shows images of vehicle untreated and GYY4137 treated (50 mg/kg body weight) lungs. Right panel shows fluorescent intensity measured using Living Image software.

Page left Blank

Reference List

1. Chen Y, Wang R. The message in the air: hydrogen sulfide metabolism in chronic respiratory diseases. *Respiratory Physiology & Neurobiology* 2012;184:130-138.

2. Wang P, Zhang G, Wondimu T, Ross B, Wang R. Hydrogen sulfide and asthma. *Experimental Physiology* 2011;96:847-852.

3. Wang R. Physiological Implications of hydrogen sulfide: a whiff exploration that blossomed. *Physiol Rev* 2012;92:791-896.

4. Wang R. Signaling pathways for the vascular effects of hydrogen sulfide. *Curr Opin Nephrol Hypertens* 2011;20:107-112.

5. Li L, Whiteman M, Guan YY, Neo KL, Cheng Y, Lee SW, Zhao Y, Baskar R, Tan CH, Moore PK. Characterization of a novel, water-soluble hydrogen sulfide-releasing molecule (GYY4137): new insights into the biology of hydrogen sulfide. *Circulation* 2008;117:2351-2360.

6. Szabo C. Hydrogen sulphide and its therapeutic potential. *Nat Rev Drug Discov* 2007;6:917-935.

7. Li H, Ma Y, Escaffre O, Ivanciuc T, Komaravelli N, Kelley JP, Coletta C, Szabo C, Rockx B, Garofalo RP, Casola A. Role of hydrogen sulfide in paramyxovirus infections. *J Virol* 2015;89:5557-5568.

8. Yang G, Wu L, Jiang B, Yang W, Qi J, Cao K, Meng Q, Mustafa AK, Mu W, Zhang S, et al. H_2S as a physiologic vasorelaxant: hypertension in mice with deletion of cystathionine gamma-lyase. *Science* 2008;322:587-590.

9. Ueba O. Respiratory syncytial virus: I. Concentration and purification of the infectious virus. *Acta Med Okayama* 1978;32:265-272.

10. Olszewska-Pazdrak B, Casola A, Saito T, Alam R, Crowe SE, Mei F, Ogra PL, Garofalo RP. Cell-specific expression of RANTES, MCP-1, and MIP-1alpha by lower airway epithelial cells and eosinophils infected with respiratory syncytial virus. *J Virol* 1998;72:4756-4764.

11. Kisch AL, Johnson KM. A plaque assay for respiratory syncytial virus. *Proc Soc Exp Biol Med* 1963;112:583.

12. Castro SM, Guerrero-Plata A, Suarez-Real G, Adegboyega PA, Colasurdo GN, Khan AM, Garofalo RP, Casola A. Antioxidant Treatment ameliorates respiratory syncytial virus-induced disease and lung inflammation. *Am J Respir Crit Care Med* 2006;174:1361-1369.

13. Kolli D, Gupta MR, Sbrana E, Velayutham TS, Hong C, Casola A, Garofalo RP. Alveolar macrophages contribute to the pathogenesis of hmpv infection while protecting against rsv infection. *Am J Respir Cell Mol Biol* 2014.

14. Guerrero-Plata A, Baron S, Poast JS, Adegboyega PA, Casola A, Garofalo RP. Activity and regulation of alpha interferon in respiratory syncytial virus and human metapneumovirus experimental infections. *J Virol* 2005;79:10190-10199.

15. Schwarze J, Hamelmann E, Bradley KL, Takeda K, Gelfand EW. Respiratory syncytial virus infection results in airway hyperresponsiveness and enhanced airway sensitization to allergen. *J Clin Invest* 1997;100:226-233.

16. Graham BS, Perkins MD, Wright PF, Karzon DT. Primary respiratory syncytial virus infection in mice. *J Med Virol* 1988;26:153-162.

17. Garofalo RP, Haeberle H. Epithelial regulation of innate immunity to respiratory syncytial virus. *Am J Respir Cell Mol Biol* 2000;23:581-585.

18. Guerrero-Plata A, Casola A, Garofalo RP. Human metapneumovirus induces a profile of lung cytokines distinct from that of respiratory syncytial virus. *J Virol* 2005;79:14992-14997.

19. Haeberle H, Takizawa R, Casola A, Brasier A.R., Dieterich H-J, van Rooijen N, Gatalica Z, Garofalo RP. Respiratory syncytial virus-induced activation of NF-KB in the lung involves alveolar macrophages and toll-like receptor 4-dependent pathways. *J Infect Dis* 2002;186:1199-1206.

20. Haeberle HA, Kuziel WA, Dieterich HJ, Casola A, Gatalica Z, Garofalo RP. inducible expression of inflammatory chemokines in respiratory syncytial virus-infected mice: Role of MIP-1alpha in lung pathology. *J Virol* 2001;75:878-890.

21. Haeberle HA, Casola A, Gatalica Z, Petronella S, Dieterich HJ, Ernst PB, Brasier AR, Garofalo RP. IkappaB kinase is a critical regulator of chemokine expression and lung inflammation in respiratory syncytial virus infection. *J Virol* 2004;78:2232-2241.

22. Bennett BL, Garofalo RP, Cron SG, Hosakote YM, Atmar RL, Macias CG, Piedra PA. Immunopathogenesis of respiratory syncytial virus bronchiolitis. *J Infect Dis* 2007;195:1532-1540.

23. Hasegawa K, Jartti T, Mansbach JM, Laham FR, Jewell AM, Espinola JA, Piedra PA, Camargo CA, Jr. Respiratory syncytial virus genomic load and disease severity among children hospitalized with bronchiolitis: multicenter cohort studies in the United States and Finland. *J Infect Dis* 2015;211:1550-1559.

24. Devincenzo JP, El Saleeby CM, Bush AJ. Respiratory syncytial virus load predicts disease severity in previously healthy infants. *J Infect Dis* 2005;191:1861-1868.

25. El Saleeby CM, Bush AJ, Harrison LM, Aitken JA, Devincenzo JP. Respiratory syncytial virus load, viral dynamics, and disease severity in previously healthy naturally infected children. *J Infect Dis* 2011;204:996-1002.

26. Paul BD, Snyder SH. H(2)S Signalling Through protein sulfhydration and beyond. *Nat Rev Mol Cell Biol* 2012;13:499-507.

27. Johnson TR, Mertz SE, Gitiban N, Hammond S, Legallo R, Durbin RK, Durbin JE. Role for innate IFNs in Determining respiratory syncytial virus immunopathology. *J Immunol* 2005;174:7234-7241.

28. Goritzka M, Durant LR, Pereira C, Salek-Ardakani S, Openshaw PJ, Johansson C. Alpha/Beta interferon receptor signaling amplifies early proinflammatory cytokine production in the lung during respiratory syncytial virus infection. *J Virol* 2014;88:6128-6136.

29. Vina J, Vento M, Garcia-Sala F, Puertes IR, Gasco E, Sastre J, Asensi M, Pallardo FV. L-Cysteine and glutathione metabolism are impaired in premature infants due to cystathionase deficiency. *Am J Clin Nutr* 1995;61:1067-1069.

30. Zlotkin SH, Anderson GH. The development of cystathionase activity during the first year of life. *Pediatr Res* 1982;16:65-68.

31. Fitzgerald R, DeSantiago B, Lee DY, Yang G, Kim JY, Foster DB, Chan-Li Y, Horton MR, Panettieri RA, Wang R, An SS. H_2S Relaxes Isolated Human Airway Smooth Muscle Cells Via the Sarcolemmal K(ATP) Channel. *Biochem Biophys Res Commun* 2014;446:393-398.

32. Castro-Piedras I, Perez-Zoghbi JF. Hydrogen Sulphide inhibits Ca2+ release through InsP3 receptors and relaxes airway smooth muscle. *J Physiol* 2013;591:5999-6015.

33. Wu R, Yao WZ, Chen YH, Geng B, Tang CS. [Plasma level of endogenous hydrogen sulfide in patients with acute asthma]. *Beijing Da Xue Xue Bao* 2008;40:505-508.

34. Zhang G, Wang P, Yang G, Cao Q, Wang R. The Inhibitory role of hydrogen sulfide in airway hyperresponsiveness and inflammation in a mouse model of asthma. *Am J Pathol* 2013;182:1188-1195.

35. Chen YH, Yao WZ, Geng B, Ding YL, Lu M, Zhao MW, Tang CS. Endogenous hydrogen sulfide in patients with COPD. *Chest* 2005;128:3205-3211.

36. Chen YH, Wu R, Geng B, Qi YF, Wang PP, Yao WZ, Tang CS. Endogenous hydrogen sulfide reduces airway inflammation and remodeling in a rat model of asthma. *Cytokine* 2009;45:117-123.

37. Whiteman M, Winyard PG. Hydrogen Sulfide and inflammation: the good, the bad, the ugly and the promising. *Expert Rev Clin Pharmacol* 2011;4:13-32.

38. Li HD, Zhang ZR, Zhang QX, Qin ZC, He DM, Chen JS. Treatment with exogenous hydrogen sulfide attenuates hyperoxia-induced acute lung injury in mice. *Eur J Appl Physiol* 2013;113:1555-1563.

39. Kalayarasan S, Sriram N, Sudhandiran G. Diallyl sulfide attenuates bleomycin-induced pulmonary fibrosis: critical role of INOS, NF-KappaB, TNF-Alpha and IL-1beta. *Life Sci* 2008;82:1142-1153.

40. Xu DQ, Gao C, Niu W, Li Y, Wang YX, Gao CJ, Ding Q, Yao LN, Chai W, Li ZC. Sodium hydrosulfide alleviates lung inflammation and cell apoptosis following resuscitated hemorrhagic shock in rats. *Acta Pharmacol Sin* 2013;34:1515-1525.

41. Wu Z, Peng H, Du Q, Lin W, Liu Y. GYY4137, a hydrogen sulfide releasing molecule, inhibits the inflammatory response by suppressing the activation of nuclear factorkappa b and mitogenactivated protein kinases in coxsackie virus b3infected rat cardiomyocytes. *Mol Med Rep* 2015;11:1837-1844.

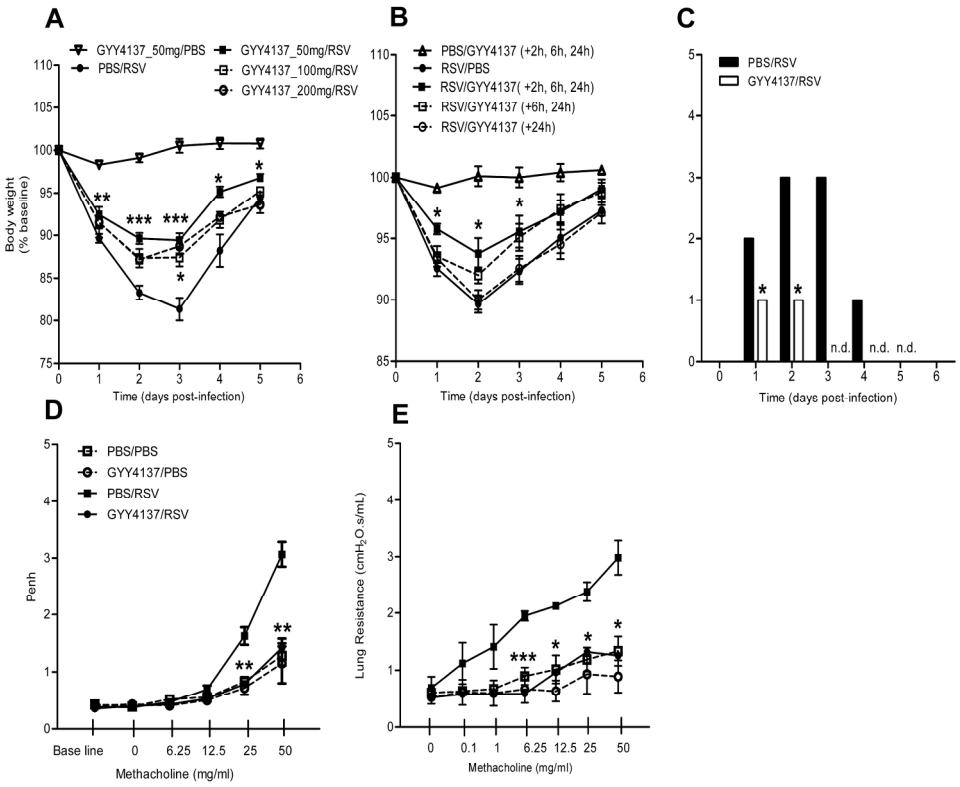

Figure 1. GYY4137 treatment attenuates RSV-induced disease and pulmonary lung function. (**A**) GYY4137 dose response *in vivo*. Mice were treated i.n. with different doses of GYY4137 (50 mg, 100mg, and 200mg/kg body weight) or an appropriate volume of vehicle (PBS) 1h before, 6h and 24h after infection. Mice were inoculated with either RSV or PBS. (**A**) Mice were monitored daily and body weight was calculated based on the original weight before the infection. Data are expressed as mean ± SEM (n = 3-4 mice/group). (**B**) Disease parameters - BALB/c mice were infected with 106 PFU RSV and treated with GYY4137 or vehicle as follows: (1) three doses, at 2h and at 6h and 24h after infection, (2) two doses, one at 6h and one at 24h after infection, (3) one dose, at 24h before infection. Data are expressed as mean ± SEM (n = 4 mice/group). *p<0.05 compared with PBS/RSV at days 1, 2, and 3 p.i. (C, D, E) Mice were treated i.n. with GYY4137 (50 mg/kg body weight) or an appropriate volume of vehicle (PBS) 1h before, 6h and 24h after infection. Mice were inoculated with RSV or PBS. (**C**) Clinical illness scores of GYY4137 RSV (open squares) and RSV vehicle (solid squares) were measured from day 1 to day 7 p.i. (data shown for the 50 mg/kg dose). GYY4137/RSV infected mice were assigned illness score 0 starting with day 3 post-infection (data shown as n.d, not detected). Sham (mock) infected mice treated with either vehicle or GYY4137 received a healthy illness score 0 throughout the course of the experiment (data not shown). (**D**) Unrestrained, whole-body plethysmography (Buxco Electronics, Inc. Sharon, CT) was used to measure the Enhanced Pause (Penh) to evaluate AHR. Baseline and post-methacholine challenge Penh values were determined at day 5 after infection. Penh values are presented as mean ± SEM (n = 4-6 mice/group). (**E**) Airway resistance (day 5 p.i.) measured in mechanically ventilated mice by the Flexivent system. Data are means ± SEM (n = 3 mice/group). *p<0.05, **p<0.001, and ***p<0.0001 compared with PBS/RSV group.
103x82mm (600 x 600 DPI)

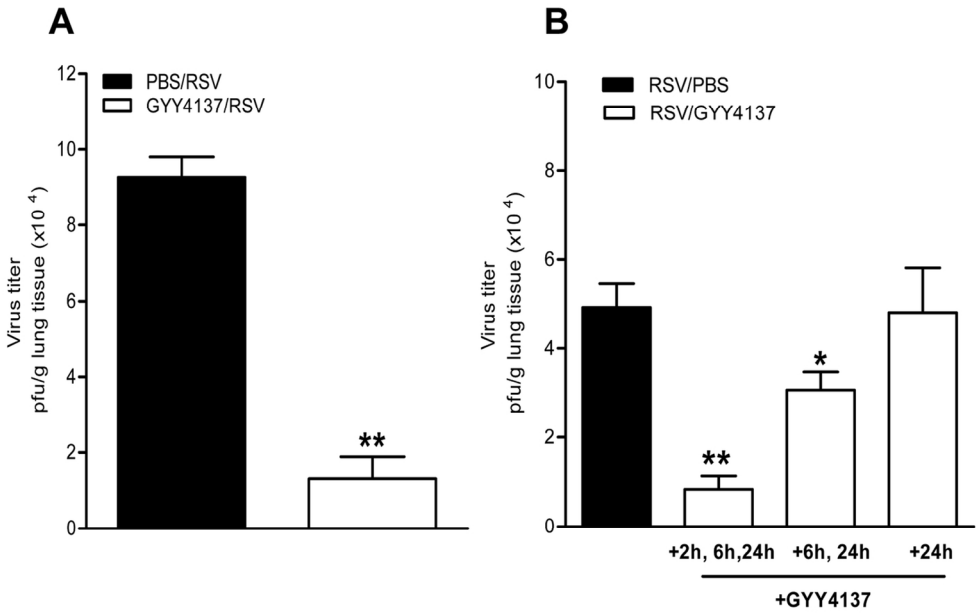

Figure 2. GYY4137 treatment reduces viral replication in RSV infected mice. (**A**) Mice were treated with GYY4137 or vehicle and infected with either RSV or PBS and harvested at day 5 p.i. to determine viral replication by plaque assay, expressed as pfu/g of lung tissue. The bar graph represents mean ± SEM (n = 4 mice/group), *p<0.001 compared with PBS/RSV group. (**B**) Mice were infected with 106 PFU RSV and treated with GYY4137 after infection as indicated. Data are expressed as mean ± SEM (n = 4 mice/group). At day 5 post-infection, virus titer in the lung was determined by plaque assay. *p<0.05 compared with PBS/RSV group.
61x38mm (600 x 600 DPI)

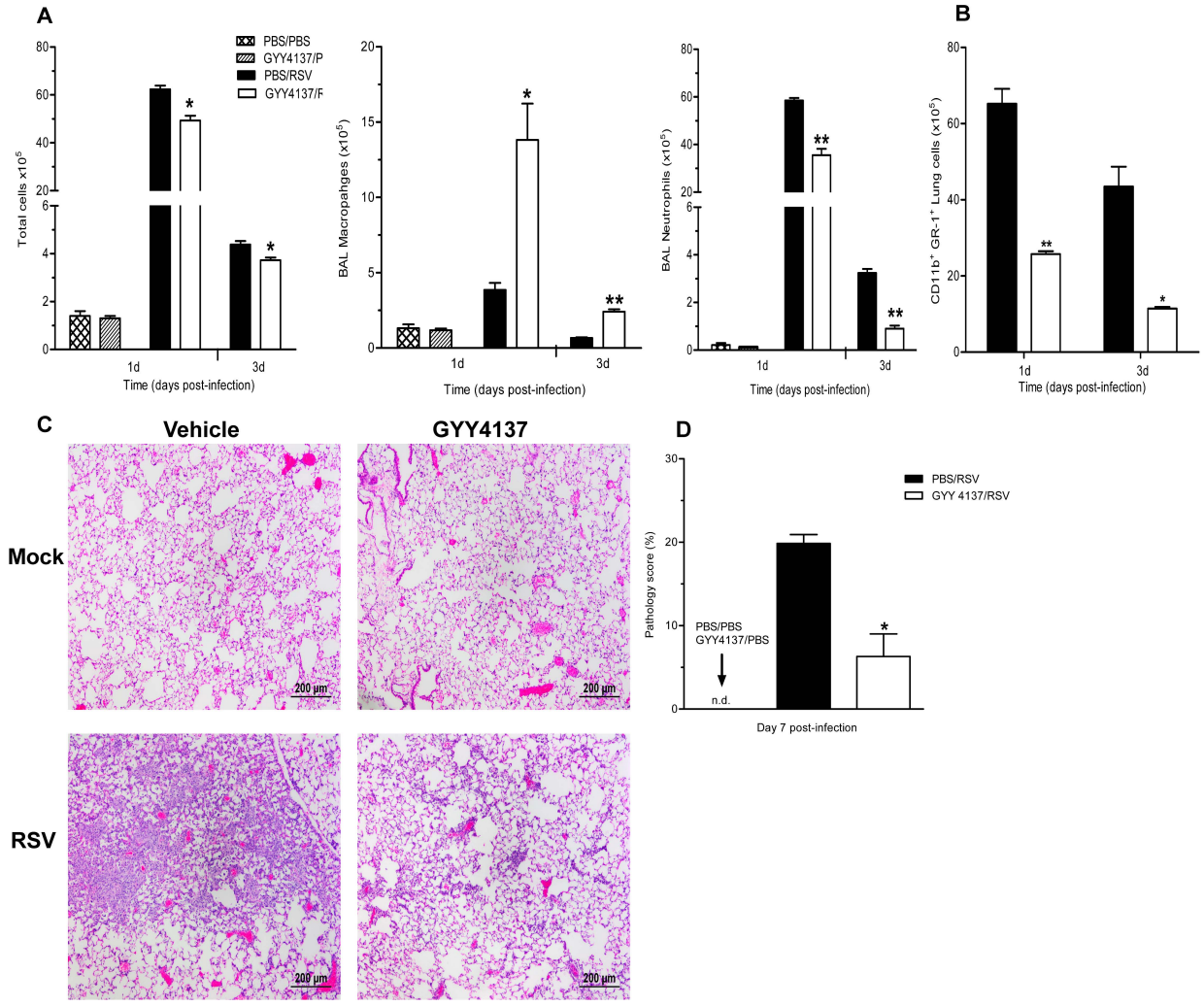

Figure 3. GYY4137 reduces airway neutrophilia and lung inflammation after infection. Mice were treated i.n. with GYY4137 (50 mg/kg body weight) or an appropriate volume of vehicle (PBS) 1h before, 6h and 20h after infection. Mice were inoculated with either RSV or PBS as described in Material and Methods. BAL and lungs were collected at different time points after infection to determine differential cell counts by hematoxylin and eosin staining in BAL (A) and neutrophils (CD11b+Gr1+) recruitment to the lung (B) by flow cytometry analysis after staining with specific antibodies. (**C**) Lung samples were harvested at day 7 post-infection, fixed for slide preparation and H&E stained. Representative stained lung tissue sections from the indicated treatment. (**D**) Pathology score of prepared slides (scored as described in Materials and Methods). The bar graph represents mean ± SEM (n = 3-4 mice/group). *p<0.05, **p<0.001, and ***p<0.0001 compared with PBS/RSV mice.
159x131mm (300 x 300 DPI)

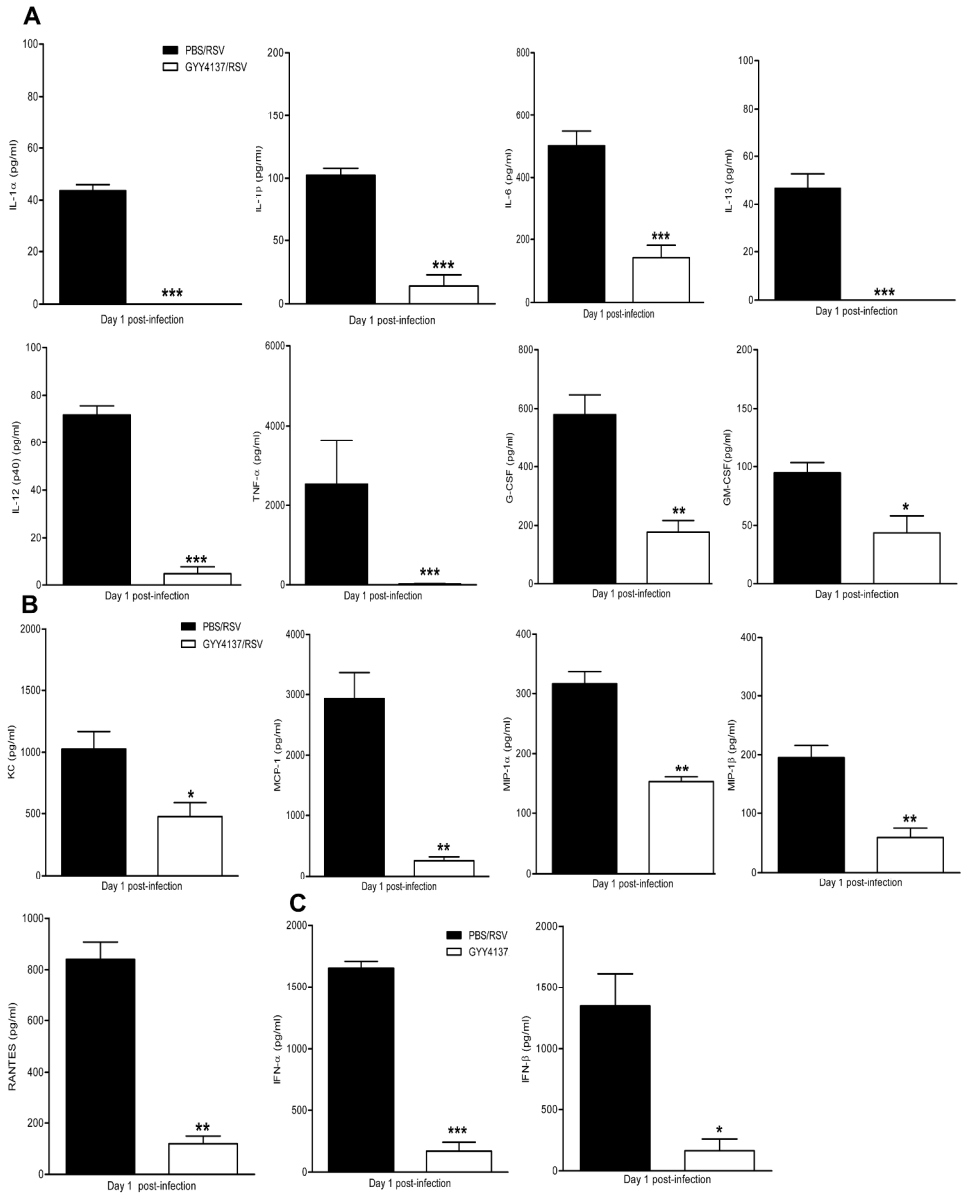

Figure 4. GYY4137 inhibits proinflammatory mediator secretion in response to RSV infection. Mice were treated with GYY4137 or vehicle, RSV at the dose of 106 PFU or sham-infected and harvested at day 1 p.i. to collect BAL samples to measure cytokines (**A**) and chemokines (**B**) by multi-Plex Cytokine detection system, and type I IFN by ELISA (**C**). The bar graph represents mean ± SEM (n = 4-6 mice/group). **p*<0.05; ***p*<0.001; ****p*<0.0001 compared with PBS/RSV group.
172x212mm (600 x 600 DPI)

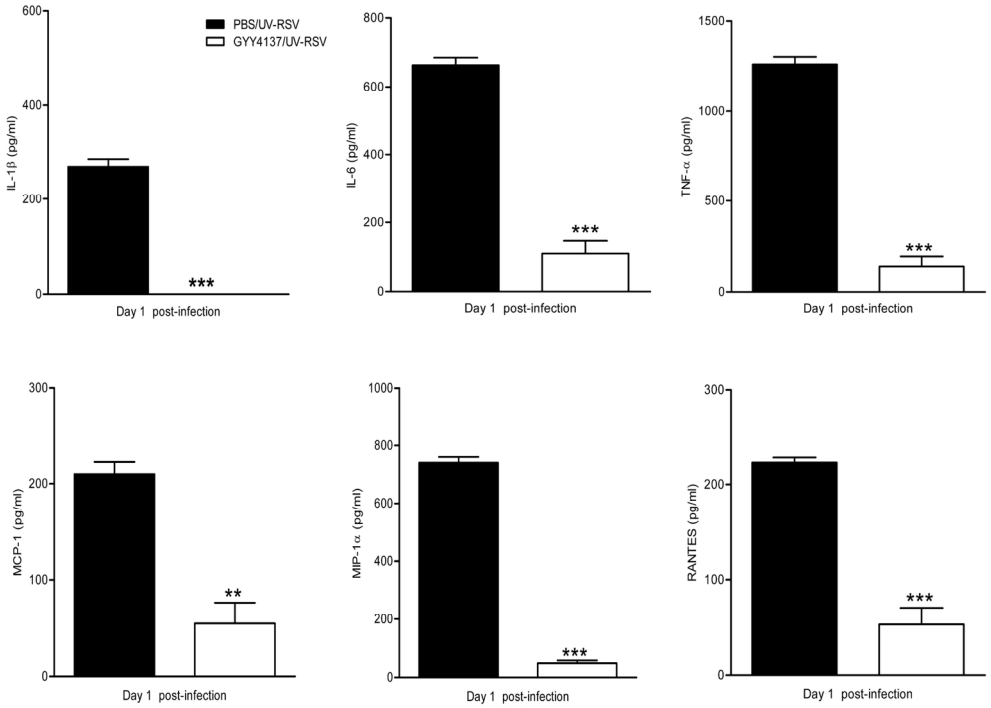

Figure 5. Effect of GYY4137 on cytokines/chemokine secretion in response to UV-inactivated RSV. Mice were treated i.n. with GYY4137 or vehicle and inoculated with either UV-inactivated 107 PFU RSV or mock-infected. BAL was collected at day 1 p.i. to measure cytokines and chemokines by a multi-Plex Cytokine detection system. The bar graph represents mean ± SEM (n = 4 mice/group). $^{**}p<0.001$; $^{***}p<0.0001$ compared with PBS/UV-RSV group.
77x56mm (600 x 600 DPI)

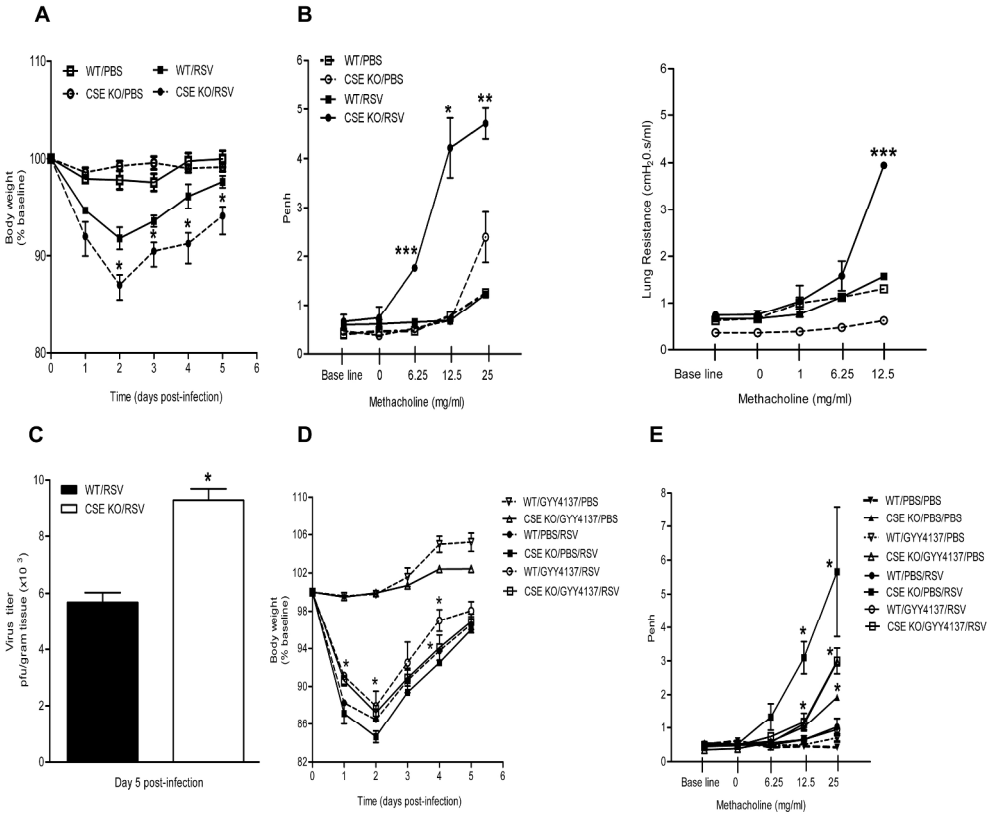

Figure 6. CSE-deficient mice have increased disease severity, viral replication and lung inflammation. C57BL/6 (WT) and CSE -/- (CSE KO) mice were infected i.n. with 107 PFU of RSV or PBS. (**A**) Mice were monitored daily and body weight was calculated based on the original weight before the infection. Data are expressed as mean ± SEM (n = 3-4 mice/group). (**B**) Left panel: Unrestrained, whole-body plethysmography (Buxco Electronics, Inc. Sharon, CT) was used to measure the Enhanced Pause (Penh) to evaluate AHR. Baseline and post-methacholine challenge Penh values were determined at day 1 p.i. Data are expressed as means ± SEM (n = 3-4 mice/group). **Right panel**: Airway resistance (day 1 p.i.) was measured in mechanically ventilated mice by the Flexivent system. Data are expressed as means ± SEM (n = 3-4 mice/group). (**C**) Viral replication. At day 5 p.i., lungs were excised and viral titers were determined by plaque assay. The bar graph represents mean ± SEM (n = 3-4 mice/group). (**D, E**) C57BL/6 (WT) and CSE -/- (CSE KO) mice were given GYY4137 or vehicle at dose 50mg/kg 1h before, 6h and 24h after infection. Mice were infected i.n. with 107 PFU of RSV or PBS. (**D**) Mice were monitored daily and body weight was calculated based on the original weight before the infection. Data are expressed as mean ± SEM (n = 2-3mice/group). **p*<0.05 CSE KO GYY4137/RSV vs. CSE KO PBS/RSV and WT GYY4137/RSV vs. WTPBS/RSV at day 1 post-infection; CSE KO GYY4137/RSV vs.. CSE KO PBS/RSV and CSE KO PBS/RSV vs. WT PBS/RSV at day 2 post-infection, WT GYY4137/RSV vs. WT PBS/RSV and CSE KO PBS/RSV vs. WT PBS/RSV at day 4 post-infection. (**E**) Unrestrained, whole-body plethysmography (Buxco Electronics, Inc. Sharon, CT) was used to measure the Enhanced Pause (Penh) to evaluate AHR. Baseline and post-methacholine challenge Penh values were determined at day 5 p.i. Data are expressed as means ± SEM (n = 2-3 mice/group).).**p*<0.05 compared with WT/RSV, WT/GYY4137/RSV groups and between CSE KO/RSV and CSEKO/GYY4137/RSV mice.
133x110mm (600 x 600 DPI)

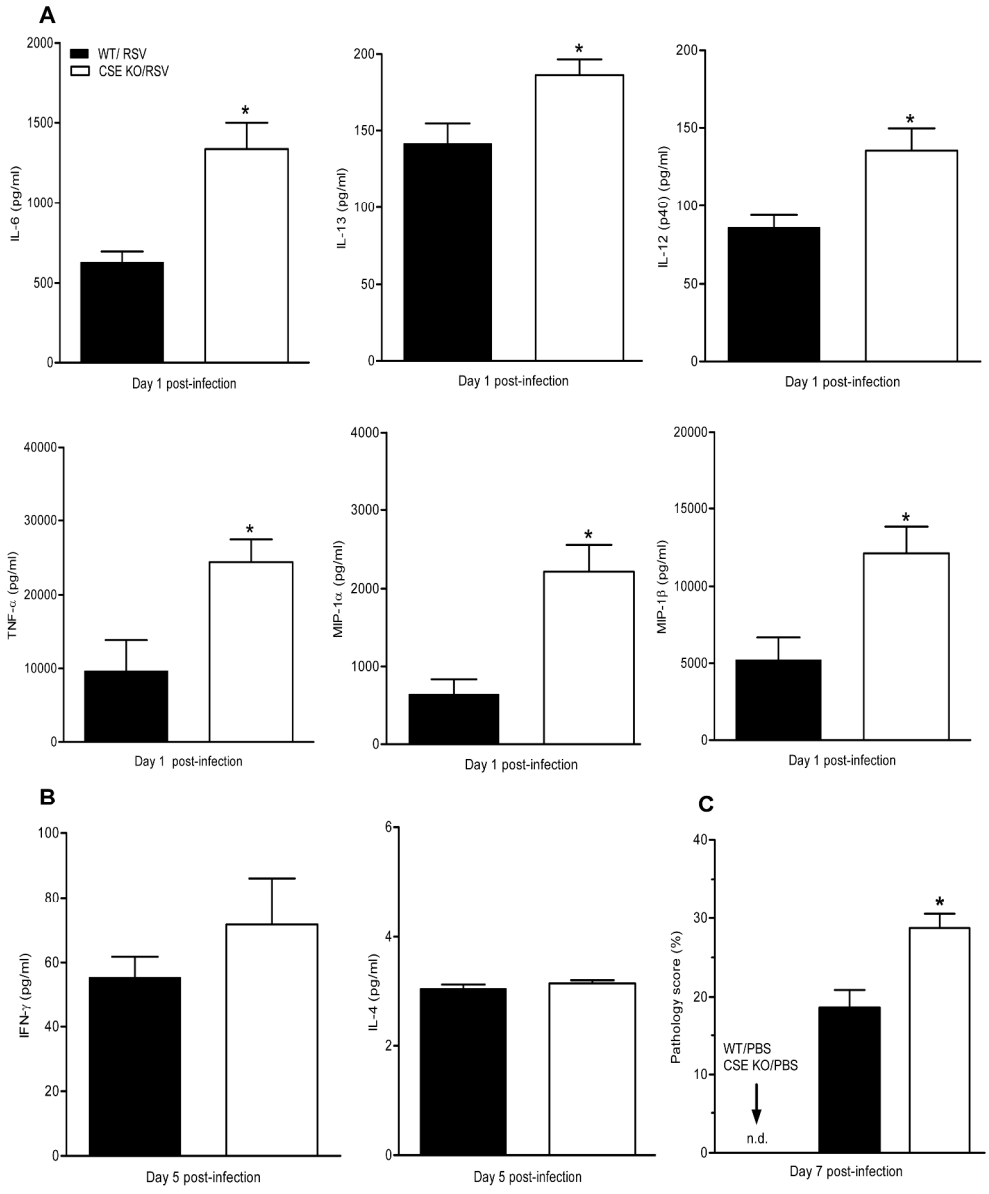

Figure 7. Effect of CSE-deficiency on cytokines, chemokines production and pulmonary inflammation after infection. C57BL/6 (WT) and CSE -/- (CSE KO) mice were infected i.n. with 107 PFU of RSV or PBS. (**A**) Mice were infected with RSV or mock-infected and sacrificed at day 1 p.i. to collect BAL samples. Cytokine/chemokine production was measured by a multi-Plex Cytokine detection system. The bar graph represents mean ± SEM (n = 3-4 mice/group. (**B**) BAL was collected at day 5 after infection to measure INF-γ and IL-4 by ELISA. Data are expressed as mean ± SEM (n = 4 mice/group). (**C**) Pathology score of lungs harvested at day 7 p.i., fixed and H&E stained. The bar graph represents mean ± SEM (n = 3-4 mice/group). *p<0.05 compared with WT/RSV group.
183x219mm (600 x 600 DPI)

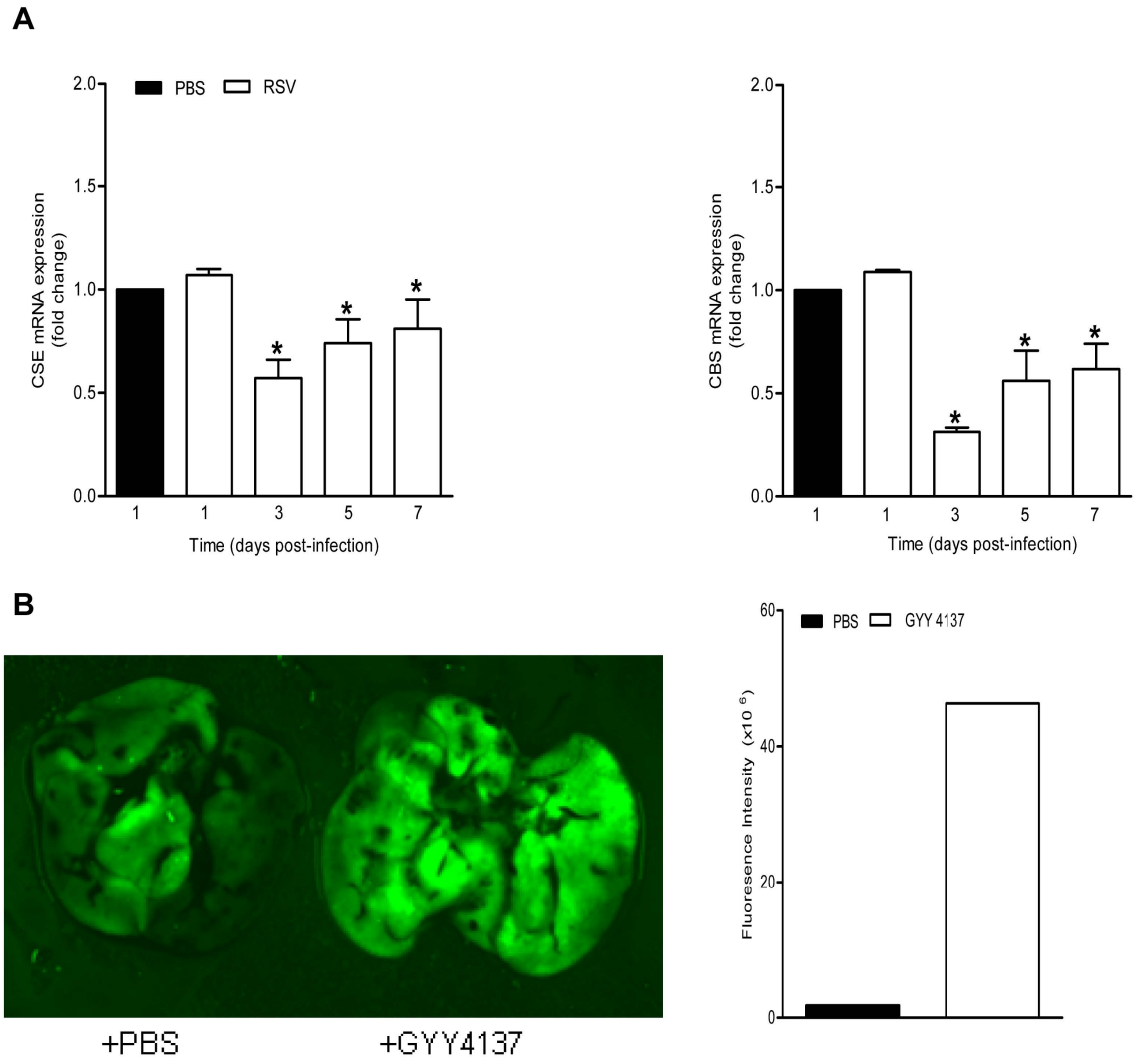

Figure ES1. H2S expression in lung tissue. (**A**) Effect of RSV infection on CSE and CBS gene expression in lungs of mock or RSV-infected mice. BALB/c mice were either inoculated with PBS (sham-infected) or infected with 5x106 pfu of RSV and harvested at different days post-infection to isolate total RNA from lungs. CSE and CBS mRNA levels in sham and viral-infected mice were measured by qRT-PCR. The bar graph represents mean ± SEM (n = 4 mice/group). * $p<0.05$ compared to sham. (**B**) Hydrogen sulfide expression in the lungs by *ex vivo* imaging using a novel fluorescent probe (SF-7AM). SF-7AM probe was delivered to vehicle or GYY4137 treated mice as described in Methods section. Left panels shows images of vehicle untreated and GYY4137 treated (50 mg/kg body weight) lungs. Right panel shows fluorescent intensity measured using Living Image software.
124x110mm (300 x 300 DPI)